Hydrogeologic Analysis of a Complex Aquifer System and Impacts of Changes in Agricultural Practices on Nitrate Concentrations in a Municipal Well Field: Woodstock, Ontario

by

Claus Philip Haslauer

A thesis
presented to the University of Waterloo
in fulfilment of the
thesis requirement for the degree of
Master of Science
in
Earth Sciences

Waterloo, Ontario, Canada, 2005
© Claus Philip Haslauer 2005

I hereby declare that I am the sole author of this thesis. This is a true copy of the thesis, including any required final revisions, as accepted by my examiners.

I understand that my thesis may be made electronically available to the public.

Abstract

The Thornton Well Field, located in an area of dominantly ($\sim$80%) agricultural land-use, produces $\sim$50% of the drinking water for the city of Woodstock. Since the mid 1990's nitrate concentrations in some of the supply wells are above the Maximum Allowable Concentration (MAC) of 10mg-N/L. The source of the nitrate is believed to be from agricultural fertilizing practices. As response to this problem, the County of Oxford purchased 111 hectares of farmland within the capture zone of the Thornton Well Field. This land is rented back to farmers with restrictions placed on the amount of nitrate fertilizer that can be applied in an attempt to sustainably reduce the nitrate concentrations in the Thornton Well Field below MAC.

The objective of this thesis is to improve the site conceptual hydrogeologic model, both at a spatial scale suitable for numerical analysis through regional groundwater flow modelling (representative distance $\sim$9km) and at a smaller scale (representative distance $\sim$2km) for nitrate transport modelling in the vicinity of the Thornton Well Field and the purchased land. Field investigations aimed to support the site hydrogeologic model involved drilling, geologic logging, and instrumentation of a 72m deep borehole completed to bedrock in the center of the nitrate plume, at the border of the farmland under consideration. The shallow subsurface features encountered during this initial drilling operation were tracked below the farm fields with geophysical tools and additional drilling and core logging throughout the field site. Transient hydraulic head observations in combination with on-site precipitation measurements were used to indicate where a hydraulic connection between ground surface and deeper layers exists, which allow rapid infiltration to occur into a glaciofluvial outwash channel which was identified as one important pathway for nitrate transport to the Thornton Well Field. One receptor at the end of that pathway, the screen of the supply Well 01, was depth-discrete profiled for water inflow and nitrate concentrations to obtain better characteristics of the receptor.

A method was developed to estimate the nitrate mass stored in the unsaturated zone below Parcel B, permitting an estimation of the time frame required for flushing the nitrate out of this zone, and the anticipated effects on nitrate concentrations in the supply wells. The spatial distribution of nitrate concentrations in the unsaturated zone and in the aquifer units was analyzed. It was found that the nitrate concentration within the unsaturated zone below Parcel B is $\sim$16mg-N/L, resulting in a total nitrogen mass of $\sim$20t within that zone. It was shown that significant reductions ($\sim$10%) in nitrate concentrations in the supply wells of the Thornton Well Field can be achieved, assuming zero nitrate mass influx into the domain from Parcel B.

A comprehensive data base was developed to organize, manage, and analyze all site measured data for that purpose, and regional hydrogeologic data from the MOE Water Well Record Database. The contents of this database in conjunction with the MOE Water Well Record Database were used to construct a three-dimensional digital repre-

sentation of the hydrostratigraphic units at a regional and at a local scale. This three-dimensional hydrostratigraphic unit spatial distribution along with surface watershed information and potentiometric surfaces of the various aquifer units will be used to define a suitable spatial domain and associated boundary conditions for future modelling efforts. This hydrostratigraphic model will serve as basis for predicting the effects of agricultural land-use changes within the capture zone of the Thornton Well Field (Parcel B) on the nitrate concentrations in the supply wells of the Thornton Well Field.

Acknowledgements

Contents

List of Tables

List of Figures

1

Introduction

Nitrate originating from fertilizer applied on farm fields is the largest anthropogenic non-point source of contaminated water worldwide (*Bouchard et al.*, 1992; *Hallberg*, 1987). The United States Geological Survey (USGS) found in a nation-wide study that 15% of groundwater samples from shallow aquifers below agricultural and urban areas exceeded the United States Environmental Protection Agency (USEPA) drinking-water standard of 10mg-N/L (*USGS*, 1999). The European Environmental Agency (EEA) points to agricultural non-point pollution as the primary cause of water quality deterioration in many European regions (*European Environment Agency*, 1999).

Nitrogen is one of the three essential plant nutrients, and nitrate (NO_3^-), the non-toxic highest oxidation state of nitrogen, is very soluble in water (300g/L to 900g/L), mobile, and is the form of nitrogen that is most easily assimilated by plants (*Mengel and Kirkby*, 1982; *OMAF*, 1998). In 1918, when Fritz Haber invented a Nobel Prize worthy method to synthesize ammonia (the basis for industrial nitrogen fertilizer production), only 2% of the total nitrogen available for agricultural fertilizer use came from inorganic sources. By the early 1970's that number had increased tenfold (*Fraser and Chilvers*, 1981). The dramatic increase of fertilizer consumption in Canada since the 1950's is shown on Figure 1.1. Parallel and linked to this increase in fertilizer consumption was an increase in average farm size, intensification of the farm process, and externalizing of farming costs to the detriment of the environment (*Phipps*, 1991).

Bacteria in mammals' stomachs can reduce nitrate to nitrite. The corresponding oxidation reaction converts hemoglobin's constituent Fe^{2+} to Fe^{3+}. This oxidized form, methaemoglobin, is unable to release oxygen to other cells, resulting in cyanosis, and eventually to asphyxia and death. Nitrites in a mammal's stomach can react with other nitrogen compounds such as amides and amines to form carcinogen N-nitroso-compounds (*Canadian Council of Ministers of the Environment*, 1992). Newborns are especially prone to methemoglobinemia ("Blue Baby Syndrome") since at this early stage of human development the ratio of water intake (with potentially elevated nitrate concentrations) to body mass is extremely high and a gastric acid barrier which prevents a grown-up's bowel from being colonized throughout its length by iron-oxidizing bacteria, is not yet developed (*Hill*, 1999). *Fraser and Chilvers* (1981) determined a fatality rate

of $\sim$8% amongst 2000 methemoglobinemia cases between 1945 and 1981 worldwide, and stated that "*there is an inverse relationship between cumulative fertilizer usage and mortality in the rural aggregates of the standard regions of England and Wales*". Epidemiological evidence linking intake of nitrate and nitrite with cancer occurrences in human beings is equivocal (*Ward et al.*, 2003; *Roos et al.*, 2003; *Weyer et al.*, 2001).

Despite the lack of a clear defined threshold, the Canadian Council of Ministers of the Environment (CCME) recommended a maximum acceptable concentration (MAC) of 45mg-NO_3^-/L in drinking water as a Canada-wide guideline (*Canadian Council of Ministers of the Environment*, 1992). This guideline is incorporated into the Ontario Safe Drinking Water Act (Ontario Regulation 169/03) as a MAC of 10mg-N/L (*Government of Ontario*, 2002). When this limit is exceeded, drinking water advisories are issued. For example, a nitrate-related drinking water advisory was put into effect in the town of Strathroy, Ontario on 23-March-2005 (*Middlesex-London Health Unit*, 2005).

A precautious approach to environmental protection is necessary to reach sustainability (*NRC*, 1993; *Rajagopal and Tobin*, 1989). Implementing a sustainable approach to secure a public drinking water supply in an agricultural setting is only possible by minimizing environmental impacts and maximizing crop yields simultaneously. Arising opportunity costs and their distribution between applying nitrate on farm fields as fertilizer to maximize crop quantity and quality, and between protecting the groundwater resource to minimize costs for drinking water treatment or costs for new, often deeper wells prevent this desired state (*Pfister*, 2002). The European Union (EU) Water Framework Directive suggests pricing water at full cost recovery to increase water use efficiency. *Martinez and Albiac* (2004) evaluated different taxing schemes for water and nitrogen to optimize policy decisions for non-point pollution. They used a dynamic bio-economic model that evaluates effects of nitrate leaching to show that taxing of emissions would lead to an optimal policy. *Lee and Kim* (2002) used a similar method in the United States and concluded that a tax on the nitrate input is the least-cost policy.

Providers of drinking water derived from groundwater resources need to know quantitatively the effects of land-use on concentrations of different contaminant species in their supply wells. In an agricultural setting this refers to fertilizing and cropping practices and their effect on concentrations of nitrate, other nutrients, and pathogen species. Evaluating and predicting the effects of non-point sources on concentrations in supply wells requires a groundwater flow- and transport model. Such a model has to be based on the physical setting within the study area. One of the first physically based approaches to modelling regional transport of nitrogen was presented by *Kinzelbach et al.* (1992) in which a simple geologic setting was represented in two dimensions, concentrations in the supply wells predicted, and effects of different land-uses considered. *Foster* (2000) stressed the importance of the unsaturated zone and the time-lag that it causes in the appearance of contaminants at the receptor. Various authors stated that spatial heterogeneity added complexity to evaluating non-point nitrate contamination (*Knapp*, 2005; *Woldt et al.*, 1996).

Pro-active Land-Use Changes within the Capture Zone of the Thornton Well Field in Woodstock, Ontario | 1.1

The Thornton Well Field is situated in an agricultural setting and faces the issues issues of non-point nitrate contamination discussed above. This well field supplies $2 \cdot 10^6 m^3$ to $4 \cdot 10^6 m^3$ water per year to the City of Woodstock – about half of the city's demand. Nitrate concentrations in extracted water from this well field have been steadily increasing since the 1970's. The water in some wells started to exceed Ontario's MAC of 10mg-N/L in 1994 (Figure 1.2). Currently, groundwater of different compositions from different sources is being blended before distribution to satisfy the MAC. In response to this continued and worsening nitrate contamination problem, the County of Oxford – the agency responsible for the water supply for the City of Woodstock – undertook a pro-active step in source water protection by purchasing 111 hectares of farmland within the capture zone of the Thornton Well Field. The land has been subsequently rented back to farmers with restrictions placed on the amount of fertilizer that can be applied in order to reduce excess nitrogen loading near this well field. The farmers managing this land are required to develop a Nutrient Management Plan (NMP) based on the guidelines provided by the Ontario Ministry of Agriculture and Food (*OMAF*, 1998). The NMP is intended to assist farmers in optimizing the use and management of all nutrients within the overall agricultural operation and is a tool to implement Best Management Practices (BMPs).

The county grants the farmers a compensation equalling the damage cost that results in applying a sub-optimal amount of nitrate fertilizer. The intention of reducing the nitrate loading within the capture zone is to reduce and maintain the nitrate concentrations in the supply wells below the drinking water MAC. The County of Oxford is assessing the prospects of achieving these intentions with a research project whose goal is to quantify and evaluate the influence that changing nutrient management practices on the purchased land will have on the regional groundwater quality, with specific emphasis on predicting the long-term impacts on the quality of the water extracted by the wells in the Thornton Well Field.

Previous hydrogeologic investigations in the vicinity of the Thornton Well Field have indicated that the aquifer system in general consists of aquifer- and aquitard- units of glacial origin (*Padusenko*, 2001). At a regional scale, the main hydrostratigraphic units appeared to be discontinuous although the detailed distribution of the main units was not well understood and likely plays a significant role in the subsurface distribution of nitrate originating from the agricultural land-use practices in the area. In addition, the unsaturated zone, presumed to store significant mass of excess nitrate leached below the root zone is highly variable in nature and plays a significant role controlling the temporal release of nitrate to the water table. In order to quantitatively evaluate the influence of the modified nutrient management practices in the area around the Thorn-

ton Well Field on the nitrate concentrations in the production wells, a more detailed understanding of the hydrogeologic system is required.

Objectives | 1.2

The objective of this thesis is to improve the site conceptual model, both at a spatial scale suitable for numerical analysis through regional groundwater flow modelling and at a smaller scale for nitrate transport modelling in the vicinity of the Thornton Well Field and purchased lands. To satisfy this objective, a host of field- and historical data investigations were completed. The focus of these investigations was to enhance the pre-existing conceptual site model with respect to data quality, spatial coverage, and level of detail. The field investigations consisted of a deep well installation, various shallow well installations, extracting and logging various soil cores, geophysical surveys, water sampling, water level measurements, tile drain monitoring, and depth-discrete profiling along one of the key supply wells.

The spatial distribution of nitrate throughout the unsaturated and saturated zones beneath the purchased lands was mapped and used to gain an understanding of the impact of the nitrate-mass loading from these fields on the supply wells. Finally, three-dimensional visualization techniques were used to construct hydrostratigraphic units suitable for use in a numerical modelling investigation. "Hydrostratigraphic units" in the context of this thesis are formational or lithologic units that are grouped together based on similar hydraulic properties into zones capable of transmitting water (aquifers) and zones that retard flow due to lower hydraulic permeabilities (aquitards) – following definitions of *Maxey* (1964) and *Weight and Sonderegger* (2000). The representation of the spatial distribution of the hydrostratigraphic units results in a hydrostratigraphic model

The above described independent complimentary data sets, augmented with information from borehole logs of wells drilled in the area since 1941, were analyzed and used to gain an improved understanding of the flow and transport processes in the subsurface. The main focus of this study is the land purchased by the County of Oxford and the transport pathway from the surface of this land to the screen of the supply wells of the Thornton Well Field (receptor).

4

Chapter 2 provides related background information on physiography, hydrology, (hydro-) geology, geochemistry, well extraction rates, and the pre-existing site conceptual model. Chapter 3 presents the methods used in this investigation to address the thesis' objective. Chapter 4 discusses the results of each field-investigation technique and the analysis of the nitrate mass stored in the unsaturated zone below the farm fields purchased by the County of Oxford, and Chapter 5 combines and integrates all results to present the constructed enhanced conceptual site model. Chapter 6 summarizes the most important conclusions from this research, and Chapter 7 recommends future actions and identifies critical issues.
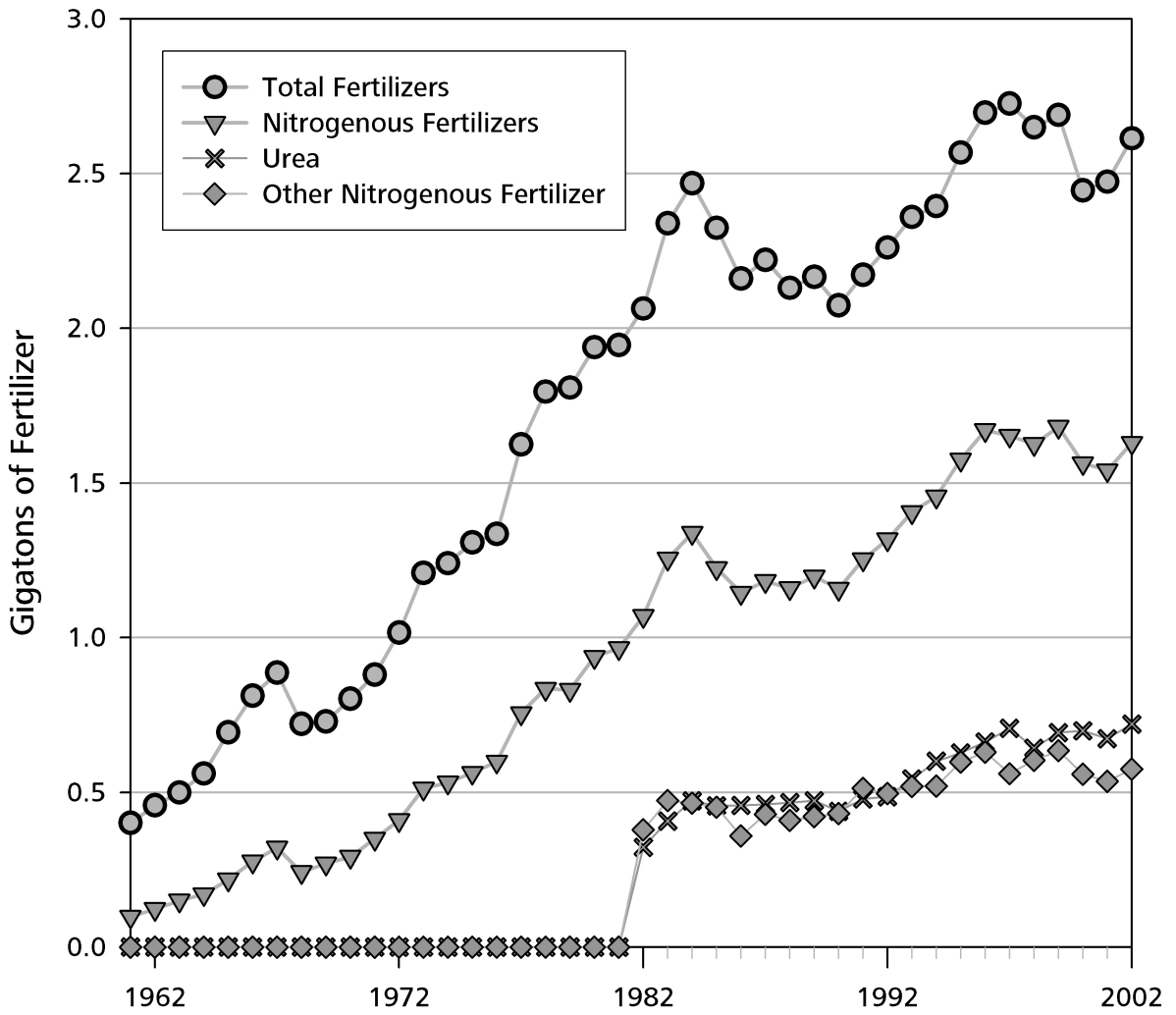
Figure 1.1:
Development of fertilizer consumption in Canada. Some minor nitrogen-containing fertilizers, including calcium nitrate and calcium ammonium nitrate, are not shown. Data from the *Food and Agriculture Organization of the United Nations* (2005).
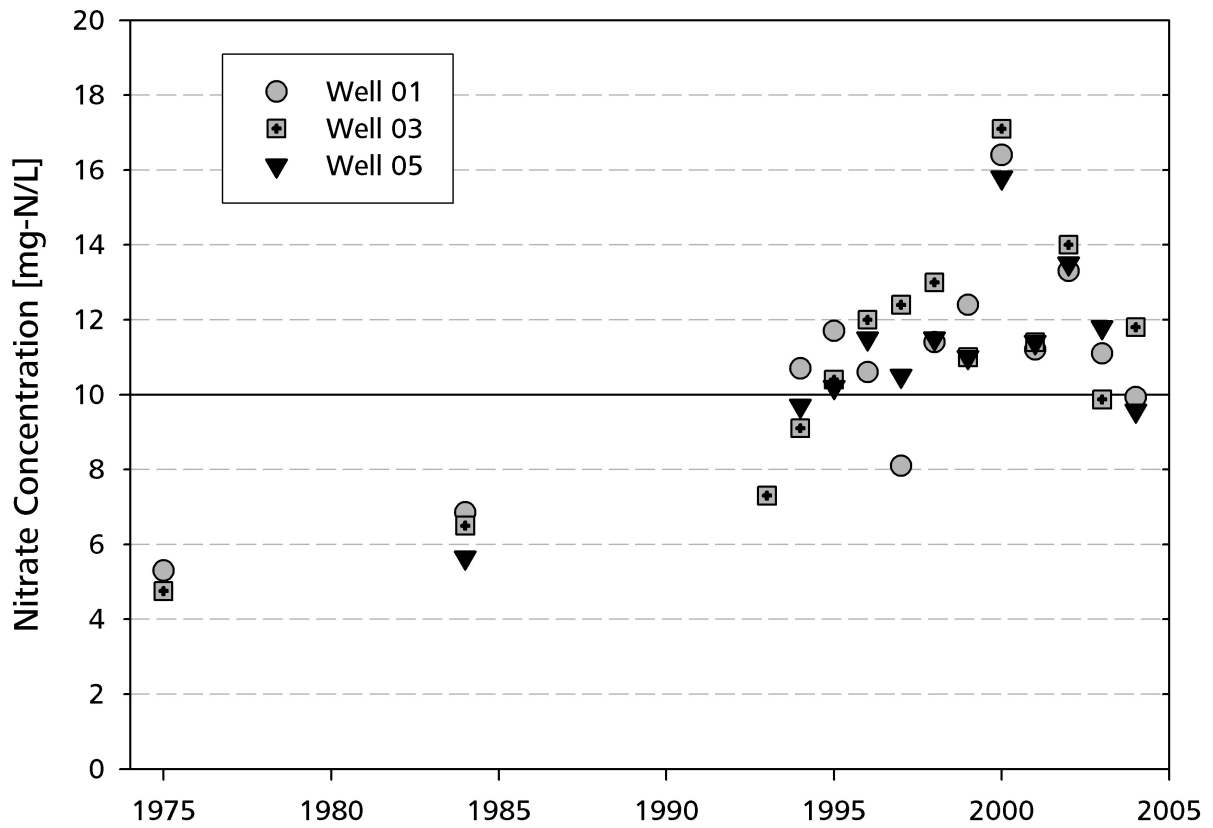
Figure 1.2:
Maximum annual nitrate concentrations [mg-N/L] observed in three of the five Thornton Supply Wells.

2

Background

The County of Oxford is located in south-western Ontario between the cities of Waterloo and London, north of Lake Erie. The main city in this county is Woodstock, located in the center of the county (Figure 2.1) with a population of 33,640 in 2001 (*County of Oxford*, 2001).

The ground surface varies county-wide from 390 meters above sea level (masl) in the north to 180masl in the south, as shown on Figure 2.2. One dominant ground surface feature, captured by a Digital Elevation Model (DEM), is the Thames River channel. This channel is the main drainage feature in the area and cuts into the bedrock surface. The study site is located within the Thames Watershed, with the Thames River draining into Lake St. Clair. The eastern part of the study site drains into Cedar Creek, a tributary to the Thames River, while the western part drains directly into Thames River (Figure 2.3). East of the Thornton Well Field (Wells 01, 05, 03, 08 and 11) in a flat area of about 290masl Cedar Creek forms the Sweaburg Swamp.

Within the area of interest three hill-features with longitudinal axes from south-west to north-east can be identified (Figure 2.2): (1) between the Thames river and Highway 401 (HW401) which comprises the point of highest ground surface elevation of about 375masl, (2) between HW401 and Sweaburg Rd., and (3) south of Sweaburg Rd. Imposed on these features are smaller scale hilly features ("drumlins") with longitudinal axes orientated from north-west to south-east. These features are prominent in the area around Woodstock ("Woodstock Drumlin Field", Figure 2.7) and are the reason why this landscape is usually described as having a "rolling surface" (*Cowan*, 1975).

The average annual rainfall depth in Woodstock between 1870 and 2002 is 795mm/year (data from *Environment Canada* (2002)). In the course of a year rainfall is evenly dis-

tributed, with a minor high in June and a minor low in February (Figure 2.4). Temperature characteristics show a typical continental climate trend with a pronounced high between June and August, and a pronounced low in January and February (Figure 2.4).

<div align="right">

Geology | # 2.2

</div>

2.2.1   Pre-Quaternary

The bedrock geology is described in detail by *Karrow* (1973) and *Cowan* (1975), and mapped by *Davies and McClymont* (1962). The bedrock surface generally slopes from north-east to south-west, and is flat or gently rolling with few drainage indentations. Figure 2.5 shows the succession of formations in south-western Ontario. The northern part of the Detroit River Formation, consisting of "*very fine grained, light brown to grey high-calcium limestone containing numerous corals and stromatoporoids*" (*Cowan*, 1975), which forms the upper most bedrock surface within the study area, is described as a "*very good*" water supply aquifer; the overlying Bois Blanc Formation as an "*excellent*" water supply aquifer (*MacRitchie et al.*, 1994; *Ontario Ministry of the Environment*, 2003*a*). *Cowan* (1975) points out that in the Ingersoll (∼6km down the Thames River from Woodstock) area the Detroit River Formation is capped by up to 10m of sandy limestone formerly known as the Columbus Limestone .

2.2.2   Quaternary

The Quaternary Geology of the area is described by *Cowan* (1975), *Karrow* (1973), and recently by *Krzyszkowski and Karrow* (2001). Summaries were given by *Sebol* (2000) and *Padusenko* (2001). The area around the Thornton Well Field is an interlobate zone where advancing and receding ice lobes that moved in different directions deposited material at different times.

The location of the field site between deposits from two different icelobes is shown at two different scales on Figure 2.6. In the larger-scale map, the Zorra Till, also called "Tavistock Till", shaded in yellow, can be identified in the north-west and the Port Stanley Till, shaded in green, to the south-east. The icelobe that deposited the Zorra Till came from the Huron-Georgian Bay area; the one that deposited the Port Stanley Till from the Erie-Ontario basin. Older deposits (Catfish Creek Till) are found deeper in the deposition sequence. The current bed of the Thames River is identifiable as "glaciofluvial outwash", only parts of which are filled with "modern alluvium" from the current river bed – therefore the Thames River is now an underfit stream (*Cowan*, 1975) carved

into the bedrock surface. The smaller-scale map on Figure 2.6 shows the drainage network more clearly with recent deposits ("modern alluvium" and "bog deposits"), older deposits ("glaciofluvial outwash", ice-contact– or glaciolacustrine deposits), and probably even older deposits ("Catfish Creek Till", exposed due to erosion). At this scale it is clear that the eastern boundary of the study site is the area where the ice-lobes of the Zorra Till and Port Stanley Till collided.

Drumlins (Figure 2.7) are longitudinal landforms, with the long axis being parallel to the direction of ice flow. In the Woodstock area this direction is between 280° and 330°. The mechanism of formation is unknown, and their interior can consist of deposits that are horizontally layered, layered parallel to ground surface, or randomly distributed *Karrow* (2005). These different ice advances at different times are the main cause of the highly heterogeneous deposition and consequently the highly heterogeneous and complex hydraulic conductivity distribution.

A correlation between tills and hydrostratigraphic units across the study site is not part of this thesis. Physical properties of tills were described by *Padusenko* (2001). "Till" is a collective term for the group of sediments laid down by the direct action of glacial ice without the intervention of water (*Allaby and Allaby*, 1999). The grain size of tills can vary from clay to coarse sand, and therefore some tills can conduct water as can be easily visually conceptualized at the open pits of the sand and gravel quarries within the study site (more detail in Section 2.5).

Municipal Well Fields $\Big|$ 2.3

The City of Woodstock relies solely on groundwater for its drinking water supply from two main well fields (Figure 2.2) which supply about 50% of the demand each: the Thornton Well Field (Well 01, 05, 03, 08, and 11) and the Tabor Well Field (Well 02 and Well 04). Four wells (06, 07, 09, and 10) are located within the urban area and are only used in times of peak water demand. Two other wells (SW-1 and SW-2) are located in the town of Sweaburg and used for this town's supply (Figure 2.2).

2.3.1   Pumping Rates and Nitrate Mass Loadings

Before ∼1940 the drinking water for the City of Woodstock was collected in a pond inside the area of the current well field close to Well 01. As the city grew, more and more supply wells were constructed as listed in Table 2.1. Construction details for these wells are given in Table 2.1. Pumping rates at the Thornton Well Field are dynamic as shown by the annual extracted water volumes between 1999 and 2004 on Figure 2.8.

The installation of a monitoring system by the County of Oxford in 2003 allowed daily pumping data to be collected (Figure 2.9). Appendix A.8 provides a detailed breakdown of monthly pumping volumes. The data indicates that in 1999 the total pumping volume was distributed relatively evenly between all wells, and since this time the contribution of Well 11 has doubled and rates at Well 01 and Well 08 have been cut back so dramatically that by 2004 they were running only intermittently. Overall, between 1999 and 2004 the total annual pumping volume of the Thornton Well Field has been reduced by 50% and was averaging in 2004 $\sim$7,000m^3/d.

Table 2.2 summarizes the annual pumping rate and the average annual nitrate concentrations for all five wells of the Thornton Well Field from 1999 to 2004. Based on those two parameters the total annual extracted nitrate mass (mass = concentration $*$ volume) was calculated. The annual pumping rate decreased over time, and the average concentration values decreased as well, both of which leads to the decrease of total mass extracted. The decrease in nitrate concentrations is likely due to the fact that different wells were pumped.

2.3.2 Observation Wells

Multilevel observation wells existed at 15 locations at the start of this study (Figure 2.10) with a total of 72 monitoring points. All these observation wells were installed in the years 1997/1998 with the goal of measuring hydraulic head and nitrate concentrations in what *Padusenko* (2001) described as the "Shallow Aquifer" (see Section 2.4.1). Construction details are described by *Padusenko* (2001). At most locations a depth of $\sim$10 meters below ground surface (mbgs) was reached, except at wells WO 02-D, WO 08-D, WO 11 and WO 12 ($\sim$20mbgs), and WO 04-D ($\sim$43mbgs). At each location between three and six wells were installed and screened at different depths.

The County of Oxford maintains a network of test wells, the ones where borehole logs were available are shown on Figure 2.10. The borehole logs and construction details of three of these wells with one monitoring point each were available for this study.

2.3.3 Thornton Well Field Nitrate Concentrations

One sample taken from a well is one snapshot in time from the small portion of the aquifer in which the well is screened. This concentration value is influenced by parameters that influence the flow system (areas of differing recharge characteristics, the hydraulic properties and spatial distribution of of hydrostratigraphic units), parameters determining the contaminant input (varying land-use and related input rates of contaminant sources), parameters that influence the contaminant along its flowpath (decay, retardation), and parameters that relate to sampling methods and analytical determination. These complex dependencies make it difficult to estimate a trend based on

relatively sparse data. Temporal dynamic extraction rates are an additional difficulty for those predictions around a well field (*Knapp*, 2005).

Nitrate concentrations in the supply wells of the Thornton Well Field have been increasing since the 1970's. They exceeded the MAC of 10mg-N/L the first time in the mid 1990's. The wells that first surpassed this threshold were Wells 01, 03, and 05 (Figure 1.2). The period of increase in aqueous nitrate concentration from the 1970's to the late 1990's corresponds to the period of increase in fertilizer consumed (Figure 1.1) and is commonly observed in agricultural areas (*Hallberg and Keeney*, 1993). Notable in the temporal development of annual maximum concentrations plotted on Figure 1.2 is the increase of nitrate concentrations in Well 03 in 2004. The timing of this increase might correspond to an earlier increase in the pumping rate of that well. The five wells of the Thornton Well Field are located within a 1.5km distance, and therefore a time-lag between a substantial change in pumping rate and the arrival of the newly configured plume has to be expected.

The current (2004) management of the Thornton Well Field leads to nitrate concentrations in all wells (except for Well 03) at or below MAC (see Appendix A.9). After decreasing nitrate concentrations in 2003, especially Well 01 and Well 03 show increasing nitrate concentrations in 2004.

Figure 2.11 shows the nitrate plume as mapped by *Padusenko* (2001). The trend-analysis of nitrate concentrations in observation wells up-gradient of the Thornton Well Field are part of the current study.

Hydrogeology | # 2.4

2.4.1   Physical Hydrogeology

The complex depositional environment at this study site results in complex hydrostratigraphy and complex spatial distribution of aquifers and aquitards which is the primary control on the nitrate migration pathways from the farm fields to the extraction wells. This section describes what was known about this spatial distribution before the start of this study.

Golder Associates (2001) in their groundwater protection study distinguished between "Shallow Overburden Aquifers", "Intermediate Overburden Aquifers", "Deep Overburden Aquifers", and "Bedrock Aquifers". These categories were based on a simple average depth-scheme, but not on a conceptual hydrogeological model.

Padusenko (2001) interpreted approximately 100 borehole-logs inside his domain to set up the two aquifer, three aquitard conceptual model shown on Figure 2.12. The aquifer units were divided into a shallow aquifer and a deep aquifer, which are connected in places. *Padusenko* (2001) described the deep aquifer as a local, relatively narrow feature with hydraulic conductivities ranging from $2.5 \cdot 10^{-06}$m/s to $5.0 \cdot 10^{-04}$m/s. The upper aquifer corresponds to the sand unit in the southern part of Figure 2.12 and its hydraulic conductivity ranges between $9.0 \cdot 10^{-06}$m/s to $2.4 \cdot 10^{-05}$m/s.

A recovery test conducted when one of the deep production wells (Well 01) was shut off for a week, demonstrated that both aquifers are connected in the vicinity of the well field (Figure 2.12). A fairly continuous surficial aquitard consisting of silty material forms the near surface sediment over much of the study area. *Padusenko* (2001) indicated that the groundwater flow direction in the upper aquifer is from west to east, with little or no vertical component except around the supply wells.

In a surfacewater – groundwater interaction study, that involved drilling and logging of two deep boreholes in the vicinity of the two deepest supply wells (Well 01 and Well 05), *Lotowater* (2002) defined three lithologic layers: a surficial sand and gravel layer with fine sediments, an intermediate silty sand and gravel layer, and one sand and gravel layer that forms the main, nitrate-contaminated aquifer. Bedrock underlies the main aquifer at approximately 4m below the bottom of Well 05 ($\sim$1m below the bottom of Well 01). Borelog analysis indicated that this aquifer unit is the same one that feeds Wells 11, 08, and 03, and slopes down 15m over a 100m distance south of Well 05 (see Figure 2.2 for location). In summary, *Lotowater* (2002) conceptualized one (nitrate-contaminated) aquifer, whereas *Padusenko* (2001) conceptualized two aquifers: one shallow aquifer, that is in places unconfined and feeds the three supply wells (Well 03, Well 08, and Well 11), and one local deeper aquifer that feeds the deep supply wells (Well 01 and Well 05). The study by *Lotowater* (2002) was spatially confined to the area around Supply Wells 01, 05, and 03, and thus there is no indication on hydrostratigraphy at a larger scale. A study by *Lotowater* (2002) proved, that Well 01 and Well 05 are flowing artesian wells under natural conditions.

2.4.2   Geochemistry and Age Dating

Geochemically, the groundwater in the area around the Thornton Well Field can be divided into three distinct geochemistry zones (*Heagle*, 2000). One zone extends from the well field westward and was identified as the source-area of the nitrate in the supply wells. It shows high dissolved oxygen concentrations, indicative of a non-denitrifying environment. The second zone is to the north of the well field with encountered high sulfur concentrations that tend to support the attenuation of nitrate (pyrite oxidation). The third zone, located to the east of the well field, is characterized by reducing conditions, high concentrations of dissolved organic carbon, and low nitrate concentrations. These are again conditions favourable to support denitrification.

Sebol (2000) pointed out, that the aquifers to the east and to the west of Sweaburg Rd. are distinct and not connected due to different geochemistry and age dates. Significantly different groundwater ages were found in the two regions (pre-1953 in the east and post-1953 in the west). During the recovery test conducted by *Padusenko* (2001) (see Section 2.4.1) no pressure response was observed in the eastern region, which supports the notion that the two regions are not hydraulically connected. *Sebol* (2004) re-sampled wells below the water table, conducted age dating analysis with enhanced methods, and concluded that water in the main aquifer (Aquifer 1 as defined in *Padusenko* (2001)) along a line between WO 11 and WO 02 (Figure 2.10) is very young (<10 years). A trench dug perpendicular along this line near WO 02 (*Yeung*, 2004) revealed a highly productive, sand and gravel aquifer stratified with gravel lenses. *Yeung* (2004) believes that water is flowing fast in that portion of the aquifer, which offers one explanation for the young groundwater age.

Padusenko (2001) developed a numerical flow model to delineate capture zones and travel times from the water table to the wells. Travel times are <10 years for all supply wells, and the age of the water within the system was shown to be <30 years. *Padusenko* (2001) stressed the importance of the unsaturated zone as a storage reservoir for (nitrate) mass and estimated a timeframe of 10 to 30 years for changes in land-use management focussed on reducing nitrate to cause a decrease of nitrate concentrations within the supply wells.

Land-Use and Management around the Thornton Well Field | **2.5**

The Thornton Well Field is located just outside the city limits of Woodstock (Figure 2.13) where the dominant (80% of the area) land-use is agricultural. Principal crops are corn, soy beans, and wheat (Figure 2.13), which are generally planted in a three-year succession. Romano beans, grass (alpha-alpha), and continuous corn are common as well. The area around the Thornton Well Field has been under agricultural cultivation since the late part of the the 19th century. As indicated by a quote from the historical atlas of the counties of Oxford and Brant (*Walker and Miles*, 1875): *"except the nucleus of a village [Woodstock], all else was a comparative wilderness as late as 1832"*. Livestock farms are common; the closest one up-gradient to the Thonton Well Field with ~2,000 hogs is located a few hundred meters to the south-west of WO 28-D.

Surface mining operations in the area are notable: there are two sand and gravel quarries in the vicinity of the Thornton Well Field. One is located north of the HW 401 between the Thornton Well Field and the City of Woodstock. The other quarry is located adjacent and west of the Tabor Well Field (both are visible on Figure 2.13). In Ingersoll (~6km down the Thames River from Woodstock), the Detroit River Forma-

tion is "*one of the most important centres in Canada for the production of chemical limestone and chemical lime*" (*Cowan*, 1975).

In 2003, the County of Oxford purchased two parcels of farmland totalling 111 ha (275 acres) within the 2-year time of travel capture zone of the Thornton Well Field, as determined by *Golder Associates* (2001), with the intention of reducing excess nitrogen loading near the well field. The land has been subsequently rented back to farmers with restrictions placed on the amount of fertilizer that may be applied. On one 38 ha (95 acre) parcel of farmland (Parcel A, Figure 2.14) fertilizer application is timed to maximize crop uptake. The farmer managing this parcel of land was required to develop a NMP. On the other parcel of farmland comprising 73 ha (180 acres, Parcel B, Figure 2.14) minimal nutrient inputs are prescribed. The soil was tested extensively across the fields to determine the spatial distribution for nutrient requirements. Based on the soil test data, minimum nutrient requirements were determined relative to the selected crop type. Fertilizer is being applied with the aid of a global positioning system- (GPS-) assisted fertilizer spreader, and detailed loading records are being collected for subsequent use in mass loading estimates. Due to the tight restrictions on fertilizer applications in Parcel B, the County of Oxford compensates the agricultural activity by renting the land for less than market value.

Table 2.1:
Overview over construction dates, recommended pumping rates, and construction details for the supply wells of the Thornton Well Field sorted by location from north to south. Data from well records from the County of Oxford.

	Well Name	Year Constructed	Estimated potential pumping rate [m³/min]	Ground Surface Elevation [masl.]	Depth to Top of Screen [mbgs.]	Top of Screen [masl.]	Bottom of Screen [masl.]	Length of Screen [m]	Inner Diameter [cm]
Thornton Wells	Well01	1905	4.5	294.1	24.8	269.3	264.7	4.6	40.6
	Well05	1962	5.7	294.3	22.6	271.7	267.1	4.6	40.6
	Well03	1945	6.0	294.9	13.1	281.8	278.7	3.1	40.6
	Well08	1966	1.8	298.9	11.6	287.3	284.2	3.1	30.5
	Well11	1993	not available	317.5	25.6	291.9	285.7	6.3	30.5
Tabor Wells	Well02	1945	7.3	294.7	15.5	279.1	274.8	4.3	40.6
	Well04	1958	10.0	298.9	14.3	284.6	275.5	9.1	45.7

Table 2.2:
Observed yearly average pumping rate and nitrate mass extraction considering all five supply wells of the Thornton Well Field (Wells 01, 05, 03, 08, and 11).

Year	Pumping Rate $[1 \cdot 10^6 \text{m}^3/\text{year}]$	Yearly Avg. Conc. [mg-N/L]	Yearly extracted mass [t-N]
2004	2.2	6.6	14
2003	2.6	7.4	18
2002	2.9	9.0	25
1999	4.2	8.6	36

Location of the Study Site

Toronto

Ontario

Great Lakes Area

Lake St. Clair

0   250   500   1,000 km

Waterloo

HW 401

Study Site

Woodstock

1

2

3

4

5

6

7

8

London

County of Oxford

Lake Erie

0 10 20   40 km
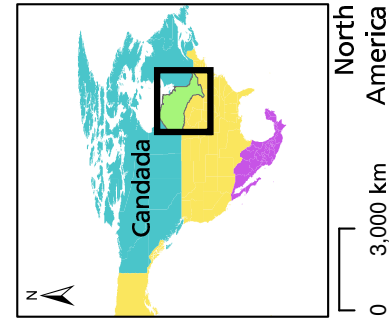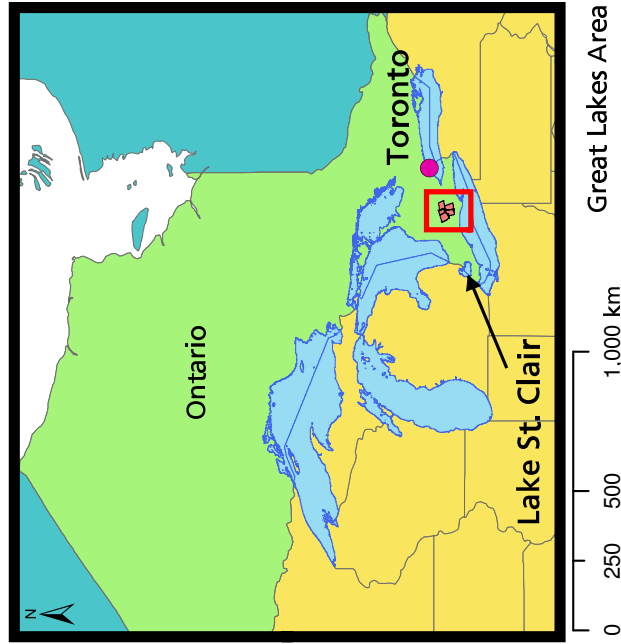
Townships within the County of Oxford

Zorra 1
E. Zorra-Tavistock 2
Blandford-Blenheim 3
SW. Oxford 4
Norwich 5
Woodstock 6
Ingersoll 7
Tillsonburg 8

North America

Candada

0   3,000 km
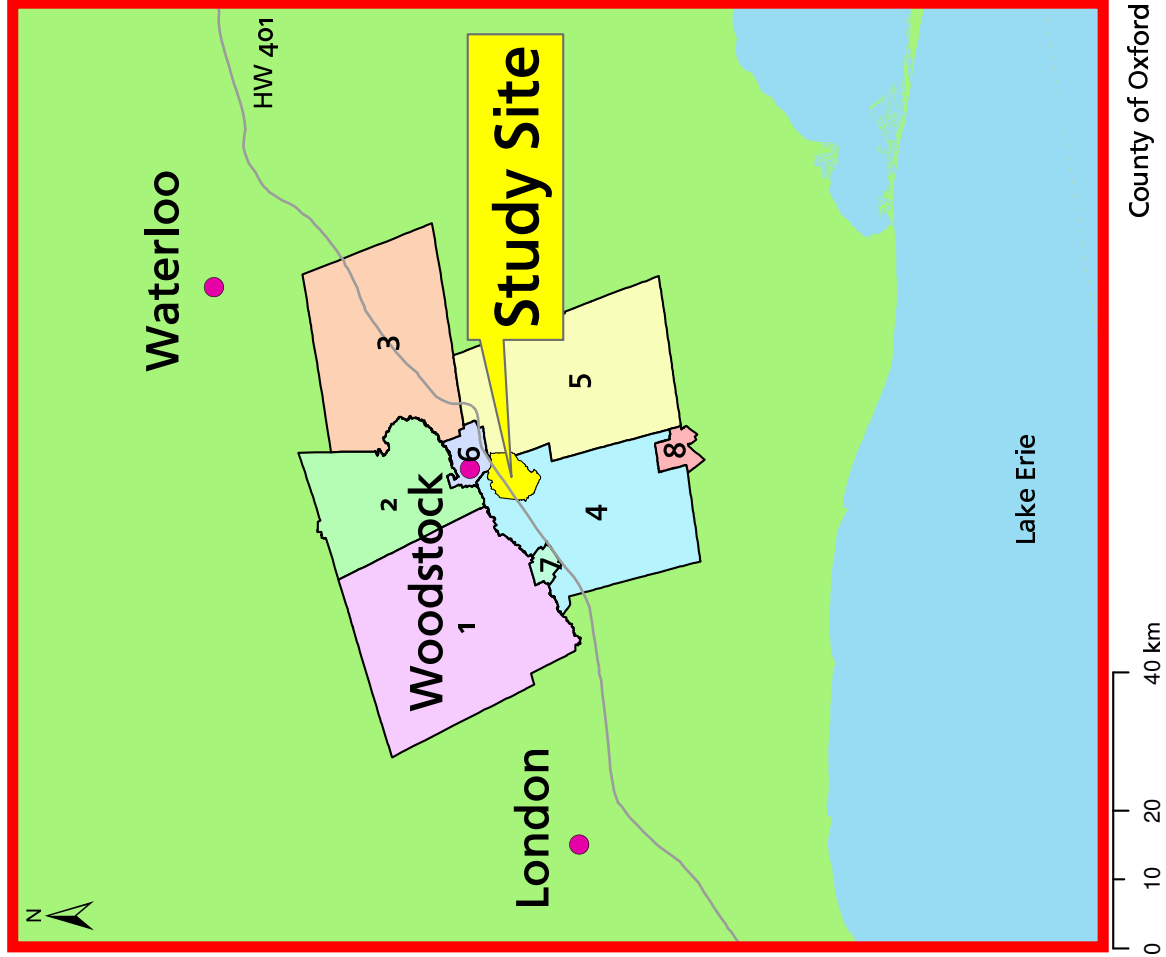
Figure 2.1:

Study site location. The study site is located in south-western Ontario, Canada, in the center of the County of Oxford. The map contains data from *Environmental Systems Research Institute* (2003), *County of Oxford* (2005b), and *Ontario Ministry of Transportation* (2000).

18
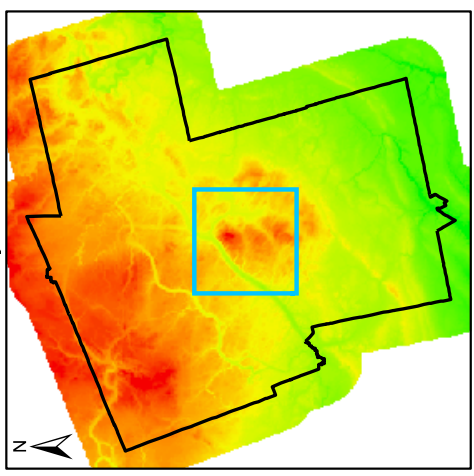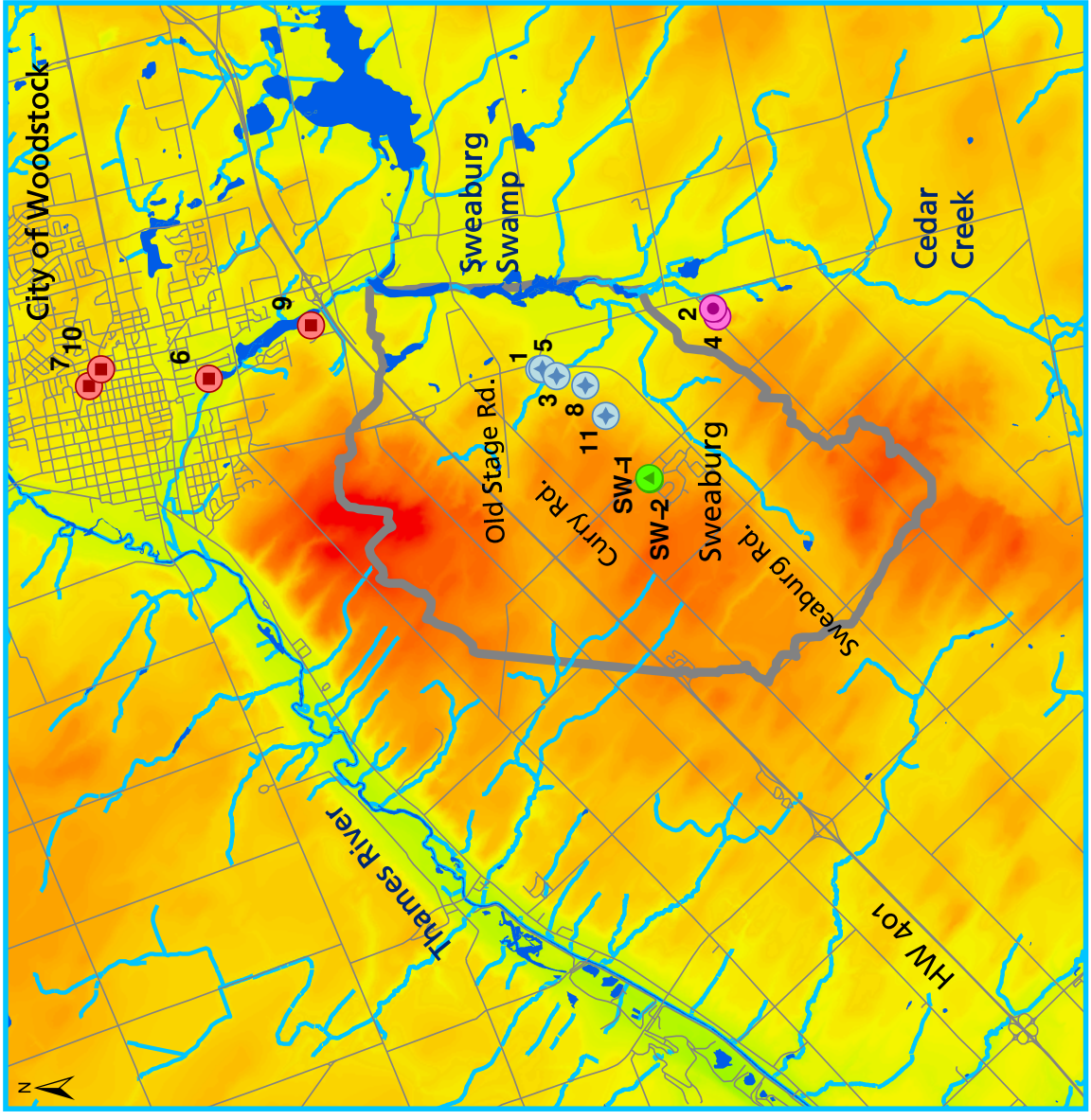
Figure 2.2:
Topographic elevation of the area of interest between the Thames River and Cedar Creek. Identification Numbers of all Supply Wells of the County of Oxford are indicated. The map contains data from *County of Oxford* (2005a), *Ontario Ministry of Natural Resources* (2002), and *Ontario Ministry of Transportation* (2000).

19
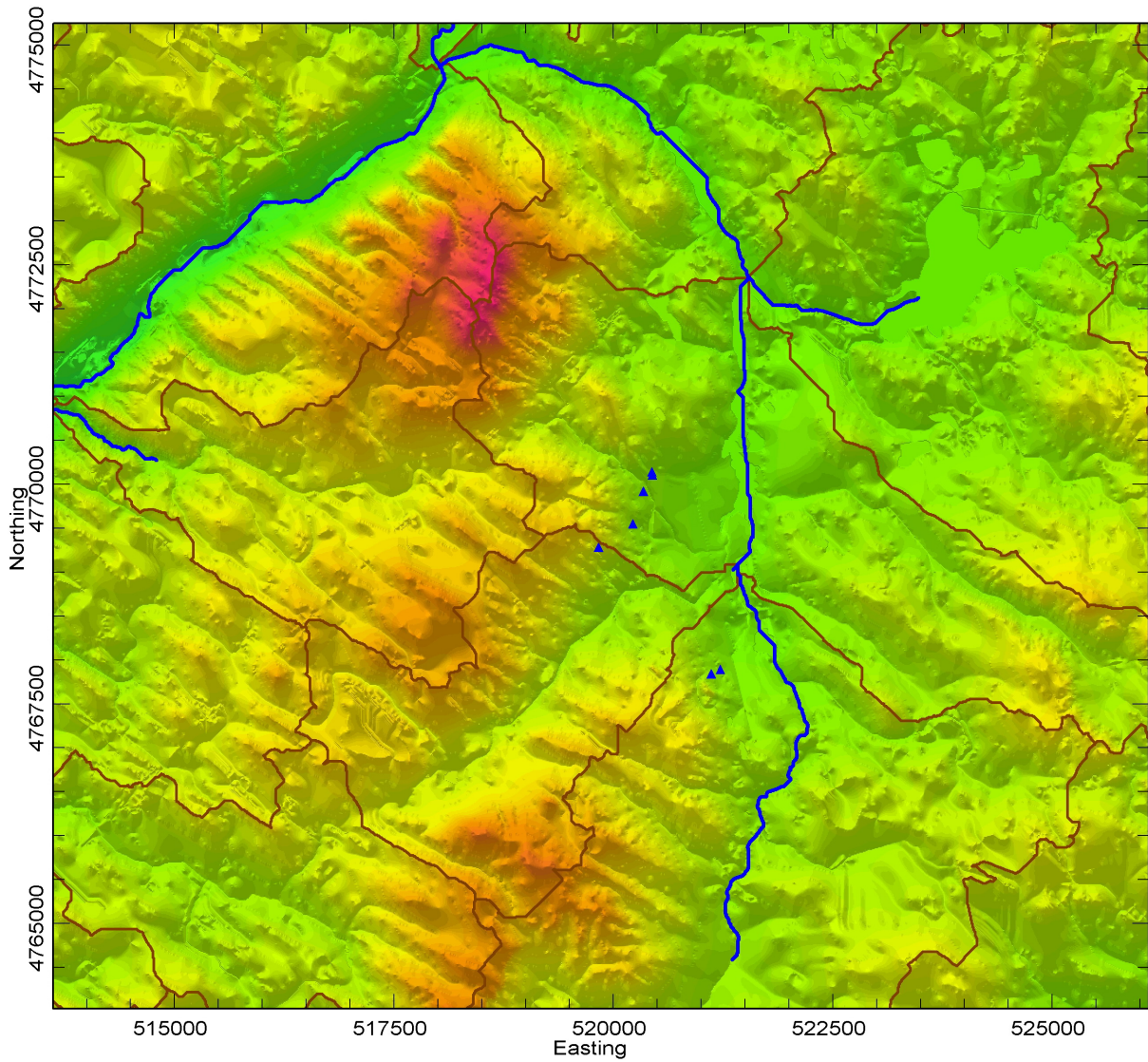
Figure 2.3:
Sub-watersheds (brown lines) in the area around the Thornton Well Field. Shaded in the background in topographic elevation – the three hill-like features are clearly visible. The supply wells of the Thornton- and the Tabor Well Field are indicated by blue triangles.
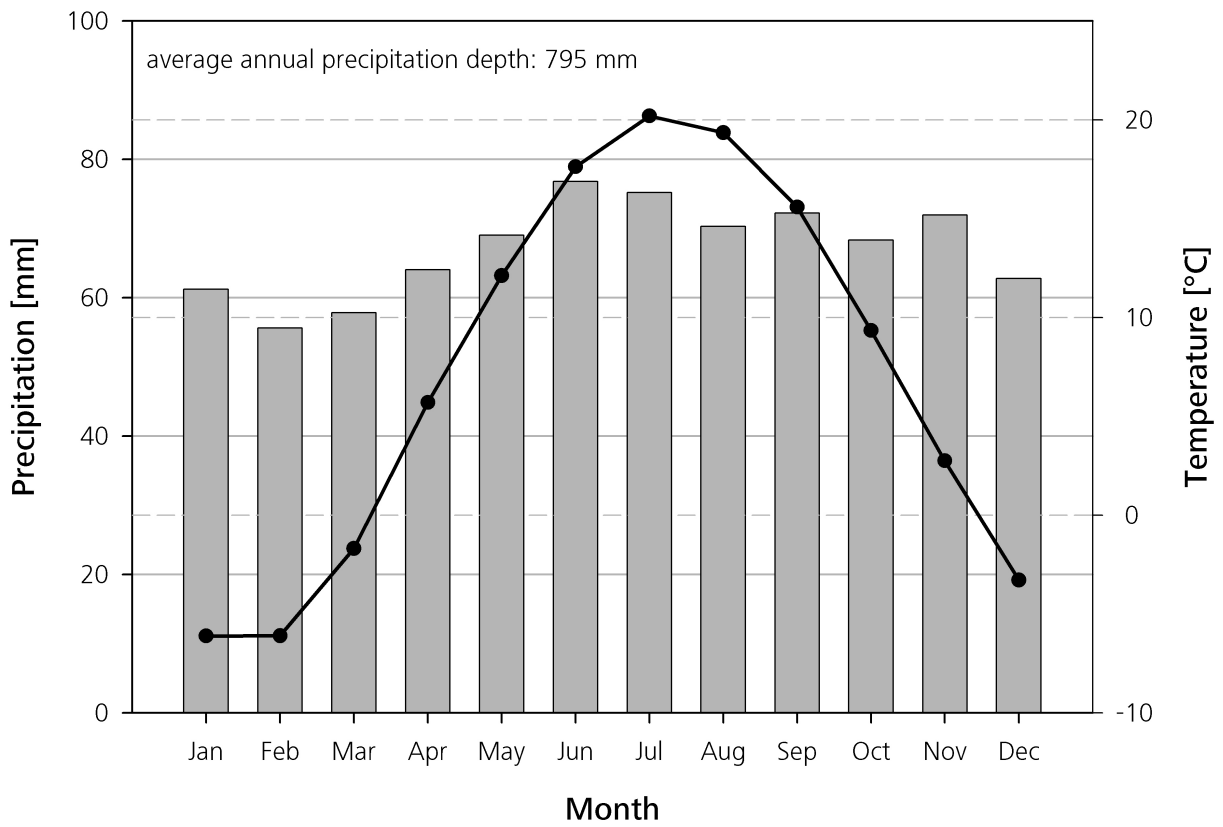
Figure 2.4:
Average monthly precipitation (bars) and air temperature (line) over the year. Data from *Environment Canada* (2002) averaged from 1870 to 2002.

Bedrock Geology

Formation Name

- Salina Fm.
  Dolostone, Shale, Gypsum
- Bass Island Fm.
  Dolostone
- Bois Blanc Fm.; Oriskany Fm.
  Cherty Limestone
- Detroit River Gp.; Onondanga Fm.
  High-Calcium Limestone
- Dundee Fm.
  Limestone

Study Site

20 km

0

200 km

0
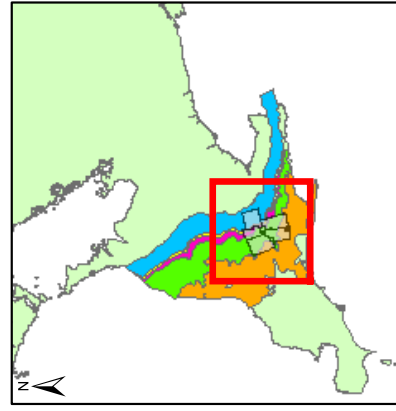
Figure 2.5:
Bedrock formations between the Upper Silurian Salina Formation and the Middle Devonian Dundee Formation, south-western Ontario.
This figure contains data from *Ontario Geologic Survey* (1988*b*)
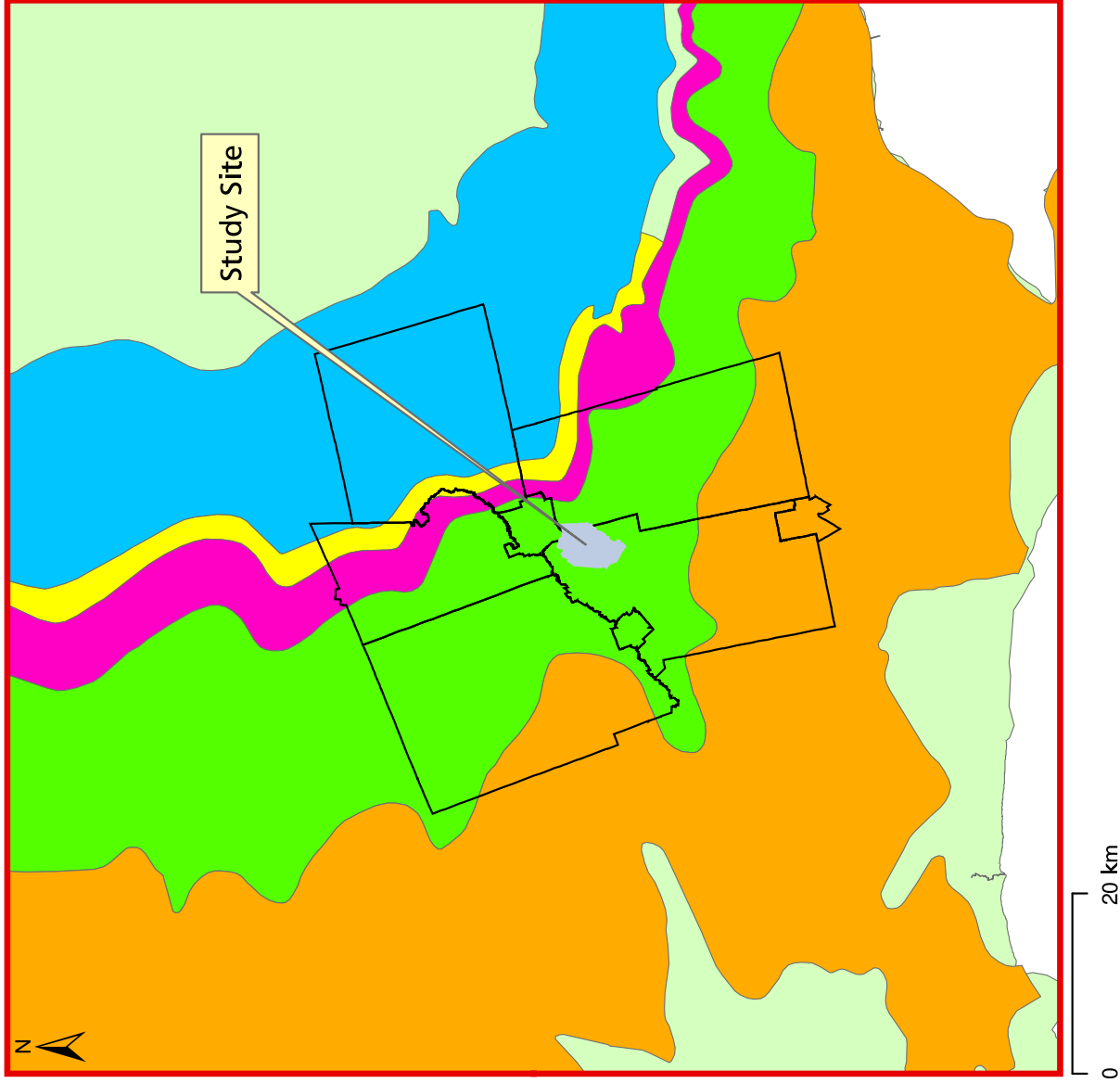
Quaternary Deposits

- Zorra Till
- Port Stanley Till
- Catfish Creek or Zorra Till
- Catfish Creek Till
- Catfish CreekTill
- Bog deposits
- Glaciolacustrine or pond deposits
- Fine-grained glaciolacustrine or pond deposits
- Ice-contact stratified drift
- Modern alluvium
- Glaciofluvial outwash
- Important Glaciofluvial Outwash Channel
- Thornton Supply Wells
- Study site
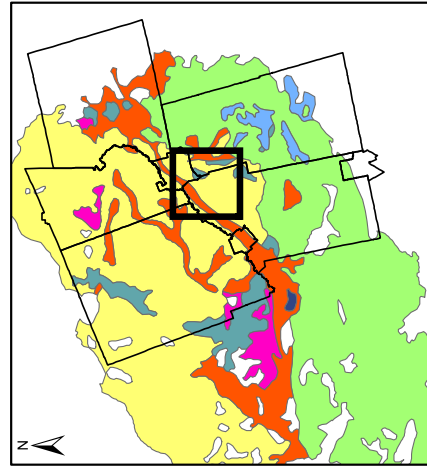
Figure 2.6:
The study site is located in the interlobate zone between the Zorra Till and the Port Stanley Till. This figure contains data from *Ontario Geologic Survey* (1988*b*), and *Ontario Geologic Survey* (1988*a*).
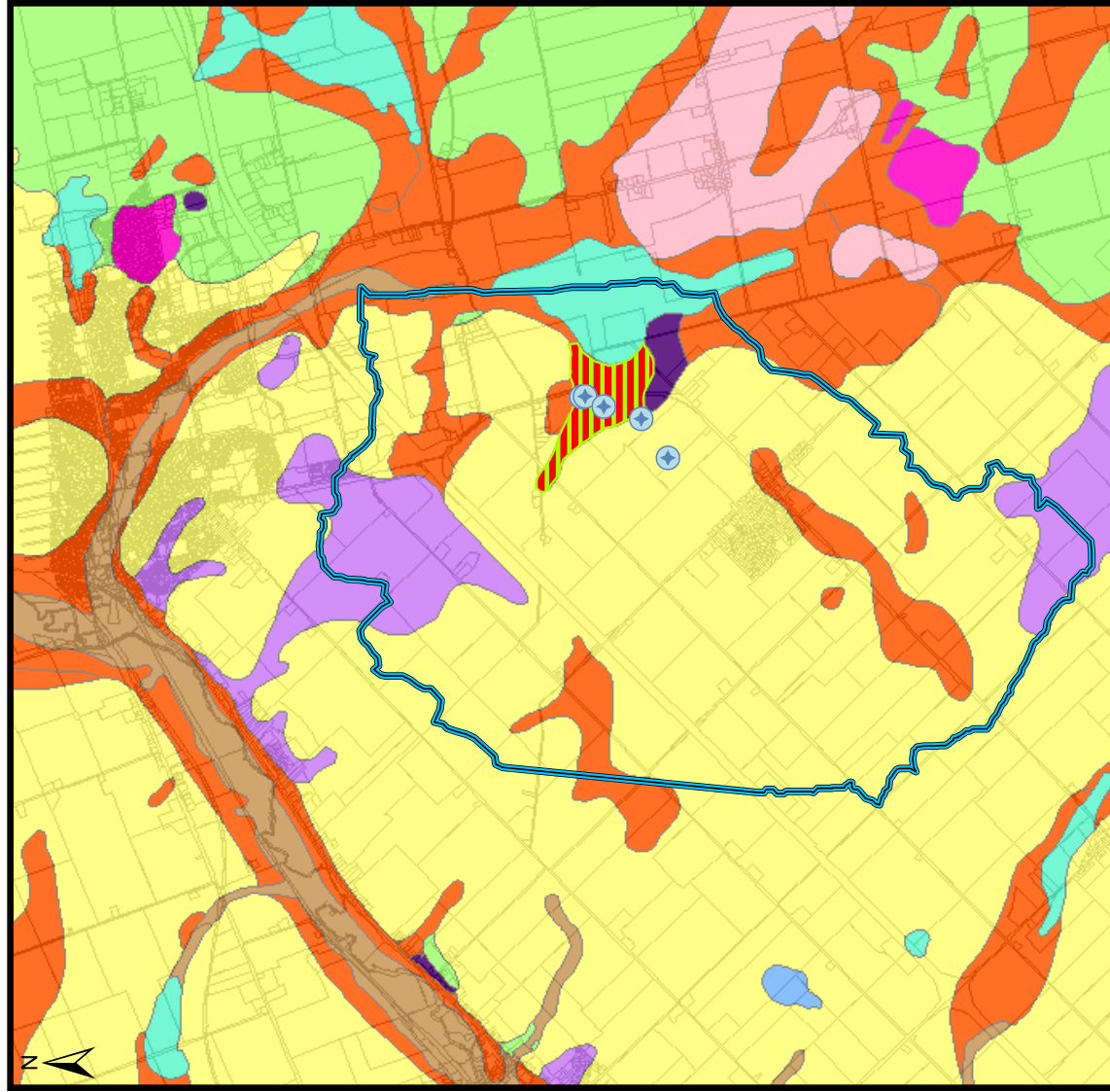
Zorra Till to the North-East and Port Stanley Till to the South-West

0   2 km

0   16 km

Quaternary Features

— Drumlin or Area of Drumlins

-·-· Trend of Ingersoll Moraine

☐ Study site

DEM

High : 390

[masl.]

Low : 180

Drumbo

Gobles

Eastwood

Oxford Centre

Oriel

Holbrook

0   10 km

N

0   20 km

N
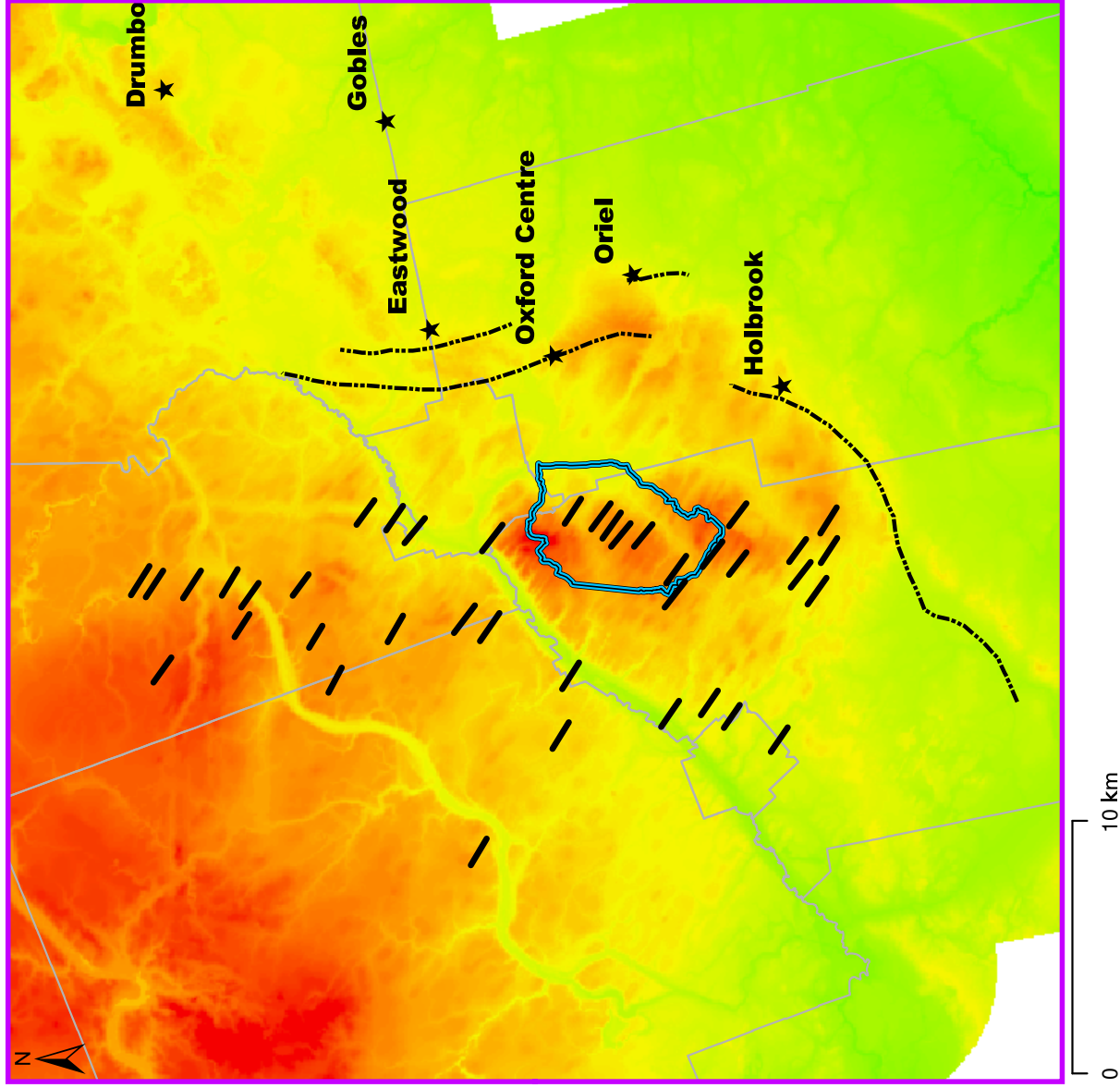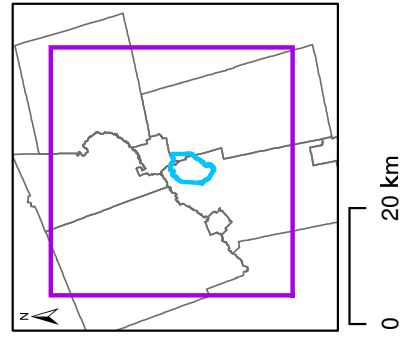
Figure 2.7:
Location and longitudinal extent of drumlins (thick solid lines). The crest of the Ingersoll Moraine is indicated by the dashed lines. The area shown is commonly referred to as the "Woodstock Drumlin Field". The map contains data from *Ontario Geologic Survey* (1988*b*). Locations of drumlins were spatially adjusted.
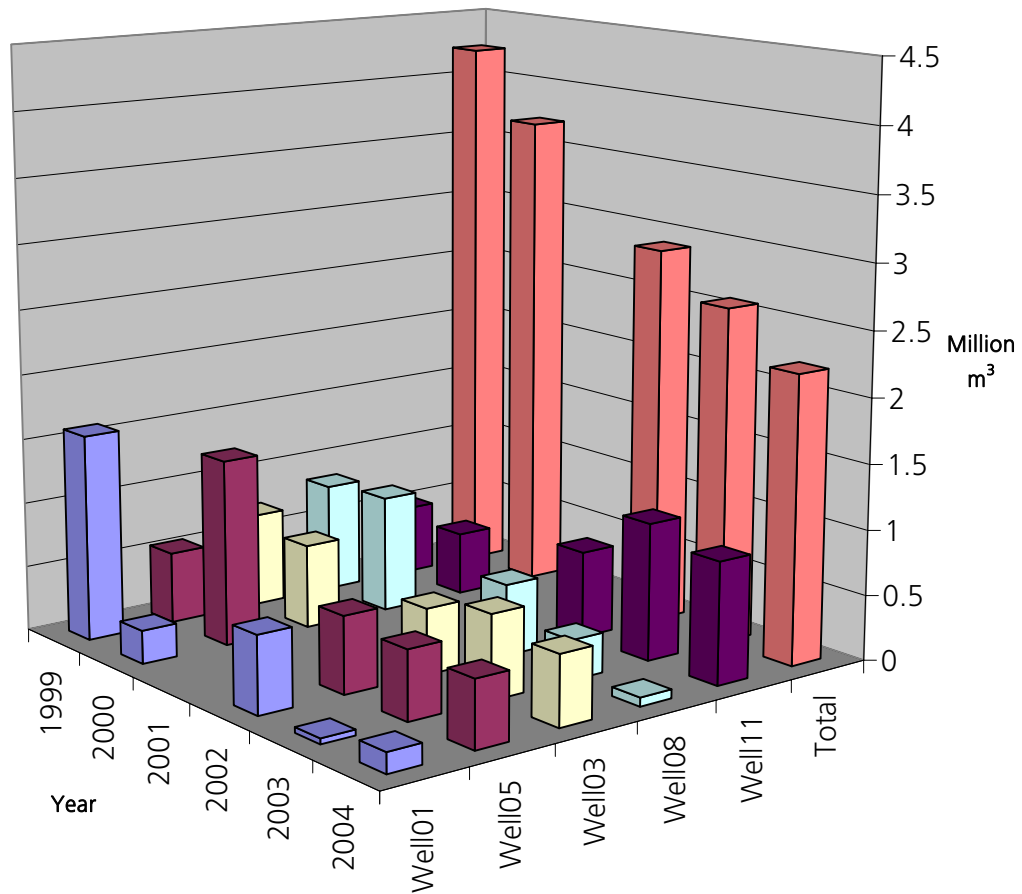
Figure 2.8:
Annual pumping volume from the Thornton Well Field. Note the 2001 data were not available.
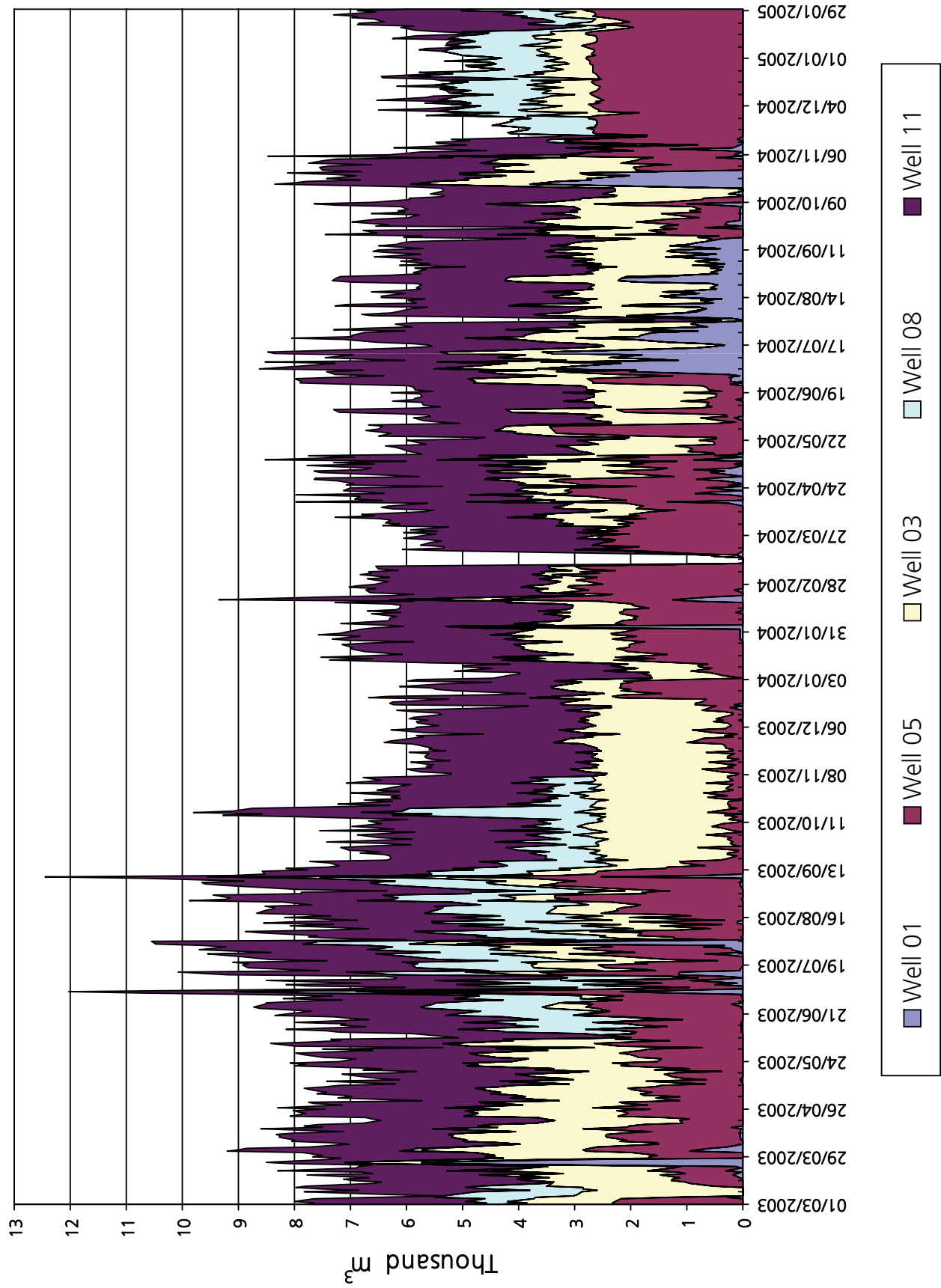
Figure 2.9:
Daily pumping volume from the Thornton Well Field from March 2003 to January 2005.

Figure 2.10:
Monitoring well network at the beginning of this study.

Plan View of the Study Site

Thornton Supply Wells

Farmland Parcel A

Farmland Parcel B

Thornton Well Field

2 yr tot Capture Zone

Property Boundaries

Nitrate Plume Contours

[mg-N/L]

1

10

Nitrate Plume Contours

[mg-N/L]

1

10

500 m

0

5.000 m

0
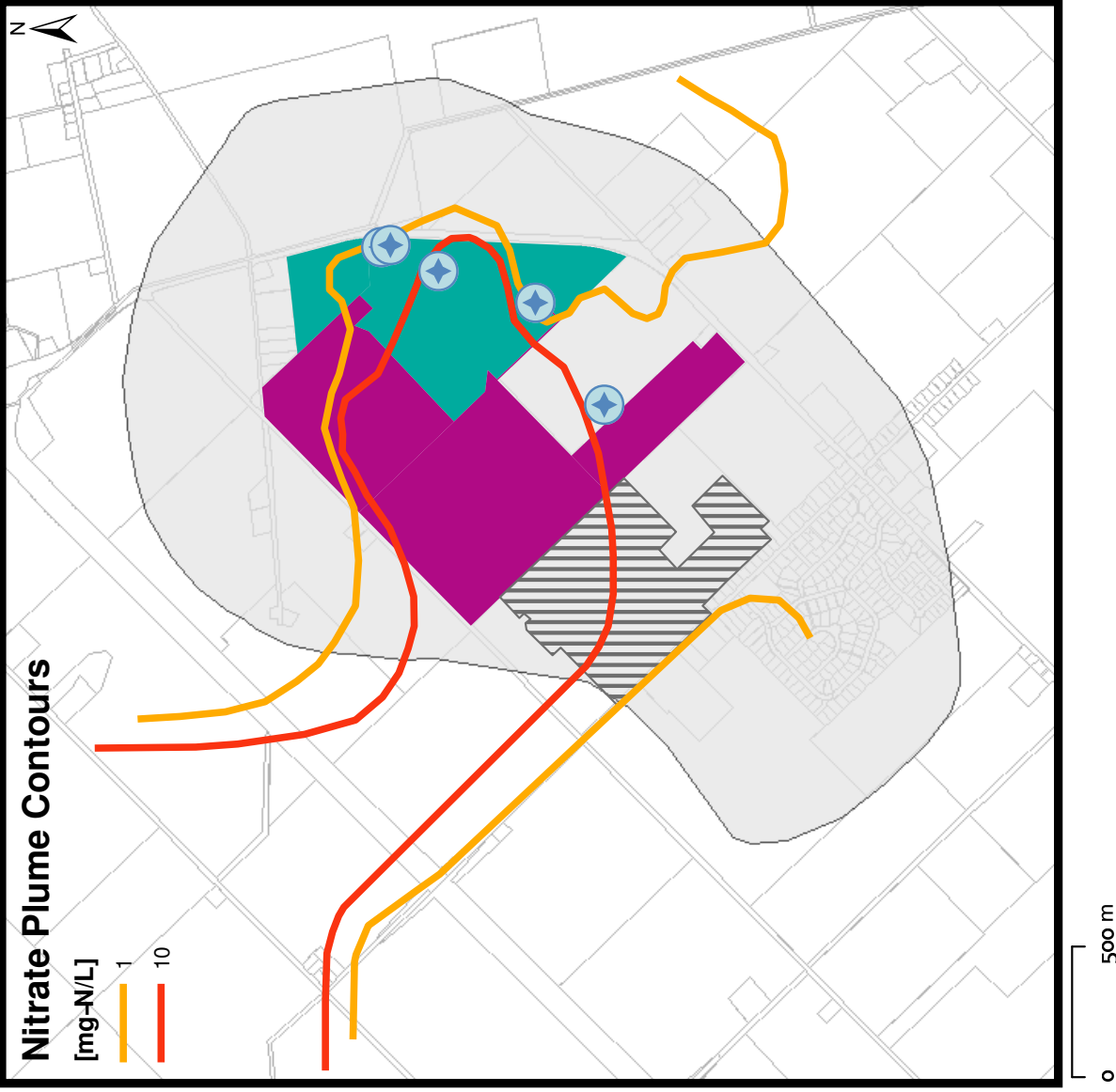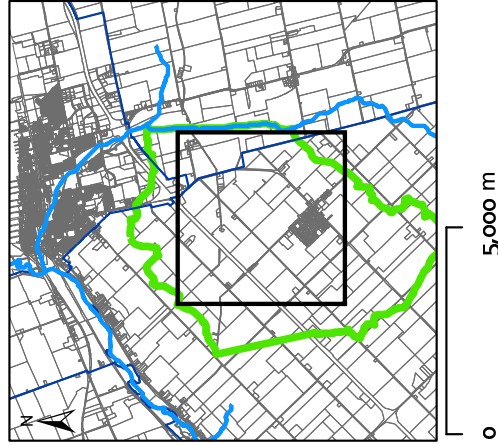
Figure 2.11:
Plan View of the vicinity of the Thornton Well Field. The supply wells of the Thornton Well Field are shown. The recently purchased farmland (Parcels A and B) are indicated. The 2-year time of travel (tot) capture zones were extracted from a wellhead protection study performed by *Golder Associates* (2001)). Nitrate concentration contours (1 and 10 mg-N l-1) were taken from *Padusenko* (2001) and are based on the maximum concentration observed until 2001 at each monitoring location.

28
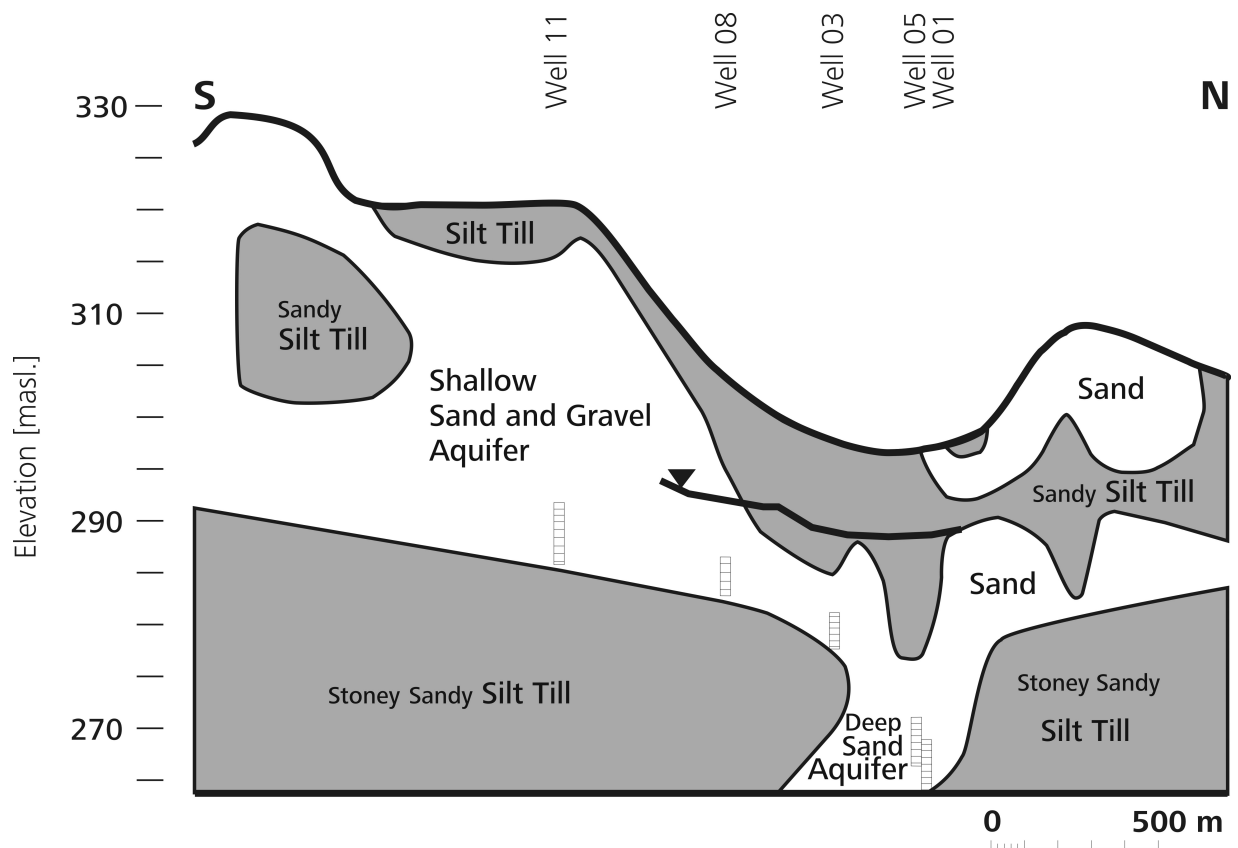
Figure 2.12:
Existing conceptual model after *Padusenko* (2001). Location of extraction well screens are indicated. Wells 1 and 5 are in the deep section of the sand and gravel aquifer unit that is connected to the screens of Wells 3, 8 and 11 at higher elevations. The bold dark line represents the water table in the shallow aquifer, which is based on measurements in the UW observation well network.
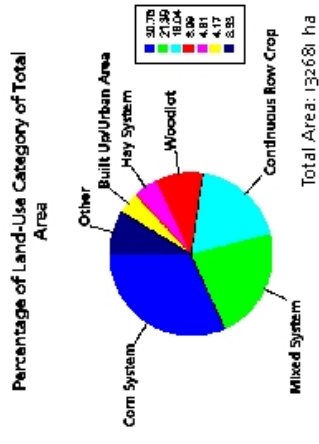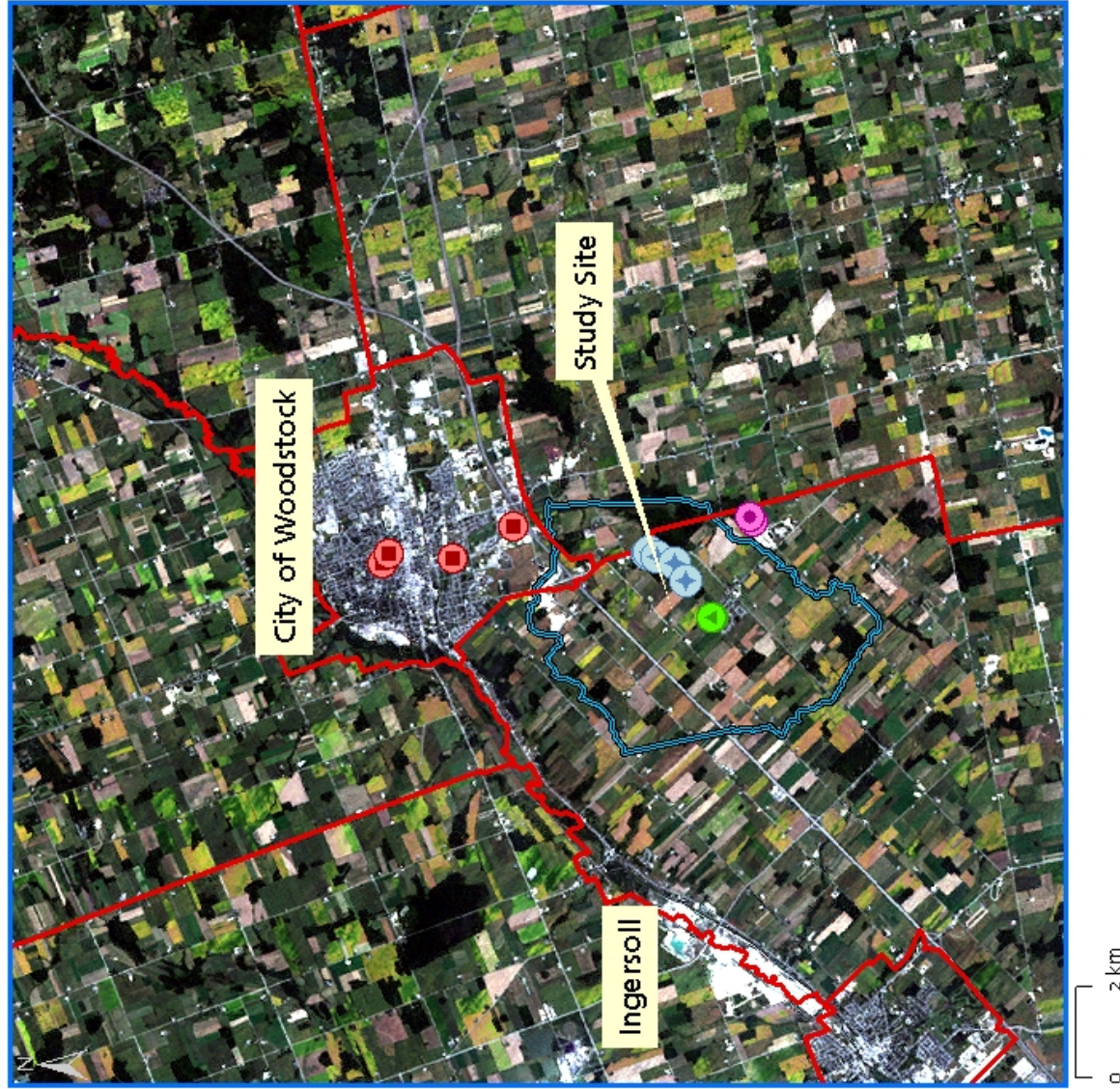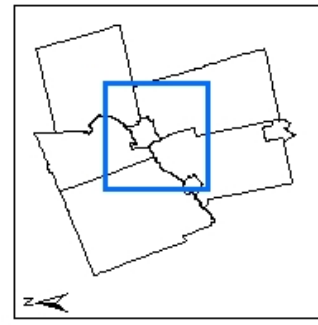
Figure 2.13:
Land-use in the area of interest. Identifiable are urban areas (City of Woodstock in the center and Ingersoll to the south-west along the Thames River), and predominantly agricultural areas. This figure includes data from *Natural Resources Canada* (2003) and *Ontario Ministry of Agriculture, Food, and Rural Affairs* (2000)

Farm Land

Legend:

- ⊕ Thornton Supply Wells
- Farmland Parcel A
- Farmland Parcel B
- 2yr tot Capture Zone
- Thornton Wellfield

Old Stage Rd.

Curry Rd.

01, 02, 03a, 03b, 04, 05, 06, 07

500 m

Sweaburg

HW 401

1,000 m
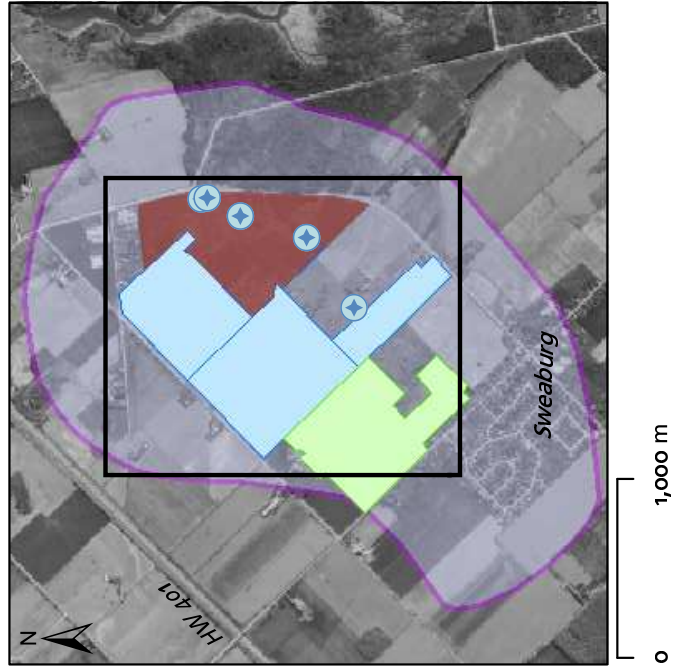
Figure 2.14:
Managed farm land around the Thornton Well Field. The recently purchased farmland (Parcels A and B) are indicated. The 2-year time of travel (tot) capture zones were extracted from a wellhead protection study performed by Golder Associates Ltd. (*Golder Associates*, 2001). Each field in Parcel B is numbered for reference.

3

Methodology and Approach

This chapter explains the tools used to enhance the hydrogeological understanding of the site, including rationale, procedure, and location.

Initial field investigations at the site involved the drilling and instrumentation of a 71.5m deep borehole completed to bedrock in the center of the nitrate plume (Figure 2.11), at the border of the farmland under consideration (Section 3.1.1). The lithologic information from this boring and data from the multilevel monitoring well cluster that was installed were used to enhance the understanding of the hydrostratigraphy and the groundwater flow system. The shallow subsurface features encountered during this initial drilling operation were tracked below the farm fields with geophysical tools (Section 3.2) and additional drilling and core logging throughout the field site (Section 3.1.2). Transient hydraulic head observations (Section 3.3.1) in combination with on-site precipitation measurements (Section 3.4) were used to indicate where a hydraulic connection between ground surface and deeper layers exists, which leads to rapid infiltration.

Along the screen of Well 01 a nitrate loading profile was determined, which involved depth-discrete measurements of water inflow rate and the nitrate concentration under pumping conditions (Section 3.5). The general understanding of the site was improved with the help of on-site interviews with farmers and collection of anecdotal information . For example, this information led to a compilation of tile-outfall locations and mapping of the areas they drain. During the spring-melt in 2005 the nitrate loading of one of these tile drain outlets was determined (Section 3.6).

A method was developed to estimate the nitrate mass stored in the unsaturated zone below farm fields where agricultural practices have been changed. This approach also permitted an estimation of the time frame required for flushing the nitrate out of this zone, and the anticipated effects on nitrate concentrations in the supply wells (Section 3.8). This methodology is largely based on geochemical and spatial analysis of the cores taken from borings drilled to examine the existence of the shallow subsurface features. The spatial distribution of nitrate concentrations in the unsaturated zone and in the aquifer units was analyzed.

Electronic data analysis tools (data bases, geographical information systems (GIS), and three dimensional visualization and analysis software) were used to store, compile and analyze newly and previously collected data. This includes well construction records, borehole logs, nitrate concentration profiles in the unsaturated zone, hydraulic head measurements, results of aqueous concentration samples, pumping rates, and rainfall measurements. These tools were used to enhance the existing conceptual model (Section 3.7) so that these data can be used directly as input for a future numerical modelling investigation.

Coring and Drilling | # 3.1

At the start of this study, the deep borehole WO 28-D was drilled at the south-western boundary of the farm-fields under investigation and in the center of the regional nitrate plume. The goal of this borehole investigation was to estimate the nitrate concentrations in groundwater entering into the study area below the farm fields where modified agricultural land-use practices were being employed, and to gain further understanding of the geology and hydrogeology of the site. Twenty additional shallower holes were subsequently drilled and geologically logged (Figure 3.1). Besides augmenting hydrostratigraphical information, the goal of these shallower borings was to obtain cores which were analyzed for nitrate content. The depth of each borehole was limited by the power of the rig. Monitoring wells were installed at the fourteen locations where the water table was reached.

The existing monitoring network as well as every new borehole location were surveyed with a total station (*Sokkia SET 600*) in the standard geographic projection format UTM NAD 83 17N. With this method the accuracy could be improved to a few decimeters in the x-, y-, and z-directions. This procedure assured control over depth during the drilling process, allowed for comparison of stratigraphy with other borehole logs, and proved to be critical to decide at what levels to install piezometers. Additionally, this new universal data format allowed compatibility and exchange of data with the County of Oxford's engineering- and planning departments.

In summer 2005 every well and core location was re-surveyed with centimeter-accurate GPS (Thales Navigation Z-Max RTK). The latter, more accurate survey-data was used for hydraulic head analysis, which requires the greatest accuracy.

3.1.1 Deep Well WO 28-D

Between 09–March–2004 and 20–April–2004 a 71.5m deep hole was drilled along Curry Rd. The drilling method was "straight air rotary"; the rotation was generated by a top-head-60 drive. Pressurized air was used to lift cuttings to ground surface, so that no foreign water was introduced into the subsurface at any time, nor was the formation altered with drilling mud. The air compressor of the rig supplied $\sim$15m^3/min (550 cubic feet per minute (cfm)). A second compressor with $\sim$21m^3/min (750 cfm) (both at $\sim$13kg/cm^2 (180 pounds per square in.)) was used for several tasks: to lift cuttings and water from below $\sim$20mbgs to ground surface in order to meet the target of reaching bedrock; to solve bentonite bridging-problems that occurred below the water table while backfilling the entire zone between screens with bentonite; and to develop the installed wells.

Cuttings were constantly released from the borehole through a discharge tube, and were collected with a catcher on average every 1.5m to 3m or after a material change was observed. They were geologically logged (texture, colour, moisture content as visibly determined) on-site, and were stored in sample bags, for future reference at the University of Waterloo.

The hole was started with a $\sim$25cm (10 in.) diameter three-cone bit, and at a depth of 46mbgs the bit was changed to $\sim$20cm (8 in.) diameter, to decrease the necessary moment to rotate it. The hole was continuously cased with a steel casing, and, on average $\sim$61m (20 ft.) long sections of casing were hammered into the hole, behind the drill-bit, and welded together.

The dimensions of the hole allowed for four Schedule 40 PVC $\sim$5cm (2 in.) ID – diameter piezometers. The deepest piezometer was installed in bedrock, two piezometers were installed in a water bearing sand- and gravel-zone directly above bedrock, and the fourth piezometer in a water bearing zone at $\sim$30mbgs. The screens were $\sim$1.5m (5 ft.) long and had a $\sim$1mm (0.4 in.) screen size. The bottom of the screen was sealed with a cap and placed at the desired depth. Sand was filled into the hole around the screen up to $\sim$0.5m above the top of the screen. The annular space to the bottom of the next screen upwards was sealed with chips of swelling clay (bentonite). The casing was pulled out of the hole as the fill (sand and bentonite) was placed. Table 3.1 lists the screened intervals for the four piezometers that were installed.

3.1.2 Coring and Multilevel Installation

Following the drilling of WO 28-D, nineteen cores were taken with an Envirocore SD-1 rig and a $\sim$6.4cm (2.5 in.) Envirocore core system. Due to the complex geology and a considerable pebble- and gravel content, most of the casing had to be hammered into the subsurface. Rarely, when clay content was sufficient would the vibratory method be used to advance the casing. When the water table was reached, a monitoring well con-

sisting of a ~3cm (1.25 in.) diameter Schedule 40 PVC pipe with a location-dependent screen length (usually ~0.75m (2.5 ft.) long) was installed in the borehole. A sand filter was placed around the screened section, and the remaining annular space filled with bentonite. Construction details are given in the Appendix A.1.

The boreholes were continuously cored in ~80cm (3 ft.) long sections. Each segment was immediately sealed in the clean core liner after being brought to ground surface. Preliminary logging for texture, colour, and dimensions of the material was conducted in the field, and after transport to the Universtiy of Waterloo, were stored upright in a cold-room at 4°C to prevent biological decay of contaminants of concern.

In the laboratory at the University of Waterloo, gravimetric moisture content (ω) was determined on ~5cm long discs of the core. Such sub-samples were extracted from the core every ~30cm, or more frequently if lithology or moisture content visibly changed. These sub-samples were analyzed for bulk soil nitrate concentration at the *Soil and Nutrient Laboratory* at the University of Guelph following the method described in *Tel and Heseltine* (1990). A detailed description of the nitrate analysis in the unsaturated zone below Parcel B is provided in Section 3.8.

<div align="right">

Geophysics | # 3.2

</div>

Geophysical tools were used to gain an improved understanding of the distribution of shallow subsurface lithology than was possible with the point data offered by logged cores. The extent of these shallow deposits was mapped by two geophysical techniques:

1. Resistivity surveys with a Syscal Junior Switch 48 resistivity imaging system from IRIS instruments, and

2. Electromagnetic surveys with a Geonics EM 34 system.

The two methods complement each other and allow surveys of large areas at low cost and in a relatively short amount of time. Electrical resistivity is measured along a plane perpendicular to ground surface, and electromagnetic surveys provide a two-dimensional view parallel to ground surface. The resistivity-surveyed lines and the area of the EM 34 survey are shown on Figure 3.2. The EM 34 measurements are integrated over a certain depth below ground surface. Therefore, the ground surface elevations are important for the interpretation of the results. Resistivity results are corrected for topographic elevation, which was measured along the survey lines with a total station (*Sokkia SET 600*).

Both methods are based on measurements and interpretations of the response from earth materials with different electrical properties. Those measurements are positively correlated to: (1) the moisture content in the material since water is a better conductor than most minerals; moisture content varies over time and is a function of porosity and macropore-distribution; (2) the clay content of the material, since clay minerals allow for conduction of ions on their surface, even at low moisture contents; (3) the ion concentration in the pore water, since more ions allow for more conduction; (4) the passage of electrons, which only applies for metals.

The plotted quantity for both methods is electrical conductivity (σ) in units of siemens per meter [S/m], which quantifies the conductance of a unit volume to current flowing between opposite faces and is the inverse of restivity (ρ). In the following subsections both methods are described in more detail.

3.2.1 Electrical Resistivity Survey

When electrical current is introduced into the ground between a pair of electrodes as part of an electrical resistivity survey, the patterns of subsurface current flow reflect the electrical conductivities of the subsurface (*Kearey and Brooks*, 1991). These patterns can be inferred by measuring the variations in voltage at the surface using another pair of electrodes. For the surveys in this study a dipole-dipole electrode configuration was chosen. In this configuration, the current circuit is completely separated from the voltage circuit and therefore the vulnerability to inductive noise is reduced. Twenty-four electrodes at either side of a programmable control unit were set at a 5m spacing into the ground and individually connected through a multi-core cable. The spacing between the pairs of transmitter- and receiver electrodes and the distance between the center of both pairs were automatically varied for each set of measurements, in order to achieve varying depth penetrations, and to allow the effects of lateral changes in conductivity to be separated from changes with depth (*Milson*, 2003). With the existing layering of the geological material, a maximum penetration depth of about 30m was achieved. The apparent conductivities measured with the different configurations of electrode-geometries as boundary conditions were inversely modelled (*Gan*, 2004) to obtain a depth-profile of electrical conductivity.

Five lines were surveyed. WO 28-D was the starting point for Line 01 and Line 02 since the lithology was well documented at this location (Figure 3.2). Line 01 is perpendicular to the long axis of the drumlin (along Curry Rd). Lines 02 through 05 run along the crest of the drumlin and later follow the bottom of the developing gully (topographic low) that leads then towards the Thornton Welll Field. Due to natural obstructions, and to ensure that each of the individual Lines 2 through 5 was straight, successive lines did not point in the same direction.

3.2.2 Electromagnetic Survey

Electromagnetic surveys involve passing alternating current through a wire loop producing a local magnetic field called the primary field. This primary field produces current flow in the earth, which creates a secondary magnetic field which has a different amplitude and phase. The secondary field induces a current flow in a receiver coil. The characteristics of the secondary field depend on intercoil spacing (s), the operating frequency (f), and the ground conductivity (σ). From the differences between the primary and secondary fields, the distribution of electrical conductivity in the subsurface can be inferred.

Each measurement integrates electrical conductivity over specified depths depending on the mode of use. The horizontal mode creates a horizontal magnetic field, the vertical mode a vertical magnetic field. Intuitively, the horizontal mode integrates over shallower depths. Details about the depth penetration for each mode of use are presented in Appendix A.4. The area of the EM34 survey, as marked on Figure 3.2 was chosen to cover the zone where low permeable features of the shallow subsurface were anticipated to intercept ground surface.

Groundwater Monitoring | # 3.3

In all observation wells (existing and new, see Figure 3.3) associated with the monitoring network, hydraulic head and chemical composition of groundwater were measured. Details of the field protocols are contained below.

3.3.1 Hydraulic Head

Hydraulic head conditions and their change over time are the driving force for groundwater flow. Mapping hydraulic head within a hydrostratigraphic zone allows the determination of groundwater flow direction and magnitude; and mapping vertical hydraulic head profiles at multilevel observation locations gives an indication of vertical flow direction and magnitude, as well as information about the spatial extent of hydrostratigraphic units. Water levels in observation wells were taken throughout the period of this study in a network of 100 monitoring piezometers at 30 locations with a water level tape. One full set of hydraulic head observations was taken within two weeks at the end of October 2003. Additionally water level measurements were taken at different times in various sections of the well network during the course of fieldwork.

To investigate the vertical hydraulic connection between the different hydrostrati-graphic units within the groundwater flow system, the hydraulic response to recharge events was monitored with pressure transducers (*Solinst Levellogger 3001*) placed in piezometers at various spatial locations within the study area. During the spring-melt in 2004 data were collected from WO 12 and WO 11 at two different depths at each location. In Fall 2004 additional pressure transducers (*Solinst Levellogger 3001*) were installed in WO 40, WO 28-D, and WO 02-D to record pressure and temperature measurements during winter and spring 2005 over a larger area. The pressure-transducers were attached to a $\sim$3mm (1/8 in.) airline cable, and lowered down a known length into the well, below the average water table. For long-term observations one measurement was recorded every 2 hours and the memory of the logger was large enough to enable a download interval of a few months. In addition to the hydraulic head data, the transducer devices contain thermistors to record water temperature, which was used as a complimentary tracer.

3.3.2 Ion Samples

Groundwater was sampled several times to determine the water quality upgradient of the Thornton Well Field, and to provide snapshots of water quality to monitor changes in the degree and extent of contamination. In October 2003, water samples from all existing observation wells were obtained and analyzed. Whenever a new well was installed, water was sampled at that location and a smaller, strategically chosen set of wells were sampled more frequently during the study. During spring 2005, another comprehensive set of samples was taken by Loren Bekeris. Duplicates were taken on average every 20 samples.

Prior to taking a sample, three well volumes were purged, either with a peristaltic pump (*Geo Scientific Ltd. "Portable Peristaltic Sampling Pump"*), or, if the diameter of the piezometer and the water table depth permitted, with a gas-powered suction pump (*Honda WH15X*). After purging, a peristaltic pump was used to take the sample, which was then passed through a 0.45μm filter (*Pall corporation Supor-450 membrane filter*). The filtrate was collected in 250mL HDPE sample bottles provided by the commercial lab that did the analysis (*Maxxam Analytics, Mississauga*), cooled below 4°C to prevent any biological activity in case microbes passed through the filter, and sent to the lab for analysis within 24 hours of sampling. Water samples for metal analysis were acidified with 25mL nitric acid to keep the metal ions in solution.

3.3.3 Isotope Samples

Water samples were obtained for isotopic analysis including ^3H (tritium), ^2H (deuterium), and ^{18}O (oxygen-18). The amount of tritium in a sample provides information on when the water infiltrated into the aquifer system. The composition of Deuterium

and Oxygen-18 isotopes in the sample is a tag of the water molecule. By plotting Deuterium vs. Oxygen-18 content of samples, waters of similar composition can be traced. Tritium samples were taken in all piezometers in the WO 28-D cluster and in a surface water pond close to supply Well 01, whose water level has been shown to respond rapidly to pumping at Well 01 (*Lotowater*, 2002). Deuterium and Oxygen-18 samples were taken in all multilevel wells from WO 11, WO 2-D, WO 28-D, from all supply wells in the Thornton Well Field, and from the pond. Samples from WO 28-D were collected with a submersible Grundfos Rediflo 2 pump, samples from other observation wells were collected with a peristaltic pump (*Geo Scientific Ltd. "Portable Peristaltic Sampling Pump"*), samples from the supply wells were taken from taps inside the pump houses, and the pond sample was taken with a plastic bottle from its center. Samples were taken in 1L HDPE bottles and were analyzed at the *Environmental Isotope Laboratory* at the University of Waterloo.

<div align="right">

Meteorological Data | # 3.4

</div>

Between April and November 2004 precipitation was measured at three locations across the study site (Figure 3.1)with tipping buckets (*Aerodynamic Raingauge ARG100 from Environmental Measurements Limited*): (1) on top of the pumphouse of Well 01, (2) on a hill (about 200m) south of WO 28-D, and (3) on the corner fence post next to one tile outflow location. Each tip in each tipping bucket was digitally recorded (*Chart Pac CP-X from Lakewood Systems*) and corresponds to a rain gauge-specific amount of precipitation. The tipping buckets were installed free of tree or other cover. Plots of measured rainfall are shown in Appendix A.10. Starting in December 2004 a complete meteorological station was available on site that supplies precipitation and air temperature (Appendix A.10), data amongst other measurements, from a location in the center of the study site as marked on Figure 3.1. For long term meteorological data, the records from the Ministry of Environment Canada were evaluated (*Environment Canada*, 2002).

<div align="right">

Profiling Mass Loading into Supply Well 01 | # 3.5

</div>

This portion of the field investigation focusses on quantifying the nitrate mass loading along the screen length of supply Well 01. This information could potentially provide insight into sections of the well screen which contribute high nitrate mass flux to the extraction wells and thus indicate important hydrostratigraphic zones. Well 01 was

selected to be logged for incoming nitrate mass in detailed discrete intervals along its screen since it was the first to show an increase of nitrate concentration above MAC; the bottom of its screen is close to bedrock, so any influence of mixing waters from different hydrogeologic units might be detectable; and it was relatively easily accessible. The latter criterion was important, because in order to complete the profiling the complete pump setup (motor, ~40cm (16 in.) diameter, 20m-long connection piping, and the five-bowl submersed pump with a design flow rate of ~4.5m^3/min) had to be removed (Appendix A.6). This operation was possible because the profiling was managed to be at a time when the pump was scheduled for regular maintenance.

Flow was measured in ~3cm (0.1 ft.) intervals with the help of an impeller-type flow tool (Appendix A.6), that measured up-hole velocity inside the screen. Above the screen, the counts per second of the flow tool's impeller were calibrated to the pumping rate of the well. Concentration was measured in ~30cm (1 ft.) intervals with a submersible sample pump (*Grundfos Rediflow 1*). Flow rate along the well screen was back-calculated from differences in the total flow rate in the well for each interval using a mass-balance approach. Combined with concentration data, the mass-balance approach was extended to determine incoming mass loading into the screen per sample interval. The calculations and approach are explained in detail in Appendix A.6.

In addition to the flow tool and the sample pump, a downhole camera was inserted into the screen, in order to obtain visual control. Above those three tools, at about ~12mbgs, a safe distance above the screen and below the expected maximum drawdown of the well, another submersible pump was lowered into the well. (Appendix A.6). This pump was used to put the system under different pumping stresses, during which the mass-loading into the screen was determined. Three profiles, each representing a different stress, were logged (detailed timeline on Figure A.8). During Profile 1 the pumping rate was 3m^3/min. Measurements were taken about 1h after pumping started from natural conditions. The pumping rate during measured Profiles 2 and 3 was 4.5m^3/min. Profile 2 was measured at approximately 4h, Profile 3 at approximately 14h after pumping started. At a pumping rate <2.5m^3/min the detection sensitivity of flow tool was exceeded and therefore, a flow profile during flowing artesian conditions could not be taken.

Tile Drains | # 3.6

In a tile drain network, perforated pipes are buried a few feet into the ground to collect infiltrating water. Not all the recharge is collected, as some infiltrates between pipes deeper into the subsurface. The collected water is typically transported to larger pipes and eventually discharged to surface water systems. Drained areas and location of

outlets were compiled through various discussions with farmers and various investigations on-site. These drained areas are shown on Figure 3.4; the coloured dots on this figure indicate the location of a tile drain outlet and the corresponding drained areas are shaded in the same colour. For field 01 and field 02 (Figure 2.14) tile line construction records exist. The areas that are being drained by the tile drain TD at WO40 and TD N Parcel A were estimated.

During Spring 2004 nitrate concentrations were determined sporadically in some of the tile outlets. Samples were collected by letting the tile outlet flow into a sample bottle. This raw water was then filtered through a 45μm filter (*Pall corporation Supor-450 membrane filter*) and submitted to *Maxxam Analytics, Mississauga* for analysis.

The manhole "TD top of gully" was replaced in April 2004 by a new manhole at the boundary between Parcel A and Parcel B ("TD N Parcel A"). This manhole gives access to a major tile line, whose outlet at the south-western boundary of the well field was equipped with a weir box, instrumented in Summer 2004 to measure and record the flow rate at this location. This tile line was considered to be worth for monitoring, since it drains some of the area where the land-use changes were applied and the ∼20cm (8 in.) diameter is indicative of a major tile line. A cover was installed to prevent it from filling with snow and freezing and to enable flow and concentration measurements during spring melt 2005. This weir box allows quantification of flow rates from the tile drains. Together with concentration measurements, determination of the mass loading from this tile line is possible. The water depth was calibrated to flow rate before the weir was installed, was measured with a float in the weir box, and was recorded (*Chart Pac CP-X, Lakewood Systems*). Water samples were collected with a programmable automatic sampler (*ISCO Sampler 6712*) whose intake was directly below the outlet of the tile line (Figure 3.5). The outlet of the weir box was connected to pipeline whose outlet was directed into an existing drainage ditch. Before the weir box was installed, flow events were observed.

Hydrogeologic Database and Spatial Analysis Tools | 3.7

One of the goals of the overall research project at the Thornton Well Field, of which this thesis is a part, is to further characterize the hydrogeologic system in the area in order to better understand the mechanisms controlling nitrate concentrations in the supply wells.

An important part of the hydrogeologic system is the spatial distribution of hydrogeologic layers. The complex geology in the interlobate zone with discontinuous and vertically inter-connected layers makes a fully three-dimensional approach to data-analysis

necessary (*Frind et al.*, 2002). The current analysis of the hydrogeologic system extends farther areally than previous work, is fully three-dimensional, includes new understanding of the hydrostratigraphy, is visually comprehensible, and is able to incorporate changes in the future, and to export the digital data to other applications.

This section describes how hydrogeologic data was managed to setup the hydrogeologic layers, as well as how data analysis tools were used to determine pressure conditions in aquifers, and to model the boundaries of surface sub-watersheds within the study site.

3.7.1   Hydrogeologic System Database

As of 31-August 2004, 4552 individual aqueous chemistry samples, 1274 individual hydraulic head measurements (not including records from pressure transducers), and 280 samples in the unsaturated zone analyzed for water content and soil bulk nitrate concentration were available. All of this data is related to a location in a piezometer or a core. Managing this amount of data efficiently (every piece of information only stored once), is possible only in a relational database. Table 3.2 lists in detail what information was stored in the developed database ("CPH database"), which includes data as early as 1997, collected by *Padusenko* (2001). The County of Oxford had additional data available, including borehole logs for the supply wells and their monitoring network, pumping rates for the supply wells, water-level measurements of their monitoring network, and nitrate concentration measurements of the supply wells, which were included into the database.

3.7.2   Setup of Hydrogeological Layers

With the CPH database, including some VBA/SQL scripts, hydrogeologic analysis was possible: hydrographs in piezometers, time series of contaminant concentrations in piezometers and their statistical description, vertical profiles of hydraulic head and contaminant concentrations in the saturated- and unsaturated zones were created.

Some of the contents of the CPH database (geologic-, hydraulic head-, and contaminant concentration- data) were connected to a visualization and analysis software (*Kassenaar*, 2004), which was used as the tool to setup hydrogeologic layers in three dimensions. The area of analysis was extended to the Thames river, a medium-regional scale, and therefore 867 additional borehole logs from the Ontario Ministry of the Environment (MOE) borehole database (*Ontario Ministry of the Environment*, 2000) were linked to viewlog. These borehole logs contain basic lithologic information, construction details including screen locations, and depth to water measurements. Since the MOE database was already in MS-Access format, and since that format is the easiest to link with viewlog, the CPH database was created in the same format (*Microsoft*, 2002).

The setup of the hydrogeologic layers was a multi-step task, and is similar to the approach used by *Radcliffe* (2000):

1. All boreholes from the UW and the MOE databases can be shown on plan view and on cross sections. The course of a cross section can be user-defined, and an infinite number of cross sections can be created;

2. On each cross section, five columns are shown for each borehole: one for the three most common material textures, one for the location of the screen, and one for the water table elevation. If required, contaminant concentration data can be shown as well. The colour coding of the textures follows the proposition by *Radcliffe* (2000);

3. Some of the Well Records of the MOE database contained no logs, or very poor logs (only one material logged for the entire well), which were discarded from the analysis;

4. The ground surface elevation coordinates of the wells were corrected by assigning the elevation from the DEM to that location;

5. Depths to the interfaces of hydrostratigraphic layers were "picked" by hand on borehole logs on cross sections and those points was written into a separate table in the database. About 500 such picks were made;

6. The subset of points that represents one surface were interpolated in two dimensions onto a 10m by 10m grid, a three dimensional representation of the surface of each hydrostratigraphic unit. Different interpolation schemes were used: Triangulation, Inverse Distance, and Simple- and Ordinary Kriging. Kriging methods allow for the expression of a prediction error of the interpolated surface. The realization with the smallest root mean square error can be taken as the "best" interpolation;

7. After the grids of hydrostratigraphic layer interfaces were created, the surfaces of the hydrostratigraphic layers that intersected a cross section were drawn as lines on that cross section. If interpolation schemes led to non-realistic results, additional data points were manually inserted ("soft" data points) to assure a realistic representation.

3.7.3 GIS Analysis

Brimbicombe (2003) defines what a Geographic Information System (GIS) is:

"A GIS is a system for managing spatial data and associated attributes. In the strictest sense, it is a computer system capable of integrating, storing, editing, analyzing, and displaying geographically-referenced information.

In a more generic sense, GIS is a 'smart map' tool that allows users to create interactive queries (user created searches), analyze the spatial information, and edit data."

The data storage in this study was handled by the CPH database. One major part of data analysis was done in viewlog. Additionally, "ArcGIS", (*Environmental Systems Research Institute*, 2002)) with its extension-packages "Geostatistical Analyst" and "Spatial Analyst" was used to draw maps, to interpolate spatial data, and to determine the nitrate mass stored in the unsaturated zone below the farmland in Parcel B (Figure 2.14). All these functions are explained throughout this thesis where necessary. One additional feature of GIS analysis used in this study, the determination of surface (sub-)watersheds is explained here.

The area within which all surface water eventually reaches the same point, is defined as a sub-watershed. All sub-watersheds that feed into a major drainage feature (river) form the watershed of that river (*Dingman*, 2002). The boundaries of surface watersheds are important for hydrogeological understanding, because they typically form for the uppermost layers a no-flow boundaries, and they represent a physical boundary of the area of interest; that is, they form the spatial domain.

As described in Section 2.1, the study site is partly located in a sub-watershed that feeds directly into the Thames River, and partly in a sub-watershed that feeds into Cedar Creek, which flows into the Thames River. Sub-watersheds were determined with the "Hydro Tools" extension for Arc GIS (*Environmental Systems Research Institute*, 2004). For each cell of the DEM the direction of the steepest path is calculated. Then the number of cells that are directly connected "upstream" to a cell are calculated. The user can decide what number should be used as the threshold for cells to be disregarded in order to decide which cell contains a stream. Then, each stream is segmented between junctions, and based on the steepest path decided which cells drain into each stream segment. The polygon that encompasses all cells that drain into a segment is the sub-watershed boundary of that stream segment.

Nitrate Mass in the Unsaturated Zone | # 3.8

Another critical characteristic required to estimate the impact of land-use changes on the nitrate concentrations in the extracted water at the Thornton Well Field is the mass of nitrate stored in the subsurface system before those changes were made. This mass in the unsaturated zone represents the legacy of multiple years of fertilizer application. Its migration behaviour through the unsaturated zone and into the production aquifers

will significantly impact the magnitude and timing of any potential changes in water quality in the Thornton wells.

To estimate the mass stored in the unsaturated zone, soil cores were extracted below the root zone at 19 locations across the fields (Parcel B) where land-use is to be changed (Figure 3.1). Representative locations were selected based on the presence or absence of the shallow aquitard, electrical resistivity and electromagnetic survey data, analytical soil data, transient hydraulic response data, anecdotal evidence from local farmers, and to obtain a good coverage of the whole Parcel B. Due to variations in subsurface geology, surface topography, and nutrient loading, the vertical profiles of stored nitrate in the unsaturated zone were expected to be highly variable. Because these core data represent a "snap shot" of the near surface nitrate concentration profiles, supplementary soil cores will be extracted in proximity to previous core locations to observe the change in land-use practices on the near surface nitrate distribution below the root zone over time.

A spatial interpolation process was employed to estimate the total nitrate mass stored in the unsaturated zone based on the data derived from the soil samples. With basic assumptions for recharge an average leaching rate of nitrate from that parcel can be estimated. These leaching rates were used to estimate the maximum time of how long it would take to flush the nitrate contamination out of the subsurface below Parcel B. Furthermore, assuming it would be possible to reduce the nitrate leaching below the root zone to zero, resulted in a best-case-scenario for the reduction of nitrate concentrations at the Thornton Supply Wells was estimated. Details of the various calculation steps are described in Section 4.8 along with results and discussion.

Table 3.1:
Overview of piezeometers installed at WO 28-D.

Name	Screen Bottom	Screen Top
	[mgbs.]	
WO 28-D-1	71.1	69.5
WO 28-D-2	66.3	65.6
WO 28-D-3	62.7	61.9
WO 28-D-4	33.6	32.0

Table 3.2:
Data in the hydrogeologic database.

Details of boreholes
   location, depth, driller, date drilled;

Construction details of wells
   screen top- and screen bottom- elevations, screen diameter, screen slot size, stick-up;

Geologic information of cores taken
   the three most common materials per lithologic section and its description, such as
   colour and other properties as visibly detected;

Hydraulic head measurements in piezometers
   depth to water from measurement point, date;

Results of analyzed water samples
   chemical parameter, date sampled, value, from which observation well;

Results of unsaturated zone analysis
   from what core and what depth the sample was taken, gravimetric moisture
   content, soil bulk nitrate concentration;
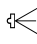
Tile drains
   location, aqueous chemistry results;
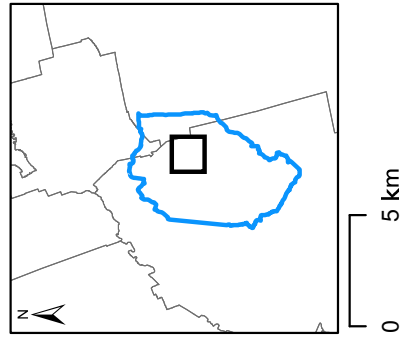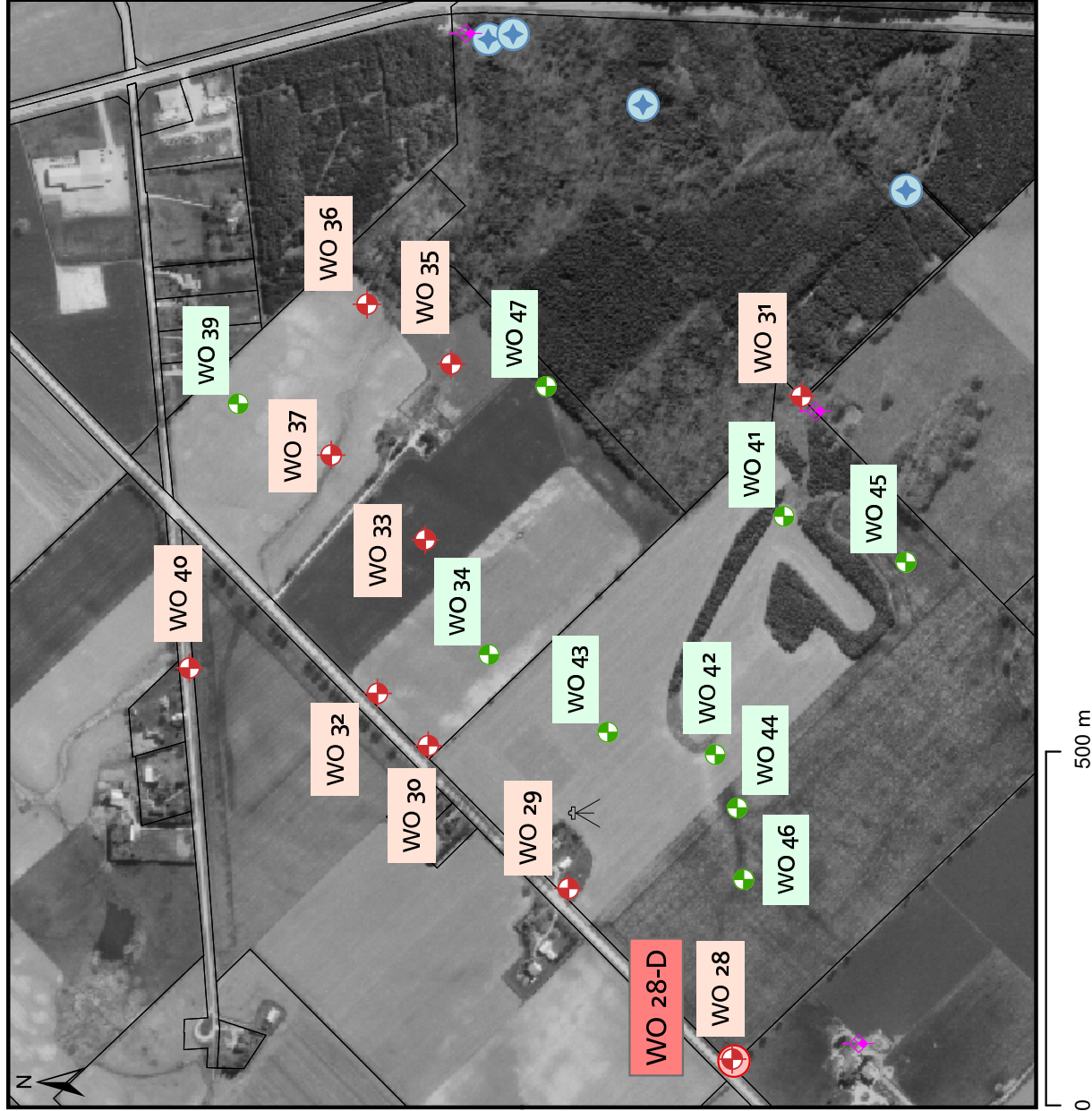
Figure 3.1:
New Core- and Well-Locations. At all locations except WO 28-D cores were taken and analyzed for gravimetric moisture content and bulk soil nitrate concentration. If the watertable was reached, a well was installed. The figure also shows the locations of the rain gauges and the meteorological station installed on site.

Geophysical Surveys

Legend:
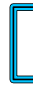
Shallow Core Location

⊙ Observation Well

Area of EM Survey

Resistivity survey lines

Topographic Elevation
— contours in 5m intervals
[masl.]
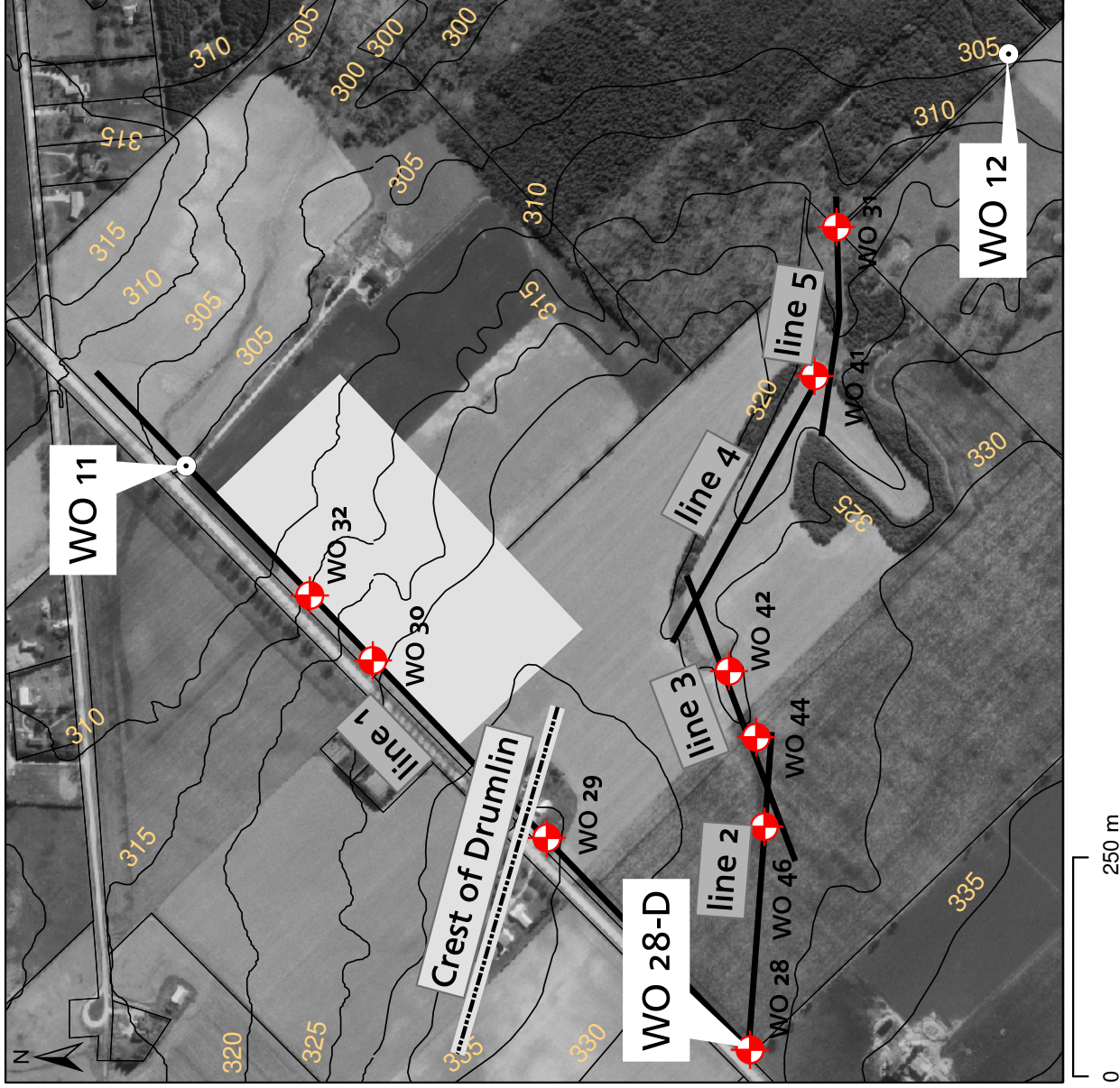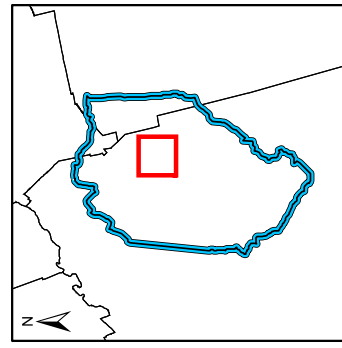
Figure 3.2:
Plan view of the locations of geophysical investigation. The thick black lines indicate the lines of resistivity surveys (line 1 through 5). The contours are topographic elevation isolines (contour interval is 5m). For orientation purposes three observation wells are shown.

48
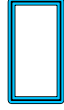
Figure 3.3:
Plan view of the locations of all observation wells.

49

Tile Drains

Thornton Supply Wells

- Thornton Well Field
- Parcel B
- Parcel A
- Study site

Labels on map:
- TD at WO 4o
- TD Weir Box
- TD SW Field o2
- TD Forrest Field o1
- TD SW Field o1
- TD top of gully
- TD N Parcel A

8 km

1,000 m
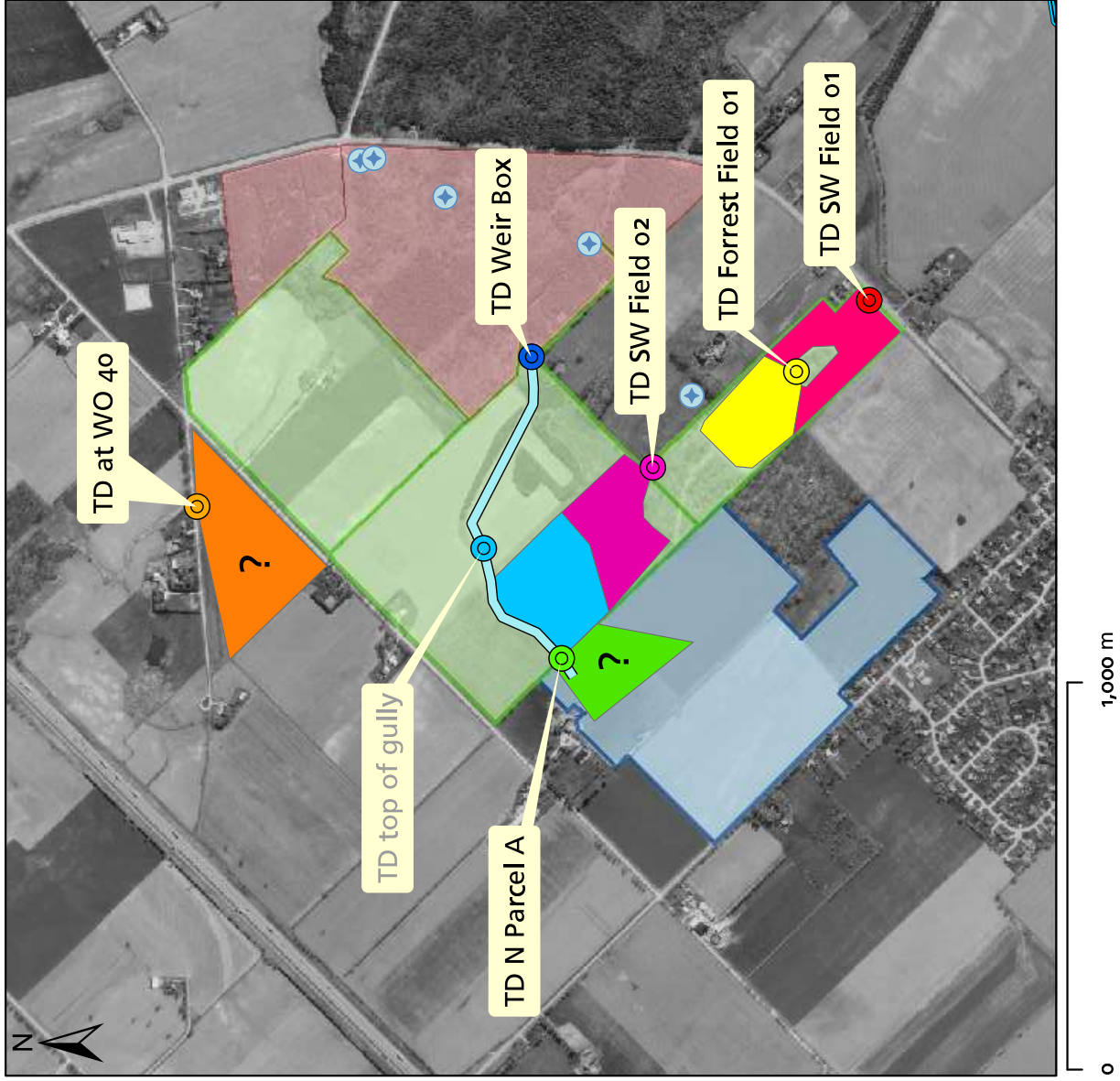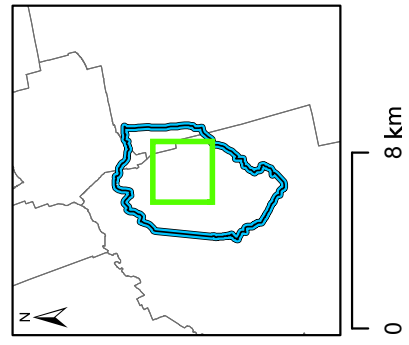
Figure 3.4:
Tile Drains and draining areas. Tile drain outlets are indicated by a circle. The drained areas are shaded in the corresponding colour.

Figure 3.5:
The Weir Box during snow melt at 30-March-2005. The white perforated pipe on the right serves as a stilling well for a float connected to a potentiometer. In the white box is a data-logger that records the output voltage of the potentiometer. This output voltage is calibrated to water hight in the weir box. The outfall plate is a $90°$ V-notch, so that the flow rate can be calculated with a standard formula. The white hose has an intake at the outlet of the tile and is connected to an automated sampling device.

4

Results

This chapter is divided into a series of sections focussed on the results of various field activities undertaken as part of the overall investigations within the study site. The hydrostratigraphic sequence is explained first through a discussion of the detailed borehole logging conducted during drilling of the deep piezometer nest at WO 28-D. Then each data set is discussed separately:

- interpretation of regional hydraulic head data;
- geophysical surveys;
- transient, local hydraulic head measurements;
- aqueous geochemistry- (including isotopes) analysis;
- depth-discrete nitrate loading profiling along the screen of Well 01; and
- quantification of nitrate loading from tile drains in the farm fields.

All results are integrated into the hydrostratigraphic model in Chapter 5

The last section in this chapter, Section 4.7, quantifies the mass of nitrate stored in the vadose zone below Parcel B and provides a prediction of the effects and implications that the in the unsaturated zone stored nitrate mass has in the long-term on the concentrations of the supply wells of the Thornton Well Field in light of land-use changes.

Deep Multilevel Well WO 28-D | 4.1

The dimensions and construction details of the monitoring well cluster WO 28-D, average hydraulic head data and the hydrostratigraphic sequence obtained from the geologically logged drill-cuttings are shown on Figure 4.1. To avoid confusion related to naming of the various water bearing zones indicated, a numerical sequence was assigned, generally based on the order of encounter in this deep borehole (note that

Aquitard 1, which was not encountered at WO 28-D, but defined elsewhere in the study area as explained later). This naming convention will be used in the remainder of the thesis.

The deepest piezometer, WO 28-D-1, was installed 3m into bedrock (Aquifer 5) at a depth of 72mbgs, two piezometers were placed in a lower highly-productive aquifer (Aquifer 4) just above bedrock at ~67mbgs, and the fourth piezometer was installed in an upper aquifer (Aquifer 3) at a depth of 30mbgs. Bedrock at the location of WO 28-D was identified to be limestone and, despite the grinding process of the drill, numerous fossils were encountered. Limestone and fossils are two characteristic parameters for the Detroit River Formation (*Cowan*, 1975), the uppermost bedrock formation in the study area, therefore it can be assumed that bedrock at the location of WO 28-D is a member of the Detroit River Formation. Drilling through the top zone of bedrock, according to the contracted driller International Water Supply (IWS), the rig showed typical behaviour for drilling through a fractured zone (hard, dry and sharp-edged, pebble sized cuttings from the process of grinding with the three-cone bit through limestone and immediate producing of water as soon as a fracture was intercepted). Such a fractured zone is where WO 28-D-1 was installed.

The drilling of this deep borehole and data from the installed piezometers produced two key pieces of information. The first key piece of information is the documented presence of Aquifer 4 at this location, which had previously been conceptualized as a local unit in vicinity to Well 01/Well 05 (Section 2.4.1). Based on bore-log analysis at a larger scale (see Chapter 5 for details), it can be concluded that this deep aquifer (Aquifer 4) is more laterally extensive than was previously thought. IWS estimated a maximum possible pumping rate of Aquifer 4 between $1m^3$/min and $1.8m^3$/min at this location. Comparing WO 28-D with the logs of the two deepest supply wells of the Thornton Well Field (Well 01 and Well 05), three hydrogeologic parameters correspond well and support the argument of an areally extensive Aquifer 4: (1) the geodetic elevation of the water bearing zones; (2) the elevation of pressure heads; (3) the material-texture as described in borehole logs. There is a ~30m drop in ground surface elevation between WO 28-D and Well 01 and Well 05, which may be one contributing factor for Well 01 and Well 05 being flowing artesian wells under natural conditions. It was not possible during this study to prove a hydraulic connection between WO 28-D-1 and Well 01 and Well 05; however, based on field data, there is no indication that a hydraulic connection does not exist.

The second key piece of information relates to the shallow groundwater flow system. The hydraulic head data (indicated on Figure 4.1) from WO 28, a piezometer installed in this shallow unit next to WO 28-D), suggest the presence of occasionally perched conditions in this shallow unit (Aquifer 1). Aquitard 2, which underlies Aquifer 1 was extremely hard to drill through at WO 28-D with the air rotary drilling method, appeared to be cemented, and its cuttings were dry and consisted of the whole spectrum of grain sizes. At places where samples of that Aquitard 2 were obtained in a core (e.g., WO 41, Figure 3.1), the clay content was determined to be ~10% by combined standard hydrometer and sieve analysis, and the matrix was found to be cemented

and therefore of decreased hydraulic permeability. These characteristics suggest that Aquitard 2 may prevent, inhibit, and/or re-distributes recharge and infiltrating nitrate mass to Aquifer 2. This finding evoked more detailed characterization effort, as discussed below.

Aquifer 3 and Aquifer 4 were found to be confined based on the static hydraulic heads (Figure 4.1). The zones directly below Aquifer 3 and above Aquifer 4 were clearly identified as aquitards; however, the drill-cuttings from an approximately 10m thick zone between 270masl and 280masl seemed to consist of dry sand. It would be very surprising if any material from this ~55m deep zone, especially aquifer-material, under the encountered hydraulic head conditions would not be saturated. Even if this sand unit was separated completely by aquitard material from other aquifers, it would be anticipated, that over time, it would have reached saturation. It could be possible that there is water in the sand, possibly as high as saturation, and that this water is held in the pores by negative pressure. One other explanation for the dry material could be the drilling method, because the cuttings are exposed to a drying airstream that pushes them from depth to ground surface. Especially if the material was cemented, implying small pore openings and low porosity, it could be possible that it was dried by the air stream after it was ground up by the drill bit, even if it was saturated, because there would be comparatively little water in the porous material. Against the drying air stream hypothesis is the observation of wet cuttings of other aquifer material, and various materials with different degrees of moisture content. In either case, this sand unit is over- and underlain by aquitard-material, and for the purpose of site conceptualization it was decided to treat the zone below Aquifer 3 and above Aquifer 4 as one low hydraulic conductivity unit (Aquitard 4). Due to the lack of hydraulic- and chemical data at WO 28-D, detailed borehole logs at that depth, and hydraulic- and chemical data at other locations, it is not possible to evaluate if another aquifer unit exists between Aquifer 3 and Aquifer 4, which might be nitrate contaminated and contribute to elevated nitrate concentrations in the supply wells of the Thornton Well Field.

In Aquifer 3 at WO 28-D nitrate concentrations of ~9mg-N/L were measured between June 2004 and August 2005. Considering the presence of the shallow Aquitard 2, the unsaturated conditions within Aquifer 2, and the presence of Aquitard 3, it is likely that the elevated nitrate levels observed in Aquifer 3 at this location are due to land-use activities outside and up-gradient of the parcel of land owned by the County of Oxford. This regional inflow of nitrate mass may be contributing to the high nitrate concentrations observed in the Thornton wells. The deep aquifer (Aquifer 4) however, never showed signs of elevated nitrate during this study, supporting the conclusion that the two aquifers are hydraulically isolated from each other in this area and that nitrate mass moving into the capture zone of the wells is predominantly located in the shallower units.

This section discusses the regional hydraulic head conditions in Aquifer 3 ("Shallow Aquifer"), Aquifer 4 ("Deep Aquifer"), and Aquifer 5 (bedrock) (Figure 4.1) based on available well records and piezometric data. These are the three main aquifers encountered within the study site. The potentiometric surface for each aquifer is shown on Figure 4.2, the vertical hydraulic pressure conditions on Figure 4.3.

The flow direction in Aquifer 3 is from south-west to north-east with an average horizontal hydraulic gradient of $\sim$0.005. As visible on Figure 4.2 (a), water flows towards Sweaburg Swamp and Cedar Creek directly to the east of the Thornton Supply Wells. The Thames River, depicted in the north-west of each panel, cuts into bedrock which is separated by Aquitard 4 from Aquifer 3, and therefore does not seem to influence the hydraulic conditions in Aquifer 3 significantly. Static potentiometric surfaces derived from static hydraulic head data in the MOE database are average surfaces because the static waterlevel at every data point was measured at a different time (at the time the well was installed). Nevertheless, the effects of pumping of the supply wells of the Thornton Well Field are clearly visible with significantly decreasing hydraulic heads around and up-gradient of the well field. A similar, but smaller, zone of influence is visible for the Tabor Well Field.

The general flow direction in Aquifer 4 and Aquifer 5 (Bedrock) is from south-east to north-west, towards the Thames River, the biggest drainage feature in the area. The potentiometric surface in the bedrock aquifer indicates an area of high hydraulic head in the center of the study site, with flow diverging in western, northern, and eastern directions. The average horizontal hydraulic gradient in Aquifer 4 is 0.002 and the average horizontal hydraulic gradient in Aquifer 5 is 0.0008. The observation of smaller horizontal gradients in deeper units than in shallower units was expected. The interpolation of the potentiometric surface of Aquifer 4 leaves room for speculation if the pumping of the Thornton Well Field might effect the potentiometric surface in Aquifer 4. The decreasing hydraulic head values in the north of the Thornton Well Field on Figure 4.2 (b) might be attributable to the supply wells within the Thornton Well Field. No influence of pumping originating in the Thornton Well Field area is detectable in Aquifer 5 (Figure 4.2 (c)).

The significantly different direction of the regional flow field in Aquifer 3 is likely due to the combined pumping effect of the Thornton and Tabor Well Fields, isolation from the influence of the Thames River, and the drainage effects of Cedar Creek / Sweaburg Swamp, which has minimal influence on the deeper units.

Regional differences in hydraulic head between Aquifers 3, 4, and 5 are illustrated on Figure 4.3. Significant upward vertical gradients were observed to the north of the Thornton Well Field. If Well 01 and Well 05 are not pumped, they are under flowing artesian conditions. This upward (negative) hydraulic gradient between Aquifer 4 and Aquifer 3 is existent in the proximity, down-gradient of the Thornton Well Field as shown on Figure 4.3. This Figure includes averaged long-time data under pumping conditions, leading to downward gradients in the zone of influence of the Thornton Well Field. Throughout the rest of the study site, flow appears to move downward from Aquifer 3 into Aquifer 4. In general, the difference in hydraulic head between these two aquifer units is higher than that observed between Aquifers 4 and 5, mainly because of the much larger vertical separation between the two shallower units. In the north-west of the study site, the flow direction is pointing from Aquifer 5 into Aquifer 4 which at that location might indicate that flow is into the Thames river, whose bed is located in the very northern edge of the study site.

Geophysics $\Big|$ # 4.3

4.3.1 Resistivity Surveys

Geophysical tools were primarily used to investigate the continuity of Aquitard 2 throughout Parcel B. As suggested in Section 4.1, Aquitard 2 is believed to play a critical role in controlling the pathway of infiltrating nitrate mass in the vicinity of the Thornton Well Field. The general results are initially presented and dicussed followed by a detailed discussion of the results of each survey line. For ease of understanding, the inverse of electrical resistivity, electrical conductivity, will be used here. The profiles of the five electrical resistivity survey lines are shown on Figure 4.4 as five 2D Finite Element rectangles. The profile below each survey line is shown individually, with locations and logs of cores in Appendix A.3.

Assuming a constant pore water ion concentration across the study site, high clay content and high moisture content are the two most significant contributing factors for high electrical conductivities. However it is not possible to tell which one is the major contributing factor unless the actual material properties were calibrated against "hard" data from borehole-logs (as shown in Appendix A.3).

The primary goal of these surveys was to map the extent of the shallow aquitard (Aquitard 2), which was known to exist at WO 28-D, the location at the very southeastern end of Figure 4.4. The areal extent of that aquitard, based on geophysical surveys, logged cores, and interviews with local farmers is shown on Figure 4.5. This aquitard appears to sit on top of the drumlin (see the drumlin's crest on Figure 3.2) like

a cap. When the ground surface declines below about ~325masl, Aquitard 2 becomes discontinuous as indicated on Line 01 and Line 02.

Across the study site, two different materials were found above Aquitard 2: cohesive, moist, organic-rich clay (Aquitard 1) or sand (Aquifer 1). Either unit is suspected to show elevated moisture content, since Aquitard 2 acts as a barrier for infiltrating water and Aquifer 1 is at least occasionally perched. Surficial zones of high electrical conductivity in the geophysical surveys represent moist and/or clayey material (Aquitard 1). This clayey material does not exist everywhere. On Line 01, for example, the area around the topographic high point (the ridge of a drumlin), and the area close to the north-eastern end of that survey line around WO 11 show only medium electrical conductivities, corresponding to surficial sands (Aquifer 1). Recharge to the deeper system can preferentially occur at locations where the following two criteria are met: (1) Aquifer 1 is found at ground surface, which is permeable for infiltrating water (sandy), and (2) below those deposits Aquitard 2 does not exist. These conditions exist in the area around WO 11 and around WO 44.

Due to the geometric configuration of the geologic layers, shielding effects of Aquitard 1 and/or Aquitard 2 decrease the informational value derived from the geophysical data about texture and moisture conditions below Aquitard 2. The anomaly below the highest point on Line 01 can be attributed to construction elements of a nearby house. The anomaly at ~235m along Line 05 may be the result of a nearby fence post or a metal tile line outlet. At both those locations cores were taken (WO 29 and WO 47) and Aquitard 2 was encountered.

The results of each resistivity line are discussed separately below (see Figures A.1, A.2, A.3, A.4, and A.5). Line 01 starts at WO 28-D, and was oriented parallel to Curry Rd., crossing a drumlin from south-west to north-east towards a valley around WO 11. Line 02 starts at WO 28-D as well, but takes an easterly course, as do Lines 03, 04, and 05, and follows the steepest gradient in topographic elevation along the topographic low towards the Thornton Well Field (Figure 3.2).

Line 01: At the origin of Line 01 in the south-west, it was known that Aquitard 2 consisting of materials of various grain sizes exists. Above Aquitard 2 partially saturated sand (Aquifer 1) was encountered, while below Aquitard 2 at this location unsaturated Aquifer 2 was encountered. This contrast was thought to be the reason for the relatively sharp contrast in electrical conductivity. The ~30m thick unsaturated sand below Aquitard 2 is marked by medium to low electrical conductivities. Aquitard 2 was found in cores at WO 28-D, WO 29, and was only a few centimeters thick at WO 30. It was possible to drill through Aquitard 2 at WO 30 below which the same sand material was encountered as at WO 28-D below Aquitard 2. The elevation of WO 30 is halfway between the bottom of the valley around WO 11 and the top of the drumlin at WO 29 and coincides with the elevation at which local farmers reported springs forming in their fields. Water moving by gravity in Aquifer 1 across the top of Aquitard 2 until this low permeable layer intercepts ground surface may be a possible explanation for these

springs.

WO 11 is located roughly at the lowest point along this profile, and its top four ports are screened in the glaciofluvial outwash channel described in Section 2.2.2. At WO 11 this channel is part of Aquifer 2 and is at this location a saturated, well yielding, sand- and gravel- aquifer that results in medium to high electrical conductivities. At ~970m along Line 01 this aquifer seems to connect to ground surface.

The borehole log of WO 11 indicates a clay layer below Aquifer 2. This clay has a high electrical conductivity, similar to the clay just below ground surface. One explanation of the geology below the bottom of the valley is that the clay in the bottom of the valley is part of the older sediments that were partially replaced by the hydraulically conductive materials of the glaciofluvial outwash channel. The deepest piezometer at WO 11 is situated in a gravel zone that seems to be encompassed by clay as indicated by the high electrical conductivities. The resistivity survey picks up the water yielding zone around the lowest port of WO 11 (highest electrical conductivities).

The distortion of the signal at ~33m along Line 01 is attributed to construction elements of a nearby house.

Line 02: Aquitard 2 seems to extent up to ~300m along Line 02. At the location of the well nest WO 44/WO 58 it was not encountered, as was confirmed by electrical conductivities in the medium range instead of the high range.

Line 03: The geologic log of WO 42 indicates a clay layer on ground surface, followed by medium sand and coarse sand. Aquitard 2 was not present. It appears that the surficial clay layer was well detected by the resistivity survey with high electrical conductivities. The sand below the clay layer is marked by very low electrical conductivities, which might be attributable to low moisture content below that shallow clay layer. There was no watertable detected while drilling WO 42. At the bottom of borehole WO 58, which was twice as deep as WO 42, water was encountered and a well installed.

Line 04: At WO 41/WO 56 Aquitard 2 was encountered, and below it a sand layer. At the bottom of WO 56 a well was installed in a water bearing zone (Aquifer 2). This succession of Aquitard 2 followed by Aquifer 2 seems to be present along the whole survey line since it shows a very uniform distribution of electrical conductivities with high values attributable to the shallow clay layer and low values attributable to the low saturated sand. At the bottom of this line a zone of high electrical conductivity appears, which is assumed to be part of Aquitard 3 since the ground elevation decreases along the profiles and compared to the origin of Line 01, where the elevation of Aquitard 3 is known, and the elevation of this zone is the same.

Line 05: At the location of WO 41/WO 56, at the west end of Line 05, the shallow layer of clay is very thin, therefore no zone of high electrical conductivity can be identified. The shallow layer of clay reappears farther along the line. The intention of drilling a hole at location WO 47 was to investigate the source of the anomalies in electrical conductivity at this location. However, aquitard material was found at ~6mbgs, which is deeper than at any other location. Within 3m of

this location a fence post and a large diameter metal tile drain outlet are present, both of which might influence the electrical signal.

4.3.2 EM34 Surveys

The results of all three EM surveys are shown on Figure 4.6 and indicate: (1) zones of high electrical conductivity in the northern part of the surveyed area corresponding to moist-clayey material in the bottom of the valley; and (2) lower electrical conductivities in the southern part of the area corresponding to the unsaturated sand below Aquitard 2 under the drumlin. The shallowest measurements (10m spacing, horizontal mode, Panel (c)) indicate an area of low electrical conductivity at about half the elevation difference between the valley and the top of the drumlin. This area corresponds with the section at ∼610m along the resistivity Line 01 – the area where sand is the dominant texture on ground surface. The connection of the glaciofluvial outwash channel to ground surface that can be identified on resistivity Line 01 is not identifiable with the three different modes of the EM survey. This is probably due to the fact that the EM survey is integrating over a large depth (see Appendix A.4), whereas the resistivity survey results in depth-discrete results.

Transient Responses to Precipitation | **4.4**

The analysis of the geophysical surveys indicated a hydraulic connection between Aquifer 2 and ground surface around WO 11 as a result of a discontinuity in Aquitard 2. Transient hydraulic head data were recorded at this location as a complimentary data set during two spring melt periods and compared to data collected at other locations where Aquifer 2 was overlain by Aquitard 2 and no direct hydraulic connection exists, and where a weaker hydraulic response was anticipated.

Figure 4.7 presents a temporal profile of hydraulic head at two discrete depths at locations WO 11 and WO 12 (see Figure 3.1 for well locations) along with daily precipitation data during Spring 2004. At WO 11 water levels at both depths responded rapidly to precipitation events indicating a direct hydraulic connection. The shape and timing of the hydrograph, at both depths is very similar, implying that the units in which the piezometers are screened, are hydraulically connected to ground surface. Directly at WO 11 the top most layer is clay (Aquitard 2), which might explain the lower amplitude of the response in the shallow piezometer WO 11-6. A few meters to the northwest and a few meters to the south-east of WO 11, the surficial layer consists of sandy material (Aquifer 2), and a connection to deeper layers exists. The minimal response to

the relatively big (28mm) rainfall on 18-June-2004 was due to the short (∼45min) duration of this event which led mostly to surface runoff instead of recharge, as observed on site.

The water level fluctuations at WO 12 can be described as "seasonal variations" rather than as responses to individual rainfall events, suggesting the existence of a hydraulic barrier between the piezometers and ground surface. These findings emphasize the need to understand the hydraulic connections between various aquifer units since these connections control the contaminant migration pathways from the surface (source) to the extraction wells (receptor).

To further investigate the subsurface behaviour in this area more piezometers (especially WO 40 ∼250m to the north-west of WO 11) were equipped with pressure transducers and thermistors in Fall 2004 to record water levels and water temperature continuously during the winter and following spring melt (data recorded every two hours, Figure 4.8). Air temperature rising above freezing point creates conditions suitable for recharge to take place. Precipitation occurs as rain, snow melts and ground thaws. These recharge conditions are indicated by the positive correlation between precipitation, air temperature, and hydraulic head on Figure 4.8. This correlation is even more pronounced at WO 40 than at WO 11. Note that WO 40 shows the higher amplitude in hydraulic head response and a pronounced water temperature decrease during recharge events. The smallest response is identified around WO 12 (as in the previous spring melt) and in the piezometers at WO 02 and WO 28-D.

Chemical Analyses | **4.5**

4.5.1 General Observations

Ninety-eight groundwater samples were taken between September 2003 and December 2004 from 67 different individual sampling ports within the observation well network around the Thornton Well Field. Table 4.1 lists the chemical parameters determined and general results. Not all the parameters were determined for every sample and sometimes duplicates were taken.

A low standard deviation (Std.Dev.) in Table 4.1 indicates that there is a low variability for that specific parameter between different samples from the monitoring network (i.e., little spatial or temporal variability). This information was used to determine which parameters should be monitored on a regular basis, and which ones are not as critical and therefore monitored over larger time intervals. Bromide, fluoride, and iron were excluded from future regular analysis, since they appeared to remain constant

over time. Because of the focus on nitrate concentrations in the area of the Thornton Well Field, nitrogen species (NO_3^-, NO_2^-, NH_3) were included in the geochemical analysis for all samples.

4.5.2 Nature of nitrate concentrations in the observation well network

The highest groundwater nitrate concentration measured in the vicinity of the Thornton Well Field prior to the commencement of the current work was 14mg-N/L recorded by *Sebol* (2000) in WO 02. The highest nitrate concentration based on the data from this study was 16.8mg-N/L measured in WO 11. The upper 25% of all nitrate concentrations were observed in eight wells that form a line from WO 40 to Well 01: WO 11, WO 02-D, WO 05, WO 07, WO 08, WO 11, WO 35 and WO 37. More detailed findings of chemical analysis along this line and the implications to the site conceptual model are discussed in Chapter 5.

In Figure 4.9, the nitrate concentrations of all samples taken between 1997 and 2005 are plotted – including data from *Padusenko* (2001) and *Bekeris* (2005). Monitoring wells installed after the start of this study are marked differently in order not to bias the results. The data from the post-2004 monitoring network produced higher nitrate concentrations indicating either that 1. these monitoring locations were placed in zones of higher nitrate concentrations, or 2. there is a general increase in nitrate concentration.

The spatial nitrate distribution for these time periods (around 1998, Fall 2003, and Spring 2005) is presented on Figure 4.10. These data sets show that the zone of nitrate concentrations above the MAC extends farther to the east in 2003/2005 than in 1998, that is farther towards the supply wells of the Thornton Well Field. The shape of the spatial nitrate distribution is similar in Fall 2003 and in Spring 2005, but in the eastern part of the contoured area, the lowest concentrations were <7mg-N/L in 2003, and between 7mg-N/L and 8mg-N/L in 2005. In the five years between 1998 and 2003 a clear increase in nitrate concentrations in the observation well network can be observed – and higher concentrations are observed closer to the supply wells in 2003 than they were in 1998. The difference between Fall 2003 and Spring 2005 is not as pronounced, but still detectable. The nitrate concentrations are slightly higher in Spring 2005 than in Fall 2003, and therefore it seems unlikely that the small increase is due to seasonal variations in nitrate concentrations, because usually higher nitrate concentrations are observed in the fall and not in the spring.

In an attempt to quantify the variability in nitrate concentrations for each piezometer, the coefficient of variation (standard deviation ÷ mean) in piezometers, where at least four nitrate samples were available, was determined and (Table 4.2). The data suggests that in some piezometers nitrate concentrations vary significantly ($\sim$ for CV>0.2). Checking the behaviour of nitrate concentrations in piezometers that indicate highest variability, it was found that especially WO 04-D-18 and all piezometers in WO 02 show

a significant increase. WO 07 and WO 05 show significant increases as well, despite a small CV or because less than 4 data points were available. Most of the piezometers with the most significant increase in nitrate concentrations are within or close to the line described above, where highest nitrate concentrations during the course of this study were measured. Increasing nitrate concentrations within the observation well network upgradient of the supply wells of the Thornton Well Field should be taken as an alarming sign. The data suggests that elevated nitrate concentrations move closer to the supply wells of the Thornton Well Field with time, and it can be anticipated that those elevated nitrate concentrations will eventually reach the supply wells. Nitrate concentrations in the piezometers of WO 09 are generally <1mg/L, therefore the mean might be small which causes the CV to be high. More detailed time series analysis work is being undertaken at the moment outside of this study.

4.5.3   Isotope Analysis

Table 4.3 lists the results of the tritium analysis. Bedrock water (WO 28-D-01) and water from Aquifer 4 (WO 28-D-03/02) indicate sub-modern water that has been recharged prior to 1952. The deep aquifer systems (Aquifer 4 and Bedrock) contain no nitrate and its water likely recharged at least 50 years ago. The result of 5.7 TU in WO 28-D-02 seems too high for the depth ($\sim$70mbgs) and considering that that piezometer is within 2m of WO 28-D-03 and WO 02-D-01 within the same or a very similar hydrogeologic unit.

WO 28-D-04, screened in Aquifer 3, contains young water, as does the pond near Well 01. Values around 15 TU have been reported by *Sebol* (2000) and *Robertson and Sebol* (2004) for water samples taken from wells that are screened in what is defined in this study as Aquifer 3. Aquifer 3 is less deep, the travel distance of infiltrating water is shorter, and at places there is a direct hydraulic connection to ground surface.

Results of the deuterium/oxygen-18 analysis are shown on Figure 4.11.   While the range of both deuterium and oxygen-18 composition is rather small, if the error of analysis is taken into account, three groups of waters with distinct composition can be identified:

1. Water of the deep aquifer just above bedrock (Aquifer 4) and bedrock water (WO 28-D-1 and WO 28-D-3).
2. Water in Aquifer 3 from WO 11, WO-02-D, WO 28-D-4. Water from the pond close to Well 01 falls into this category, which is evidence that it is being fed by groundwater.
3. Water from the supply wells.

The samples are similar to local meteoric composition (after Fritz et al., 1987 as cited in *Stottler* (2002)) observed in proximity to a field site in Simcoe, Ontario ($\sim$50km to the south-east of Woodstock. Since most of the annual recharge in the area occurs dur-

ing spring melt, it was expected that the isotopic composition of the samples would be similar to the composition indicated by the winter local meteoric water line (LMWL), that is have higher $\delta^2 H$ content, than the annual and the summer LMWL. Furthermore, it was expected that the composition of water from the supply wells would be a mixture between Aquifer 3 and Aquifer 4 water, since these two aquifers are suspected to feed the supply wells. The oxygen-18 met that expectation, but the deuterium contribution is unexpected high. One explanation might be the physical difference between the big supply wells from which water samples were directly taken for the third group, and piezometers that were used for taking all other samples (mechanical mixing effects within the well or the pump). *Clark and Fritz* (1997) report higher than expected $\delta^2 H$ content in samples taken from units that produced methane (landfill leachates). It seems unlikely that this is the case in this area. A delay in analysis and/or not perfectly stored samples might cause differeces in $\delta^2 H$ and $\delta^{18} O$ composition.

<div style="text-align:right">

Mass Loading into Well 01 | # 4.6

</div>

Water enters the screen of Well 01 along two main sections: 50% between ∼25.5mbgs (84 ft. bgs.) and ∼27mbgs (88 ft. bgs), and 13% between ∼27.5mbgs (90.5 ft. bgs.) and ∼28mbgs (93 ft. bgs) (Figure 4.12). Below ∼28.5mbgs (94 ft. bgs.) no water enters the screen. This distribution is fairly consistent, regardless of the pumping rate (Figure 4.12, Profiles 1 to 3).

Profile 1 shows the most distinct peaks at ∼26mbgs (86 ft. bgs.) and at ∼28mbgs (92 ft. bgs); however after sustained pumping, the peaks flatten out (Profiles 2 and 3). It appears that initially only narrow zones along the screen contribute water, but later as the pressure pulse from the pumping migrates farther into the aquifer, the contributing zones get wider.

Possible reasons for the determined shape of the flow profile could be a performance issue of the well (clogged, it could be poorly developed), or the contribution of the aquifer material around the upper part of the screen is significantly more hydraulic conductive, than the lower zone. For numerical modelling it might be worth considering to take the shape of the inflow distribution along the screen into account.

Nitrate concentrations measured during Profiles 2 and 3 at ∼0.3 m (1 ft.) intervals were uniform with a mean of 6.3mg-N/L and a standard deviation of 0.2mg-N/L.However, the average nitrate concentration during Profile 2 was ∼6.2mg-N/L and during Profile 3 ∼6.4mg-N/L (Figure 4.13 b and d). The concentration profiles were uniform along the screen, therefore the shape of the estimated mass loading distribution along the screen was found to be similar to the water inflow distribution (Figure 4.13 a and

c), since variations in flow dominate. Due to the mass balance approach used, anomalies in the nitrate loading profile are to be expected. For example, a higher mass load entering a given mixing cell than leaving generates a negative loading for the given mixing cell (see Profile 3 at ~28mbgs (~91 ft. bgs.)). The rate of nitrate mass extracted in Profile 2 is ~2.9kg-N/min, during Profile 3 ~3.1kg-N/min.

Tile Drain Mass Loading | # 4.7

The only times that tile flowed before installation of the weir box were during the spring melt in 2004 and during the most intensive rainfall event of the Summer 2004 on 17-June. Between the start of operation of the weir box on 01-August-2004 and December 2005 the tile did not flow. During the spring melt (March) in 2005, one flow event at the installed weir box was monitored (Figure 4.14). As soon as the air temperature rose above the freezing point and was coupled with precipitation, the tile started flowing. Note that the tile line did not flow during the day, but at night, about 6h after the maximum air temperature was observed during the day. This delay might be related to the time needed for the water to infiltrate into the tile after it melted, or, if the water in the tile was frozen, for that water to thaw.

Nitrate concentrations in tile drain samples are listed in (Table 4.4). During the period when the flow rate was measured by the weir, the nitrate concentration at this location varied from 14.3mg-N/L on 17-March, to 18.1mg-N/L on 21-March, to 19.2mg-N/L on 23-March, and to 10.1mg-N/L after the flow declined to almost zero on 30-March (Figure 4.14). Using an average nitrate concentration of 18mg-N/L and the total water volume of 1500m^3 that were measured during this flow event, the total mass of nitrate discharged through the weir box for this event was ~30kg-N. Assuming there are 10 flow events with similar characteristics per year (in 2004 only four events were observed) the yearly nitrate mass discharged from that weir box would be ~300kg-N. Compared to the total mass of 10t to 30t of nitrate extracted by the Thornton Well Field per year, this is two orders of magnitude less. The estimated drained area from that tile drain is about 10% of the total area of Parcel B. Using the average of the recharge values from Section 4.8, between 250kg-N/year and 570kg-N would flush through this tile-drained area. This would mean that most of the recharge is captured by the tile drain system. This captured recharge is infiltrating directly behind the weir box back into the groundwater system and is potentially drawn into the supply wells. If the tile outlet would be placed at a location outside the capture zone of the Thornton Well Field, or if the outflow of the tile drain was treated to reduce nitrate concentrations on site, it might be possible to decrease nitrate concentrations in the supply wells.

Four steps were required for the analysis of nitrate mass in the unsaturated zone:

Step 1:   Determine the volume of the unsaturated zone below Parcel B.

Step 2:   Determine the mass of nitrate in that volume.

Step 3:   Determine the annual rate of nitrate flushed out of that volume and the time-frame until the nitrate is completely removed.

Step 4:   Determine the average yearly extracted mass of nitrogen with average annual pumping rates and concentrations lumped over the whole Thornton Well Field. Then subtract the annual nitrate loading from Parcel B and back-calculate the possible decrease of nitrate concentrations of the Thornton Well Field.

Step 1 – Volume of Unsaturated Zone

The top of the unsaturated zone is defined by the ground surface which is given by the 10m by 10m – resolution DEM (Section 2.1). The bottom surface of the unsaturated zone is the water table. In the center of each DEM cell the water table elevation was subtracted from ground surface elevation, and then multiplied by the cell area of 100m^2 to obtain the volume of the unsaturated zone per cell. To obtain the volume of the unsaturated zone below Parcel B, the volumes of all cells within that parcel were summed up. This analysis was undertaken with three different data sets:

1. Static hydraulic head data within Aquifer 3 based on data from the Water Well Record database of the Ministry of Environment (MOE).

2. A local data-set of water levels in observation wells of the UW monitoring network. This data set included only wells that were installed before May 2004. Average values from 1998 to 2004 were taken for the shallowest monitoring point, if more than one measurement existed at one location.

3. A similar data set as in (2), but including all wells installed until June 2005, and based on a "snapshot in time"- measurement (a few weeks in February 2004) of hydraulic head. Seven additional datapoints were available within Parcel B.

Each data set has its advantages and disadvantages: Data set (1) is on the largest scale, therefore primarily represents the regional trends for depth to the water table and

groundwater flow direction. The data include water level measurements taken after well constructions since 1941; each measurement was taken under a different configuration of the groundwater flow system, and therefore the resulting potentiometric surface is a relatively crude average between different conditions. Data set (2) is on a more local scale and over a shorter time-average, with monitoring points confined to within the Thornton Well Field and Parcel B. It contains fewer data points overall, but more data points within Parcel B. Data set (3) is a snapshot in time in Spring 2005, on the same area-scale as data set (2), and includes seven new wells within Parcel B which were not included in data set (2).

For each water table data set the point measurements were interpolated using Kriging which allows to express the estimation error. Different methods were used: Simple-, Universal-, and Ordinary Kriging with variations in Kriging parameters (degree of trend removal, different data-transformations, and the values of nugget and range). For each interpolation the root mean square error was determined and the one with the smallest error was taken as the best interpolation of each data set.

The upper panel on Figure 4.15 shows the best interpolations of potentiometric surfaces for the three data sets. General flow direction is from the east to the west. The MOE data set suggests a southern component to the flow vector, the averaged UW data a northern component. Variations originate in the averages over different periods of time, different averaging procedures, and in different scale and data density. Between the three data sets, the thickness and the distribution of the unsaturated zone, as shown in the lower panel of Figure 4.15, is similar and ranges between $14 * 10^6 \text{m}^3$ and $15 * 10^6 \text{m}^3$ (Table 4.5). The varying topography has a bigger influence than the relatively flat potentiometric surface.

Step 2 – Estimate Nitrate Mass in the Unsaturated Zone

This step can be divided into two parts: First the bulk soil nitrate concentration [mass nitrate per mass soil] and the gravimetric moisture content were determined in discrete sub-samples of cores. Then the nitrate mass was distributed over the domain and the total mass of nitrate stored in the unsaturated zone calculated.

Sub-sampling of Cores

In the lab, the cores described in Section 3.1.2 were divided into sections of similar moisture content and similar material properties based on visible inspection. In each section at least one representative sample of 5cm thickness was taken. Immediately after taking the sample from the fresh core the following parameters were determined:

1. The fresh weight M_{fresh} as a measure for the mass of water *and* matrix of the sample.

2. The dry weight M_{dry} after 24h drying at 80°C. At this temperature no mass of organic matter is being lost due to burning. This dry weight is a measure of the mass of the matrix. With the help of the above parameters a gravimetric moisture content ω can be determined (*Bear*, 1972; *Tindall and Kunkel*, 1999):

$$\omega = \frac{M_{fresh} - M_{dry}}{M_{dry}}.$$

3. The mass of nitrate in each sample ($M(NO_3 - N)_{sample}$), under the assumption that all nitrate originally existed in the aqueous phase and is left behind in the sample (see Section 3.1.2). Values were provided as mass nitrate per mass soil ($M(NO_3 - N)_{rel}$).

The aqueous concentration of nitrate in the pore water of the original sample was back-calculated by dividing the obtained mass of nitrate by ω and multiplying by the water density:

Example procedure:

Determined in Lab:

$$M(NO_3 - N)_{rel} = 2.8 \ \frac{mg \ NO_3 - N}{kg \ soil};$$

$$M_{fresh} = 121.33g, \ M_{dry} = 103.39g;$$

$$\Rightarrow M_{water} = M_{fresh} - M_{dry} = 17.94g \ water;$$

$$\Rightarrow \omega = 0.17 \ \frac{g \ water}{g \ soil};$$

Therefore (with a water density of 1kg/L):

$$
\begin{aligned}
C(NO_3 - N) &= \left(2.8 \ \frac{mg \ NO_3 - N}{kg \ soil}\right) \div \left(0.17 \ \frac{g \ water}{kg \ soil}\right) * \left(1 \ \frac{kg \ water}{L \ water}\right) \\[2mm]
&= 16.13 \ \frac{mg \ NO_3 - N}{L \ water} \\[4mm]
M(NO_3 - N)_{sample} &= \left(16.13 \ \frac{mg \ NO_3 - N}{L \ water}\right) * (17.94 \ g \ water) \div \left(1 \ \frac{kg \ water}{L \ water}\right) \\[2mm]
&= 0.29 \ mg \ NO_3 - N
\end{aligned}
$$

At every core location the average soil water nitrate concentration was calculated with an arithmetic mean of all soil samples. These values were then interpolated on Parcel B, as shown on Figure 4.16. Highest concentration is observed at WO 35, a plot of land

between the Thornton Well Field and an abandoned farm house, where cattle used to graze. The lowest value was obtained at WO 45 in the south-east corner. Generally, the average nitrate concentrations are variable.

Profiles of $M(NO_3 - N)_{rel}$, ω, $C(NO_3 - N)$, and $M(NO_3 - N)_{sample}$ for each core along with the corresponding geologic log are shown for each core in Appendix A.11. A trend in the data is hard to describe. Two cores (WO 34 and WO 44) exhibit sandy material along their entire depth, and no peaks in nitrate mass can be detected. This suggests that these sands conduct water fairly easily which leads to flushing of the nitrate mass through that conductive material. The location of WO 35 is in an area where cattle used to graze, leading to constant manure application. The effects of remnant excess nutrients in this area were visible in Spring 2004, when the winter wheat on that plot of land was growing faster than in the surrounding area. The reason why the nitrate peak in WO 35 is recognizeable might be attributable to the fact that it is within a clay zone that slows the rate of infiltration down. Conversely, the conductive sands of WO 34/WO 44 allow recharge and any dissolved substances in it to infiltrate deeper into the system, which may be why no peak in nitrate mass occurs in WO 34.

Calculate an Average Nitrate Concentration per Core and Distribute over the Volume

An average value of mass nitrate per mass dry soil ("soil bulk nitrate concentration") $\left(\frac{\sum (C_i l_i)}{\sum l_i} \right)$ was calculated for each core by a representative distance weighting scheme. The method is described for WO 28 in Table 4.6, and values for each core are presented in Table 4.7. These values of average bulk soil nitrate concentrations were then interpolated to every cell within a raster of the same dimensions as the DEM. The best interpolation was chosen to be the one with the smallest Root-Mean-Square error amongst a variety of kriging scenarios. Then the value in each cell was multiplied by the soil bulk density, the thickness of the unsaturated zone and the area of the grid cell to obtain the mass of Nitrate-N in each grid cell. For the bulk density an average value of 1500kg/m^3 was assumed (*Tindall and Kunkel*, 1999). The total mass of nitrate stored in the unsaturated zone below Parcel B was obtained by summing up the nitrate mass over all grid cells within Parcel B. A schematic sketch of the raster analysis is shown in Appendix A.7.

The three panels on Figure 4.17 show the mass of nitrate within every cell of the grid calculated for the three different data sets from Step 1. In Table 4.8, the most important statistical parameters are shown, providing an indication on the distribution of nitrate in the unsaturated zone. There are $\sim$20t nitrogen in the unsaturated zone below Parcel B.

The shape of the nitrate distribution is very similar in the three cases. In areas where water can infiltrate into the ground (in the topographic low around WO 11, on both sides of the driveway in the north part of Parcel B that is excluded from analysis and is

in the south-western area), the nitrate mass is lowest. These areas may reflect processes of rapid flushing as opposed to slow build up of nitrate mass. Lack of data in the southern part is the reason for the biggest differences between the three scenarios.

Step 3 – Estimate of Timeframe for Nitrate-Mass Removal

In order to provide insight into the time scale involved in realizing improvements to water quality in the Thornton wells, initial estimates were calculated of the time required to flush the nitrate stored in the unsaturated zone across the water table by infiltrating meteoric water were constructed. These initial estimates will be later used as a benchmark for the numerical modelling.

The mass-flux $\dot{m}$ $[M/T]$ leaching out of a volume of soil can be calculated, assuming vertical flow, with three parameters: the recharge R $[L/T]$ that infiltrates below a surface area A $[L^2]$ and the concentration C $[M/L^3]$ within that volume (Equation 4.1).

$$\dot{m} = C \cdot A \cdot R \tag{4.1}$$

Dividing the total mass of nitrate in the unsaturated zone (Section 4.8) by $\dot{m}$ gives the time necessary to flush the nitrate mass out of the unsaturated zone. Inherent in this step are the assumptions of constant, average, steady-state and plug-flow conditions. Furthermore it is assumed that there are no sources of nitrogen within or entering the volume of unsaturated zone below Parcel B (zero nitrate concentration in rain, no release of nitrogen from plants or the root zone, no nitrogen fertilizer inputs). In addition, no attenuation mechanisms are actively removing nitrate mass during the flushing process (no decay or degradation of nitrogen along the flow path).

These assumptions have limitations. Plug-flow unrealistically assumes no tailing in nitrate concentration as the flushing process occurs or retardation effects that would lead to longer release of nitrogen into the receptors. *Ryan et al.* (2000) showed that the assumption of plug-flow conditions might be substantiated in shallow groundwater systems. Zero nitrogen inputs are likely impossible to achieve. Furthermore, there is no relationship available between a decrease of fertilizer input and decreased plant release. In this model, an increase of fertilization would lead to an equal increase of released nitrogen. The assumption of no biodegradation along the flowpath is probably safe, since high oxygen concentrations have been observed everywhere upgradient of the supply wells (*Sebol*, 2000, 2004; *Heagle*, 2000).

An estimate of recharge for high and low permeable soils under agricultural land-use in vicinity of the Thornton Well Field is given by *Padusenko* (2001): 250mm/year and 110mm/year , respectively. Based on the overall surface area for Parcel B of 61.8ha and an average nitrate concentration in the unsaturated zone pore water based on all sediment sample analyses of 16mg-N/L (Figure 4.16), a nitrate mass ranging between 1.1t/year and 2.5t/year can be flushed through the system. This means that under the

process of steady state flushing of the unsaturated zone by fresh meteoric waters, without nitrate decay along the flowpath, around 15 years would be required to completely remove the stored nitrate mass (Table 4.9).

Step 4 – Impact on Thornton Well Field

One of the main goals of the overall project is to evaluate the potential effects on water quality in the Thornton Well field from the imposed changes in agricultural land-use practices. Annual average pumping rates, nitrate concentrations, and therefore average total extracted nitrate mass from the Thornton Well Field are known (Section 2.3.1). From this yearly extracted mass, the mass flux $\dot{m}$ from Parcel B was subtracted and the potential reduction in annual average nitrate concentration for the Thornton Well Field from decreases in nitrate loading on Parcel B was calculated. This analysis assumes that after the unsaturated zone is completely flushed of stored nitrate within Parcel B, a total decrease of annual nitrate mass flux to the water table of 1.8t-N/year (the average between the two estimates in Step 3) would be realized. Based on this reduction, possible reduction in average nitrate concentration for the Thornton Well Field were estimated and are presented in Table 4.10. This table indicates that under the assumed conditions of zero nitrate infiltration from the Parcel B area, significant improvements in overall water quality within the Thornton Well Field can be achieved. It is of interest to note that the most significant results are achieved at lower annual pumping rates, which reflects the combination of wells and related pumping rates that are selected at any given time. This suggests that an optimal well management strategy could be developed that would permit the highest extraction rate and the lowest nitrate concentrations. It should also be noted that as pumping schedules change, the effective capture zone area for the individual wells will also change which may result in slow but significant changes in the quality of water extracted from each well.

4.8.1   Discussion

In evaluating the results of this initial analysis of potential impacts on well water quality, several additional factors should be kept in mind. Firstly, it is unlikely that the mass of nitrate leaching from Parcel B will ever be reduced to zero. The actual leaching rate will depend primarily on the effectiveness of the alternative nutrient management practices currently underway within Parcel B. Secondly, due to the spatially distributed nature of the physical data, the interpolated estimates of the stored nitrate mass stored have a certain degree of uncertainty. Future numerical simulation work will provide additional insight into the fate and transport of nitrate beneath Parcel B.

A source of error might be the fact that the cores did not penetrate the whole unsaturated zone. The maximal depth of each core varies and was determined by the power of the drilling rig. Table 4.11 summarizes the depth of the core and the depth of the

unsaturated zone at the core location. However, it can be safely assumed that the loading history has not changed significantly over the last few decades, as reported by local farmers, and therefore a consistent amount of nitrate stored can be assumed in the unsaturated zone over its entire thickness. Further sources of error are:

Handling cores: Oxygen might enter through imperfectly sealed cores or temperature might not always be low enough to prevent (biological) reactions that would decrease the nitrate content.

Analytical error: The analytical error for determining nitrate content in soil is 10.8% for a 5mg-N/kg soil sample.

DEM: The digital elevation model used in this study has the fine resolution of 10m by 10m. However, due to the varying topography on site, this resolution might still contribute to errors in determining the thickness of the unsaturated zone.

Water table interpolation: By analyzing three different data sets the error in water table interpolation was sought to be minimized. The fact that three very similar volumes were calculated might indicate success. However, measurement points are still sparsely distributed, especially outside Parcel B.

Soil bulk density: For conversion purposes between mass and volume a constant of $1500 \text{kg soil}/\text{m}^3$ soil was assumed. Differences in bulk density between different material types and encountered depths were not distinguished.

Table 4.1:
Descriptive statistics of chemical analysis within the observation well network of the University of Waterloo. Samples were taken between Fall 2003 and December 2004. The units of the chemical parameter indicated in italics in the left column, except for pH, are given in [mg/L]. For the calculation of the average and the standard deviation the detection limit was used if a sample was below that threshold, and then it was also included in the sample count.

Parameter	Avg.	Std.Dev.	Min.	Max.	MAC	Det.Limit	Number
Bicarbonate (HCO_3)	308.32	101.17	0.05	478.00	—	0.05	59
Bromide (Br^-)	0.35	0.00	0.35	0.35	—	0.35	56
Chloride (Cl^-)	31.27	18.01	2.20	84.40	250.00[†]	1.0	98
Fluoride (F^-)	0.34	0.46	0.10	2.70	1.50[‡]	0.1	90
Nitrate (N^-)	7.86	5.69	0.10	16.80	10.00[‡§]	0.1	95
Nitrite (N^-)	0.11	0.03	0.10	0.30	1.00[‡§]	0.1	97
Phosphate (P^{3-})	0.30	0.04	0.30	0.70	—	0.3	86
Sulfates (SO_4^{2-})	44.26	39.54	3.50	313.00	500.00[†]	1.0	97
Alkalinity ($CaCO_3$)	241.45	73.77	1.00	456.00	500.00[†]	1.0	98
Ammonia (N)	0.19	0.30	0.05	1.29	—	0.05	84
Calcium (Ca^{2+})	102.18	35.97	22.00	230.00	—	0.2	105
Iron (Fe)	0.22	0.33	0.01	0.76	0.30[†]	0.01	8
Magnesium (Mg^{2+})	29.78	16.05	8.10	170.00	—	0.05	105
Manganese (Mn)	0.06	0.05	0.02	0.14	0.05[‡]	0.002	8
pH	8.03	0.24	7.26	8.44	9.00[†]	—	98
Potassium (K^+)	2.17	1.73	0.87	12.00	—	0.2	105
Sodium (Na^+)	19.28	16.84	1.50	82.00	200.00[†]	0.1	105

†: from MOE database;
‡: from *Ontario Ministry of the Environment* (*2003b*);
§: according to Ontario Regulations (*Government of Ontario*, *2002*), the sum of nitrate- and nitrite concentrations in one sample has to be below 10mg/L;

Table 4.2:
Descriptive statistical parameters for nitrate concentrations in individual piezometers for sample-sizes ≥4 sorted in descending order by the coefficient of variation.

Well Name	Piezometer Name	Sample Count	Avg. NO_3 Conc.	StdDev. NO_3 Conc.	Coef. Variation
		[–]	[mg-N/L]	[mg-N/L]	[–]
WO04-D	WO04-D-33	5	0.83	1.11	1.34
WO09	WO09-08	5	0.96	1.1	1.14
WO04-D	WO04-D-43	6	0.54	0.6	1.11
WO11	WO11-18	6	0.5	0.44	0.88
WO22	WO22-06	4	1.46	1.25	0.86
WO09	WO09-10	4	0.96	0.81	0.84
WO06	WO06-03	4	6.02	4.28	0.71
WO18	WO18-03	4	3.08	2.08	0.67
WO09	WO09-03	4	1.22	0.82	0.67
WO09	WO09-04	5	1.1	0.55	0.5
WO02	WO02-08	6	11.28	5.09	0.45
WO24	WO24-12	5	3.04	1.17	0.39
WO08-D	WO08-D-06	4	9.6	3.38	0.35
WO02	WO02-03	5	11.4	4	0.35
WO09	WO09-06	4	0.77	0.26	0.34
WO04-D	WO04-D-18	4	9.1	1.79	0.2
WO11	WO11-08	5	13.52	2.21	0.16
WO11	WO11-13	5	13.16	1.9	0.14
WO02-D	WO02-D-13	4	13.2	1.74	0.13
WO02-D	WO02-D-19	6	13.3	1.54	0.12
WO12	WO12-08	4	6.68	0.78	0.12
WO11	WO11-10	7	13	1.42	0.11
WO12	WO12-19	4	6.15	0.68	0.11
WO11	WO11-06	6	13.85	1.58	0.11
WO05-b	WO05-06	4	12.23	1.23	0.1
WO07	WO07-07	5	12.2	1.19	0.1
WO37	WO37-04	5	13.92	1.33	0.1
WO36	WO36-04	4	9.5	0.97	0.1
WO 28-D	WO 28-D-4	4	9	0.85	0.09
WO07	WO07-05	6	12.78	1.02	0.08
WO05-b	WO05-09	5	12.36	0.89	0.07
WO07	WO07-09	5	12.14	0.79	0.07
WO06	WO06-06	5	10.76	0.7	0.06
WO05-b	WO05-12	4	11.65	0.53	0.05
WO02	WO02-05	4	13.5	0.73	0.05
WO06	WO06-09	4	11.25	0.48	0.04
WO02	WO02-11	5	12.66	0.43	0.03
WO02-D	WO02-D-16	4	12.3	0.22	0.02

Table 4.3:
Results of Tritium Analysis.

Sample Point	Screened in Unit	Tritium Unit	
WO 28-D-01	Aquifer 5	< 0.8	†
WO 28-D-02	Aquifer 4	5.7	± 0.7
WO 28-D-03	Aquifer 4	< 0.8	†
WO 28-D-4	Aquifer 3	14.2	± 0.5
Pond at Well 01	—	13.8	± 1.1

†MDL

Table 4.4:
Measured nitrate concentration in tile outlets. "Hole in Drain west of WO40" indicates samples taken in a broken tile line in the field adjacent to the tile outlet in Spring 2005. "ISCO" indicates a cummulative sample taken from TD Weir Box.

Tile Outlet	Nitrate Concentration [mg − N/L]	Date
TD top of gully	17.95	11-Mar-04
TD at WO 40 (outside)	2.00	11-Mar-04
TD Weir Box	24.35	11-Mar-04
TD SW Field 02	9.90	17-Jun-04
TD Weir Box	8.85	17-Jun-04
TD at WO40 (inside)	18.80	17-Mar-05
TD at WO 40 (outside)	3.40	17-Mar-05
TD Weir Box	14.35	17-Mar-05
TD at WO40 (inside)	18.85	21-Mar-05
TD N Parcel A	20.85	21-Mar-05
TD Weir Box	19.25	21-Mar-05
TD at WO40 (inside)	12.60	30-Mar-05
TD at WO 40 (outside)	3.60	30-Mar-05
Hole in Drain west of WO40	12.40	30-Mar-05
ISCO 21-24 March 05	19.20	30-Mar-05
Hole in Drain west of WO40	10.70	30-Mar-05
TD Weir Box	10.10	30-Mar-05

Table 4.5:
Descriptive statistics of the unsaturated zone below Parcel B for each of the three data sets evaluated. Minimum, Maximum, Range, Mean, and Standard Deviation are calculated for all cells of the 10m by 10m grid within Parcel B.

		MOE	1998-2004	2005
Minimum	[m]	4.4	3.9	3.0
Maximum	[m]	34.7	36.6	34.6
Range	[m]	30.3	32.7	31.6
Mean	[m]	22.6	24.0	22.6
Std.Dev.	[m]	7.4	9.1	8.6
Total Volume	$[*10^6 m^3]$	14	15	14

Table 4.6:
Method how to calculate an average nitrate concentration per core, shown for WO 28.

Depth	Mass nitrate per mass dry soil	Interval Boundary	Thickness	$C_i l_i$
[mbgs]	$[mgNO_3 - N/kg]$	[m]	[m]	$[mgNO_3 - N * m]$
0		0		
-0.08	2.8	-0.58	0.58	1.61
-1.07	0.7	-1.47	0.90	0.63
-1.87	1.00	-2.07	0.60	0.60
-2.27	0.45	-2.92	0.85	0.38
-3.57	1.50	-3.96	1.04	1.56
-4.34	1.35		0.80	1.07
-4.75				

Average nitrate concentration $\dfrac{\sum(C_i l_i)}{\sum l_i}$ in this core: **1.23**

Table 4.7:

Average Nitrate Concentrations for each Core

Well Name	Length	Sum over all core intervals of N-mass times length of interval $$\sum(C_i l_i)$$	Average N-mass in each core $$\frac{\sum(C_i l_i)}{\sum l_i}$$
	[m]	[(mg-N/kg soil) $*$ m]	[mg-N/kg soil]
WO 28	4.75	5.84	1.23
WO29	3.05	4.63	1.52
WO30	9.14	20.33	2.22
WO31	2.62	4.82	1.84
WO32	5.64	7.88	1.4
WO33	2.97	4.6	1.55
WO34	7.92	2.97	0.35
WO35	6.71	5.94	0.89
WO36	4.88	4.52	0.93
WO37	4.88	7.32	1.5
WO39	4.28	8.49	1.98
WO40	8.53	2.89	0.34
WO41	3.66	3.31	0.9
WO42	9.45	1.78	0.19
WO43	5.73	4.43	0.77
WO44	8.53	2.69	0.32
WO45	4.0	0.47	0.09
WO46	3.96	0.39	0.11
WO47	4.0	4.8	1.2

Table 4.8:

Nitrate mass in the unsaturated zone below Parcel B. Minimum, Maximum, Range, Mean, and Standard Deviation for each of the three data sets used are calculated for all cells of the 10m by 10m grid within Parcel B.

		MOE data	1998-2004	2005
Minimum	[kg-N]	0.5	0.5	0.4
Maximum	[kg-N]	7.8	7.9	7.5
Range	[kg-N]	7.3	7.4	7.1
Mean	[kg-N]	3.2	3.3	3.1
Std.Dev.	[kg-N]	1.3	1.5	1.4
Total N-Mass	[t-N]	19.9	20.6	19.4

Table 4.9:

Estimated timeframe for flushing the nitrate mass out of the unsaturated zone below Parcel B. The range of estimated values for mass stored and the range of the flushing rate is given.

Nitrate mass in unsaturated zone below Parcel B [t-N]	19.9	20.6	19.4
Possible nitrate removal rate from unsaturated zone below Parcel B [t-N/year]	**Time for flushing [year]**		
1.1	18	19	18
2.5	7	8	7

Table 4.10:

Possible decrease in nitrate concentrations in the Thornton Well field, assuming no more nitrate mass is introduced into the system from Parcel B.

Year	Possible decreased yearly extracted mass [t-N]	Possible decreased yearly average concentration [mg-N/L]	Possible decrease [%]
2004	12.2	5.5	17
2003	16.2	6.2	16
2002	23.2	8	11
1999	34.2	8.1	6

Table 4.11:
Comparison between core depth and thickness of unsaturated zone. Thicknesses for WO31 and WO40 are estimated.

Well Name	Depth of Core [m]	Thickness Unsaturated Zone [m]
WO 28	4.8	31.2
WO 29	3.0	37.5
WO 30	9.1	26.1
WO 31	2.6	20.0
WO 32	5.6	17.8
WO 33	3.0	13.9
WO 34	7.9	23.6
WO 35[†]	6.7	6.6
WO 36[†]	4.9	4.8
WO 37[†]	4.9	4.2
WO 39	4.3	18.0
WO 40[†]	8.5	6.2
WO 41	3.7	20.8
WO 42	9.5	27.4
WO 43	5.7	29.1
WO 44	8.5	27.6
WO 45	4.0	31.5
WO 46	4.0	29.8
WO 47	4.0	13.5

† water table reached
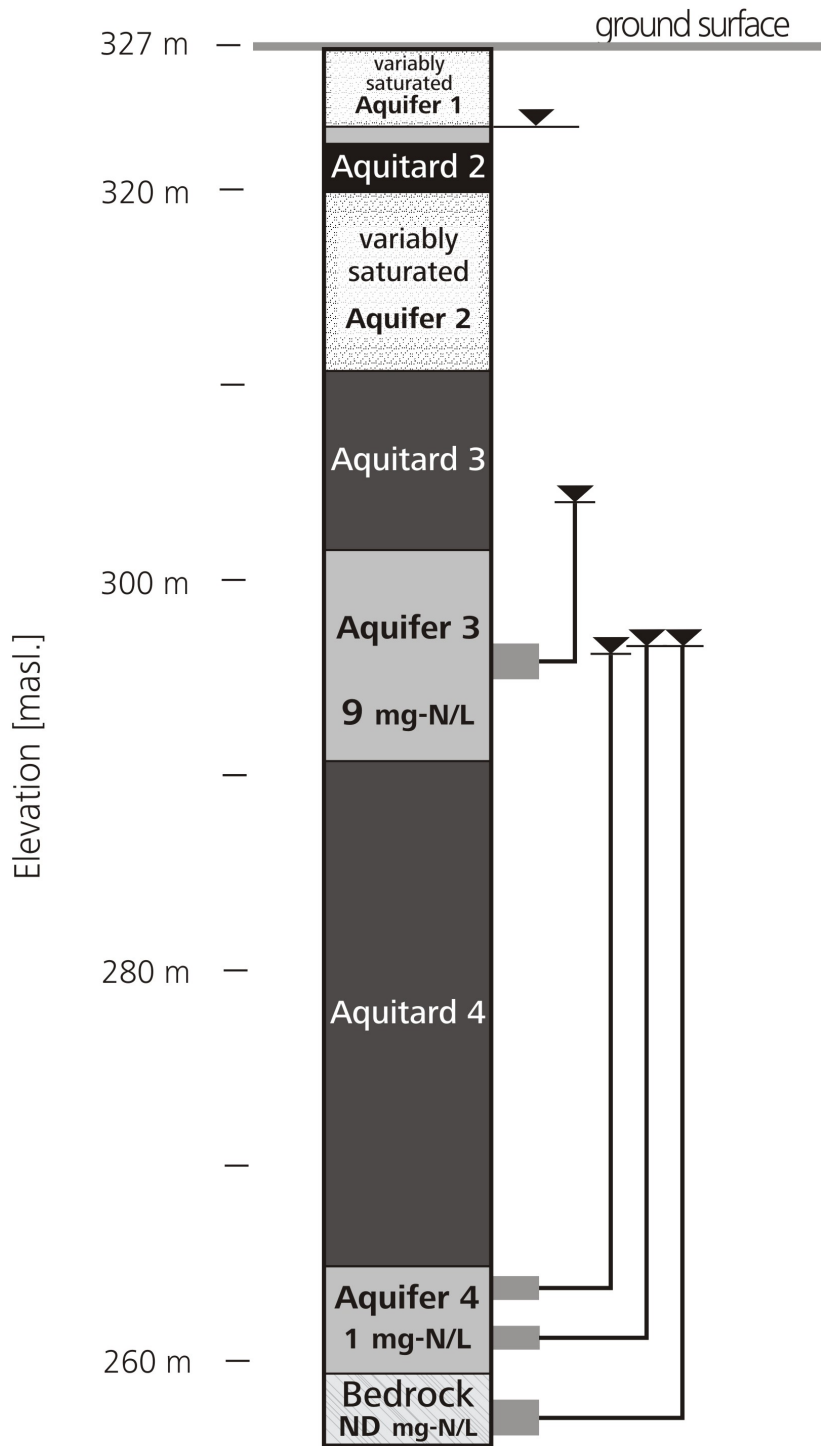
Figure 4.1:
Hydrogeologic log of borehole WO 28-D showing the location of the screened intervals, the associated average water level for each piezometer, and the average nitrate concentration measured in each water bearing zone.
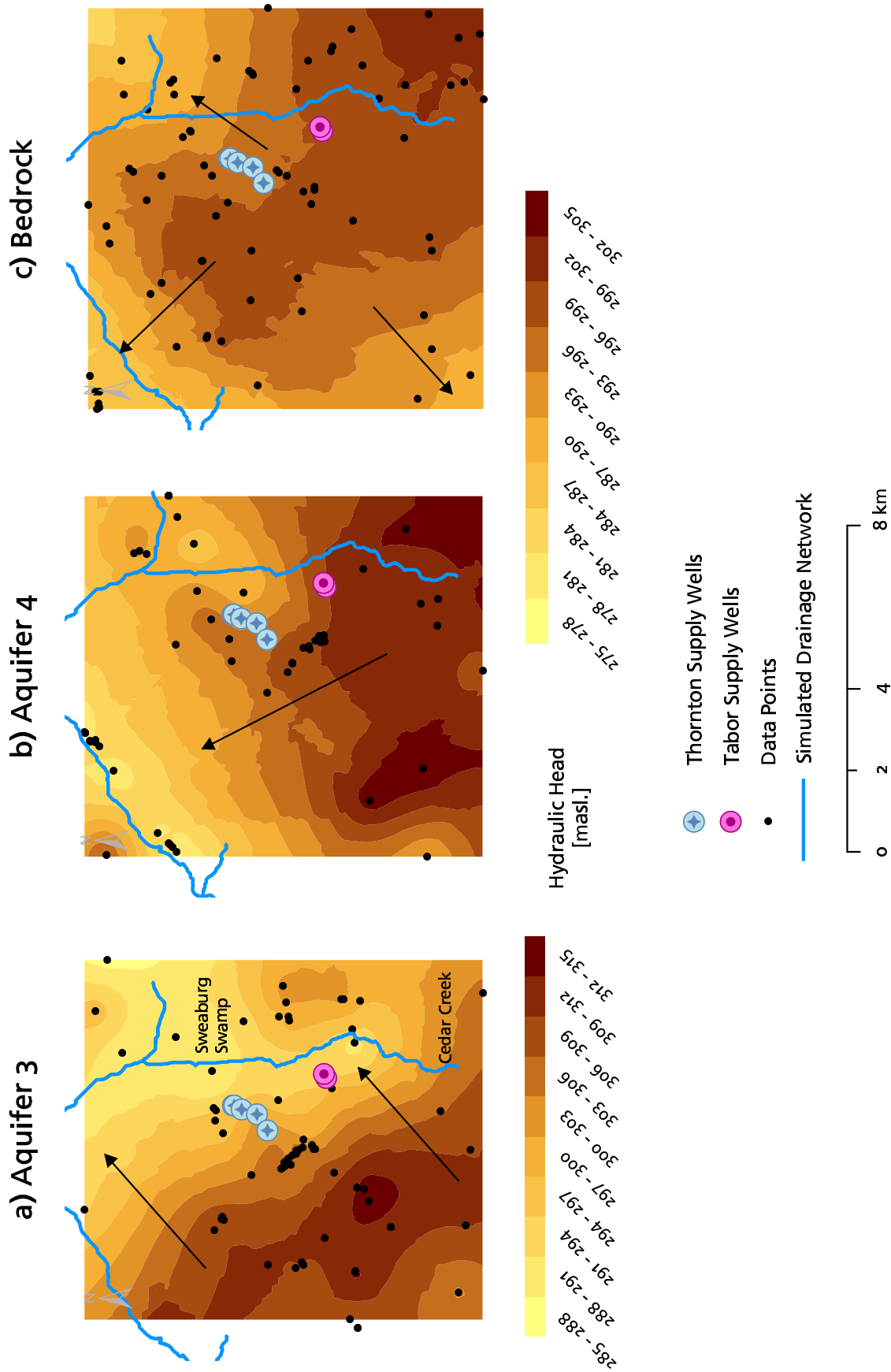
Figure 4.2:
Regional potentiometric surfaces for Aquifer 3, Aquifer 4, and Aquifer 5 (Bedrock). The trend in groundwater flow direction is indicated by the black arrows. The solid circles indicate data used to construct these surfaces. For orientation each panel includes the location of the Thornton- and the Tabor- supply wells, as well as portions of the surface water drainage network around the study site.

Hydraulic Head Difference [m] Aquifer 3 - Aquifer 4

- -2.3 - 0
- 0.1 - 4
- 4.1 - 8
- 8.1 - 12
- 12.1 - 16
- 16.1 - 21.1

Hydraulic Gradient Δh/Δl between Aquifer 3 - Aquifer 4

- -0.46 - 0
- 0.01 - 0.25
- 0.26 - 0.5
- 0.51 - 0.75
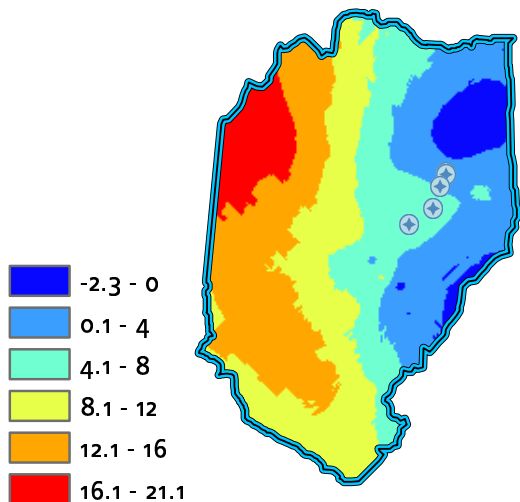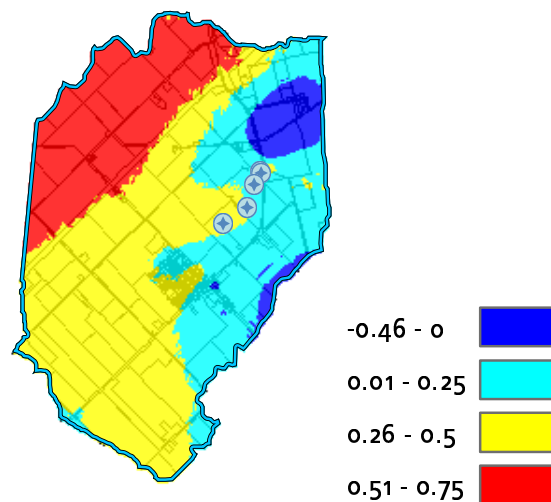
Hydraulic Head Difference [m] Aquifer 4 - Aquifer 5

- -10.0 - -6
- -5.9 - -3
- -2.9 - 0
- 0.1 - 3.5
- 3.6 - 7.1

Aquifer 3

Aquitard 4

Aquifer 4

Δh

Δl
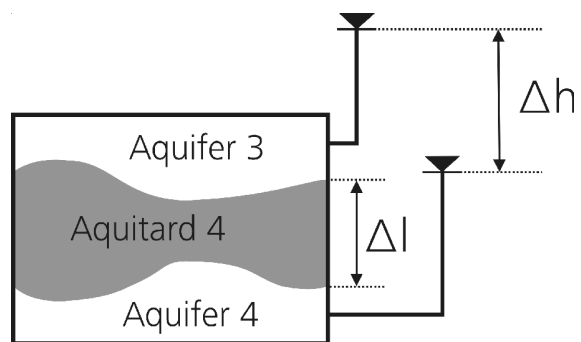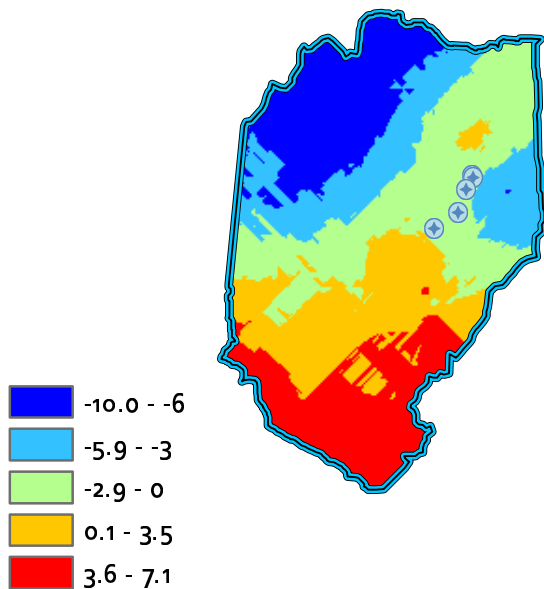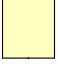
Figure 4.3:
Vertical hydraulic head variations between Aquifer 3 – Aquifer 4 and Aquifer 4 – Aquifer 5. A negative value indicates upward flow direction.
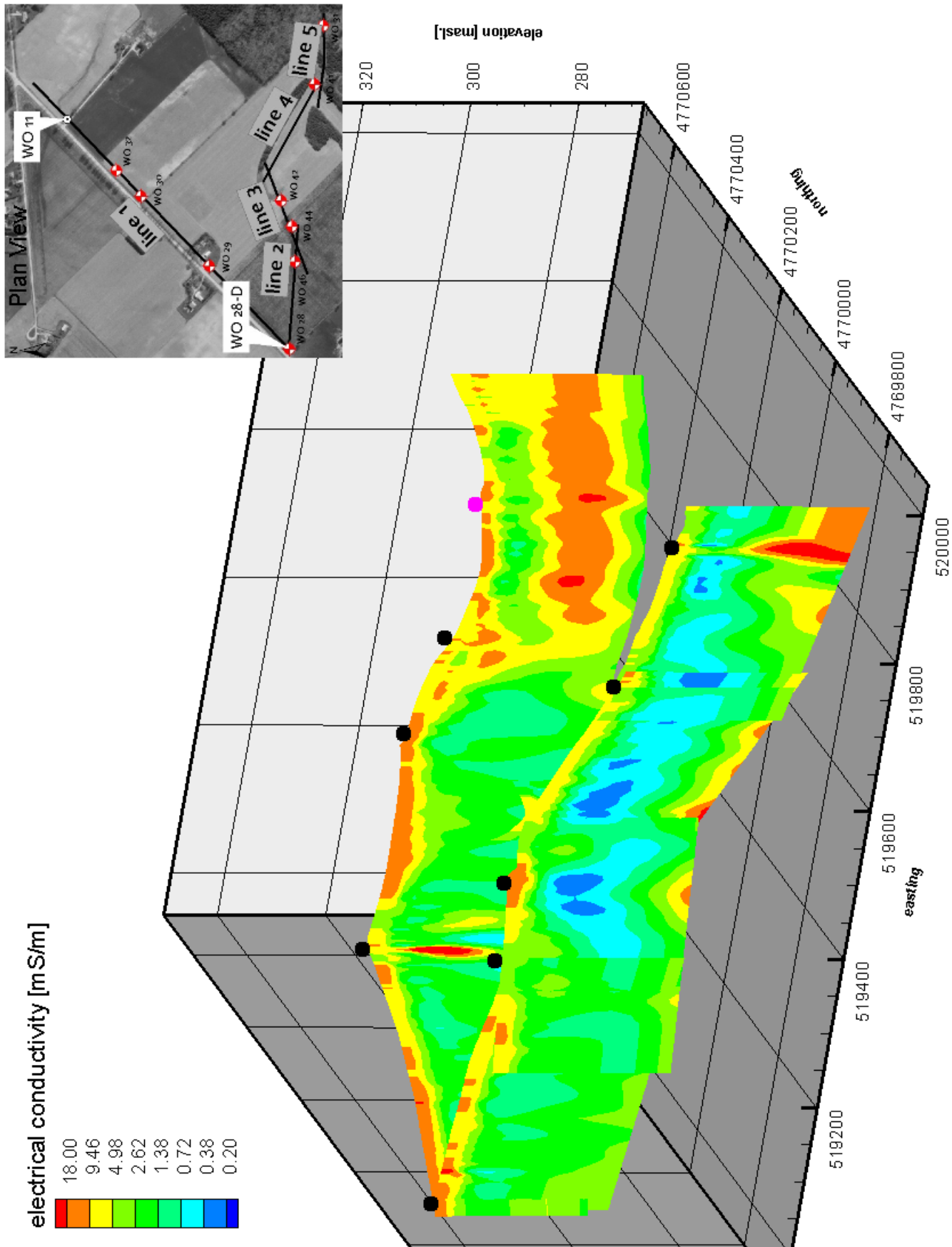
Figure 4.4:
Fence diagram of electrical resistivity surveys. The orientation of the lines can be seen in plan view on the inset map. Eastings and Northings are in UTM Nad83 17N format. Black solid circles indicate core locations directly on the geophysical survey lines that were logged during this study. The purple solid circle indicates the location of WO 11.
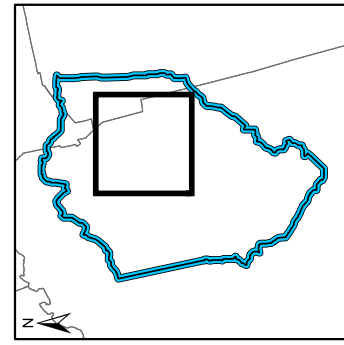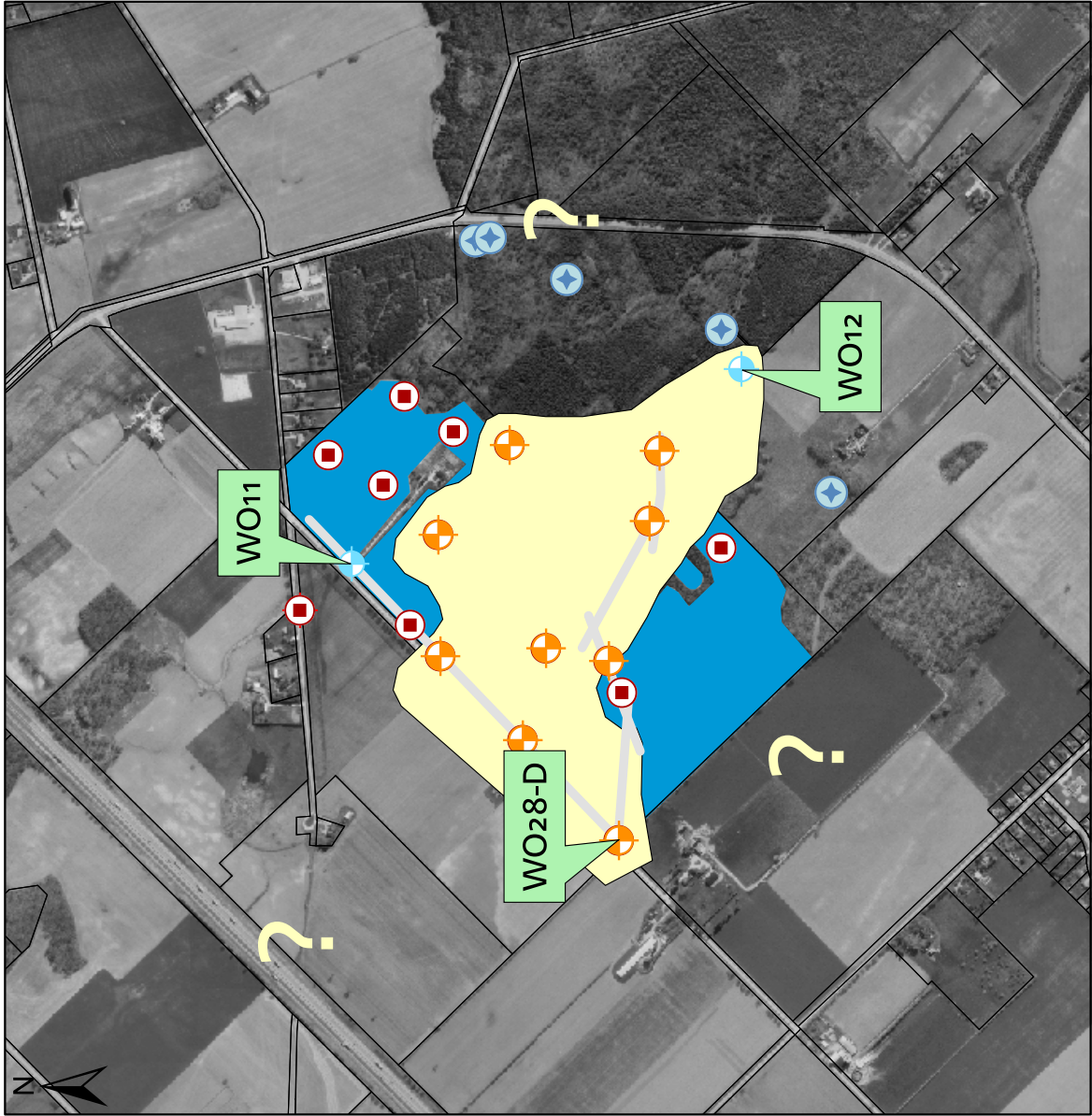
Figure 4.5:
Areal extend of Aquitard 2. Question marks indicate areas where the existence of Aquitard 2 is uncertain.

83

(a) 20m spacing, vertical mode
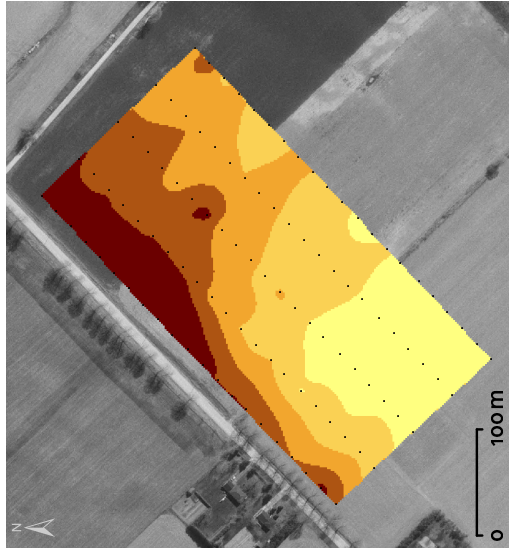
(b) 10m spacing, vertical mode
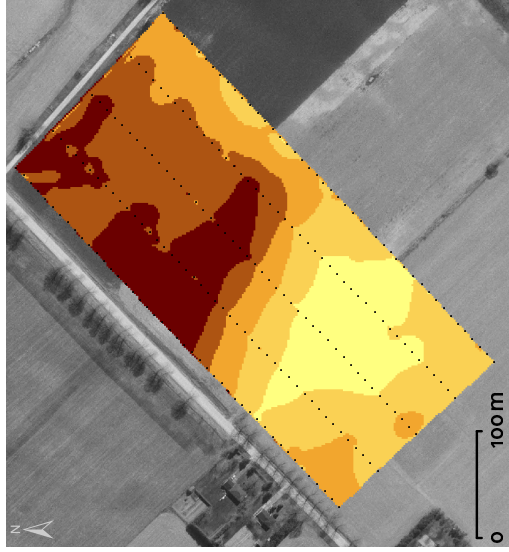
(c) 10m spacing, horizontal mode

Electrical Conductivity
[mS/m]

3　4　5　6

filled contours for panels a, b, and c
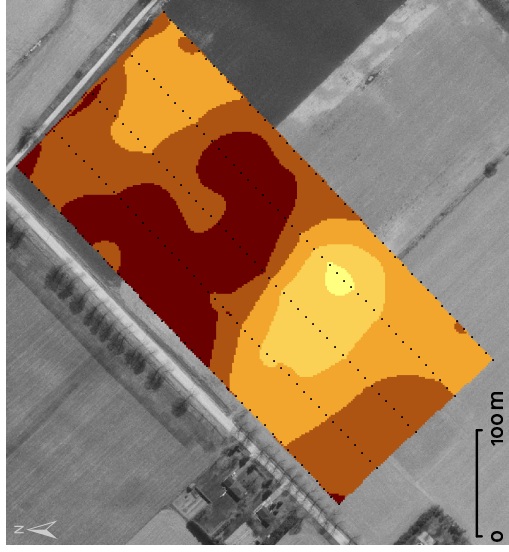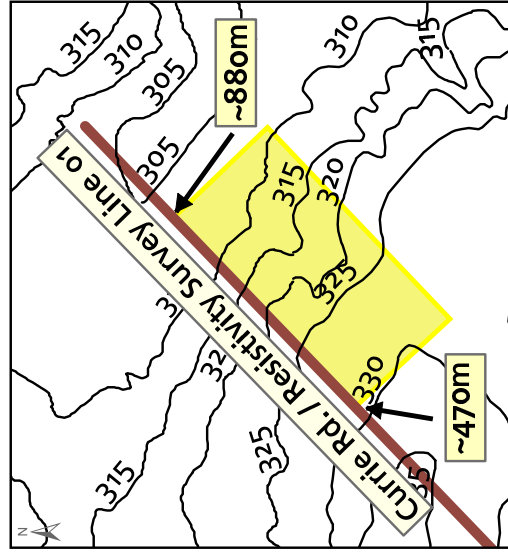
(d) Overview

Topographic elevation contours in [masl.]

Figure 4.6:
Overview over all EM 34 surveys. Panel (d) shows a plan view of the area with 5m spaced contours of ground surface elevation. The area of the EM survey for panel a is shown and its position on the resistivity Line 01 indicated. Panels a, b, and c show results of the electromagnetic surveys with different modes of use as indicated.

84

Figure 4.7:
Water level response at two discrete depths in wells WO 11 and WO 12. Monitoring piezometers WO 11-06, and WO 12-08 are the shallow piezometers at each location in 2004.
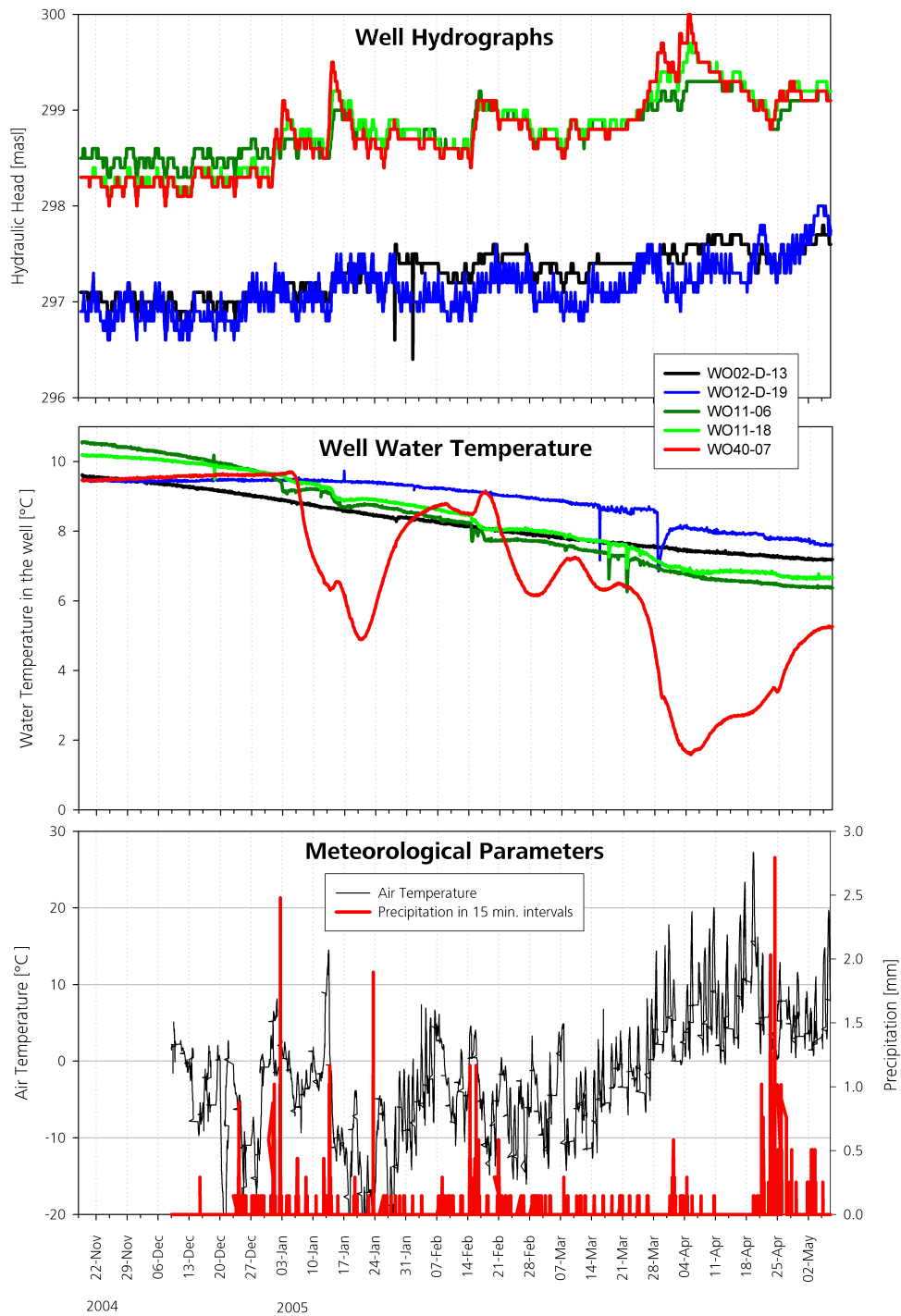
Figure 4.8:
The top panel shows the hydraulic head in observation wells screened within Aquifer 3 at locations WO 11, WO 12, and WO 40. The middle panel shows water temperature in the wells at these three locations. The lower panel shows precipitation and air temperature as recorded by the UW Weather Station located within the study site. Hydrographs of WO 28-D are not shown on this figure for scale reasons.
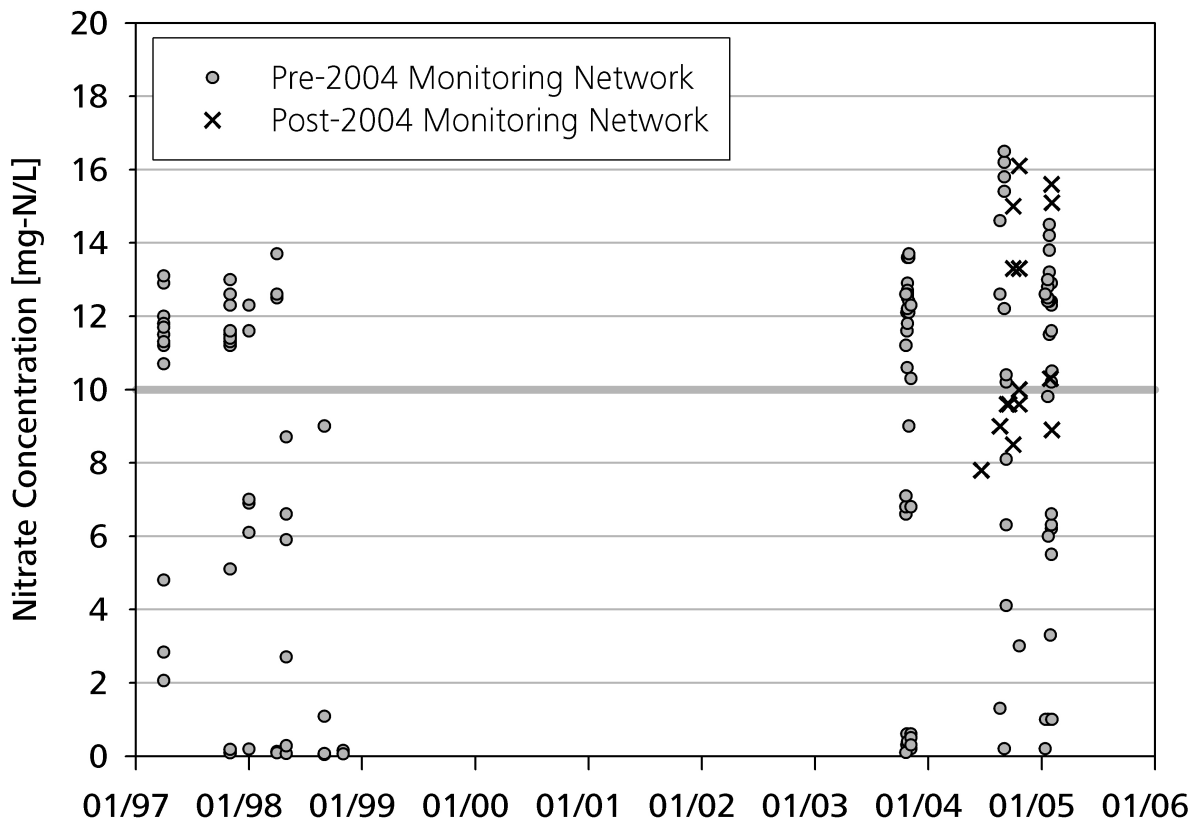
Figure 4.9:
Time-analysis of nitrate concentrations in the observation wells of the Thornton Well Field.
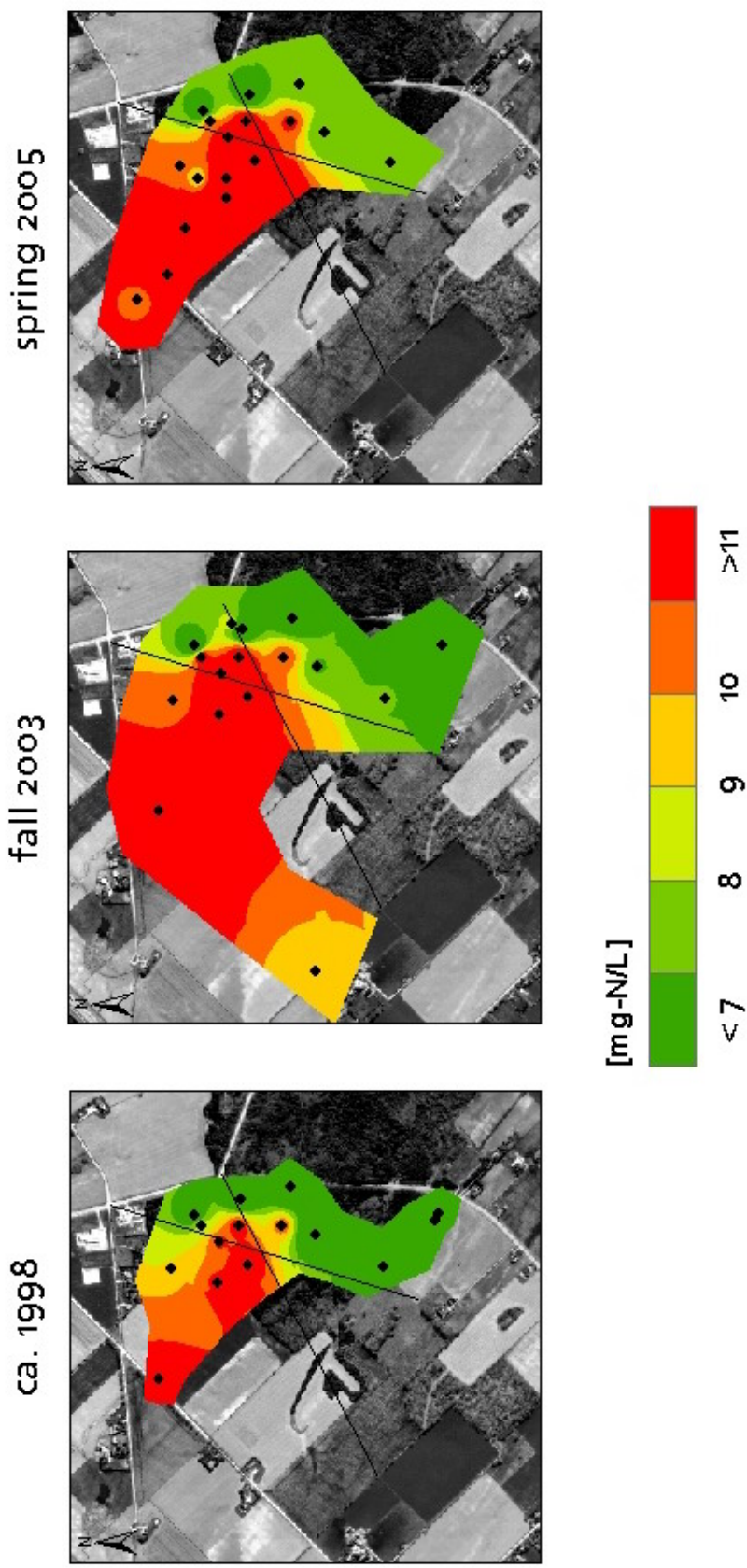
Figure 4.10:
Spatial analysis of nitrate concentrations in the observation wells of the Thornton Well Field. The crossing black lines are plotted at the same positions in each panel for comparison purposes. Plotted are the concentrations of the shallowest screen in Aquifer 3 at each of the locations indicated with a solid circle.
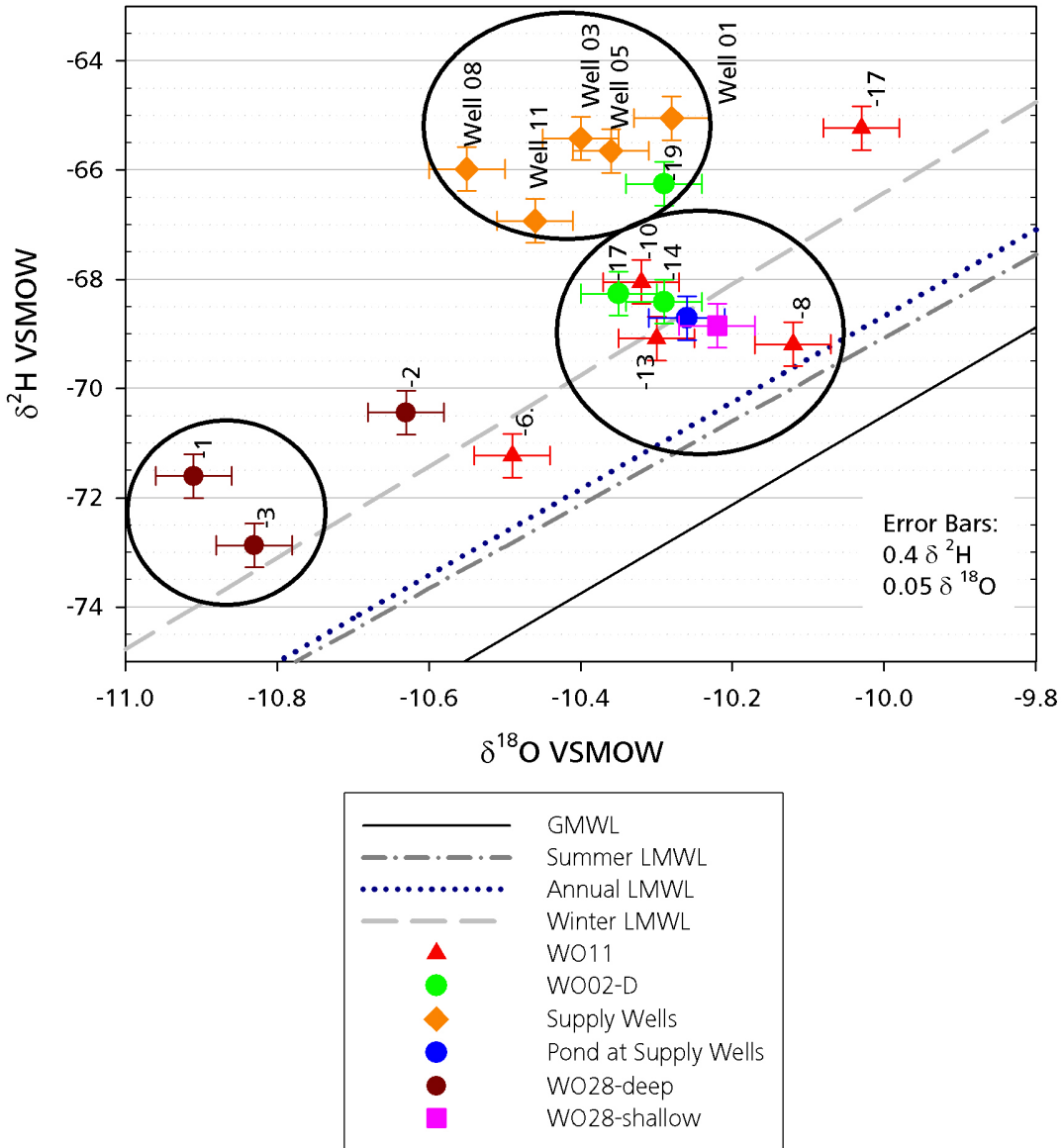
Figure 4.11:
Deuterium vs. Oxygen-18. Global Mean Meteoric Water Line (GMWL) taken from (*Clark and Fritz*, 1997). Local Meteoric Water Lines (LMWLs) after Fritz et al., 1987 as cited in *Stottler* (2002).
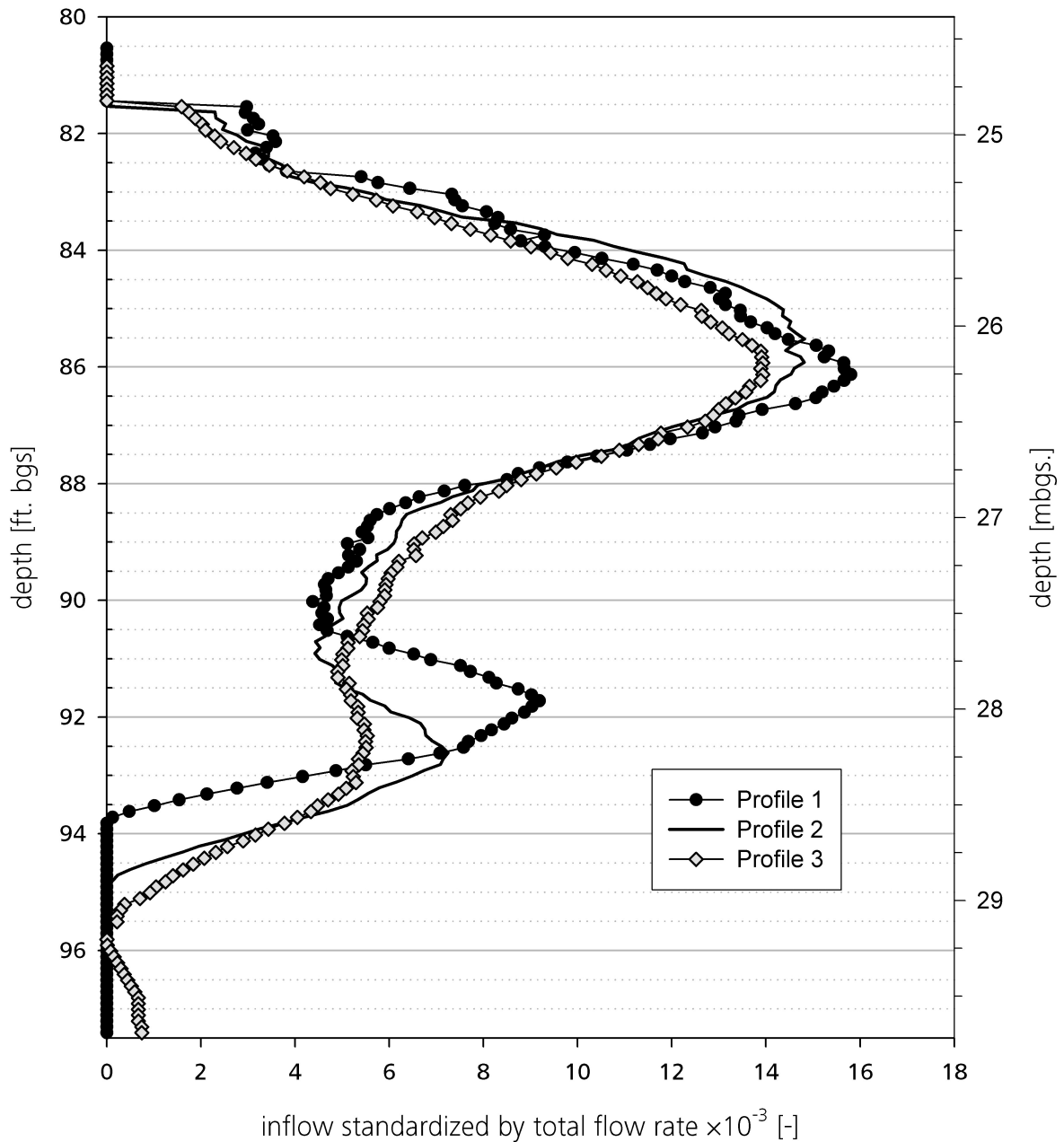
Figure 4.12:
Inflow profile along screen of Well 01. Inflow was measured every 0.5 ft. and standardized to the total flow rate from the well. Profile 1 was the first profile taken after pumping started with a rate of $3m^3$/min. Profile 2 and 3 were taken with a pumping rate of $4.5m^3$/min. Profile 3 was the last profile taken after ~14h of pumping. The small amount of inflow of water at the bottom of the screen during profile 3 is believed to be a measurement error.
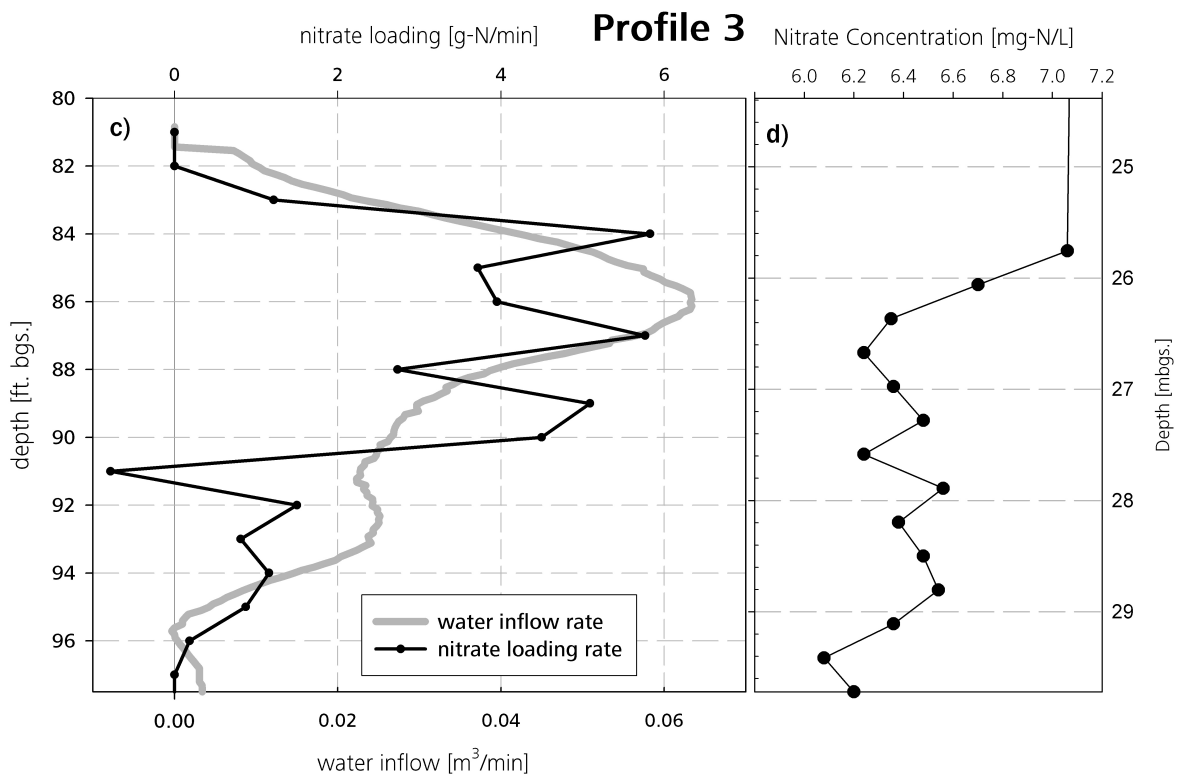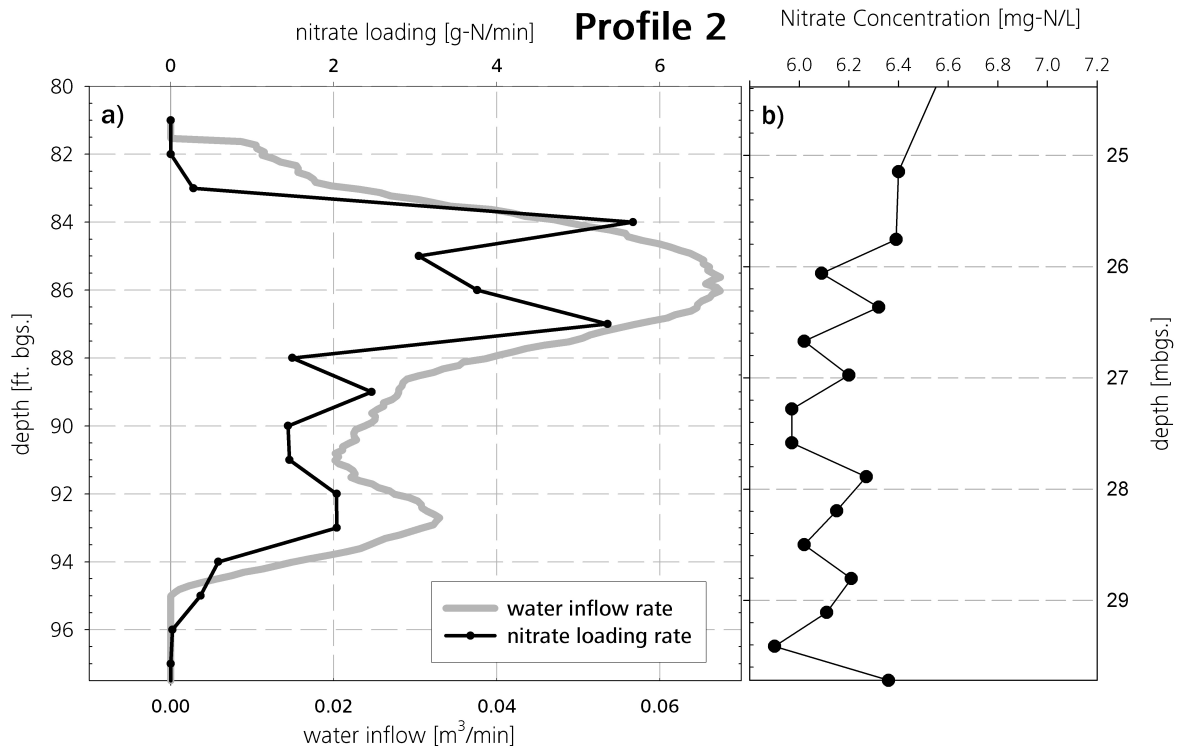
Figure 4.13:
Nitrate loading along screen of Well 01 for Profile 2.
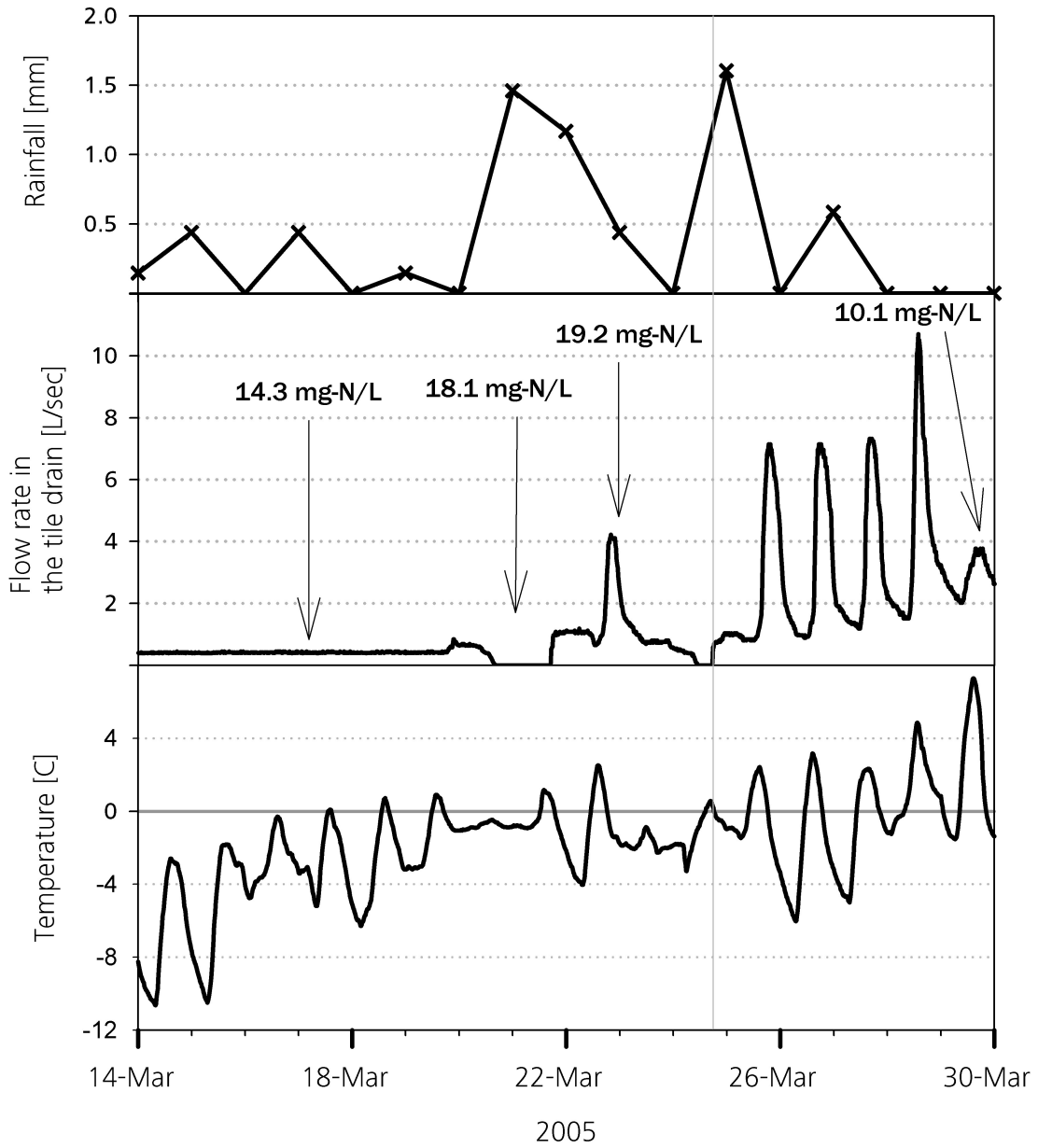
Figure 4.14:
Flow rate in main tile drain during spring melt 2005. The top panel shows daily rainfall. The middle panel flow rate calculated from measured water height. The bottom panel shows air temperature measured at ground surface next to the tile outlet. As soon as the temperatures during the day (the ticks are at midnight) increase above freezing point, flow in the tile line occurs.

Potentiometric Surface in Aquifer 3

Potentiometric Surface
in Aquifer 3
[masl.]

293 – 294.5
294.5 – 296
296 – 297.5
297.5 – 299
299 – 300.5
300.5 – 302

MOE data

1998–2004

2005

Legend does not apply

Thickness Unsaturated Zone

Thickness of
Unsaturated Zone
[m]

4.4 – 10
10.1 – 15
15.1 – 20
20.1 – 25
25.1 – 30
30.1 – 35

MOE data

1998–2004

2005

N

0   500 Meters
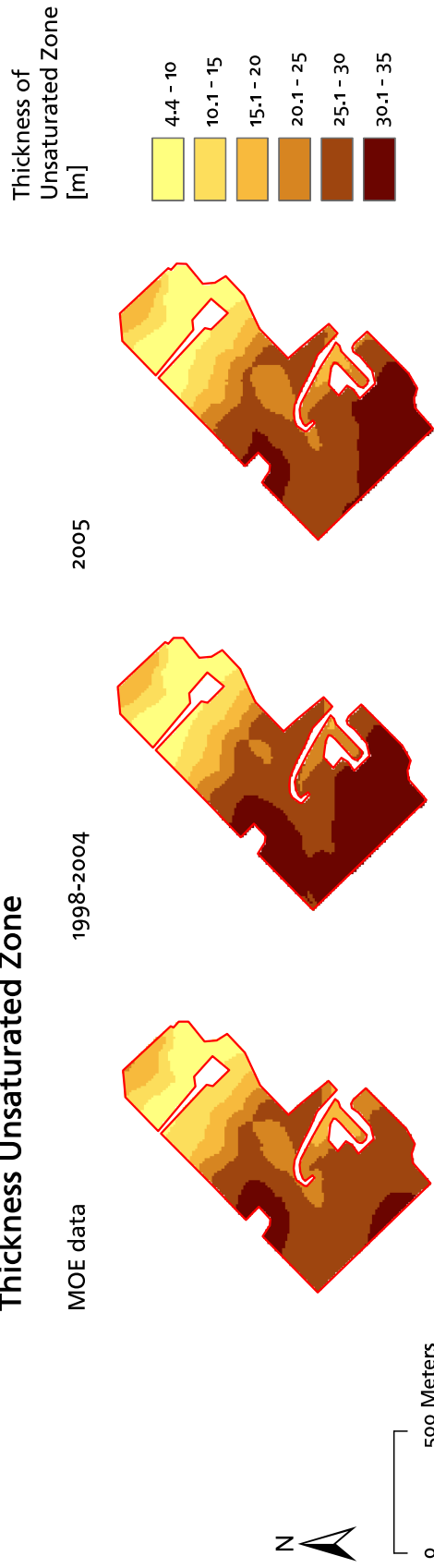
Figure 4.15:
Water table (upper panel) and unsaturated thickness (lower panel) below Parcel B. Both parameters are shown for the three different data sets used: the regional water table based on the MOE water well record database (see overview inset for used data points), one local water table interpretation based on data from 1998 to 2004, and a second local water table interpretation based on additional wells and measurements taken within a few weeks in spring 2005.

93

Average Nitrate Concentrations in the Unsaturated Zone

Location of Core

Average Nitrate Concentration

[mg-N/L]

- 0.9 - 6.7
- 6.8 - 11.5
- 11.6 - 15.0
- 15.1 - 17.8
- 17.9 - 20.5
- 20.6 - 24.9
- 25.0 - 31.0

Mean: 16.0 mg-N/L

250 m

0

5 km

0
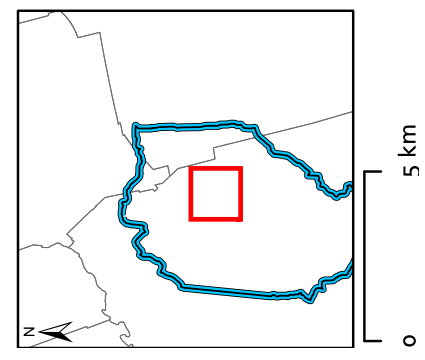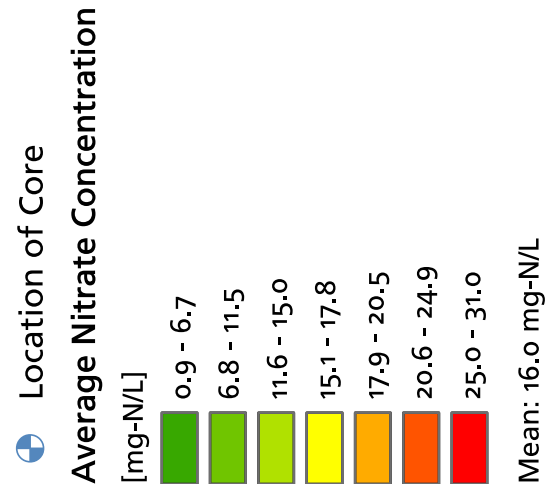
Figure 4.16:
Average aqueous nitrate concentration in the unsaturated zone.
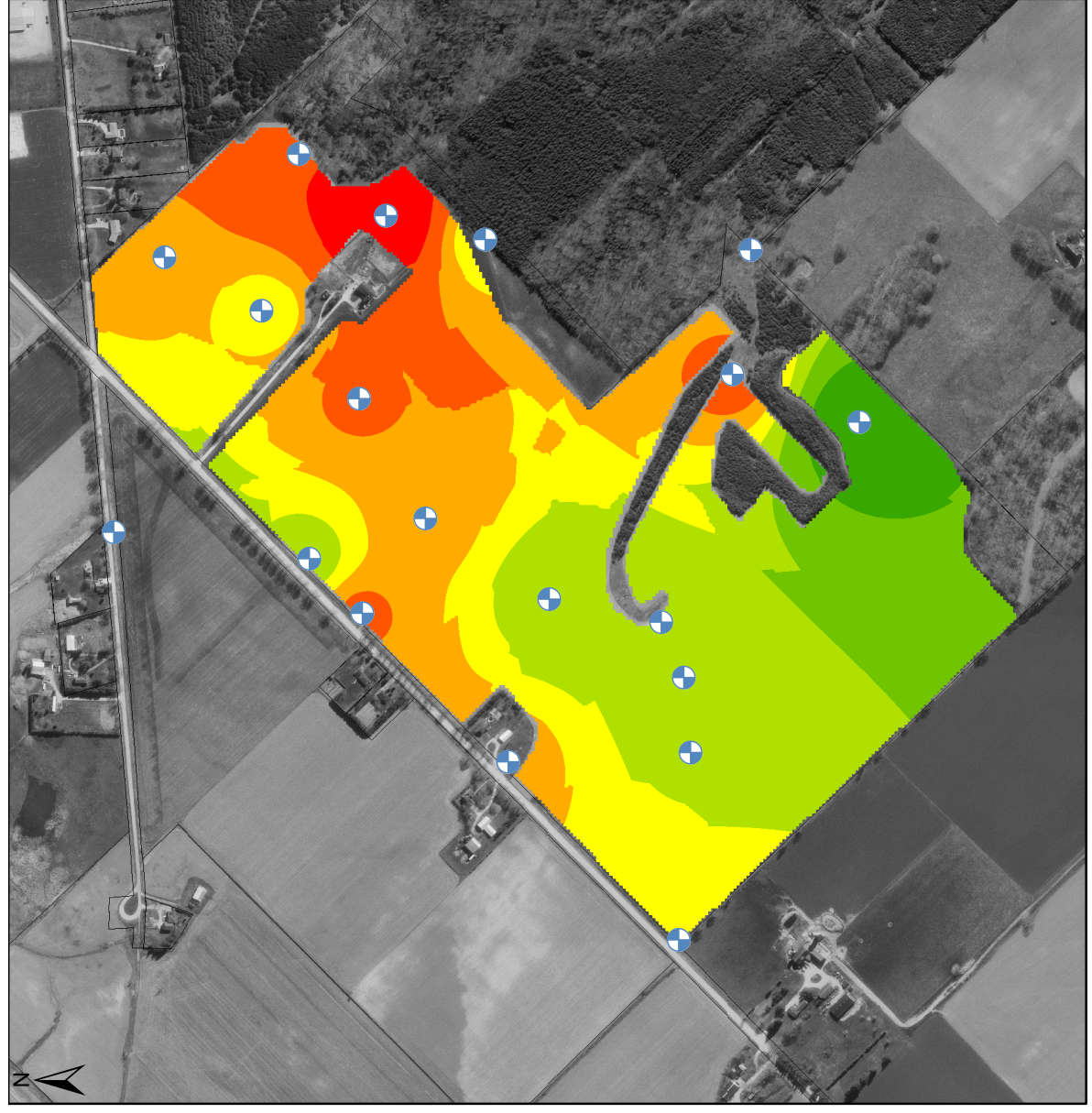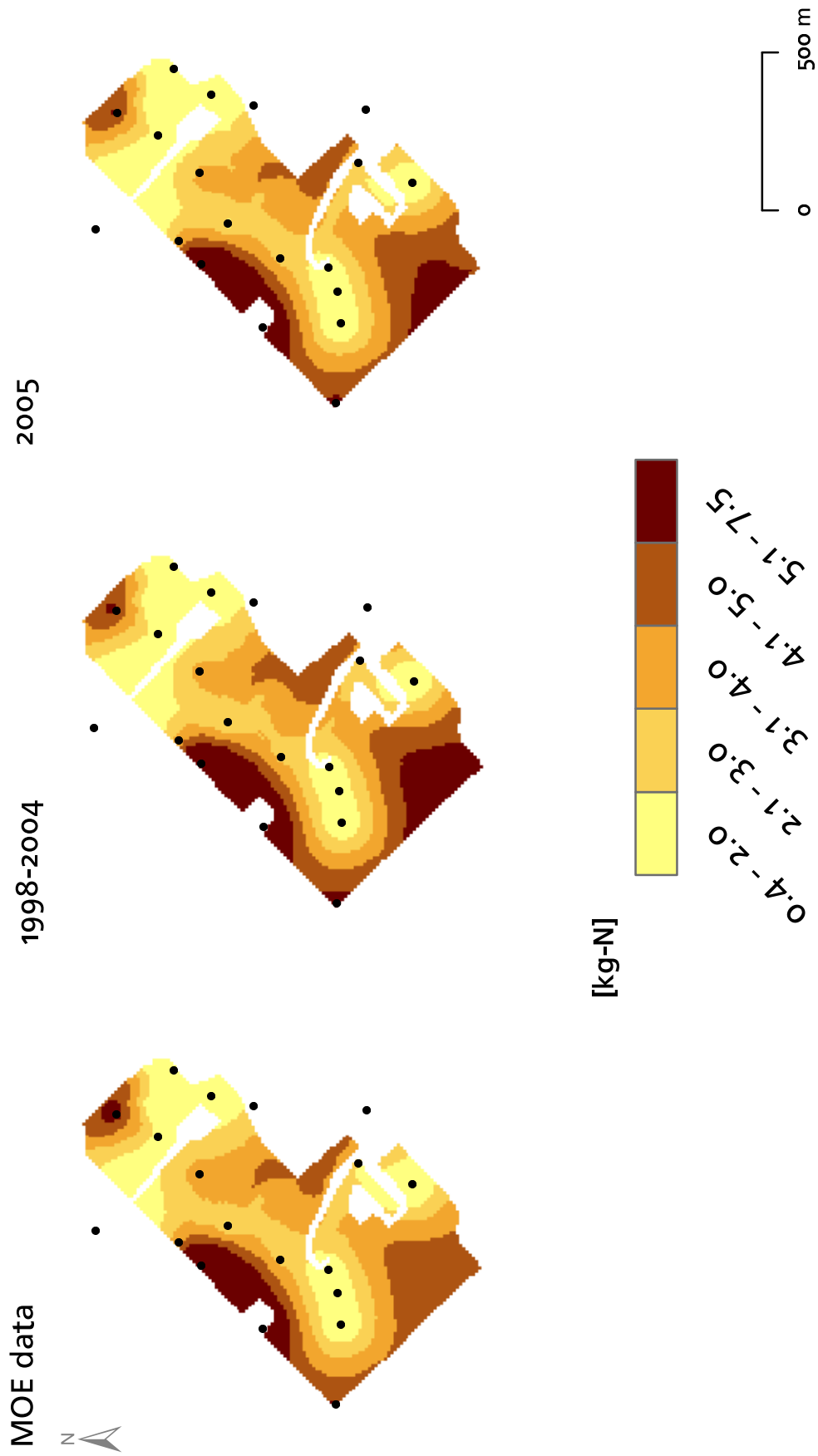
Figure 4.17:
Nitrate mass in unsaturated zone below Parcel B. Contoured is the mass in kg-N per 10m by 10m raster cell. The black dots indicate core locations. The scale and contour interval are the same for each of the three panels.

5

Enhanced Conceptual Hydrogeological Model

The spatial distribution of the hydrostratigraphic units is represented in a three-dimensional conceptual hydrogeologic model. These units which determine the flow path of groundwater and at some locations the advective nitrate pathways, are established within and beyond the study site. For support of the hydrostratigraphic model, the independent and complimentary data-sets described and analyzed in Chapter 4 were combined and integrated wherever possible. All data sets were evaluated simultaneously, but at two different spatial scales: (1) on a mid-regional scale between the two main drainage features, the Thames River and Cedar Creek (representative distance ~9km) which encompass the study site and are believed to influence the hydraulic conditions in Aquifers 3, 4, and 5; and (2) on a local scale between Parcel B and the Thornton Supply Wells (representative distance ~2km). This local scale encompasses the farm fields where the land-use changes are adopted and is the area where most of the detailed hydrogeologic information was available.

In this chapter the hydrostratigraphic sequence within the study site, its spatial distribution, and the pathways for nitrate movement that were identified, are discussed. The spatial extent of the flow model domain is then presented and discussed, followed by the description and rationale for the choice of flow boundary conditions.

Spatial Distribution of Hydrogeologic Units 5.1

The work of *Padusenko* (2001) served as basis for developing the conceptual hydrogeologic model, and was considerably enhanced by using the geologic log of the deep borehole WO 28-D, geologic logs of various shallower cores around the Thornton Well Field, borehole logs from the MOE's Well Record Database (*Ontario Ministry of the Envi-*

ronment, 2000), hydraulic head- and aqueous chemistry data, and geophysical surveys. The locations of all borehole logs used to construct this enhanced conceptual hydrogeological model are shown on Figure 5.1.

Sequence of Hydrostratigraphic Units

The geologic log of WO 28-D (Figure 4.1) served as main reference for the hydrostratigraphic sequence across the study site. These main hydrostratigraphic units are generally traceable across the study site, however due to the nature of the depositional environment (Section 2.2.2), the thickness of the hydrostratigraphic units varies, and therefore any unit can be locally discontinuous. The hydrogeological units were deposited in a layered sequence, with horizontal or slightly dipping surfaces. Each unit is listed in Table 5.1 along with a short material-description, thickness, and information on trends in average hydraulic gradients. The spatial distribution of Aquifer 1 and Aquitard 1 are known on the smaller scale only, and will be discussed primarily in Section 5.3.

Three main water supply aquifers were identified and mapped: Aquifers 3, 4, and 5. Aquifer 2 appears to be unsaturated throughout most of the study area; however, in the proximity of the well field, where this glaciofluvial outwash channel (Section 2.2.2) is part of Aquifer 2, saturated conditions were encountered. Within the general study site the distribution of wells screened in each aquifer unit were calculated (Table 5.2) to provide an indication of the contribution of each aquifer to the "non-public" water supply, although general pumping rates are not known. The data in Table 5.2 show that >60% of wells in the study site are screened in the deep units Aquifer 4 and/or Bedrock.

MacRitchie et al. (1994) stated that in the "*south-western part of South-Western Ontario*" the "*majority of wells obtain water from either a basal sand and gravel unit that lies directly on the bedrock, or from the upper* 1m *of the bedrock*". The small thickness of "*maximal* 6m *limits yield, but the unit is capable of supplying* 0.8L/s *to* 3.8L/s *of good to medium quality water*", which is in the estimated range determined at WO 28-D (Section 4.1). This basal unit most likely corresponds to the Columbus Limestone (Section 2.2.1). According to *MacRitchie et al.* (1994) the City of London, Ontario, ∼50km south-west of Woodstock, used such a basal aquifer for its municipal supply until 1967.

The distribution of the main hydrostratigraphic units on the regional scale within the study site was determined by the spatial analysis of 867 borehole logs from the MOE data base and those derived from the University of Waterloo drilling programs over the last six years. The surfaces of each hydrostratigraphic unit were spatially interpolated using kriging based on elevation "picks" of hydrostratigraphic layer surfaces from borehole logs, and in some cases the manual insertion of "soft" data points as described in Section 3.7.2. The top most layer on the regional scale is either Aquitard 2 or Aquifer 2. As previously stated, the existence and extent of the shallow units Aquitard 1 and Aquifer 1 are only known on the local scale and are discussed in Section 5.3. Aquitard 2 is originally defined on the local scale as the shallow, hard, cemented layer encountered during drilling of WO 28-D. Aquitard 2 is overlain either by Aquifer 1 (sandy material) or Aquitard 1 (clayey material). To maintain continuity of units, Aquitard 2 is defined on the regional scale as any aquitard-like material that can be spatially correlated to the local-scale Aquitard 1 or Aquitard 2.

The hydrostratigraphic layers that were established at WO 28-D were traced across the study site and generally they are continuous, but vary in thickness. Due to heterogeneity of the glacial deposits and the nature of the MOE borehole logs, it was not possible to make all data from every borehole log fit the conceptual hydrostratigraphic model, but overall, it is believed that a realistic representation was achieved. The highest data density of borehole logs in the MOE data base is in towns and along roads where private wells are located. In other areas little or no information is available. Additionally, some borehole logs are of poor quality; that is only few (sometimes even only one) material is logged for the entire depth of a borehole. Such information has little utility, because it does not provide insight into the (hydro-)stratigraphy.

Thickness of Hydrogeologic Units

The spatial distribution of each unit's thickness was estimated by subtracting the elevation of the bottom surface from the top surface. Such an isopach map is presented for each regionally known hydrogeologic unit on Figures 5.2, 5.3 and 5.4. A common feature of all these isopach maps is that the thickness of all units is zero at the center of the valley of the Thames River. This clearly illustrates that the Thames River cuts into the geologic sequence to bedrock.

Of major interest are zones where aquitards are absent and therefore two aquifers are hydraulically directly connected. *Frind et al.* (2002) and *Martin and Frind* (1998) showed that those zones, commonly referred to as "windows", have a major influence

on groundwater flow in complex geological settings. In the isopach map for Aquitard 3 (Figure 5.3) a window is clearly recognizable in the east-center of the study site. This location coincides with the location where *Padusenko* (2001) proved a connection between what in this study is called Aquifer 2 and Aquifer 3 . A similar window was identified in the north-west of the study site close to the Thames River in Aquitard 3 (Figure 5.3) and in the north-eastern corner of the study site in Aquitard 4 (Figure 5.4).

Aquifer 2 is associated with the spatial extent of the three hill features within the study site (Figure 5.2). In the vicinity of the northern hill feature, which is also the area of highest ground surface elevation within the study site, both Aquifer 2 and Aquitard 2 are estimated to be extremely thick. Unfortunately, within this ~1.5km by ~1.5km area only two borehole logs of poor quality exist, which results in a high degree of uncertainty regarding the interpolation of the surfaces of hydrogeologic units. However, the presence of extensive sand and gravel quarries in this area suggest that the interpolated thickness of Aquifer 2 may be justified. Aquitard 2 is also associated with the three hill features within the study site and seems to sit on top of Aquifer 2 wherever the overburden thickness was thick enough. In other areas, Aquitard 2 was mostly removed by erosion. At Well 01 and Well 05 of the Thornton Well Field Aquifer 3 is naturally under flowing artesian conditions, perhaps as a result of elevated pressure head due to recharge introduced into Aquifer 3 in this area of this northern hill feature. If this hydraulic support can be substantiated, then this area is important for the groundwater flow conditions in Aquifer 3.

The thickness of Aquifer 3 increases to ~22m towards the south-west of the study site, which is where highest hydraulic head values were observed. Extending from this south-west location towards the Thornton Well Field, Aquifer 3 is rather thick (10m to 20m). The thickness of Aquifer 4 is highly variable, between 0m and 5m (Figure 5.2). Aquitard 4 is the thickest unit, exceeding 30m in the south of the study site.

Spatial Distribution of Hydrostratigraphic Units

The regional distribution of hydrostratigraphic units was evaluated along the set of cross-sections shown on Figure 5.5. The scales are adjusted individually for each cross-section to fit on one page. The shape of any unit on a given cross-section can be influenced by a data point that is too far away from the section and therefore not shown. This is the main cause of changes of the distribution of hydrogeologic layers away from borehole locations. The distance [m] of a borehole perpendicular to the shown section is indicated by the value in brackets behind the name of the UW borehole. For boreholes from the MOE database the name of the boreholes are not shown.

The course of Cross-Section 3 (Figure 5.6) is along Curry Rd. and includes information drawn from the borehole logs of WO 28-D, WO 28, WO 29, WO 30, WO 32, WO 11, the resistivity-survey line 01, and various transient hydraulic head observations at WO 28-D and WO 11. The lower boundary represents the bedrock surface,

above which Aquifer 4 is located. Most of the private wells (the ones that are not labeled) along this section are completed in Aquifer 4 or Bedrock, which corresponds to the conclusions drawn from Table 5.2. Overlying Aquifer 4 is Aquitard 4, which is ~25m thick in the south-west, thinning significantly towards the north-east. The next hydrostratigraphic layer in the sequence is Aquifer 3, the main nitrate contaminated aquifer, with a maximal thickness of ~10m. At the location of WO 11 Aquifer 3 is very thin (a few meters), and overlain by an equally thin aquitard (Aquitard 3). Aquifer 2 is overlain by Aquitard 2 in the center-area of this cross-section and is unconfined or not existent elsewhere.

Cross-Section 4 (Figure 5.7) runs through the town of Sweaburg, parallel to and ~2km to the south-east of Cross-Section 3. Due to generally lower topographic elevations on this cross-section compared to Cross-Section 3, all units above Aquifer 2 are missing. Notable differences are the thicker Aquitard 4 on Cross-Section 4 and the downward slope towards the north-east of Aquifer 3. The rest of the sequence is very similar to Cross Section 3. Along Cross-Section 4, a few wells are shown with long (~40m) screens in bedrock.

Cross-Section C (Figure 5.8) is perpendicular to Cross-Sections 3 and 4, roughly between WO 28-D and the town of Sweaburg (indicated by the high density of boreholes in that area). The sequence of hydrogeological layers is very similar to that seen in Cross-Section 3. Aquitards 2 and 3 appear at ground surface and form a discontinuous semi-confining layer over Aquifer 2 and Aquifer 3. Most of Sweaburg's private wells in the north part of the town are screened in Aquifer 3, whereas most of the wells in the southern part are screened in Aquifer 4 and/or Bedrock. This is likely attributable to the fact that Aquitard 3 gets thicker farther in the south-east of the study site, and forms the bottom of the bed of Cedar Creek on this cross-section. In the north-west of Cross-Section C the valley of the Thames River appears and cuts through overburden to bedrock.

An overview with a set of regional-scale cross-sections is shown on Figure 5.9. The origin of the view is from the north of the study site, on the highest topographic location, looking southwards. It is clearly visible how some units (Aquitard 2 and Aquitard 1) exist only in areas of higher topographic elevation, how the thickness of units varies spatially, and where discontinuities in some of the hydrostratigraphic units exist.

Compared to the previous conceptual model established by *Padusenko* (2001), ~700 additional borehole logs (some of which were later deleted, because they were of poor quality) of the MOE database were included in the analysis. *Padusenko* (2001) used a ~18km^2 area for his hydrostratigraphic analysis, which was also the modelling domain. In this study, the area of analysis was increased to 100km^2, ~28km^2 within which are the new modelling domain. With this approach of establishing the hydrostratigraphic units beyond the new modelling domain, increased confidence in each hydrostratigraphic surface was achieved. By interpreting the boreholes in many different directions it was assured that the surfaces are smoother with significantly less local extrema compared to previous studies. By incorporating the independent complimen-

tary data sets and the great detail on the local scale into the analysis, a sound physical representation was achieved.

Local Scale Hydrogeologic Model | 5.3

On the local scale, in the vicinity of the Thornton Well Field and Parcel B, the majority of data across the study area (density of boreholes, depth of boreholes, detail of geologic logs of boreholes, density of complimentary data sets) are available and therefore the hydrogeologic conceptual model can be presented in more detail in this area. A series of smaller-scale cross-sections were selected from this analysis for presentation purposes and are shown on Figure 5.10. On the local-scale cross-sections (Figures 5.11, 5.12, and 5.13), the average hydraulic head for each piezometer is shown by a purple triangular water table symbol. These data were either taken from the static water level data set contained in the MOE data base (the same data was used for the potentiometric surfaces in Section 4.2), or are the average hydraulic heads observed in a UW monitoring piezometer.

Cross-Section along Curry Rd.

This Cross-Section 01 (Figure 5.11) is the same one as shown on Figure 5.6, but the presentation is now focussed specifically on the section between WO 28-D and WO 11. Apparent on this finer scale cross-section is the known presence of Aquifer 1 towards the south-west. This aquifer overlies Aquitard 2, the shallow, hard, cemented layer encountered during drilling of WO 28-D (see Figure 4.5 for the presumed extent of Aquitard 2). Aquitard 2 is believed to support occasionally a perched water table in Aquifer 1. Water within this aquifer flows under the influence of gravity towards lower lying areas and forms springs where Aquitard 2 intercepts ground surface (between WO 30 and WO 32). The formation of springs in farm fields at this location, especially during spring melt is a frequently observed phenomenon by farmers. Other evidence (*Robertson et al.*, 1996) suggests that aquitards similar to Aquitard 2 are fractured, and weathered, allowing recharge to occur and nitrate to be oxidized by Pyrite. Some additional information would be needed to further investigate into the physical properties of Aquitard 2.

Outside the area where Aquitard 2 exists (Figure 4.5), the distinction between Aquitard 1 and Aquitard 2 is difficult to interpret and therefore they are combined to form one hydrostratigraphic unit. The combined unit Aquitard 1/Aquitard 2 exists directly below ground surface at the location of WO 11. More than ∼5m away from WO 11 a connection from ground surface to Aquifer 2 exists as is indicated by the resis-

tivity survey line 01 (Section 4.3.1) and by the monitored responses of hydraulic heads to rainfall (Chapter 4.4). The geologic log at WO 11 indicates a clay layer between the deepest piezometer (screened in Aquifer 3) and the second deepest piezometer (screened in Aquifer 2), suggesting the presence of Aquitard 3 at this location. The distinctly higher hydraulic head and lower nitrate concentrations in the deeper piezometer compared to other piezometers at this location, and the interpretation of the resistivity survey (Figure A.1) support a continuous Aquitard 3 at this location.

The continuous nature of Aquifer 3 is supported by similar hydraulic head values at the lowest piezometer at WO 11 and piezometer WO 28-D-04, which are both screened in Aquifer 3. The nitrate concentrations at WO 28-D-04 were always considerably higher during this study than those at the deep piezometer at WO 11 ($\sim$9mg-N/L compared to $\sim$0.5mg-N/L). It is believed that those nitrate concentrations are different as a result of the groundwater flow direction which is perpendicular to this cross-section in Aquifer 3. The source of nitrate at WO 28-D-04 is therefore assumed to be upgradient.

The upper piezometers at WO 11 are screened in Aquifer 2 and these piezometers yield a good amount of water with elevated nitrate levels. The shallowest piezometer was observed to be dry in the Summer 2004 suggesting that occasionally unsaturated conditions are present in Aquifer 2 at WO 11. Piezometers farther away from WO 11, and located at a higher elevation in Aquifer 2 were found to be unsaturated. The observed hydrogeologic parameters and the spatial dimensions of Aquifer 2 at WO 11 suggest that the "Glaciofluvial Outwash Channel", which was described in Section 2.2.2, is part of Aquifer 2 and appears in the north-east along this cross-section.

Cross-Section 05

Figure 5.12 shows Cross-Section 05 whose orientation runs roughly parallel to Curry Rd., and through the supply wells of the Thornton Well Field. Due to lower topographic elevations along this cross-section, hydrogeologic units above Aquitard 2 are missing. In the southern part of this cross-section, Well 11, Well 08, and Well 03 are screened in approximately the same elevation in Aquifer 3. South of Well 03, the elevation of Aquifer 3 drops $\sim$20m within a horizontal distance of $\sim$200m, and in this low-lying area of Aquifer 3 the screens of Well 01 and Well 05 are located.

In the topographic low area along this cross-section the long-term average hydraulic head in some piezometers is close to or above ground surface (WO 02), indicating flowing artesian conditions in the Sweaburg Swamp area (Section 2.1).

Cross-Section along the Glaciofluvial Outwash Channel

Figure 5.13 shows Cross-Section 0d, whose course is perpendicular the two previous presented cross-sections, between WO 11 on Section 01 in the north-west and Well 01

on Section 05 in the south-east, coinciding with the middle of the "Glaciofluvial Out-wash Channel". Similar to the conditions along Cross-Section 05, Aquifer 3 dips towards Well 01 on Cross-Section 0d. It is directly connected in at least two locations to Aquifer 2, as indicated by the borehole data analysis here, and the pumping test conducted by *Padusenko* (2001). Aquitard 3 is very discontinuous in the central part of this section (Section 5.2). Towards the south-eastern end of this section it reaches considerable thickness, similar to the description provided by *Padusenko* (2001).

Cross-Section 0h

Cross-Section 0h extends from WO 28-D across Parcel B towards the Thornton Well Field, where it reaches Well 08. Bedrock and Aquitard 4 are existent everywhere along the cross section and slightly dip towards the Thornton Well Field. Aquitard 4 is ~20m thick along the entire cross section, which is only based on the geologic logs of WO 28-D and Well 01/Well 05. Aquifer 4 and Aquifer 3 are connected in the shown area of the Thornton Well Field (around Well 08 and WO 12), where Aquitard 3 does not exist, as indicated by borehole logs in the area and no hydraulic head differences between the piezometers at WO 12. To the east, Aquifer 3 and Aquifer 2 pinch out. Areas where recharge into Aquifer 2 is possible were identified around WO 42 and west of WO 45, due to pinch-outs in Aquitard 2 and Aquifer 2 reaching ground surface. The connection from those two areas allowing infiltration into the system to Well 08 is considered to be an important pathway for nitrate reaching the supply wells of the Thornton Well Field.

Local Scale 3D Fence Diagram

Figure 5.15 includes all the previous local scale cross-sections and forms an impression of the three-dimensional spatial distribution of the hydrogeological units. Aquifer 3 dipping towards Well 01 is visible, as well as the above described locations of discontinuous units.

Nitrate Migration Pathways | # 5.4

Based on the field investigation results and analyses discussed in Chapter 4 and the spatial distribution of hydrogeological units presented in Section 5.1, the conceptual model of nitrate migration pathways within the study area consists of the following components:

1. Little nitrate mass is present in Aquifer 4 based on data from WO 28 and therefore the pathways associated with Aquifer 4 are not considered significant to the nitrate loading on the Thornton Well Field. Additionally, isotope analysis suggests that the water found in Aquifer 4 is at least 50 years old, reducing the probability that it contains nitrate.

2. Figure 5.16 presents the spatial distribution of nitrate along Cross-Section 0d based on data from the Spring 2005 sampling episode. This cross-section contains eight locations that historically have had the highest nitrate concentration levels across the study site (Section 4.5.2). In this cross-section, groundwater flows primarily from the north-west towards the Thornton Well Field. Notice that upgradient nitrate concentrations are low and where a connection to ground surface occurs, elevated nitrate concentration are observed. To the north-west of WO 40, several tile drains converge and surface water ponding and rapid infiltration have been reported in this area by farmers and observed in both Spring 2004 and Spring 2005. The average nitrate concentration in water samples from a tile drain outfall near WO 40 ("TD at WO 40", see location on Figure 3.4 and see picture in Appendix A.5) is ~20mg-N/L. This tile drain is simply allowed to discharge freely into a wet well where water infiltration occurs; however, during spring melt the flow rate into the wet well exceeds the infiltration rate and water ponds over the surrounding ground surface. When environmental conditions are suitable, this ponded water infiltrates. The core log of WO 40 shows a permeable zone between ground surface and the top of Aquifer 2 which is located ~6mbgs. In January 2005 the nitrate concentration in WO 40 was observed to be 10.3mg-N/L. Nitrate concentrations in the shallow piezometers at WO 11 have been the highest observed concentrations in any observation well within the network of wells installed by the University of Waterloo (16mg-N/L in Fall 2004). The evidence presented above, along with the bore log analysis, results from the transient hydraulic head measurements from Section 4.4, observed zones of rapid flushing deeper into the system (Section 4.8), and the results of resistivity survey line 01, indicates that depression-focussed recharge occurrs in the area around WO 11 and WO 40. Therefore it is vulnerable to nitrate applications on ground surface. Nitrate mass that enters Aquifer 2 either near WO 40 or farther down-gradient due to near surface connections migrates towards the well field and spreads into Aquifer 3 where discontinuities in Aquitard 2 are present.

3. The estimated pathway of nitrate observed in Aquifer 3 in WO 28-D-04 across Parcel B towards the Thornton Well Field may be estimated from Cross-Section 0h. Unfortunately, along this cross-section, not enough nitrate concentration data are available to support the pathways estimated from geologic logs. Through the above-described locations where Aquifer 2 reaches ground surface, infiltrating nitrate can be drawn towards the connection to Aquifer 3, where it joins the nitrate-contaminated water and is being drawn towards the supply wells.

Table 5.1:
Overview over hydrostratigraphic units.

Unit	Material	Thickness	$\sim i_h$	$\sim i_v$	Comments
Aquitard 1	clay	maximal 5m	—	—	surficial clay above Aquitard 2
Aquifer 1	sand	maximal 5m	—	—	surficial sand above Aquitard 2
Aquitard 2	hard, cemented, dry, thin; consisting of a mix of clay, silt, sand, and pebbles up to diameters of 1cm	1m to 5m	—	—	shallowest confining unit, supporting at places an occasional perched water table
Aquifer 2	sand and gravel aquifer	0m to 40m	—	—	saturated within the glaciofluvial outwash channel, otherwise mostly unsaturated.
Aquitard 3	Gravelly clay, often cemented with fines (silt)	0m to 10m	—	—	
Aquifer 3 ("Upper Aquifer")	sand and gravel	laterally extensive to the west of the well field; proven to be connected to Aquifer 4 in the vicinity of the well field (*Padusenko*, 2001); 0m to 25m	0.005	downwards into Aquifer 4 in the western/north-western part of the study site 0.75;	the Thornton Supply Wells are screened in this unit
Aquitard 4	material between Aquifer 4 and Aquifer 3 (see page 54)	5m to 20m	—	—	in MOE Well Records often described as "hardpan" or as a "stoney/bouldery/hard" layer
Aquifer 4 ("Lower Aquifer")	thin, productive; gravel and (coarse) sand	nowhere >10m; pinches out at places	0.002	upwards into Aquifer 3 in the eastern part of the study site 0.25	material and possible pumping rates fit the description in *MacRitchie et al.* (1994).
Aquifer 5 (Bedrock)	fractured limestone; belongs to the Detroit River Formation	>5m	0.0008	upwards in the northern part, downwards in the southern part of the study site	

Table 5.2:
Number of screened wells within each aquifer unit.

Unit	Number of Screens in Unit	Percent of Total
Aquifer 3	64	20%
Aquifer 4	37	11%
Aquifer 4 and Bedrock	69	21%
Bedrock	96	29%
Other Units	61	19%
Total	327	100%
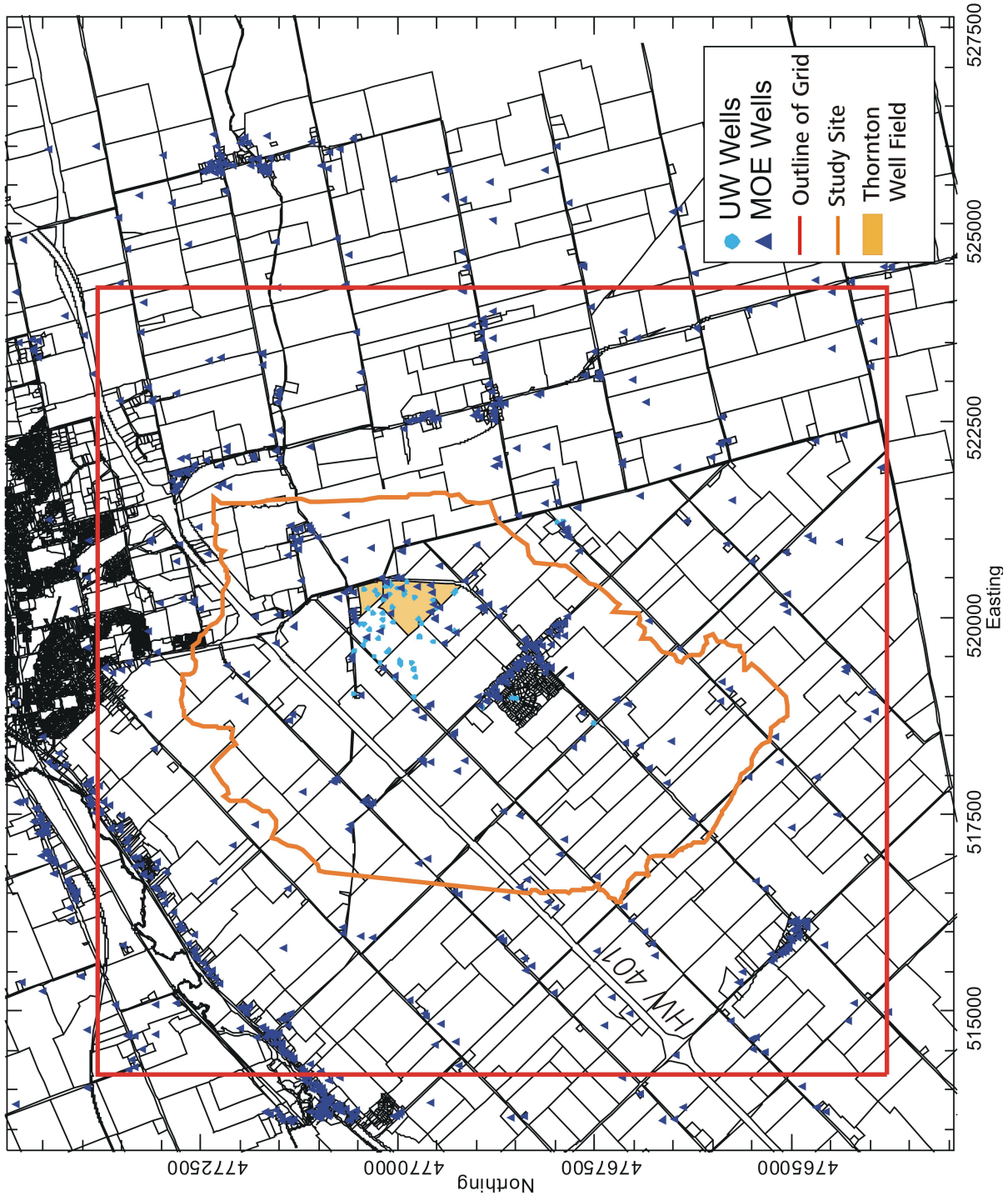
Figure 5.1:
Borehole locations used to construct the conceptual hydrogeologic model. The red rectangle indicates the boundaries of the grid used for interpolating the surfaces of the hydrogeologic units, the orange line represents the boundary of the study site. The area around the Thornton Well Field is shaded in light orange.
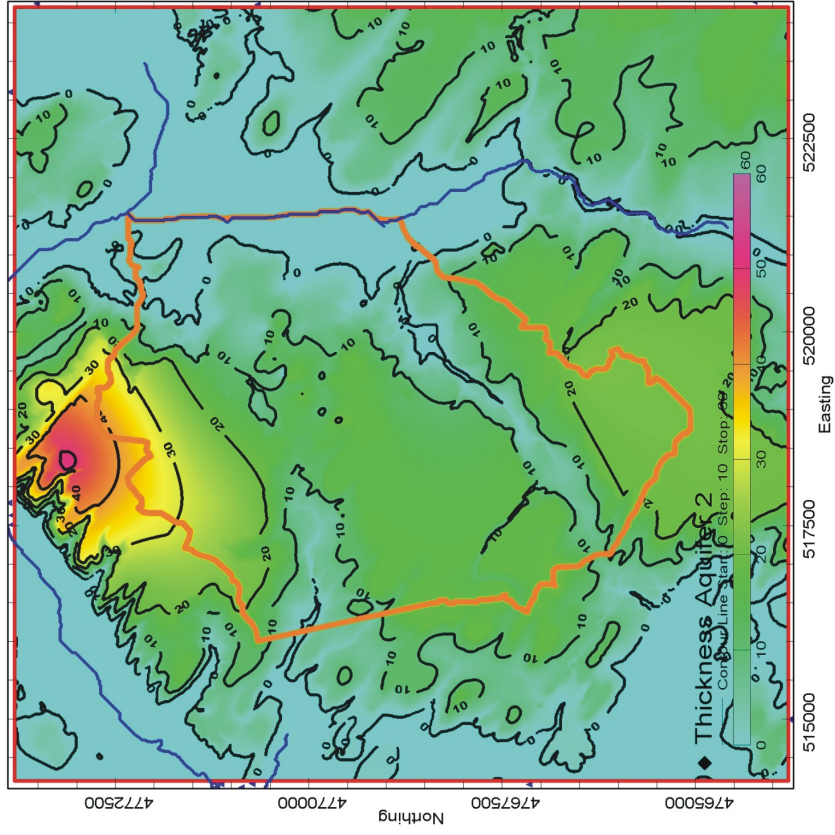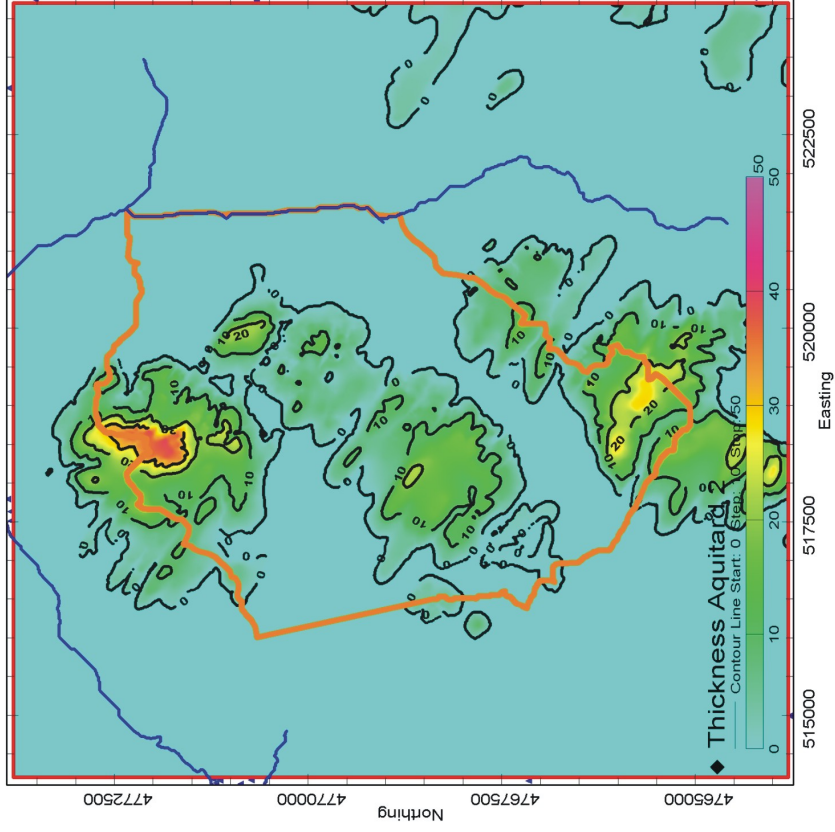
Figure 5.2:
Isopach maps for Aquifer 2 and Aquitard 2.
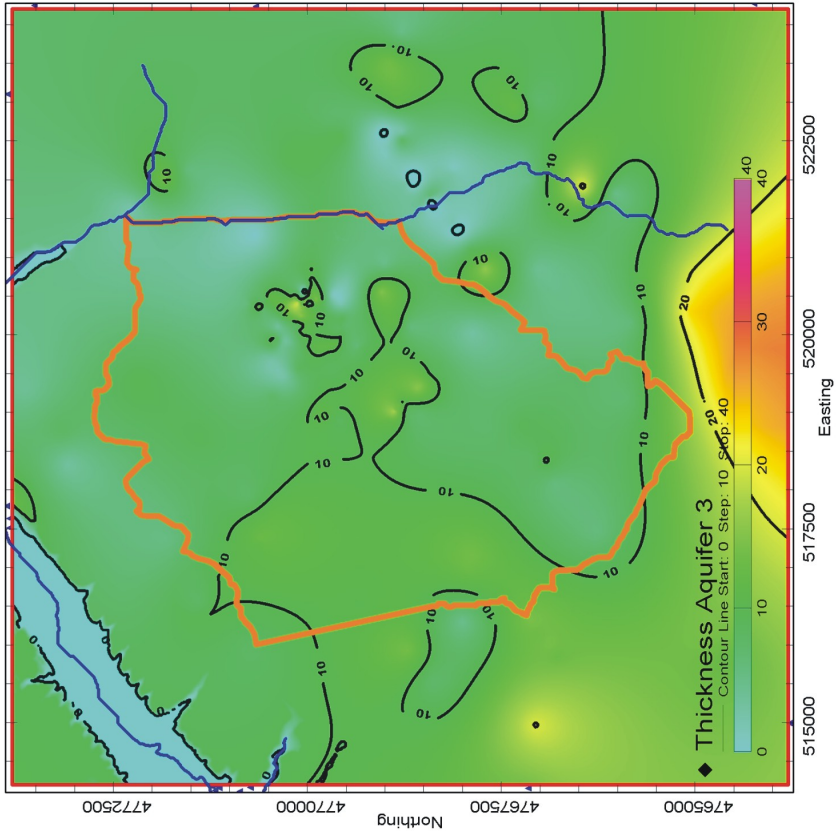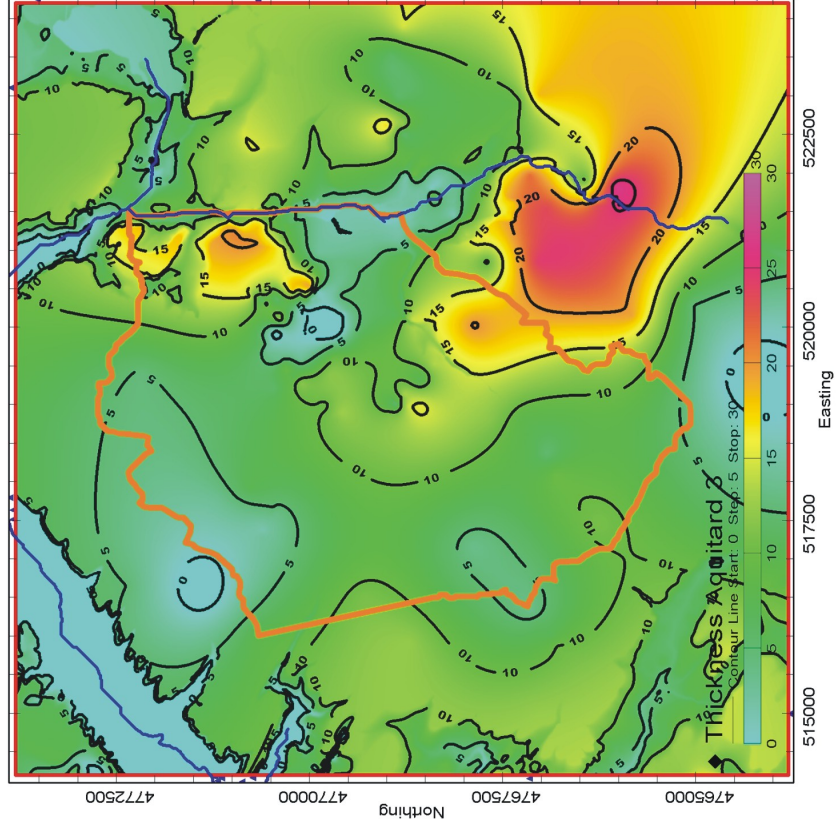
Figure 5.3:
Isopach maps for Aquifer 3 and Aquitard 3.
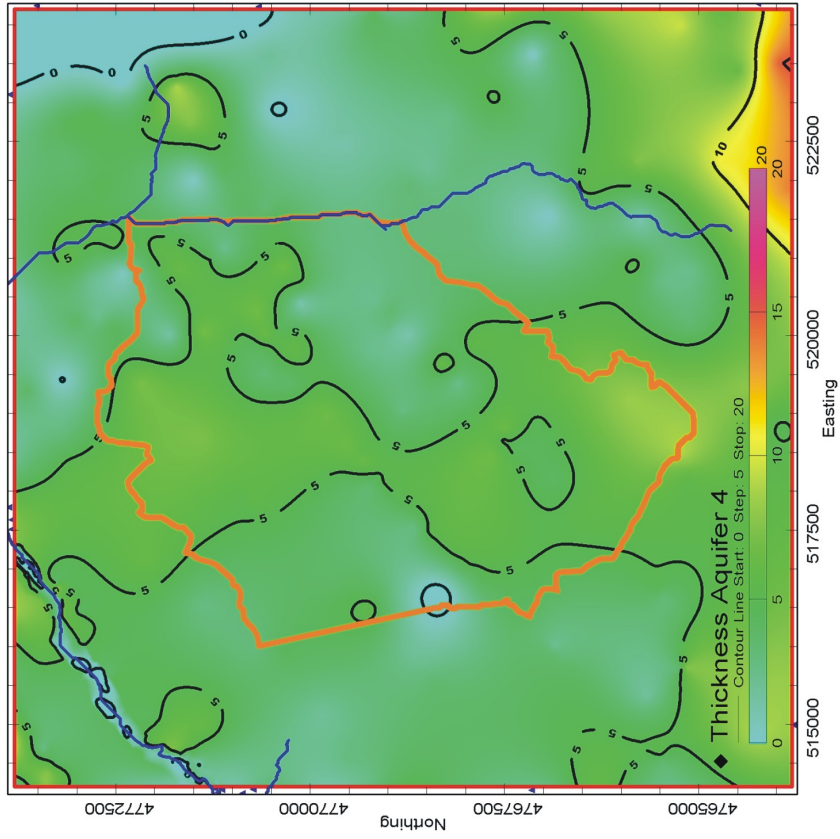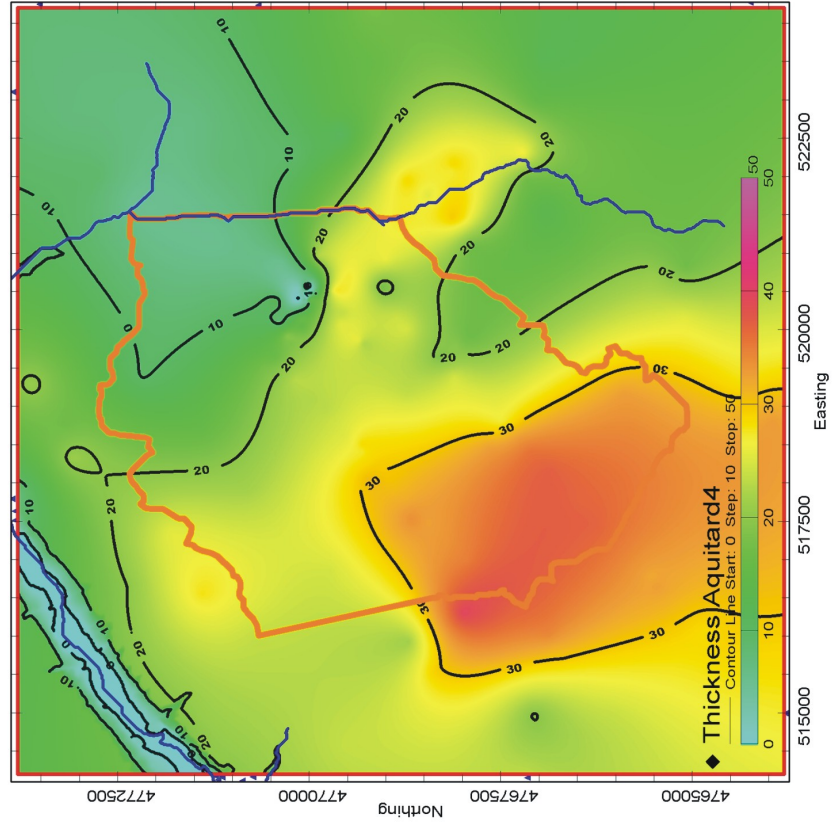
Figure 5.4:
Isopach maps for Aquifer 4 and Aquitard 4.
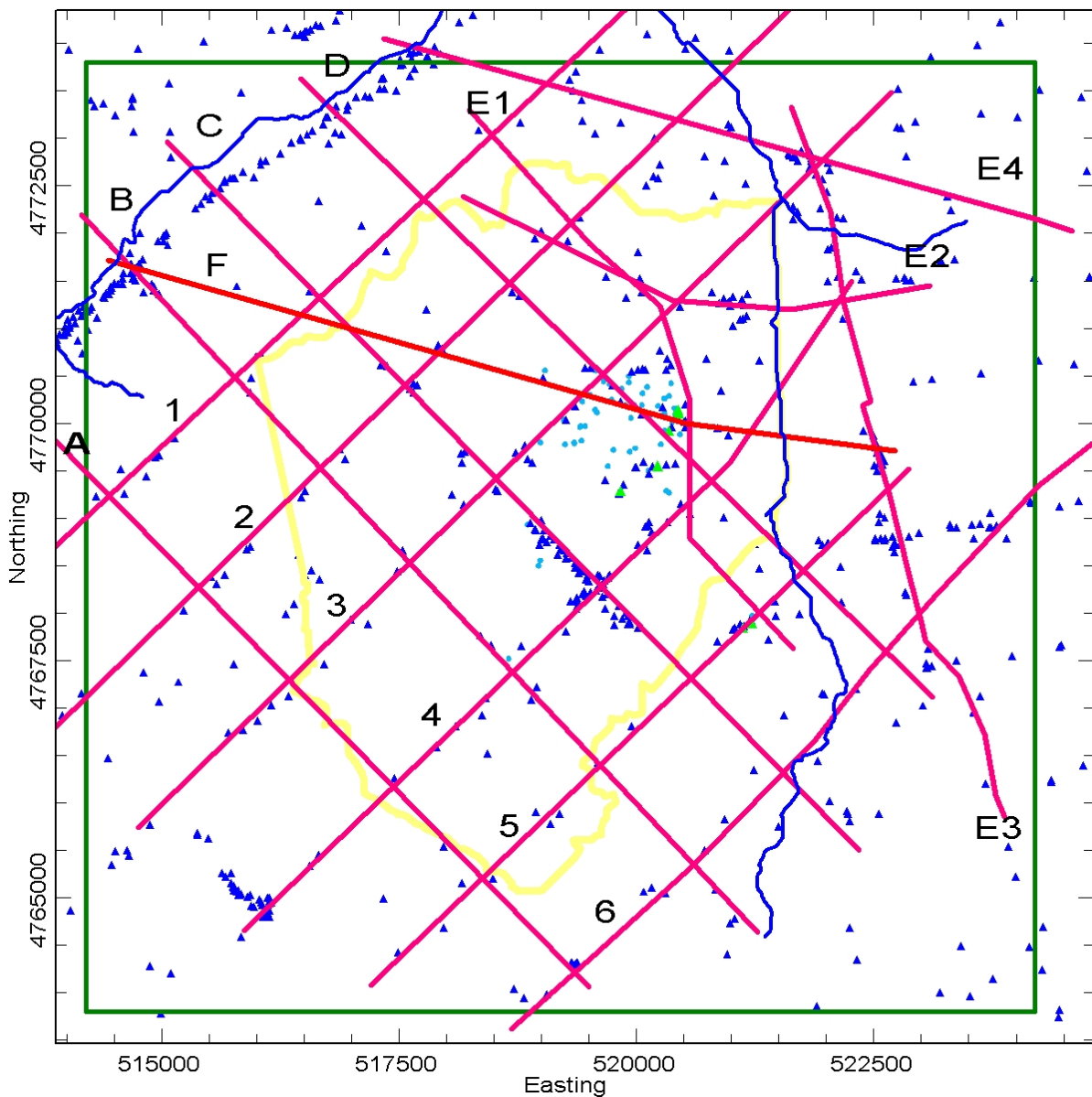
Figure 5.5:
Overview over the courses of cross-sections, set-up for the design of the regional conceptual hydrogeologic model. Shown lines are: in yellow the study site, in green the outline of the grid for interpolation of the hydrogeologic surfaces, in blue the stream network, and in magenta the course of cross-sections. Dark blue dots represent locations of boreholes in the MOE Water Well Record Database, light blue dots represent the UW borehole locations and green dots the wells of the supply wells of the Thornton Well Field.
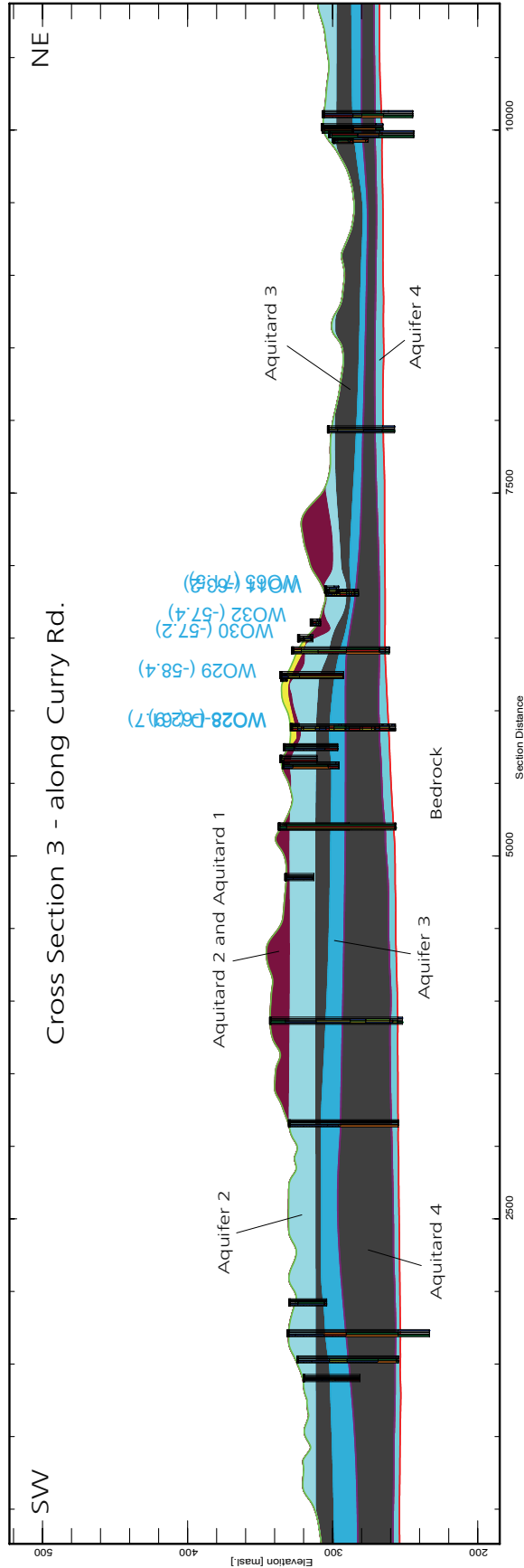
Figure 5.6:
Cross-Section 3.
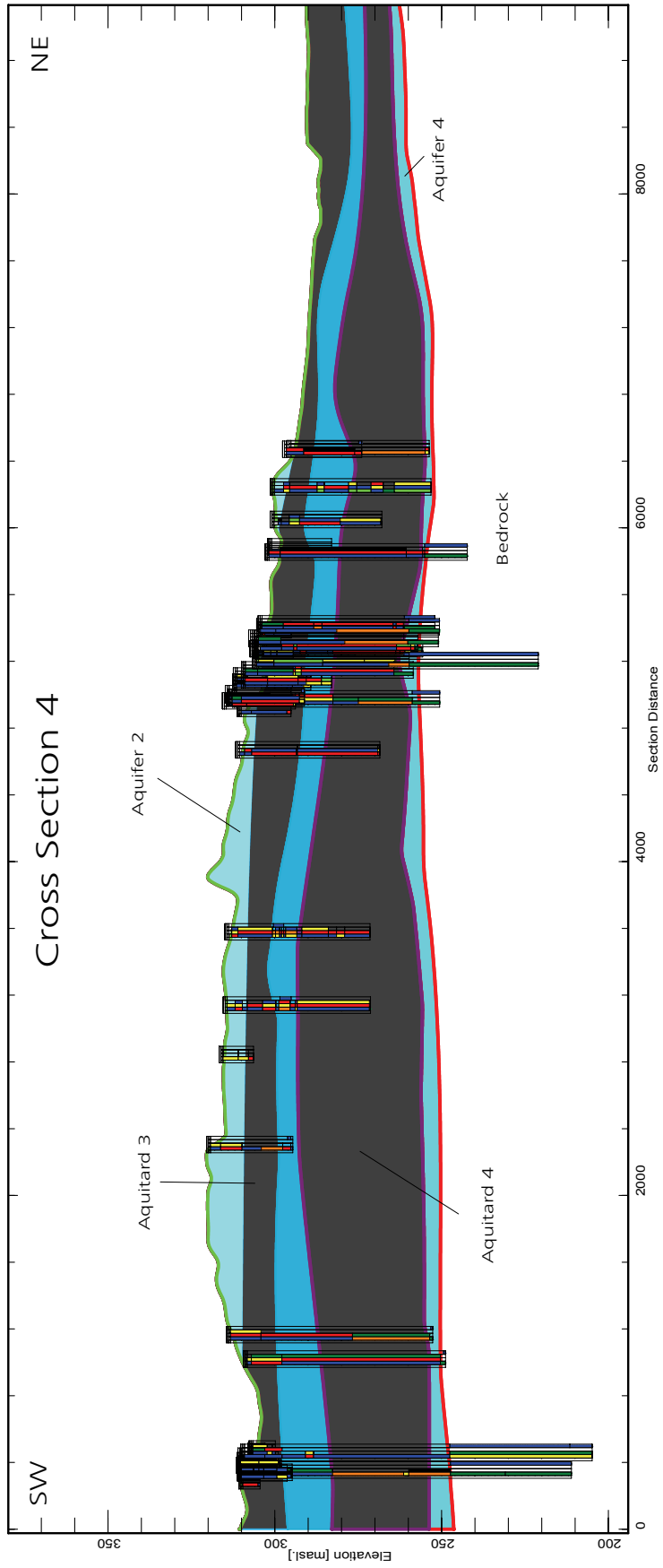
Figure 5.7:
Cross-Section 4.
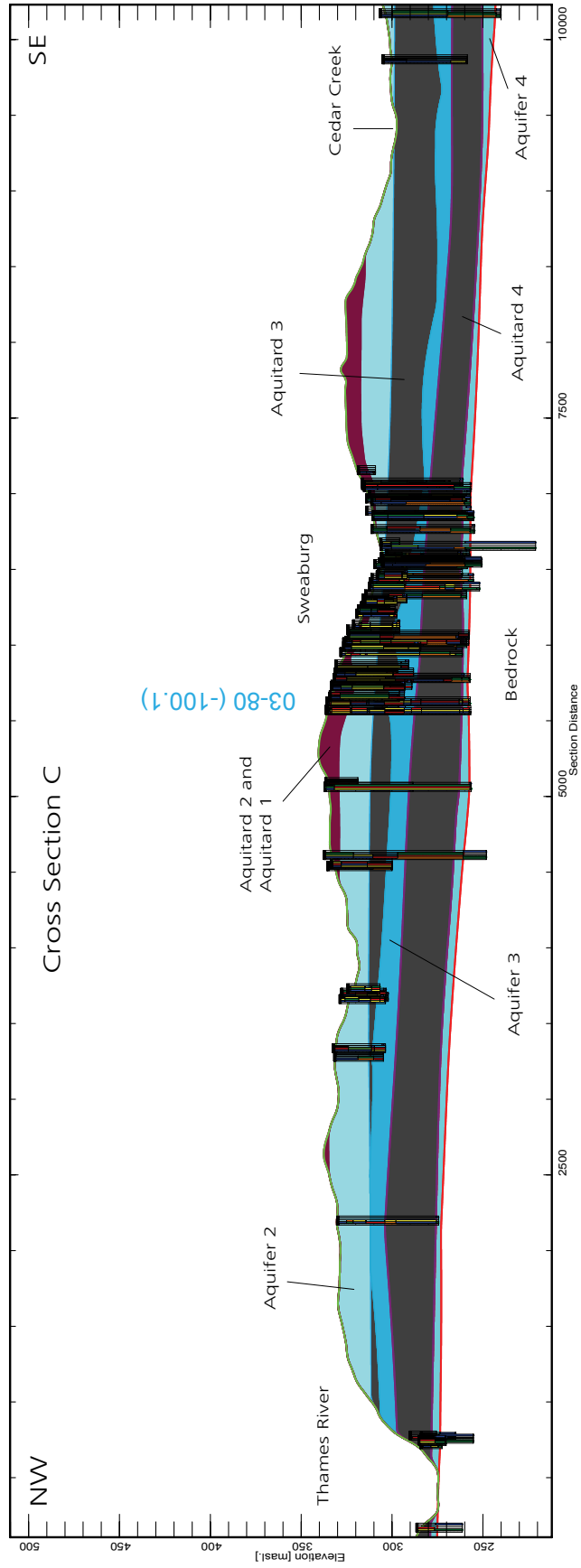
Figure 5.8:
Cross-Section C.
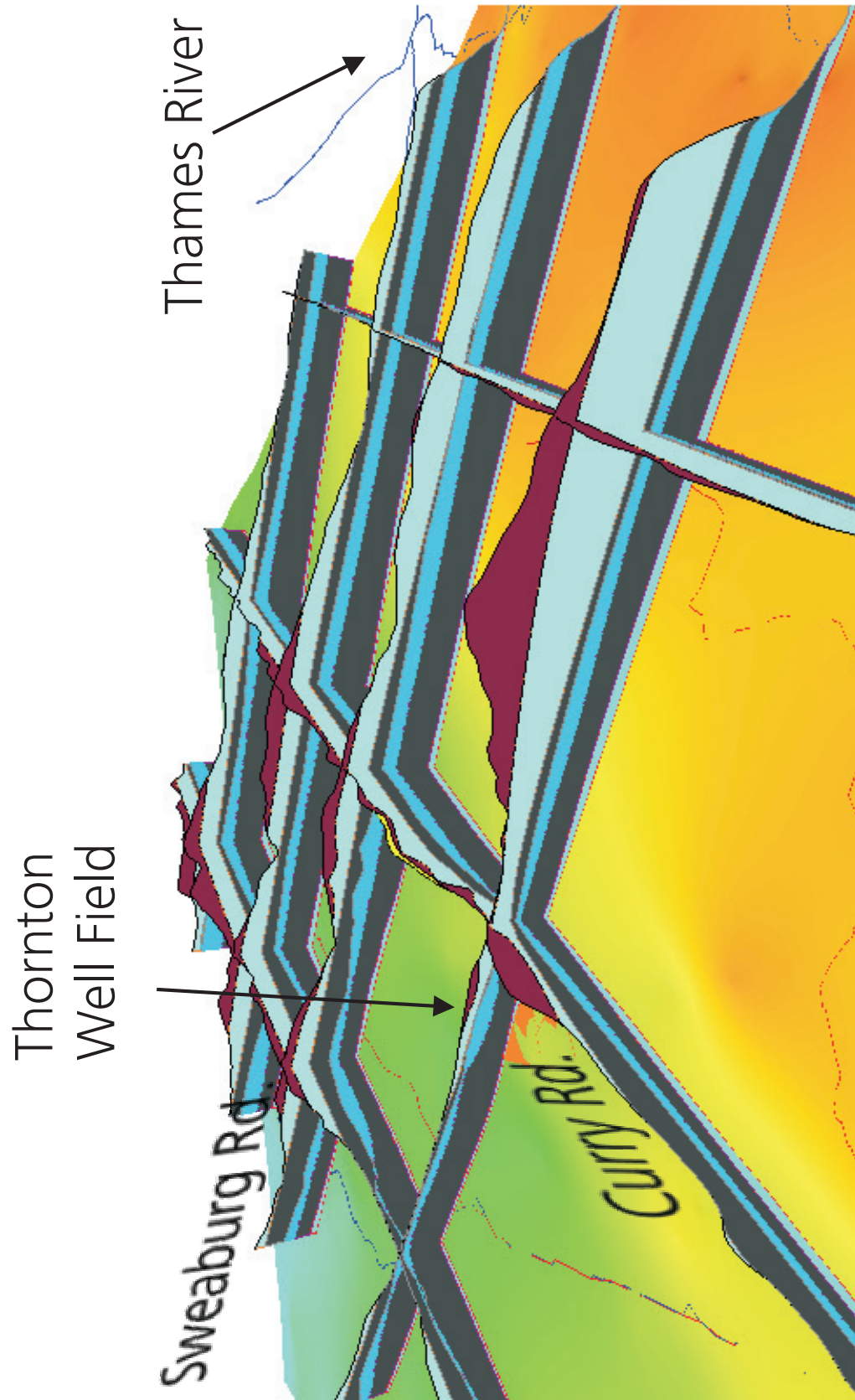
Figure 5.9: Regional 3D view of hydrostratigraphic units.
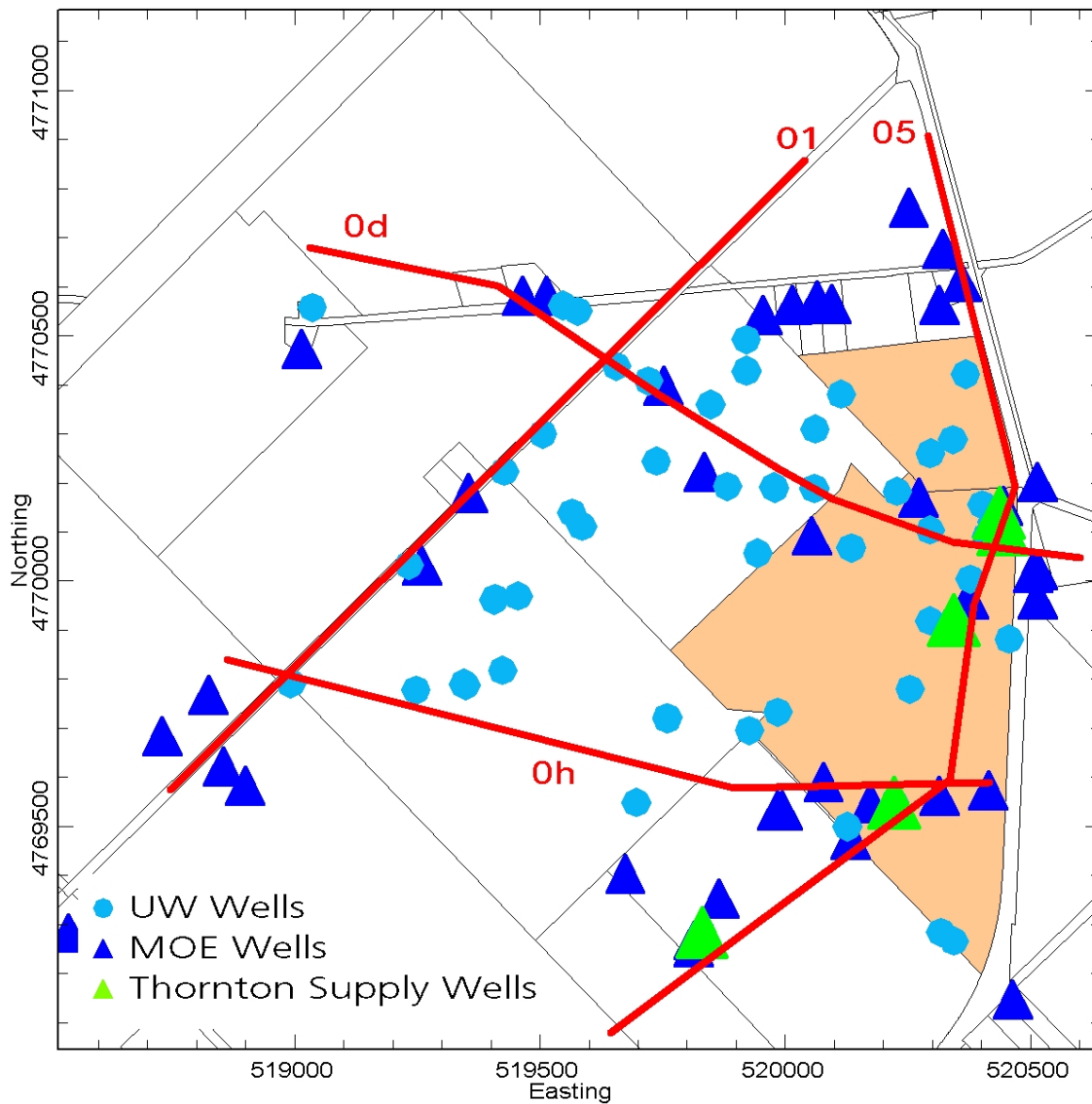
Figure 5.10:
Overview over the courses of cross-sections, set-up for the design of the small scale conceptual hydrogeologic model.
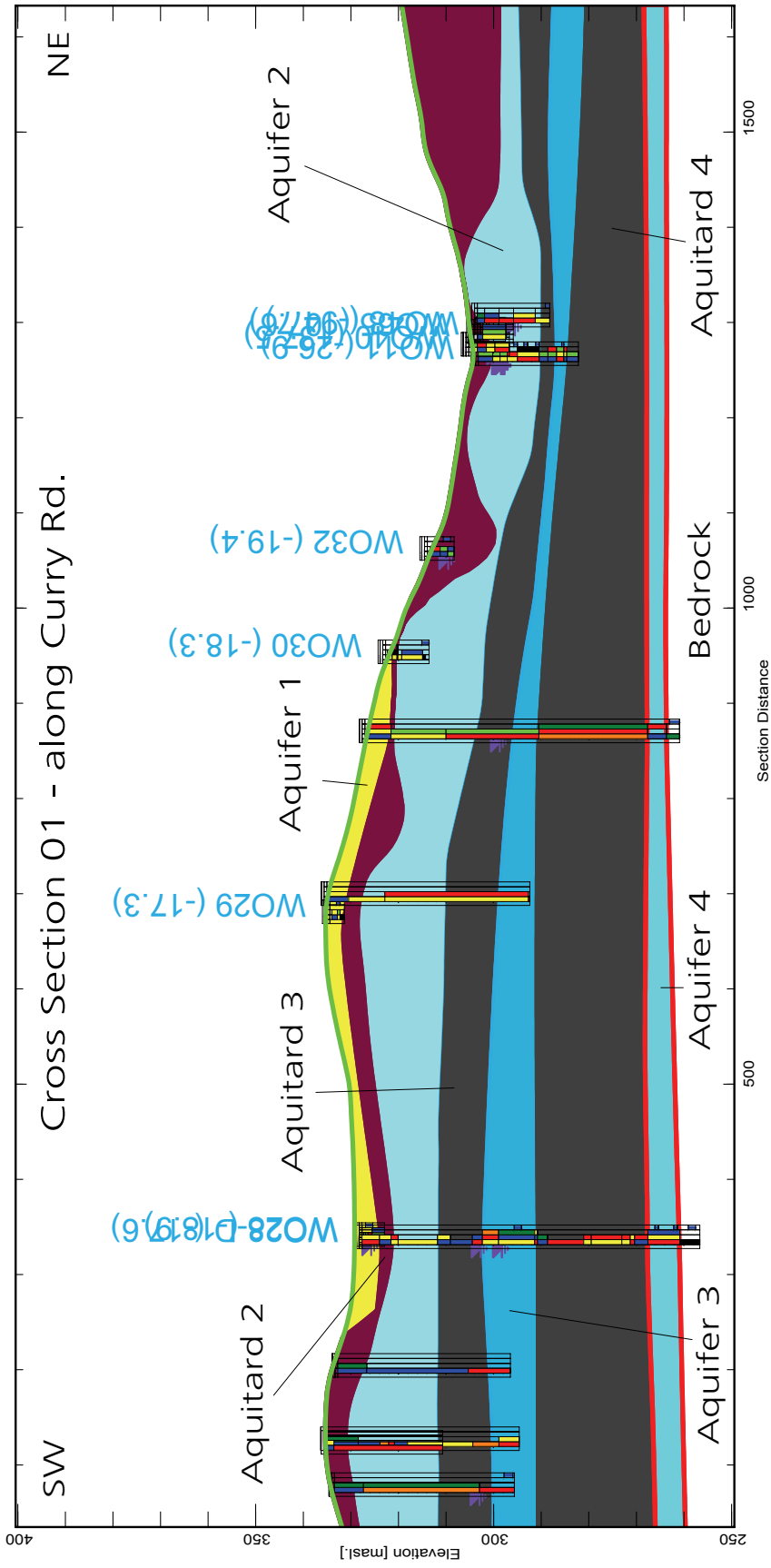
Figure 5.11:
Cross-Section 01.
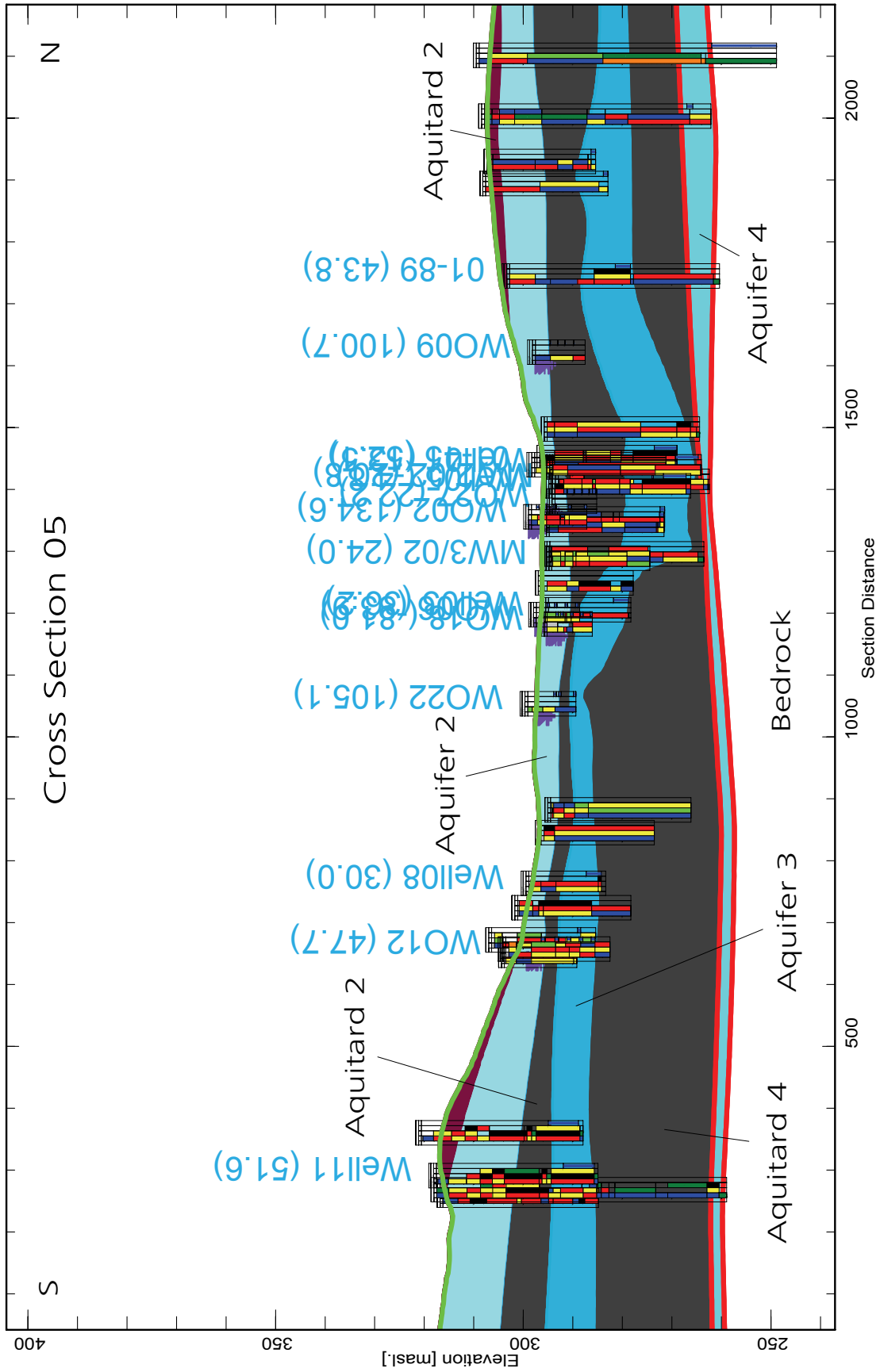
Figure 5.12:
Cross-Section 05.
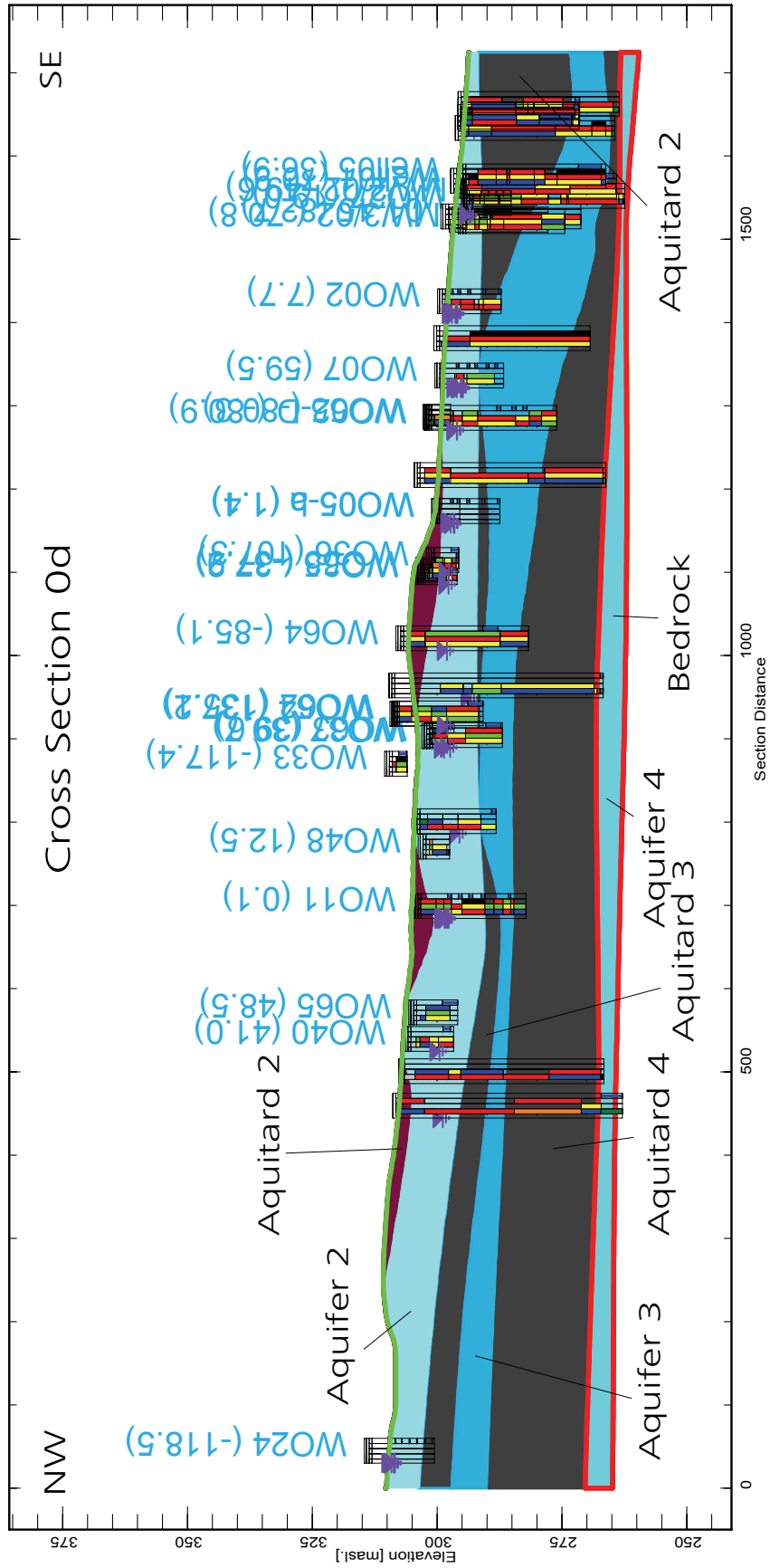
Figure 5.13:
Cross-Section 0d.
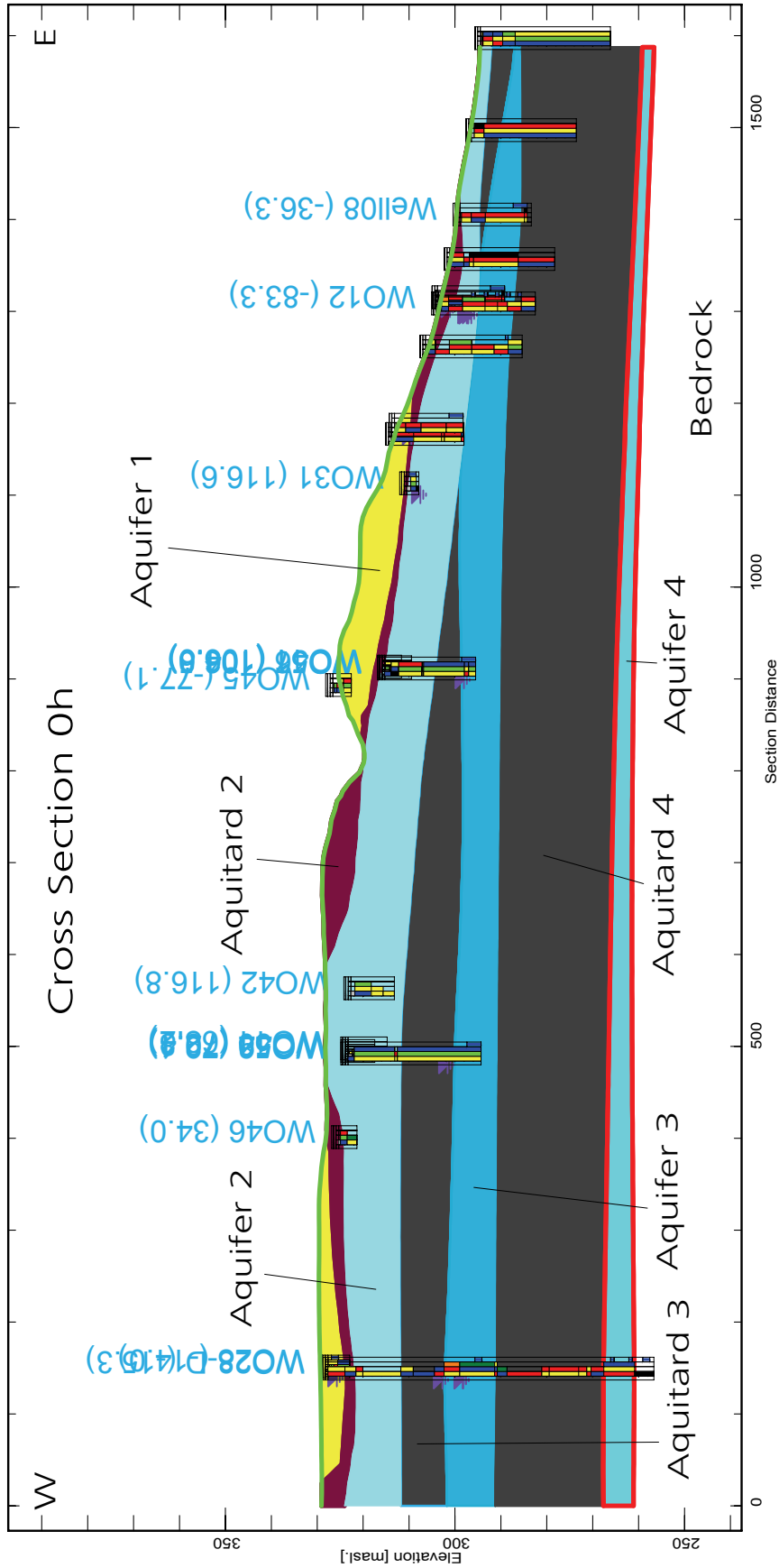
Figure 5.14:
Cross–Section 0h.
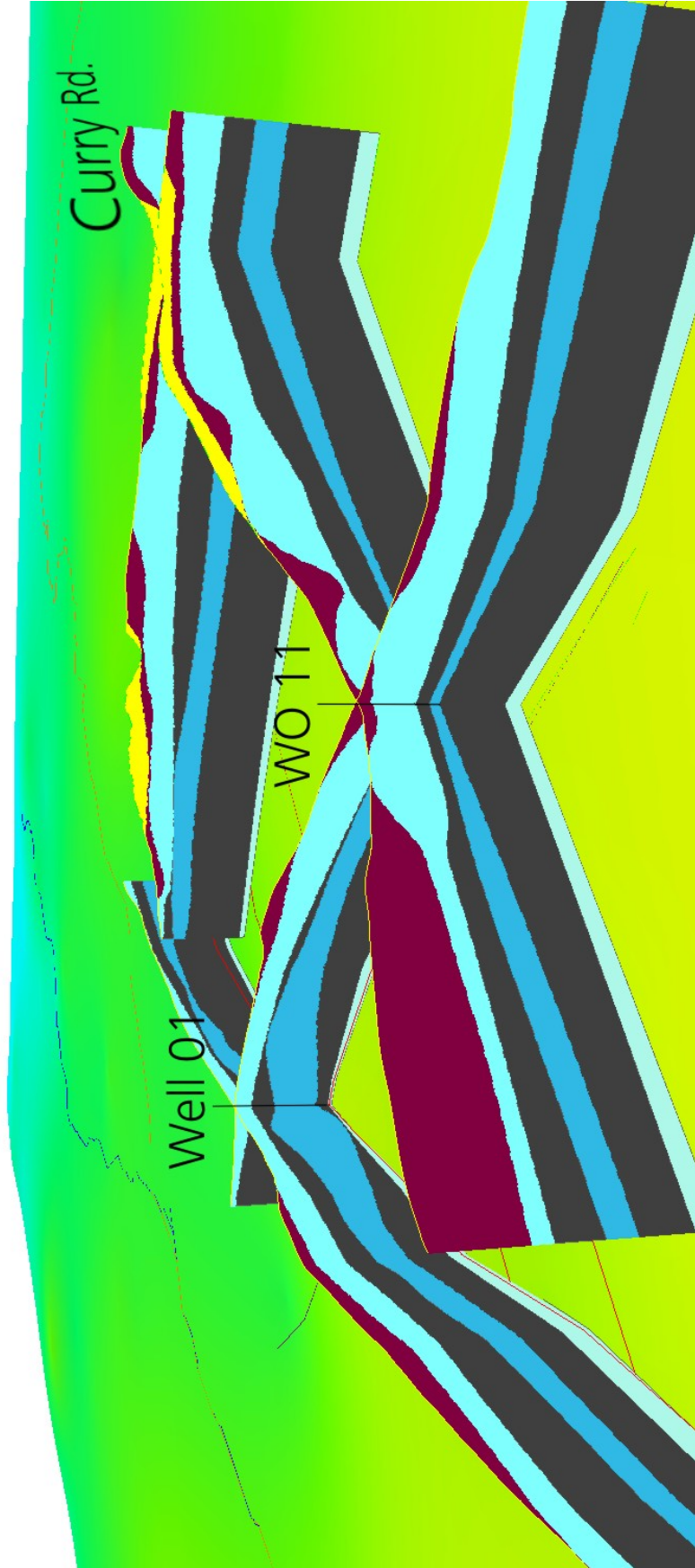
Figure 5.15:
Local 3D view of hydrostratigraphic units. Shaded in the background is the top surface of bedrock. The view is towards the south.
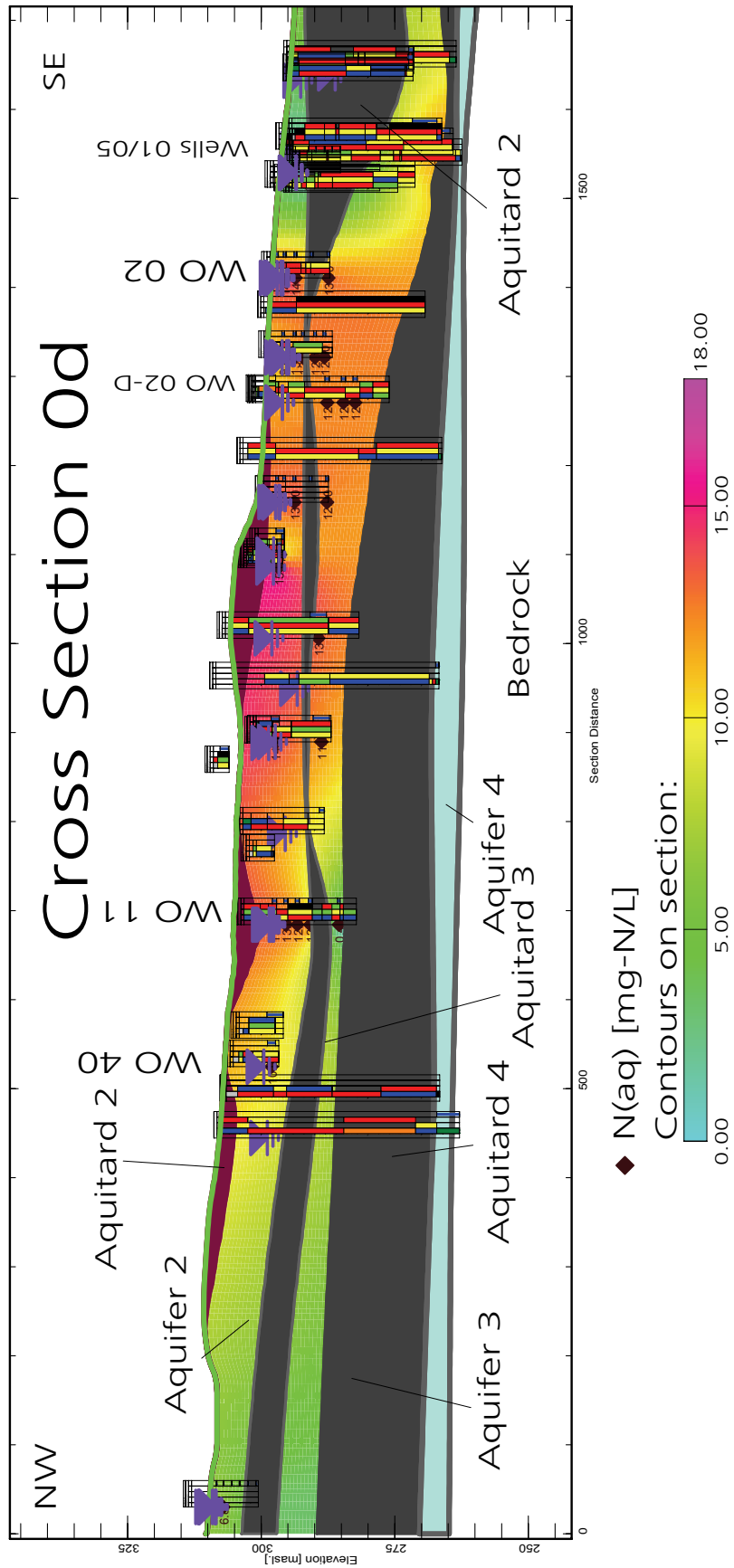
Figure 5.16:
Nitrate concentration contoured on cross-section.

6

Conclusions and Recommendations

Conclusions 6.1

As a result of the research contained in the thesis, the following notable conclusions that enhance the site hydrostratigraphic conceptual model are:

- The site hydrostratigraphy was conceptualized as a layered system of four aquitards and five aquifers. These layers are traceable across the study site, and their thickness is variable, ranging from non-existent to tens of meters.
- Conditions that allow for rapid infiltration into Aquifer 2 exist around WO 11/WO 40 and around WO 44, as indicated by geologic logs of cores, geophysical surveys, transient hydraulic head monitoring during times of maximal recharge (spring melt). These are areas highly vulnerable to ground surface contamination. Below Parcel B, a shallow, continuous, and low permeable zone (Aquitard 2) was mapped and acts as a barrier for infiltration and likely redistributes recharge to topographic lower areas (the areas around WO 11/WO 40 and WO 44 have been identified).
- Hydraulic connections between aquifers ("windows" through an aquitard) allow deeper contaminant migration pathways to be established. Such deep windows were identified along a glaciofluvial outwash channel, extending roughly along a line WO 24, WO 40, WO 37, Well 01. Analysis of nitrate concentration data demonstrated how this channel acts as a pathway for nitrate reaching the supply wells of the Thornton Well Field.
- Estimates of nitrate mass in the unsaturated zone within Parcel B combined with average groundwater recharge rates indicate that ~15 years would be needed to flush the stored nitrate out of the unsaturated zone. This time frame was based on the assumptions of piston flow displacement, recharge water containing zero nitrate, no reactions occurring along the path of infiltrating water, and no preferential infiltration occurring at any location.

123

- Depending on the well field management scheme used, complete reduction of nitrate infiltration from Parcel B could reduce the overall nitrate concentration in the supply wells of the Thornton Well Field by 6% to 17%. These estimates represent the maximum possible improvement that could be expected from the alternative nutrient management practices adopted within Parcel B. The actual improvements are likely to be somewhat lower than this.
- The majority of nitrate mass loading entering supply Well 01 comes from the top third of the screen. No nitrate mass enters the bottom third of the screen. This observation could have the following causes: Aquifer 4 was either not intercepted with the installed screen, or the performance of the well is not maximal, or the contribution of Aquifer 3 at this location is overwhelming other contributions.
- Analysis of the nitrate concentrations around the Thornton Well Field suggests that the zone of higher groundwater nitrate concentration is expanding towards the Thornton Well Field with time. This is a potential threat to the quality of the water in the supply wells; concentrations might temporarily increase in the supply wells,
- The glaciofluvial outwash channel is considered to be an important pathway for nitrate, since the upper 25% of all observed nitrate concentrations were found in eight wells whose location corresponds to that channel feature. This vulnerable area, especially the direct recharge area between WO 40 and ∼WO 35 is worth to be protected against nitrate inputs. Since this is channel is a preferential pathway (indicated by the young groundwater it contains), it is anticipated that it is a major contributor to the water being pumped in Well 01 and Well 05.

Recommendations | 6.2

- A contaminant transport modelling the study should be performed to predict the nitrate concentrations in the supply wells based on different nitrate loading scenarios on Parcel B in more detail.

- There is insufficient data to decide on the importance of tile drains in this study site. Most of the tile drain outlets are located within the capture zone and therefore only effect the location where the nitrate is infiltrating into the system. A decrease of nitrate loading into the supply wells could be achieved, if tile drain outlets were connected to surface water drains leading away from the Thornton Well Field (into Sweaburg Swamp,f.ex), or the flow of the tile drains treated on site to reduce nitrate concentrations. Due to the vulnerable area around WO 40 it seems logical to monitor the tile drain next to WO 40 more closely. The main usefulness of monitoring tile drain outlets will be as "early warning" systems for changes in NO_3 loading. The effect of reduced nitrate loading on Parcel B should

be reflected within a few years in the nitrate concentrations of the tile drains. Another possibility to evaluate the effects of the reduced nitrate loading on Parcel B is to re-core and re-analyze the locations presented in this study.

- A comprehensive analysis of pumping rates of the supply wells of the Thornton Well Field and observed nitrate concentrations in those wells should be performed to understand potential correlations. This may lead to an improved well field management scheme.

- There is a lack of hydrogeologic information in the area of the "northern hill" feature. This area is considered important because it likely contributes significantly to the hydraulic head conditions in Aquifer 3. Geologically logged boreholes are anticipated to improve the knowledge in this area.

- The results of the resistivity surveys were useful to support the hydrogeological model. Similar surveys, especially in the area of the glaciofluvial outwash channel should improve the understanding of the spatial distribution of hydrostratigraphic units in this key area even better.

- It should be resolved why the lower part of the screen in Well 01 is not producing water. A similar well profiling test could be conducted in Well 05 and the results compared to Well 01.

Bibliography

Allaby, A. and Allaby, M. *A Dictionary of Earth Sciences, 2nd etition*. Oxford University Press, 1999.

Bear, J. *Dynamics of Fluids in Porous Media*. Dover Publications, 1972.

Bekeris, L. Nitrate data from the Thornton Well Field, Woodstock, Ontario. Personal Communication, 2005.

Bouchard, D.C., Williams, M.K., and Surampalli, R.Y. Nitrate Contamination of Groundwater: Sources and Potential Health Effects. Journal of the American Water Works Association, vol. 84, no. 9, (1992) pp. 85–90.

Brimbicombe, A. *GIS, Environmental Modelling and Engineering*. Taylor & Francis, 2003.

Canadian Council of Ministers of the Environment. Nitrate/Nitrite Guideline. Electronic Source: http://www.hc-sc.gc.ca/hecs-sesc/water/pdf/dwg/nitrate.pdf, 1992. Access Date: 2005/07/26.

Clark, I. and Fritz, P. *Environmental Isotopes in Hydrogeology*. Lewis Publishers, 1997.

County of Oxford. Population and Household Projections, 1996 – 2021. *Tech. Rep.*, County of Oxford, 2001.

County of Oxford. Digital Elevation Model; 10m by 10m cell size [`computer file`]. Woodstock, ON, 2005*a*.

County of Oxford. Townships within the County of Oxford; [`computer file`]. Woodstock, ON, 2005*b*.

Cowan, W.R. Quaternary Geology of the Woodstock Area – Southern Ontario; Geological Report 119. *Tech. Rep.*, Ontario Ministry of Natural Resources, Division of Mines, 1975.

Davies, L.L. and McClymont, W.R. Bedrock Topography Series, Woodstock Sheet, Preliminary Map No. P169, 1962. Scale: 1:50000.

Dingman, S.L. *Physical Hydrology*. Prentice Hall, 2002.

Environment Canada. Canadian Daily Climate Data on CD-ROM - Eastern Canada, 2002.

Environmental Systems Research Institute. Arc GIS Desktop. Computer Program by Environmental Systems Research Institute, Redlands, CA, version 8.3, 2002.

Environmental Systems Research Institute. Countries and Administrative Units in North America; Global GIS [`computer file`]. Redlands, CA, 2003.

Environmental Systems Research Institute. Arc Hydro Tools. Computer Program by Environmental Systems Research Institute, Redlands, CA, version 1.1, 2004.

European Environment Agency. Nutrients in European Ecosystems. Electronic Source: http://reports.eea.eu.int/ENVIASSRP04/en/enviassrp04.pdf, 1999. Access Date: 2005/07/13.

Food and Agriculture Organization of the United Nations. Fertilizer Dataset of the Agriculture Database within the Statistics Section of the FAO. Electronic Source: http://faostat.fao.org/faostat/form?collection=Fertilizers&Domain=Means&servlet=1&hasbulk=0&version=ext&language=EN, 2005. Access Date: 2005/07/06.

Foster, S.S.D. Assessing and Controling the Impacts of Agriculture on Groundwater – from Barley Barons to Beef Bans. Quarterly Journal of Engineering Geology and Hydrogeology, vol. 33, (2000) pp. 263–280.

Fraser, P. and Chilvers, C. Health Aspects of Nitrate in Drinking Water. The Science of the Total Environment, vol. 18, (1981) pp. 103–116.

Frind, E.O., Muhammad, D.S., and Molson, J. Delineation of Three-Dimensional Well Capture Zones for Complex Multi-Aquifer Systems. Ground Water, vol. 40, no. 6, (2002) pp. 585–598.

Gan, Y. Res2dinv – 2D Resistivity and IP Inversion. Computer Program by Geotomo Software, http://www.geoelectrical.com, Malaysia, version 3.5, 2004.

Golder Associates. Phase II Groundwater Protection Study County of Oxford: Volume I. *Tech. Rep.*, 2001.

Government of Ontario. Ontario Regulation 169/03. Electronic Source: http://www.e-laws.gov.on.ca/DBLaws/Regs/English/030169_e.htm, 2002. Access Date: 2005/07/26.

Hallberg, G.R. Agricultural Chemicals in Ground Water: Extent and Implications. American Journal of Alternative Agriculture, vol. 2, no. 1, (1987) pp. 3–15.

Hallberg, G.R. and Keeney, D.R. *Regional Ground-Water Quality*, chap. Nitrate, pp. 297–322. 12 - Nitrate. Van Nostrand Reinhold, 1993.

Heagle, D.J. *Nitrate Geochemistry of a Regional Aquifer in an Agricultural Landscape, Woodstock, Ontario.* Master's thesis, University of Waterloo, Department of Earth Sciences, 2000.

Hill, M.J. Nitrate toxicity: Myth or Reality. British Journal of Nutrition, vol. 81, no. 5, (1999) pp. 343–344.

Karrow, P.F. Bedrock Topography in Southwestern Ontario: A Progress Report. Reprint from The Geological Association of Canada, Proceedings — Volume 25.

Karrow, P.F. Drumlins – Quaternary Landforms. Personal Communication, 2005.

Kassenaar, Dirk. Viewlog. Computer Program by Earth FX, Toronto, version 3.0, 2004.

Kearey, P. and Brooks, M. *An Introduction to Geophysical Exploration*. Blackwell Scientific Publications, 1991, second edition edn..

Kinzelbach, W., Ploeg, R.v.d., Rohmann, U., and Rodelsperger, M. *Schadstoffe im Grundwasser – Wärme und Schadstofftransport*, vol. 1, chap. Modellierung des Regionalen Transports von Nitrat: Fallbeispiel Bruchsal-Karlsdorf, pp. 414–469. DFG - Deutsche Forschungsgemeinschaft, 1992.

Knapp, M. Diffuse Pollution Threats to Groundwater: a UK Water Company Perspective. Quarterly Journal of Engineering Geology and Hydrogeology, vol. 38, (2005) pp. 39–51.

Krzyszkowski, D. and Karrow, P.F. Wisconsinan inter-lobal stratigraphy in three quarries near Woodstock, Ontario. Geographie Physique et Quaternaire, vol. 55, no. 1, (2001) pp. 3–22.

Lee and Kim. Nonpoint source groundwater pollution and endogenous regulatory policies. Water Resources Research, vol. 38, no. 12, (2002) pp. 11–1–11–13.

Lotowater. Woodstock and Sweaburg Water Supply Class EA Hydrogeologic Study for GUDI at the Thornton and Tabor Well Fields. *Tech. Rep.*, 2002.

MacRitchie, S.M., Pupp, C., Grove, G., Howard, K.W.F., and PLapcevic, P. Groundwater in Ontario: Hydrogeology, Quality Concerns and Management. *Tech. Rep.*, 1994.

Martin, P.J. and Frind, E.O. Modelling a complex multi-aquifer system: The Waterloo Moraine. Ground Water, vol. 36, no. 4, (1998) pp. 679–690.

Martinez, Y. and Albiac, J. Agricultural Pollution control under Spanish and European environmental Policies. Water Resources Research, vol. 40, no. 10, (2004) p. W10501.

Maxey, G.B. Hydrostratigraphic Units. Journal of Hydrology, vol. 2, (1964) pp. 124–129.

McNeil, J.D. Electromagnetic Terrain Conductivity Measurement at low Induction Numbers. *Tech. Rep.*, 1980.

Mengel, K. and Kirkby, E.A. *Principles of Plant Nutrition*. International Potash Institute, 1982.

Microsoft. Access. Computer Program by Microsoft, Redmond, WA, version 10.6 SP3, 2002.

Middlesex-London Health Unit. Drinking Water Advisory - Mar 23/05: Infants Less Than 6 months of Age in Strathroy. Electronic Source: http://www.thehealthline.ca/viewnews.asp?newsid=400, 2005. Access Date: 2005/07/06.

Milson, J. *Field Geophysics*. The Geological Field Guide Series. John Wiley and Sons Ltd, 2003, 3rd edn..

Natural Resources Canada. Canimage 40P02 GeoTiff "Woodstock"; LANDSAT 7 Imaginary [`computer file`]. Ottawa, ON, 2003.

NRC. *National Research Council – Soil And Water Quality: an Agenda for Agriculture*. National Academy Press, 1993.

OMAF. *Ontario Ministry of Agriculture and Food Soil Fertility Handbook*, vol. 611. 1998.

Ontario Geologic Survey. Geologic Maps; 40P2 map area [`computer file`]. Toronto, Ontario, 1988*a*.

Ontario Geologic Survey. Geologic Maps; [`computer file`]. Toronto, Ontario, 1988*b*.

Ontario Ministry of Agriculture, Food, and Rural Affairs. Agricultural Land Use of Ontario; [`computer file`]. Guelph, ON, 2000.

Ontario Ministry of Natural Resources. Waterbodies – Natural Resources and Values Information System; [`computer file`]. Toronto, ON, 2002.

Ontario Ministry of the Environment. Well Record Database; [`computer file`], 2000.

Ontario Ministry of the Environment. The Hydrogeology of Southern Ontario, second etition. *Tech. Rep.*, 2003*a*.

Ontario Ministry of the Environment. Technical Support Document for Ontario Drinking Water Standards, Objectives and Guidelines. Electronic Source: http://www.ene.gov.on.ca/envision/gp/4449e.htm, 2003*b*. Access Date: 2005/08/15.

Ontario Ministry of Transportation. Digital Cartographic Reference Base of Ontario, version 2.0; [`computer file`], 2000.

Padusenko, G. *Regional Hydrogeologic Evaluation of a Complex Glacial Aquifer System in an Agricultural Landscape: Implications for Nitrate Distribution*. Master's thesis, University of Waterloo, Department of Earth Sciences, 2001.

Pfister, G. Zur Effizienz des Grundwasserschutzes – eine ökonomische Analyse. *Tech. Rep.*, Akademie für Technikfolegenabschätzung in Baden-Württemberg, 2002.

Phipps, T.T. Commercial Agriculture and the Environment: An Evolutionary Perspective. Northeastern Journal of Agriculture and Resource Economics, pp. 143–150.

Radcliffe, A.J. *Physical Hydrogeology and Impact of Urbanization at the Waterloo West Side: A Groundwater Modelling Approach.* Master's thesis, University of Waterloo, Department of Earth Sciences, 2000.

Rajagopal, R. and Tobin, G. Expert Opinion and Ground-Water Quality Protection: The Case of Nitrate in Drinking Water. Ground Water, vol. 27, no. 6, (1989) pp. 835–847.

Robertson, W.D., Russell, B.M., and Cherry, J.A. Attenuation of Nitrate in Aquitard Sediments of Southern Ontario. Journal of Hydrology, vol. 180, (1996) pp. 267–281.

Robertson, W.D. and Sebol, L.A. Age Characterization of Groundwater in the Thornton Well Field using Tritium/Helium Analyses. *Tech. Rep.*, University of Waterloo, Department of Earth Scineces, 2004.

Roos, A.J.d., Ward, M.H., Lynch, C.F., and Cantor, K.P. Nitrate in Public Water Supplies and the Risk of Colon and Rectum Cancers. Epidemiology, vol. 14, no. 6, (2003) pp. 640–649.

Ryan, M. C., MacQuarrie, K.T.B., Harman, J., and McLellan, J. Field and Modeling Evidence for a "Stagnant Flow" Zone in the Upper Meter of Sandy Phreatic Aquifers. Journal of Hydrology, vol. 233, (2000) pp. 223–240.

Sebol, L.A. *Determination of Groundwater Age Using CFC's in Three Shallow Aquifers in Southern Ontario.* Master's thesis, University of Waterloo, Department of Earth Sciences, 2000.

Sebol, L.A. *Evaluating Shallow Groundwater Age Tracers: Br^-, CFCs, $^3H/^3He$, SF_6, and HCFCs/HFCs.* Ph.D. thesis, University of Waterloo, Department of Earth Sciences, 2004.

Stottler, R. *Change in Geochemistry, Isotope Composition, and Residence Time within the Waterloo Moraine Aquifer Complex.* Master's thesis, University of Waterloo, Department of Earth Sciences, 2002.

Tel, D. and Heseltine, C. The Analyses of KCl Soil Extracts for Nitrate, Nitrite and Ammonium Using a TRAACS 800 Analyzer. Communications in Soil Science and Plant Analysis, vol. 21, (1990) pp. 1681–1990.

Tindall, J.A. and Kunkel, J.R. *Unsaturated Zone Hydrology for Scientists and Engineers.* Prentice Hall, 1999.

USGS. U.S. Geological Survey Circular 1225 – The Quality of Our Nation's Waters – Nutrients and Pesticides. *Tech. Rep.*, 1999.

Walker and Miles. *Illustrated historical atlas of the counties of Oxford and Brant, reprint 1972.* 1875.

Ward, M.H., Riley, D., Merkle, S., and Lynch, C.F. Nitrate in Public Water Supplies and Risk of Bladder Cancer. Epidemiology, vol. 14, no. 2, (2003) pp. 183–190.

Weight, W.D. and Sonderegger, J.L. *Manual of Applied Field Hydrogeology*. Mc Graw Hill, 2000.

Weyer, P.J., Cerhan, J.R., Kross, B.C., Hallberg, G.R., Kantamneni, J., Breuer, G., Jones, M.P., Zheng, W., and Lynch, C.F. Municipal Drinking Water Nitrate Level and Cancer Risk in Older Women: The Iowa Women's Health Study. Epidemiology, vol. 12, no. 3, (2001) pp. 327–338.

Woldt, W., Goderya, F., Dahab, M., and Bogardi, I. Consideration of spatial variability in the management of non-point source pollution to groundwater. In *Spatial accuracy assessment in natural resources and environmental sciences; second international symposium*, (edited by H.T. Mowrer and R. H. Czaplewski, R.L.H.), pp. 49–56. U.S. Department of Agriculture, Forest Service, Rocky Mountain Forest and Range Experiment Station, 1996.

Yeung, N. In-situ groundwater velocity measurements using the borehole dilution method. B.Sc. Thesis, Department of Earth Sciences, University of Waterloo, 2004.

A

Appendix

A.1

Details of Cores and Piezometers

Table A.1:
Construction Details of Cores taken with the Envirocore Method.

Well Name	MonitorName	Easting	Northing	top	bottom
		[UTM NAD 83 17 N]		[masl.]	
WO 28	WO 28-02	518992.9	4769792.2	326.91	325.39
WO 28-D	WO 28-D-01	518990.4	4769791.5	259.09	257.57
WO 28-D	WO 28-D-02	518990.4	4769791.5	262.14	261.38
WO 28-D	WO 28-D-03	518990.4	4769791.5	266.10	265.34
WO 28-D	WO 28-D-04	518990.4	4769791.5	295.67	294.14
WO29	WO29-02	519232.5	4770032.1	333.04	332.28
WO30	WO30-08	519427.1	4770223.7	315.11	313.57
WO31	WO31-01	519926.8	4769695.3	309.99	308.47
WO32	WO32-04	519505.0	4770299.4	310.59	309.07
WO33	WO33-02	519737.0	4770244.4	307.68	306.15
WO34	WT not reached	519565.1	4770138.4		
WO35	WO35-06	519976.3	4770191.9	297.54	296.02
WO36	WO36-04	520060.5	4770310.3	297.22	295.69
WO37	WO37-04	519847.5	4770360.9	298.15	296.62
WO38	hole had to be abandoned – hit bolder				
WO39	WT not reached	519919.9	4770492.5		
WO40	WO40-07	519546.8	4770561.8	298.84	297.32
WO41	WT not reached	519760.8	4769721.2		

Hydraulic Head Measurements

Monitor Name	Date of sampling	Water level [masl.]
WO02-01	25/01/2005	297.15
WO02-03	11/10/2003	296.69
WO02-03	26/10/2003	296.74
WO02-03	25/01/2005	297.09
WO02-05	11/10/2003	296.67
WO02-05	26/10/2003	296.76
WO02-05	25/01/2005	297.18
WO02-08	11/10/2003	296.67
WO02-08	26/10/2003	296.77
WO02-08	25/01/2005	297.19
WO02-11	11/10/2003	296.59
WO02-11	26/10/2003	296.64
WO02-11	25/01/2005	297.01
WO02-D-13	11/10/2003	296.64
WO02-D-13	26/10/2003	296.70
WO02-D-13	19/05/2004	297.29
WO02-D-13	30/08/2004	297.14
WO02-D-13	28/01/2005	297.11
WO02-D-16	11/10/2003	296.64
WO02-D-16	26/10/2003	296.70
WO02-D-16	19/05/2004	297.29
WO02-D-16	30/08/2004	297.14
WO02-D-16	28/01/2005	297.11
WO02-D-19	11/10/2003	296.64
WO02-D-19	26/10/2003	296.69
WO02-D-19	19/05/2004	297.28
WO02-D-19	30/08/2004	297.05
WO02-D-19	28/01/2005	297.10
WO04-D-18	19/10/2003	297.01
WO04-D-18	21/10/2003	297.0
WO04-D-18	19/05/2004	297.8
WO04-D-18	02/02/2005	297.48
WO04-D-33	19/10/2003	295.66
WO04-D-33	21/10/2003	295.83
WO04-D-33	19/05/2004	296.50
WO04-D-33	02/02/2005	295.93
WO04-D-43	19/10/2003	295.84

Table A.2:
(continued)

Monitor Name	Date of sampling	Water level [masl.]
WO04-D-43	21/10/2003	295.89
WO04-D-43	19/05/2004	296.48
WO04-D-43	02/02/2005	295.92
WO05-03	25/10/2003	
WO05-03	25/01/2005	297.47
WO05-04	25/10/2003	
WO05-04	25/01/2005	297.62
WO05-06	25/10/2003	296.99
WO05-06	25/01/2005	297.6
WO05-09	25/10/2003	296.99
WO05-09	25/01/2005	297.6
WO05-12	25/10/2003	296.99
WO05-12	25/01/2005	297.59
WO06-03	25/10/2003	296.29
WO06-03	21/01/2005	296.89
WO06-04	25/10/2003	296.33
WO06-04	21/01/2005	296.88
WO06-06	25/10/2003	296.25
WO06-06	21/01/2005	296.81
WO06-09	25/10/2003	296.22
WO06-09	21/01/2005	296.74
WO07-03	30/10/2003	296.12
WO07-03	19/05/2004	296.55
WO07-03	20/01/2005	
WO07-05	30/10/2003	296.16
WO07-05	19/05/2004	296.55
WO07-05	20/01/2005	
WO07-07	30/10/2003	296.18
WO07-07	19/05/2004	296.58
WO07-07	20/01/2005	
WO07-09	30/10/2003	296.17
WO07-09	19/05/2004	296.55
WO07-09	20/01/2005	296.39
WO07-11	30/10/2003	296.22
WO07-11	19/05/2004	296.6
WO07-11	20/01/2005	296.43
WO08-03	19/10/2003	295.88
WO08-03	21/10/2003	295.90
WO08-03	19/05/2004	297.46
WO08-03	01/02/2005	
WO08-05	19/10/2003	295.81

134

Table A.2:
(continued)

Monitor Name	Date of sampling	Water level [masl.]
WO08-05	21/10/2003	295.76
WO08-05	19/05/2004	297.39
WO08-05	01/02/2005	
WO08-D-06	19/10/2003	295.65
WO08-D-06	21/10/2003	295.62
WO08-D-06	19/05/2004	295.89
WO08-D-06	01/02/2005	295.33
WO08-D-12	19/10/2003	295.68
WO08-D-12	21/10/2003	295.65
WO08-D-12	19/05/2004	295.89
WO08-D-12	01/02/2005	295.37
WO08-D-17	19/10/2003	295.74
WO08-D-17	21/10/2003	295.66
WO08-D-17	19/05/2004	295.91
WO08-D-17	01/02/2005	295.38
WO09-03	24/10/2003	295.38
WO09-03	19/05/2004	296.97
WO09-03	20/01/2005	296.97
WO09-04	24/10/2003	295.36
WO09-04	20/01/2005	296.98
WO09-06	24/10/2003	295.37
WO09-06	19/05/2004	296.96
WO09-06	20/01/2005	296.98
WO09-08	24/10/2003	295.37
WO09-08	19/05/2004	296.98
WO09-08	20/01/2005	296.97
WO09-10	24/10/2003	295.34
WO09-10	19/05/2004	296.97
WO09-10	20/01/2005	296.97
WO11-06	19/10/2003	297.94
WO11-06	26/10/2003	297.96
WO11-06	28/04/2004	298.88
WO11-06	19/05/2004	298.96
WO11-06	27/05/2004	299.14
WO11-06	05/07/2004	298.69
WO11-06	29/07/2004	298.63
WO11-06	30/08/2004	298.58
WO11-06	11/01/2005	298.65
WO11-08	26/10/2003	297.58
WO11-08	19/05/2004	298.58
WO11-08	27/05/2004	298.76

Table A.2:
(continued)

Monitor Name	Date of sampling	Water level [masl.]
WO11-08	05/07/2004	298.28
WO11-08	29/07/2004	298.25
WO11-08	30/08/2004	298.19
WO11-08	11/01/2005	298.28
WO11-10	19/10/2003	297.56
WO11-10	26/10/2003	297.58
WO11-10	19/05/2004	298.57
WO11-10	27/05/2004	298.76
WO11-10	05/07/2004	298.29
WO11-10	29/07/2004	298.25
WO11-10	30/08/2004	298.2
WO11-10	11/01/2005	298.27
WO11-13	19/10/2003	297.86
WO11-13	26/10/2003	297.88
WO11-13	19/05/2004	298.88
WO11-13	27/05/2004	299.07
WO11-13	05/07/2004	298.69
WO11-13	29/07/2004	298.56
WO11-13	30/08/2004	298.50
WO11-13	11/01/2005	298.58
WO11-18	19/10/2003	297.88
WO11-18	26/10/2003	297.92
WO11-18	28/04/2004	297.9
WO11-18	19/05/2004	299.15
WO11-18	27/05/2004	299.47
WO11-18	05/07/2004	298.85
WO11-18	29/07/2004	298.65
WO11-18	11/01/2005	298.75
WO12-08	11/10/2003	296.56
WO12-08	21/10/2003	296.75
WO12-08	25/03/2004	297.49
WO12-08	28/04/2004	297.52
WO12-08	19/05/2004	297.62
WO12-08	27/05/2004	297.67
WO12-08	05/07/2004	297.50
WO12-08	01/10/2004	297.45
WO12-08	01/02/2005	296.96
WO12-10	11/10/2003	296.65
WO12-10	21/10/2003	296.76
WO12-10	25/03/2004	297.52
WO12-10	28/04/2004	297.55

Table A.2:
(continued)

Monitor Name	Date of sampling	Water level [masl.]
WO12-10	19/05/2004	297.64
WO12-10	27/05/2004	297.69
WO12-10	05/07/2004	297.53
WO12-10	01/10/2004	297.48
WO12-10	01/02/2005	296.97
WO12-13	11/10/2003	296.65
WO12-13	21/10/2003	296.79
WO12-13	19/05/2004	297.63
WO12-13	27/05/2004	297.70
WO12-13	05/07/2004	297.53
WO12-13	01/10/2004	297.48
WO12-13	01/02/2005	296.98
WO12-15	11/10/2003	296.63
WO12-15	21/10/2003	296.78
WO12-15	19/05/2004	297.63
WO12-15	27/05/2004	297.70
WO12-15	05/07/2004	297.53
WO12-15	01/10/2004	297.49
WO12-15	01/02/2005	296.95
WO12-19	11/10/2003	297.67
WO12-19	21/10/2003	296.81
WO12-19	25/03/2004	297.55
WO12-19	19/05/2004	297.67
WO12-19	27/05/2004	297.73
WO12-19	05/07/2004	297.56
WO12-19	01/10/2004	297.51
WO12-19	01/02/2005	296.96
WO18-02	25/10/2003	293.36
WO18-02	13/01/2005	293.83
WO18-03	25/10/2003	293.35
WO18-03	13/01/2005	293.84
WO18-05	25/10/2003	293.36
WO18-05	13/01/2005	293.82
WO18-07	25/10/2003	293.36
WO18-07	13/01/2005	293.82
WO18-09	25/10/2003	293.36
WO18-09	13/01/2005	293.82
WO19-01	19/05/2004	295.46
WO19-01	13/01/2005	295.99
WO19-02	30/10/2003	294.73
WO19-02	19/05/2004	295.44

Monitor Name	Date of sampling	Water level [masl.]
WO19-02	13/01/2005	295.99
WO19-04	30/10/2003	294.73
WO19-04	19/05/2004	295.34
WO19-04	13/01/2005	295.99
WO19-05	30/10/2003	294.60
WO19-05	19/05/2004	295.46
WO19-05	13/01/2005	295.66
WO20-01	19/05/2004	294.81
WO20-06	30/10/2003	293.28
WO20-06	19/05/2004	294.77
WO22-06	11/10/2003	295.92
WO22-06	11/10/2003	295.92
WO22-06	19/05/2004	296.98
WO22-06	21/01/2005	296.89
WO22-07	11/10/2003	296.00
WO22-07	19/05/2004	296.69
WO22-07	21/01/2005	296.58
WO22-10	11/10/2003	296.14
WO22-10	19/05/2004	296.90
WO22-10	21/01/2005	296.75
WO24-04	02/09/2004	214.02
WO24-04	28/01/2005	309.43
WO24-06	28/01/2005	309.39
WO24-07	28/01/2005	
WO24-09	28/01/2005	311.75
WO24-11	28/01/2005	
WO24-12	02/09/2004	308.70
WO24-12	28/01/2005	309.55
WO27-02	19/05/2004	293.46
WO27-02	02/02/2005	293.46
WO27-04	15/06/2004	293.50
WO27-04	02/02/2005	293.44
WO27-05	15/06/2004	293.49
WO27-05	02/02/2005	293.42
WO27-06	15/06/2004	293.39
WO27-06	02/02/2005	293.44
WO27-08	15/06/2004	293.56
WO27-08	02/02/2005	293.44
WO28-D-01	20/04/2004	298.46
WO28-D-01	28/04/2004	298.48
WO28-D-01	19/05/2004	298.56

Monitor Name	Date of sampling	Water level [masl.]
WO28-D-01	25/05/2004	298.71
WO28-D-01	10/06/2004	298.46
WO28-D-01	15/06/2004	298.41
WO28-D-01	08/07/2004	298.26
WO28-D-01	16/08/2004	297.95
WO28-D-01	30/08/2004	297.94
WO28-D-01	02/09/2004	297.95
WO28-D-01	08/06/2005	298.34
WO28-D-02	20/04/2004	298.45
WO28-D-02	28/04/2004	298.47
WO28-D-02	19/05/2004	298.57
WO28-D-02	25/05/2004	298.70
WO28-D-02	10/06/2004	298.45
WO28-D-02	15/06/2004	298.39
WO28-D-02	08/07/2004	298.25
WO28-D-02	16/08/2004	297.95
WO28-D-02	30/08/2004	297.94
WO28-D-02	02/09/2004	297.94
WO28-D-02	08/06/2005	298.34
WO28-D-03	20/04/2004	298.44
WO28-D-03	28/04/2004	298.46
WO28-D-03	19/05/2004	298.55
WO28-D-03	25/05/2004	298.65
WO28-D-03	10/06/2004	298.44
WO28-D-03	15/06/2004	298.34
WO28-D-03	08/07/2004	298.24
WO28-D-03	16/08/2004	297.89
WO28-D-03	30/08/2004	297.74
WO28-D-03	02/09/2004	297.84
WO28-D-03	08/06/2005	298.49
WO28-D-04	20/04/2004	302.75
WO28-D-04	28/04/2004	301.97
WO28-D-04	19/05/2004	302.15
WO28-D-04	25/05/2004	302.18
WO28-D-04	10/06/2004	307.10
WO28-D-04	15/06/2004	302.15
WO28-D-04	08/07/2004	302.17
WO28-D-04	16/08/2004	302.25
WO28-D-04	30/08/2004	302.27
WO28-D-04	02/09/2004	302.52
WO28-D-04	08/06/2005	302.72

Table A.2:
(continued)

Monitor Name	Date of sampling	Water level [masl.]
WO32-04	30/06/2004	309.78
WO32-04	06/07/2004	309.54
WO32-04	08/07/2004	309.54
WO32-04	29/07/2004	309.36
WO32-04	02/02/2005	
WO35-06	01/10/2004	297.57
WO35-06	02/02/2005	297.59
WO35-06	08/06/2005	298.16
WO36-04	01/10/2004	297.56
WO36-04	02/02/2005	297.58
WO36-04	08/06/2005	297.99
WO37-04	01/10/2004	298.49
WO37-04	01/02/2005	298.59
WO37-04	08/06/2005	298.98
WO40-07	01/10/2004	299.22
WO40-07	28/01/2005	299.42

Table A.2:
Hydraulic Head Measurements. Empty cells represent either dry wells or taking a measurement was not possible (frozen).

Aqueous Chemical Samples Fall 2003

Monitor	Sampling Date	Nitrate N	Alkalinity CaCO3	Fluoride F	Chloride Cl	Bromide Br	Phosphate P	Sulfates SO4	Bicarbonate HCO3	Magnesium Mg	Potassium K	Sodium Na	Calcium Ca	Ammonia N	Nitrite N	pH
Well01-27	30-Oct-03	9	290	0.3	63.2	0.35	0.3	38.9	353	30	2	26	110	0.05	0.1	8.1
WO02-03	26-Oct-03	13.2	297	0.1	31.7	0.35	0.3	38.5	363	30	1.5	8	100	0.05	0.1	8.03
WO02-05	26-Oct-03	13.6	295	0.1	33.3	0.35	0.3	40.2	360	31	1.5	8.5	110	0.05	0.1	8.06
WO02-08	26-Oct-03	12.9	312	0.1	34.3	0.35	0.3	40.7	381	31	1.4	9.1	100	0.05	0.1	8.03
WO02-11	26-Oct-03	12.7	292	0.1	34.4	0.35	0.3	41.2	357	30	1.2	10	100	0.05	0.1	8.16
WO02-D-13	26-Oct-03	12.1	289	0.1	30	0.35	0.3	40.8	353	31	1.2	8.2	110	0.05	0.1	7.77
WO02-D-16	26-Oct-03	12.1	290	0.1	30.1	0.35	0.3	40.6	354	30	1.2	8	110	0.05	0.1	7.85
WO02-D-19	26-Oct-03	12.55	292.5	0.1	32.8	0.35	0.3	41	357	29.5	1.15	8.5	103	0.05	0.1	7.97
WO04-D-18	06-Nov-03	10.3	255	0.4	38.3	0.35	0.3	35.6	311	22	1.6	30	78	0.14	0.1	7.87
WO04-D-33	06-Nov-03	0.2	232	1.8	4.93	0.35	0.3	28.1	283	13	1	66	23	0.71	0.1	8.13
WO04-D-43	06-Nov-03	0.2	237.5	1.8	5.06	0.35	0.3	28.8	290.5	13	1.1	69	23	0.65	0.1	8.075
WO05-06	24-Oct-03	12.6	134	0.1	39.7	0.35	0.3	31.8	164	27	3	11	100	0.05	0.1	7.9
WO05-09	24-Oct-03	12.1	169	0.1	43.7	0.35	0.3	37.1	206	29	2.7	13	100	0.05	0.1	7.72
WO05-12	24-Oct-03	11.6	180	0.1	49.5	0.35	0.3	37.9	219	28	1.8	14	100	0.05	0.1	7.58
WO06-03	25-Oct-03									170	9.1	13	120			
WO06-04	25-Oct-03	11.1	173	0.1	30.5	0.35	0.3	39.9	211	29	1.2	11	100	0.05	0.1	7.61
WO06-06	24-Oct-03	11.2	158	0.1	35.5	0.35	0.3	40.7	193	30	1.2	13	95	0.05	0.1	7.6
WO06-09	25-Oct-03	10.6	154	0.1	26.2	0.35	0.3	33.8	188	29	1.2	12	100	0.05	0.1	7.77
WO07-05	30-Oct-03	13.65	292.5	0.3	34	0.35	0.3	38.4	357	29.5	1.8	10.5	120	0.05	0.1	8.02
WO07-07	30-Oct-03	12.9	296	0.3	39.8	0.35	0.3	39.65	361	30.5	1.75	13.5	110	0.125	0.1	8.17
WO07-09	30-Oct-03	12.4	300	0.1	46.4	0.35	0.3	40.8	366	31	1.9	14	120	0.05	0.1	8.03
WO08-05	21-Oct-03	0.8	386	0.3	3.05	0.35	0.3	37.4	471	25	2.6	4.2	130	0.05	0.1	8.1
WO08-D-06	21-Oct-03	11.9	316	0.3	42.9	0.35	0.7	36.6	386	29	2.9	16	100	0.05	0.1	7.99
WO08-D-12	21-Oct-03	12.6	307	0.3	47.6	0.35	0.3	36.5	375	32	3.3	17	140	0.05	0.1	7.99
WO08-D-17	21-Oct-03	11.2	303	0.3	52.8	0.35	0.3	39.6	370	29.5	2.85	21.5	105	0.05	0.1	7.97
WO09-03	24-Oct-03	2.3	156	0.1	3.1	0.35	0.3	18.4	191	22	0.97	1.8	100	0.09	0.1	7.79
WO09-04	24-Oct-03	1.35	187	0.1	2.51	0.35	0.3	15.55	228	21.5	1	1.55	110	0.05	0.1	7.565
WO09-06	24-Oct-03	1	168	0.1	3.15	0.35	0.3	18.5	205	21	1.1	1.8	110	0.05	0.1	7.61
WO09-08	24-Oct-03	0.3	141	0.1	2.2	0.35	0.3	48	172	24	1.1	1.7	110	0.05	0.1	7.49
WO09-10	24-Oct-03	0.6	197	0.1	3.19	0.35	0.3	31.3	240	24	1.3	2.9	97	1.22	0.1	7.78
WO11-06	06-Nov-03	13.5	282	0.3	32.5	0.35	0.3	29.3	336	26	1.9	13	100	0.05	0.1	8.34
WO11-08	06-Nov-03	12.2	286	0.2	44.1	0.35	0.3	40.6	349	26	1.95	15	105	0.05	0.1	8.02
WO11-10	06-Nov-03	12.25	294.5	0.2	44.6	0.35	0.3	45.35	359.5	29.5	1.8	14.5	110	0.085	0.1	8.045
WO11-13	26-Oct-03	11.8	302	0.1	46.3	0.35	0.3	47.6	368	31	1.1	15	110	0.05	0.1	8.07
WO11-18	26-Oct-03	0.4	292	0.2	16.8	0.35	0.3	84.6	356	34	2.3	9.1	130	0.07	0.1	8.16
WO12-08	21-Oct-03	6.2	335	0.3	36.6	0.35	0.3	39.4	409	36	2.3	15	100	0.05	0.1	7.72
WO12-10	21-Oct-03	6.6	300	0.3	39.5	0.35	0.3	40.5	367	33	2.3	15	110	0.05	0.1	8.01
WO12-13	21-Oct-03	0.1	1	0.1	36	0.35	0.3	46.1	0.05	34	2.3	17	110	0.05	0.1	7.69
WO12-15	21-Oct-03	6.8	300	0.3	42.9	0.35	0.3	42.2	367	35	2.5	17	110	0.05	0.1	8.06
WO12-19	21-Oct-03	7.1	302	0.3	47.6	0.35	0.3	44.2	369	35	3.25	19	89.5	0.05	0.1	8.06
WO18-02	06-Nov-03	3.4	141	0.1	30.7	0.35	0.3	38.5	172	13.5	1.6	35	74	0.06	0.1	7.87
WO18-03	25-Oct-03	3	190	0.1	40	0.35	0.3	41.1	232	20	2.45	41	125	0.1	0.1	7.26
WO18-05	06-Nov-03									28	3	14	75			
WO18-07	06-Nov-03	0.6	298	0.5	34.9	0.35	0.3	54.3	364	29.5	2.55	18.5	35.5	0.4	0.1	8.15
WO18-09	06-Nov-03			0.3	34.5	0.35	0.3	27.4	100	15.05	4	35	55	1.2	0.1	7.36
WO19-05	30-Oct-03	1.4	230	0.5	13.8	0.35	0.3	6	281	23	1.5	14	85	0.05	0.1	8.1
WO22-06	06-Nov-03	1.65	299	0.35	8.47	0.35	0.3	40.4	364.5	25	2.2	4.05	69	0.05	0.2	8.06
WO22-07	06-Nov-03	0.5	261	0.4	3.9	0.35	0.3	50.3	318	24	1.7	4.8	87	1.29	0.1	8.14
WO22-10	06-Nov-03	6.8	285	0.5	26.2	0.35	0.3	48.4	348	32	2.6	10		0.05	0.1	8.17
WO27-02	06-Nov-03									31	2	19	230			
WO27-04	06-Nov-03	1.6	392	0.3	21.7	0.35	0.3	159	478	34	2.2	6.4	160	1.27	0.1	8.06
WO27-05	06-Nov-03	0.9	386	0.3	21.1	0.35	0.3	228	471	50	2.3	7.2	140	0.56	0.1	8.02
WO27-06	06-Nov-03	0.3	341	0.3	21.1	0.35	0.3	97.8	416	37	2.3	7	110	0.79	0.1	8.15
WO27-08	06-Nov-03	0.3	314	0.3	22.3	0.35	0.3	313	383	47		6.1	150	0.45	0.1	8.04
Standard Deviation		5.3	76.9	0.3	15.7	0	0.1	50.5	97.7	20.4	1.2	13.3	31.3	0.4	0	0.2
Mean		7.13	258.62	0.28	29.6	0.35	0.31	50.99	311.25	31.11	2.05	15.12	103.78	0.21	0.1	7.93

Aqueous Chemical Samples During 2004

Monitor	Sampling Date	Nitrate N	Alkalinity CaCO3	Fluoride F	Chloride Cl	Bromide Br	Phosphate P	Sulfates SO4	Bicarbonate HCO3	Magnesium Mg	Potassium K	Sodium Na	Calcium Ca	Ammonia N	Nitrite N	pH
Well01-27	08-Sep-04	10.2	299	0.2	49.7		0.3	38		27	1.7	19	100		0.1	8.27
Well03-15	08-Sep-04	10.4	280	0.2	37.8		0.3	38.8		32	1.4	16	94		0.1	8.22
Well05-25	08-Sep-04	8.1	286	0.2	42.7		0.3	41.2		32	1.2	16	85		0.1	8.1
Well11-30	08-Sep-04	6.3	294	0.2	45.3		0.3	44.2		30	1.5	17	110		0.1	8.26
WO02-D-13	02-Sep-04	15.8	164	0.2	34.7		0.3	45.4		34	1.1	9.5	120	0.05	0.1	8.16
WO02-D-16	02-Sep-04	12.2	204	0.2	26.6		0.3	35.8		35	1.3	9.7	120	0.05	0.1	8.16
WO02-D-19	02-Sep-04	16.2	155	0.2	36.5		0.3	45.9		32	1	9.4	110	0.05	0.1	8.17
WO11-06	19-Aug-04	14.7	170	0.1	24.8		0.3	15.1		25	1.7	7.1	110	0.05	0.1	8.23
WO11-06	02-Sep-04	16.3	166	0.2	33.3		0.3	21.5		29	1.7	9.9	130	0.05	0.1	8.07
WO11-08	19-Aug-04	14.5	165	0.2	42.2		0.3	28.9		32	2	17	140	0.05	0.1	8.33
WO11-08	02-Sep-04	16.8	164	0.1	54.3		0.3	38.1		34	2.1	18	130	0.05	0.1	8.16
WO11-10	19-Aug-04	14.6	171	0.2	39.6		0.3	27.8		32	2	17	120	0.05	0.1	8.28
WO11-10	02-Sep-04	15.4	175	0.2	51.7		0.3	47.5		37	2.7	22	150	0.05	0.1	8.1
WO11-13	19-Aug-04	12.6	181	0.2	42.2		0.3	35		35	2.4	20	150	0.05	0.1	8.28
WO11-13	02-Sep-04	16.5	171	0.2	56.6		0.3	51.2		35	1.9	22	150	0.05	0.1	8.09
WO11-18	19-Aug-04	1.3	234	0.5	18.9		0.3	74.5		37	1.3	12	100	0.05	0.1	8.37
WO11-18	02-Sep-04	0.2	201	0.6	20.6		0.3	101		40	1.3	8.9	120	0.05	0.1	8.21
WO24-12	08-Sep-04	4.1	456	0.3	78.4		0.3	77.1		46	12	25	150		0.1	8.16
WO24-12	20-Oct-04	3	304	0.3	84.4		0.3	68.8		52	12	27	190		0.1	8.05
WO28-D-01	20-Jun-04	0.1	211	2.2	5.75			3.5		13	1.7	56	33	0.25	0.1	8.43
WO28-D-01	11-Sep-04	0.1	243		5.05			4.7		11	1.6	54	27	0.2	0.1	8.33
WO28-D-01	17-Sep-04	0.1	243		5.05			4.7		11	1.6	54	27	0.2	0.1	8.33
WO28-D-02	20-Jun-04	0.1	188	1.4	18.1		0.3	20.6		17	0.91	37	41	0.17	0.1	8.3
WO28-D-02	11-Sep-04	0.2	231		31			25.6		20	1.1	30	49	0.16	0.1	8.29
WO28-D-02	17-Sep-04	0.2	231		31			25.6		20	1.1	30	49	0.16	0.1	8.29
WO28-D-03	20-Jun-04	0.3	228	2.7	8.38		0.3	16.5		11	2.1	71	31	0.24	0.1	8.37
WO28-D-03	11-Sep-04		262		5.37			13.7		9.3	1.4	82	22	0.35	0.1	7.5
WO28-D-03	17-Sep-04		262		5.37			13.7		9.3	1.4	82	22	0.35	0.1	7.5
WO28-D-04	20-Jun-04	7.8	215	0.5	29.9		0.3	60.2		27	1.4	31	78	0.15	0.1	8.01
WO28-D-04	19-Aug-04	9	160	0.4	29.2		0.3	60.5		35	1.7	27	110	0.05	0.2	8.44
WO28-D-04	11-Sep-04	9.6	298		27.2			52.7		32	1.4	15	86	0.05	0.2	8.18
WO28-D-04	17-Sep-04	9.6	298		27.2			52.7		32	1.4	15	86	0.05	0.2	8.18
WO32-04	10-Jul-04	3.5	278	0.1	6.83		0.3	7		31.7	4	14	91.7	0.89	0.1	8.22
WO35-06	20-Oct-04	16.1	205	0.2	33		0.3	33.9		35	4.8	12	140		0.1	8.03
WO36-04	01-Oct-04	8.5	130	0.1	71.2		0.3	35.1		33	2.7	35	130		0.1	8.11
WO36-04	20-Oct-04	10	167	0.3	68.6		0.3	30.7		31	2	29	130		0.1	7.99
WO37-04	01-Oct-04	14.15	171.5	0.1	33.35		0.3	36.35		36	3.25	13	145		0.1	8.09
WO37-04	20-Oct-04	13.3	160	0.2	31.1		0.3	34.1	0.05	30	1.5	11	130		0.1	8.2
WO40-07	20-Oct-04	9.6	157	0.2	61.1		0.3			30	0.87	18	110		0.1	8.13

Resistivity Measurements | A.5

In this section of the appendix, the results of each individual resistivity survey line (line 01 through line 05, Figures A.1 through A.5) are shown. Whenever a core was taken on or within a few meters of the surveyed line, a simplified log of that core is shown on the section. The darker the shading, the finer the material. The lighter the shading, the coarser the material.

Depth Penetration of the EM34 Method | A.6

The relationship between the relative contribution (Φ) of the material at a certain depth and the specific depth $z = \dfrac{d}{s}$ to an electric conductivity measurement, where (d) is the depth [m] and (s) is the spacing between transmitter and receiver in [m], for the vertical and horizontal mode is given by equations A.1 and A.2, respectively (**?**):

$$\Phi_V = \frac{4z}{(4z^2 + 1)^{\frac{3}{2}}} \tag{A.1}$$

$$\Phi_H = 2 - \frac{4z}{(4z^2 + 1)^{\frac{1}{2}}} \tag{A.2}$$

The cumulative response (R) from all material below a certain depth is obtained by integrating Equations A.1 and A.2 over a depth-interval. Solutions are given by equations A.3 and A.4 (**?**):

$$R_V = \frac{1}{(4z^2 + 1)^{\frac{1}{2}}} \tag{A.3}$$

$$R_H = (4z^2 + 1)^{\frac{1}{2}} - 2z \tag{A.4}$$

Equations A.1, A.2, A.3 and A.4 are plotted on Figure A.6 for a set of different spacings (s) (1m, 5m, 10m, and 20m).
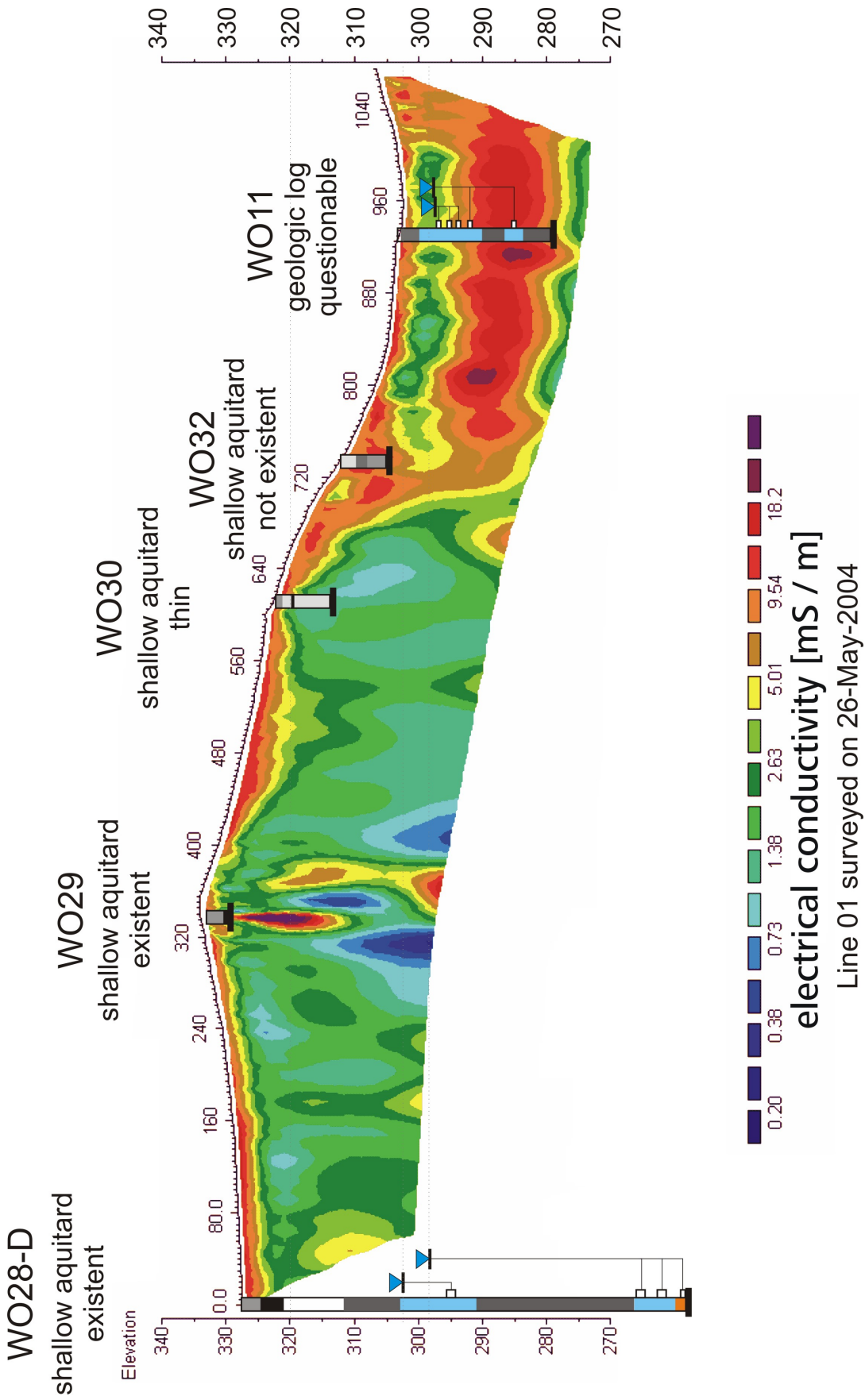
Figure A.1:
Resistivity Line 01
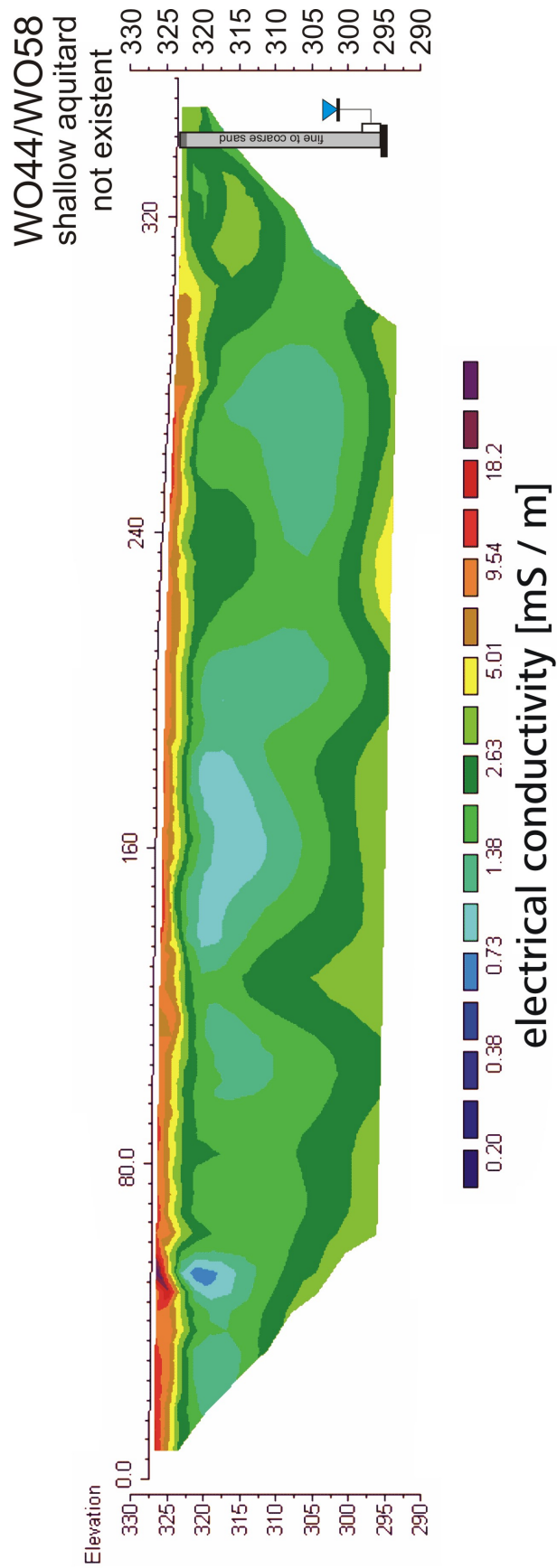
Figure A.2:
Resistivity Line 02
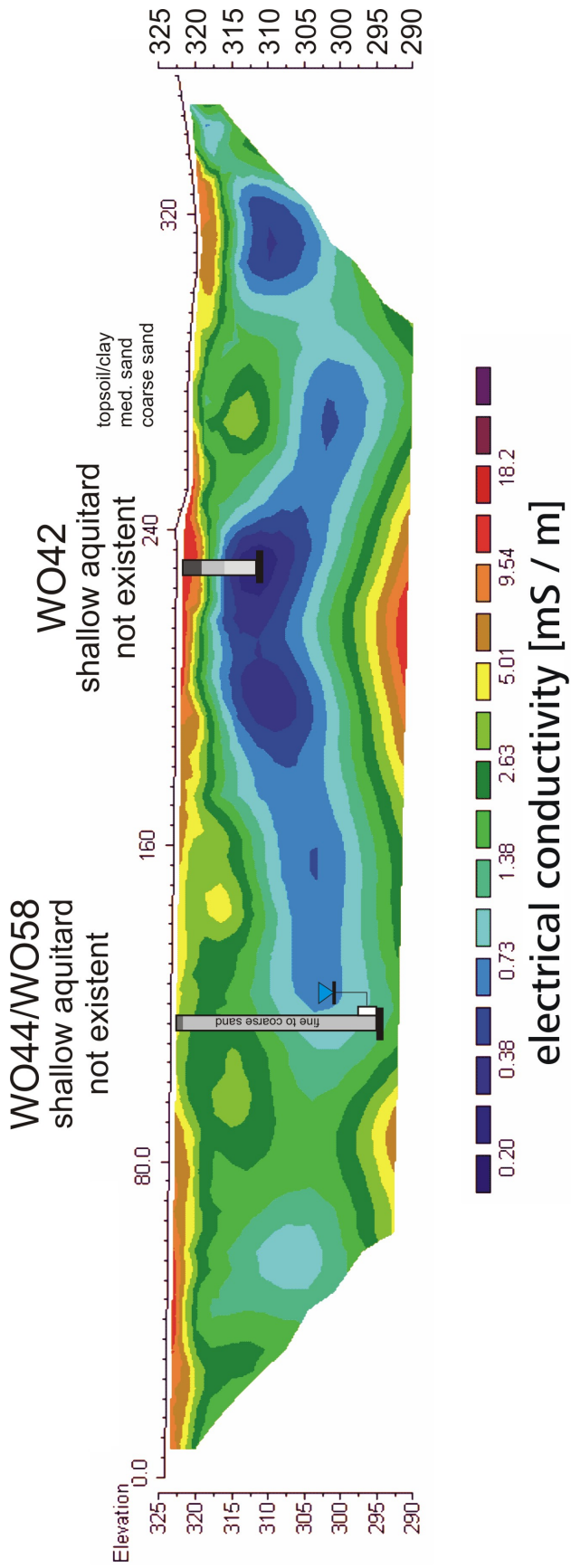
Figure A.3:
Resistivity Line 03
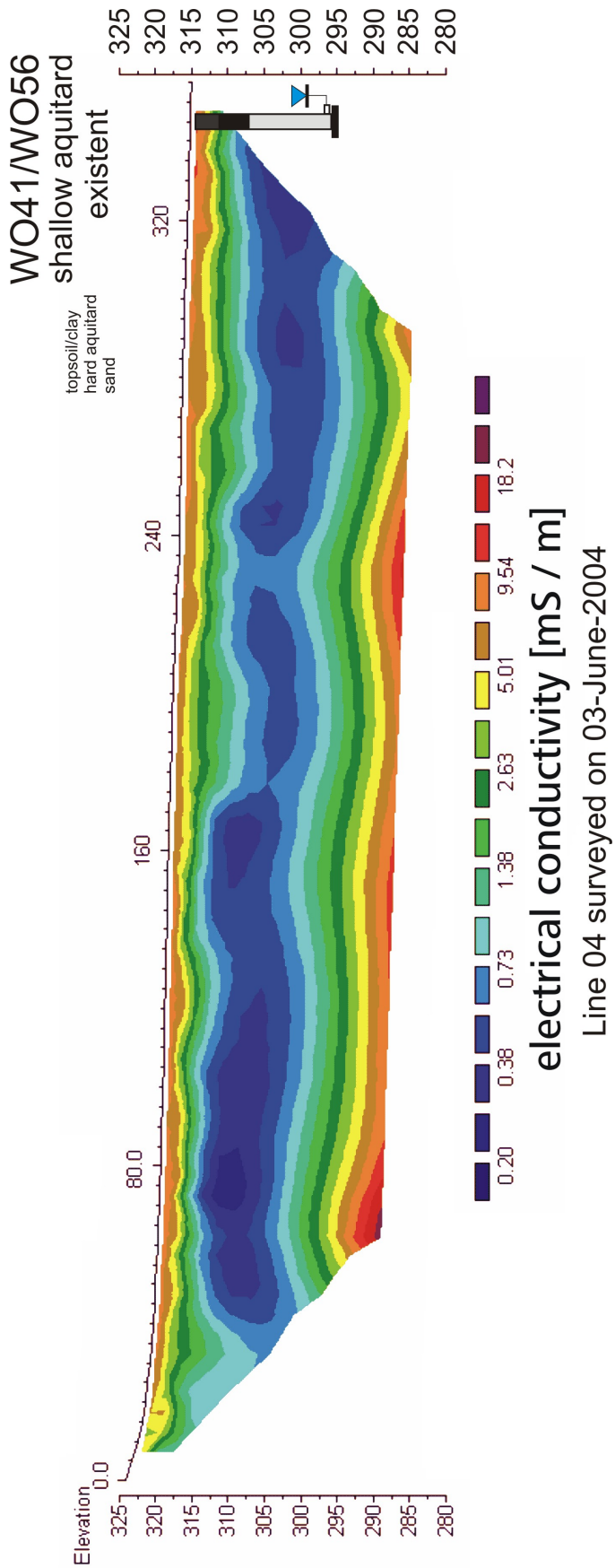
Figure A.4:
Resistivity Line 04

Figure A.5:
Resistivity Line 05

electrical conductivity [mS / m]
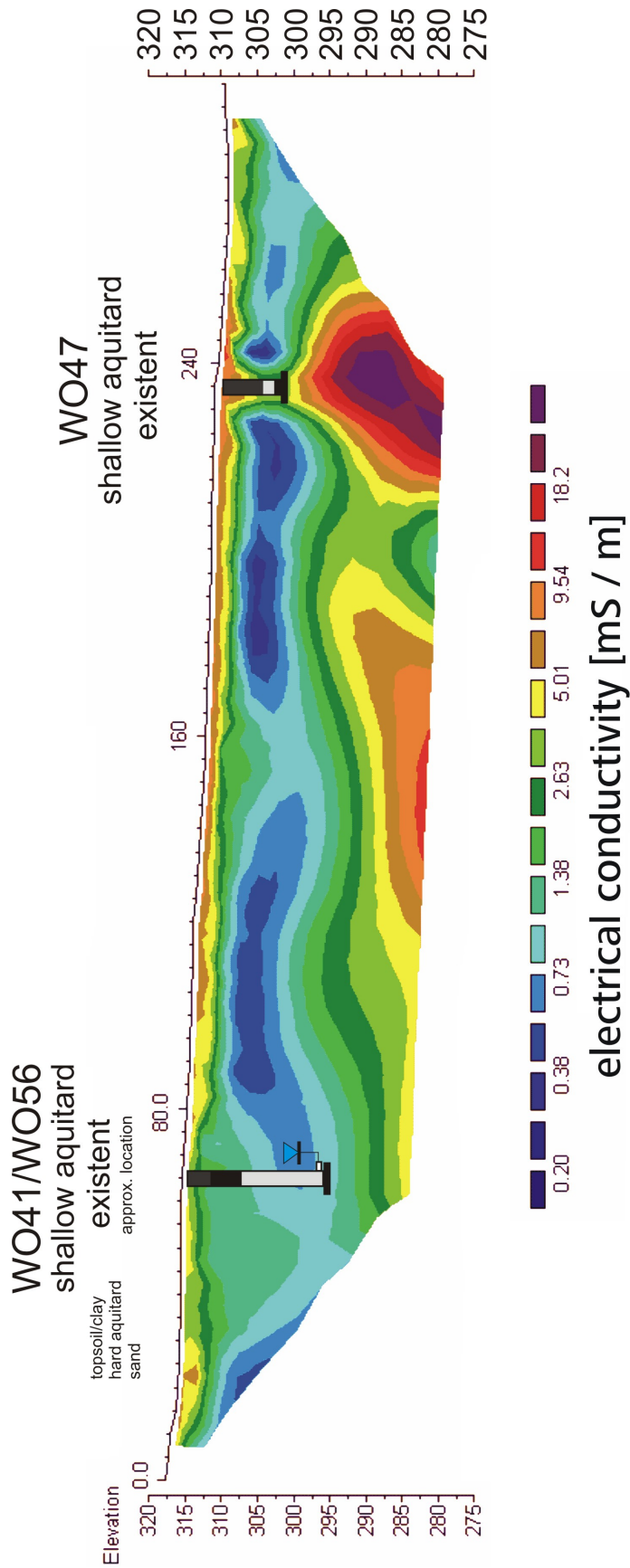
Line 5 surveyed on 03-June-2004

Relative Contribution of Material at a Specific Depth to the Apparent Conductivity

Horizontal Mode

Vertical Mode
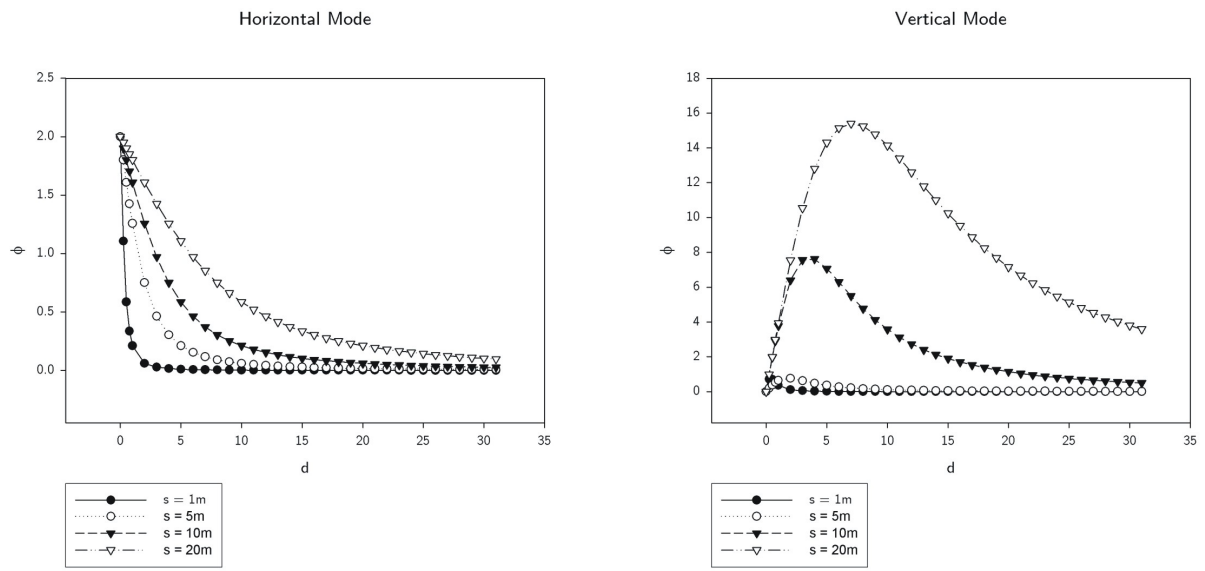
Cumulative Response from All Material Below a Specific Depth

Horizontal Mode

Vertical Mode
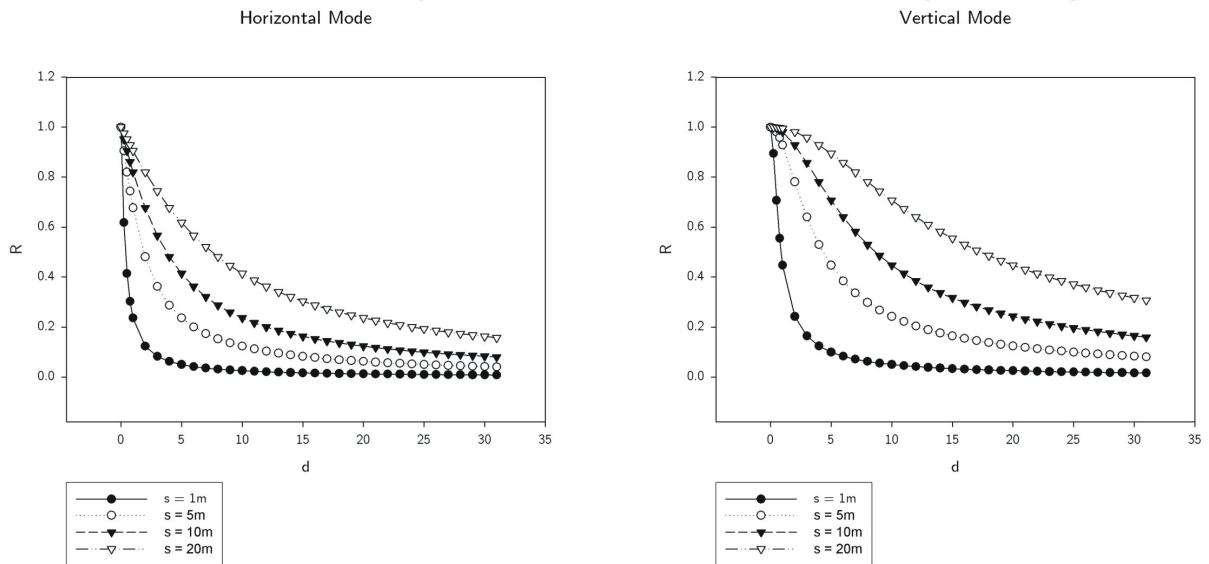
Figure A.6:
Relative contribution of the material at a specific depth to the apparent conductivity.

In total three sets of measurements were undertaken with different coil spacings and operation modes, as outlined in Table A.3.

Table A.3:

The three different sets of EM 34 measurements

Measurement ID	spacing s	mode
1	20m	vertical
2	10m	horizontal
3	10m	vertical

Table A.4 summarizes for each set of measurements, the 20%, 50%, and 80% cumulative contribution of material below a given depth to a measurement. The 20m spacing with vertical operation mode results in the greatest penetration depth, with matrix properties at depth greater than 20m contributing 50% to the measurement.

Table A.4:

Summary for each set of measurements of the 20%, 50%, and 80% cumulative contribution of material below a given depth to a measurement

mode	20V	10V	10H
80 %	8 m	4 m	2 m
50 %	20 m	9 m	4 m
20 %	>30 m	25 m	13 m
	deepest	medium depths	shallowest

Figure A.7:
Tile drain TD at WO 40. Picture taken on 07-March-2004. The tile lines converge ~1mbgs into the bottom of the plastic barrel. The pressure head in those pipes is big enough that the water gets pushed to ground surface through an opening where it ponds and infiltrates as soon as the ground thaws. The plastic barrel has no outlet-pipe and is not connected to a drainage ditch.

Figure A.8 shows the detailed timeline for the downhole work on Well 01 in November 2004. Figure A.9 shows how the pump-setup consisting of a white PCV screen below the five-bowel pump was lifted out of the well and the pump-house with a crane. Figure A.10 shows the setup of the tools used for downhole-profiling. Figure App:fig:DownholeScreens shows the monitoring setup during the downhole profiling work. Figure A.14 shows the flow-tool used for measuring the flow velocity within the screen of Well 01.

The screen was divided into n 1 ft. long blocks, as symbolized by the blue rectangles on Figure A.13. $\dot{m}_i$ is the mass loading into block i in units [Mass/Time]. $\dot{V}_i$ is the inflow of water into block i in units [Volume/Time]. The indices -1 and $+1$ indicate loading or flow coming from the block below the current block or leaving the current block, respectively.

The mass balance for block i is:

$$\frac{\dot{m}_{i-1}}{\dot{V}_{i-1}} + \frac{\dot{m}_i}{\dot{V}_i} - \frac{\dot{m}_{-1} + \dot{m}_i}{\dot{V}_{i-1} + \dot{V}_i} = C_i \tag{A.5}$$

The desired parameter in Equation A.5 is $\dot{m}_i$:

$$\dot{m}_i = \frac{\left[\left(C_i - \frac{\dot{m}_{i-1}}{\dot{V}_{i-1}}\right) \cdot \dot{V}_i \cdot \left(\dot{V}_{i-1} + \dot{V}_i\right)\right] + \left(\dot{V}_i \cdot \dot{m}_{i-1}\right)}{\dot{V}_{i-1}} \tag{A.6}$$

Figure A.9:
A crane takes the pump out of Well 01.
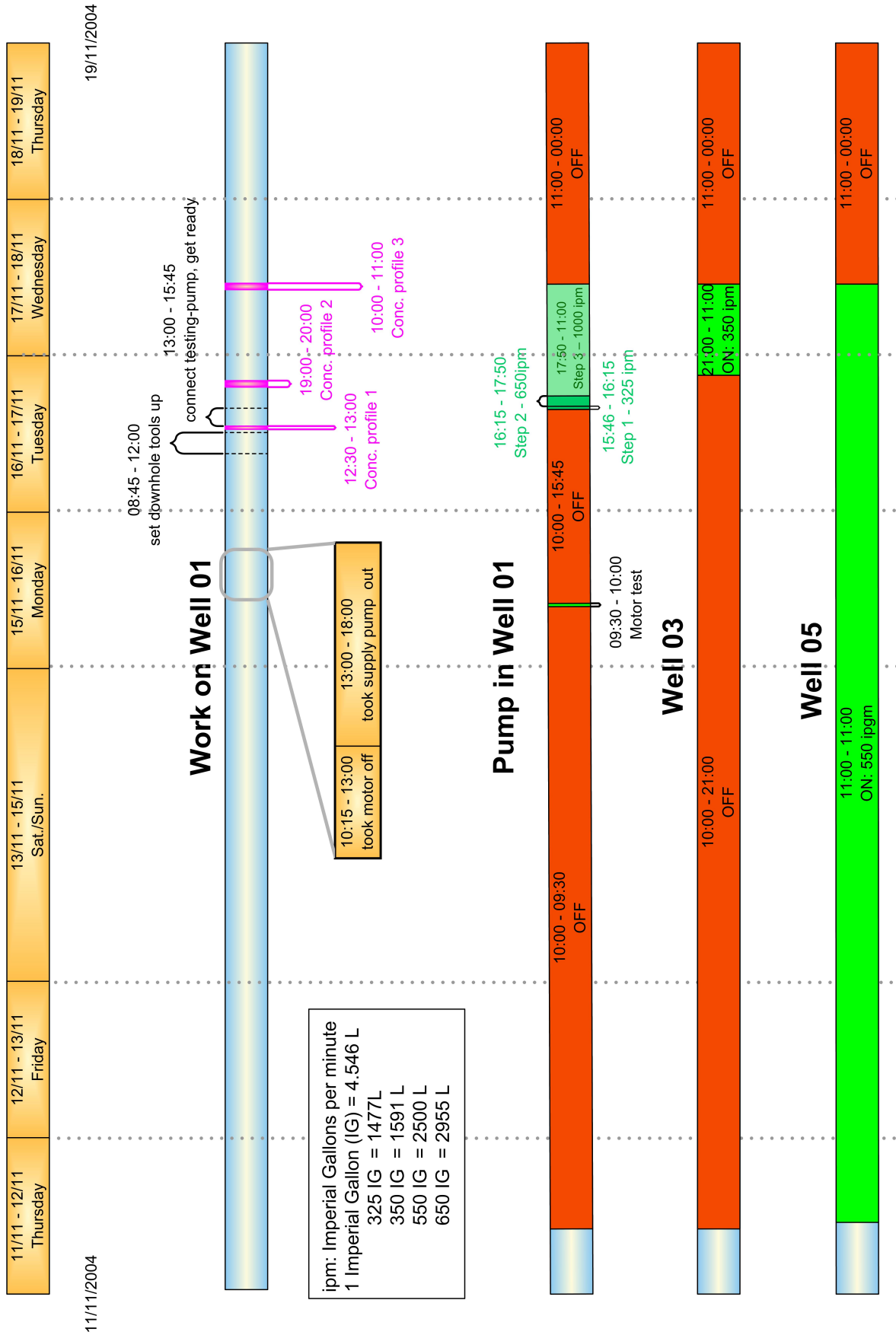
Figure A.8:
Timeline for work during downhole profiling.

153
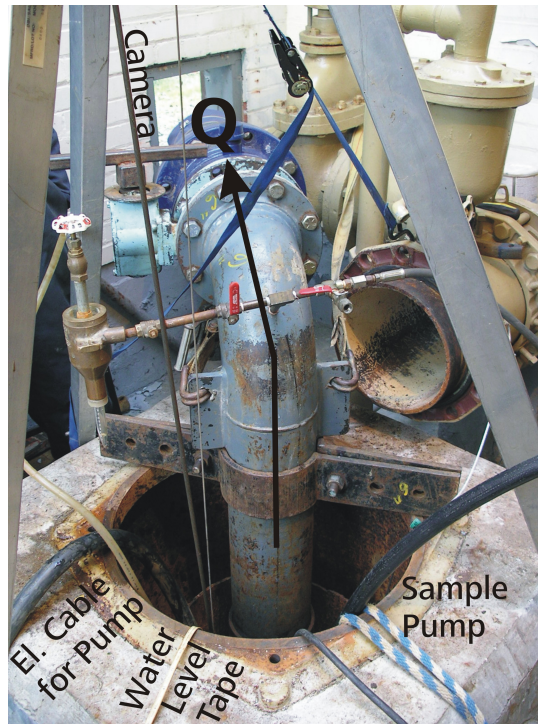
Figure A.10:
Tools setup for profiling Well 01.

Figure A.11:
Monitoring setup for profiling Well 01.

Figure A.12:
The flow tool used for profiling Well 01.
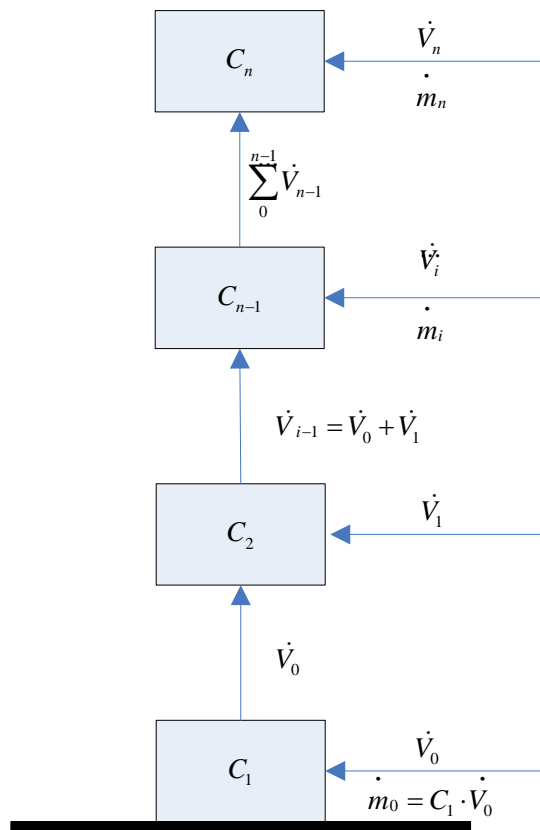
Figure A.13:
Conceptualization for Mass Balance.

For the whole domain:

1595mg NO$_3$-N
* (5*5 cells)
* 100 m^2 per cell
* 1500 kg soil / m^3 soil
= 6 t NO$_3$-N

60+60+50+50+25
+80+80+60+50+50
+75+80+80+40+40
+75+60+80+60+40
+90+75+75+80+80 = 1595mg NO$_3$-N

60	60	50	50	25
80	80	60	50	50
75	80	80	40	40
75	60	80	60	40
90	75	75	80	80

There are 25mg NO$_3$-N in this 10m by 10m cell and they are already summed up over the depth of the unsaturated zone

4*3

15	15	10	10	5
20	20	15	10	10
25	20	20	10	10
25	20	20	15	10
30	25	25	20	20

Thickness of the unsaturated zone [meter]

4

All values: mass nitrate per core-length [mg NO$_3$-N / kg soil]

10m

10m

4	4	5	5	5
4	4	4	5	5
3	4	4	4	4
3	3	4	4	4
3	3	3	4	4
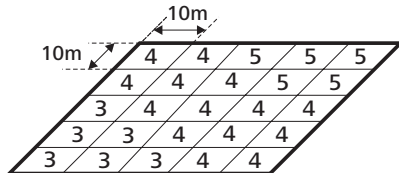
Proper value assigned to the corresponding cell of the grid

3

5

4

3
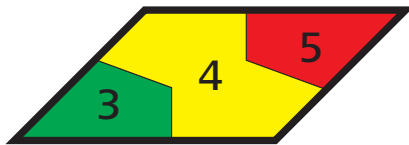
Interpolated values within domain

2

4   5

3   4
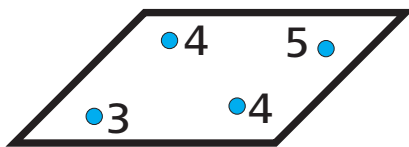
Measured values at cores (points)

1

Figure A.14:
Sketch for Raster Analysis. To be read from bottom up. Orders of magnitude of numbers are made up to be similar to reality, but are not reality.

Table A.5:
Monthly average pumping rates of individual wells and the total average of the Thornton Well Field in m^3/min.

Year	Month	Well 01	Well05	Well03	Well08	Well11	Overall Average
2003	Mar	0.4	0.68	1.63	0.43	1.81	4.95
2003	Apr	0.07	1.29	1.72	0.04	2.02	5.13
2003	May	0	1.05	1.7	0.01	2.09	4.85
2003	Jun	0.01	1.45	0.41	1.05	2	4.92
2003	Jul	0.23	1.34	0.72	1.45	2.04	5.78
2003	Aug	0.15	1.21	0.84	1.38	2.03	5.61
2003	Sep	0.07	0.97	1.12	1.05	1.94	5.16
2003	Oct	0	0.2	1.63	0.93	2.01	4.77
2003	Nov	0	0.23	1.58	0.12	1.94	3.87
2003	Dec	0.01	0.63	1.35	0	1.81	3.8
2004	Jan	0.01	1.04	1.14	0	1.92	4.11
2004	Feb	0.22	1.43	0.71	0	1.85	4.2
2004	Mar	0.01	1.34	0.22	0	1.62	3.18
2004	Apr	0.13	1.47	0.75	0	2.02	4.37
2004	May	0.08	1.11	1.24	0	1.98	4.4
2004	Jun	0.03	0.68	1.38	0	2.02	4.12
2004	Jul	1.26	0.03	1.32	0	2.07	4.68
2004	Aug	0.67	0.04	1.36	0	2.03	4.11
2004	Sep	0.33	0.36	1.34	0	1.92	3.95
2004	Oct	0.63	0.42	1.51	0	1.95	4.51
2004	Nov	0.06	1.56	0.31	0.49	0.93	3.35
2004	Dec	0	1.8	0.59	1.01	0.26	3.66
2005	Jan	0	1.71	0.46	0.77	0.88	3.82

Table A.6:
Contributing Percentage of Each Well to the Total Flow Rate

Year	Month	Well 01	Well05	Well03	Well08	Well11
2003	Mar	8.1	13.7	32.8	8.7	36.6
2003	Apr	1.3	25.1	33.5	0.8	39.3
2003	May	0	21.7	35.1	0.2	43
2003	Jun	0.2	29.6	8.3	21.3	40.6
2003	Jul	4	23.2	12.4	25.1	35.3
2003	Aug	2.7	21.6	15	24.6	36.1
2003	Sep	1.5	18.9	21.8	20.3	37.6
2003	Oct	0	4.2	34.2	19.5	42.1
2003	Nov	0	5.8	40.8	3.2	50.1
2003	Dec	0.3	16.5	35.6	0	47.7
2004	Jan	0.2	25.4	27.6	0	46.8
2004	Feb	5.3	34	16.8	0	44
2004	Mar	0.2	42.2	6.8	0	50.8
2004	Apr	3	33.6	17.3	0	46.1
2004	May	1.8	25.2	28.1	0	44.9
2004	Jun	0.8	16.5	33.5	0	49.2
2004	Jul	26.9	0.6	28.2	0	44.3
2004	Aug	16.4	0.9	33.2	0	49.5
2004	Sep	8.3	9.1	33.9	0	48.7
2004	Oct	14	9.3	33.4	0	43.3
2004	Nov	1.7	46.5	9.3	14.8	27.8
2004	Dec	0	49.1	16.2	27.6	7.1
2005	Jan	0	44.6	12.1	20.2	23
Overall average		4.2	22.5	24.6	8.1	40.6

A.11

Nitrate Concentration in Well 01
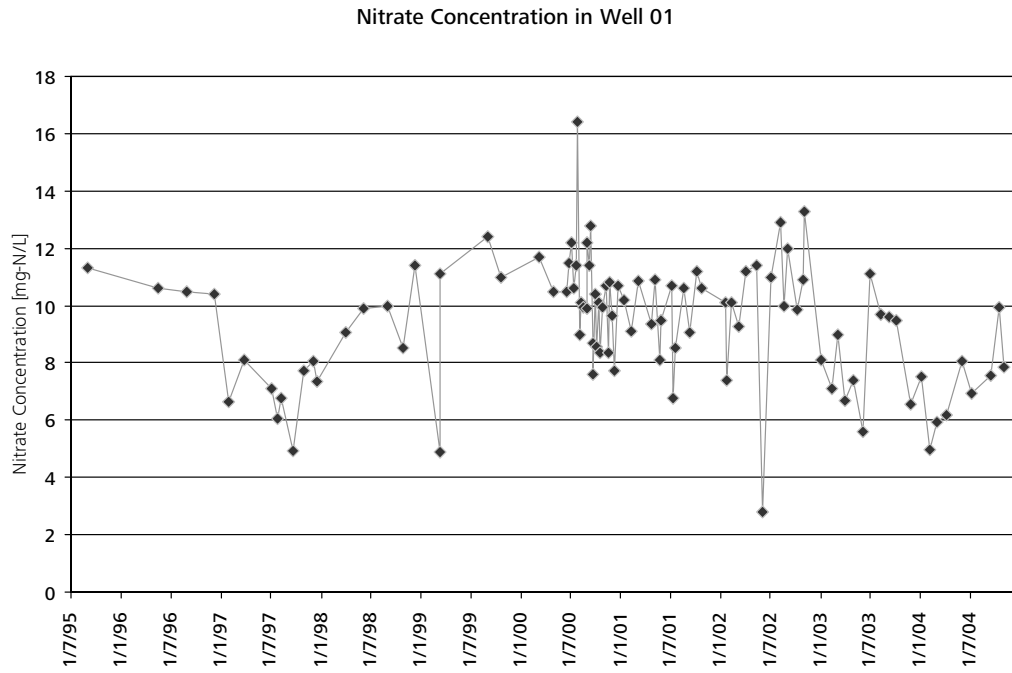
Figure A.15:
Trend of nitrate concentrations in Well 01
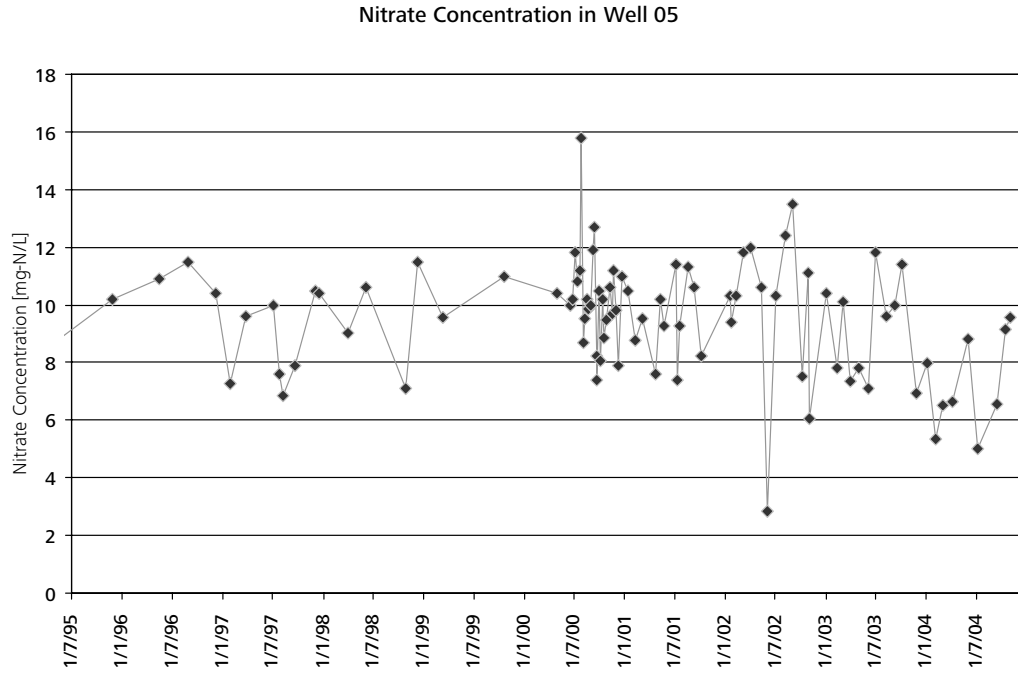
Figure A.16:
Trend of nitrate concentrations in Well 05
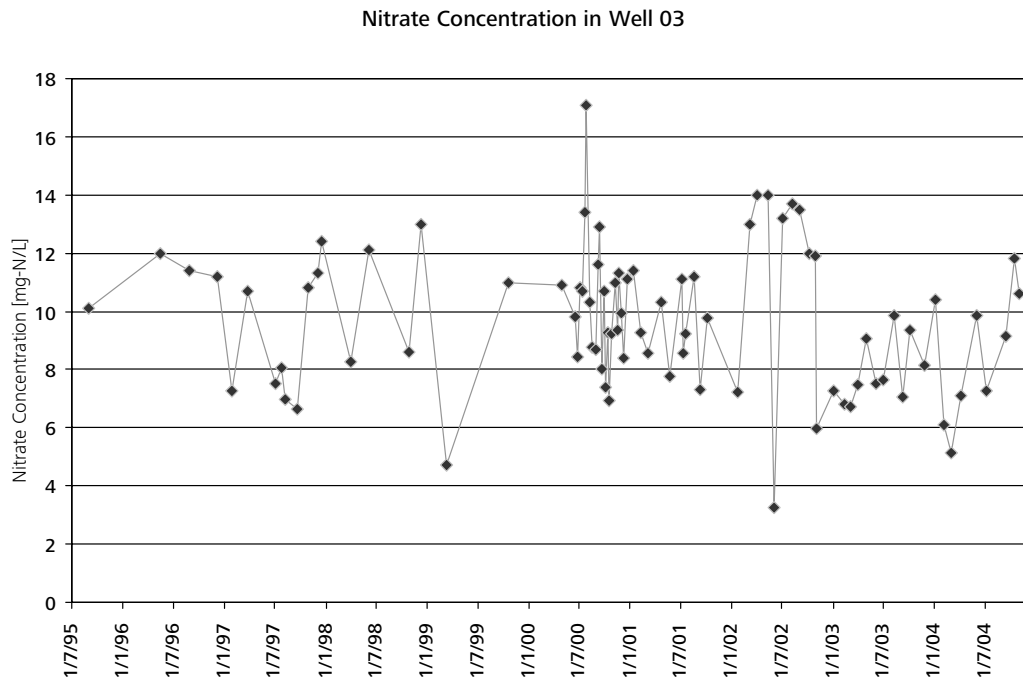
Figure A.17:
Trend of nitrate concentrations in Well 03

Nitrate Concentration in Well 08
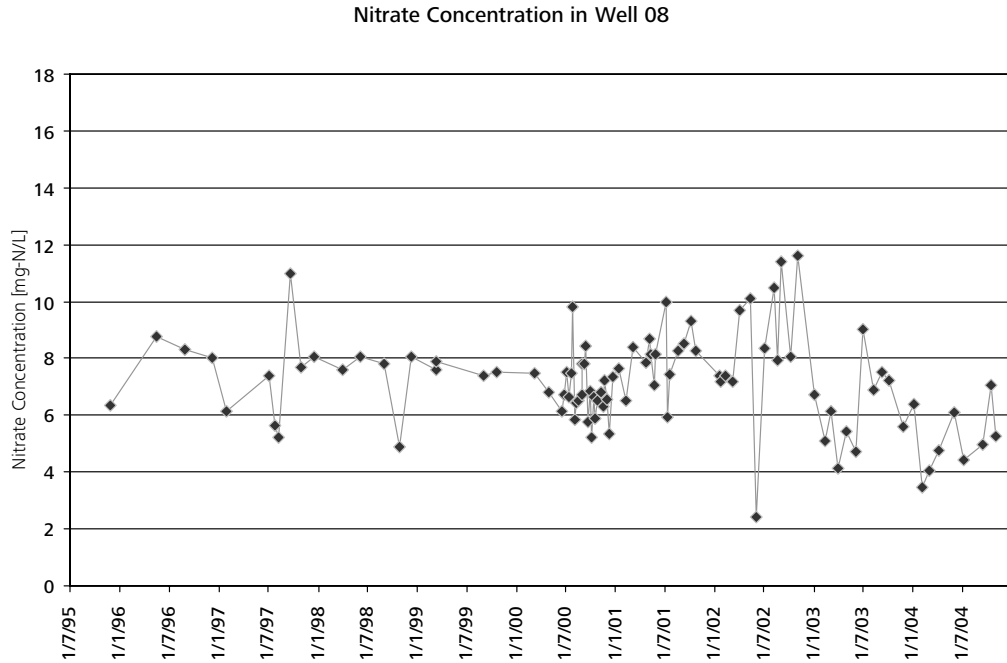
Figure A.18:
Trend of nitrate concentrations in Well 08

Nitrate Concentration in Well 11
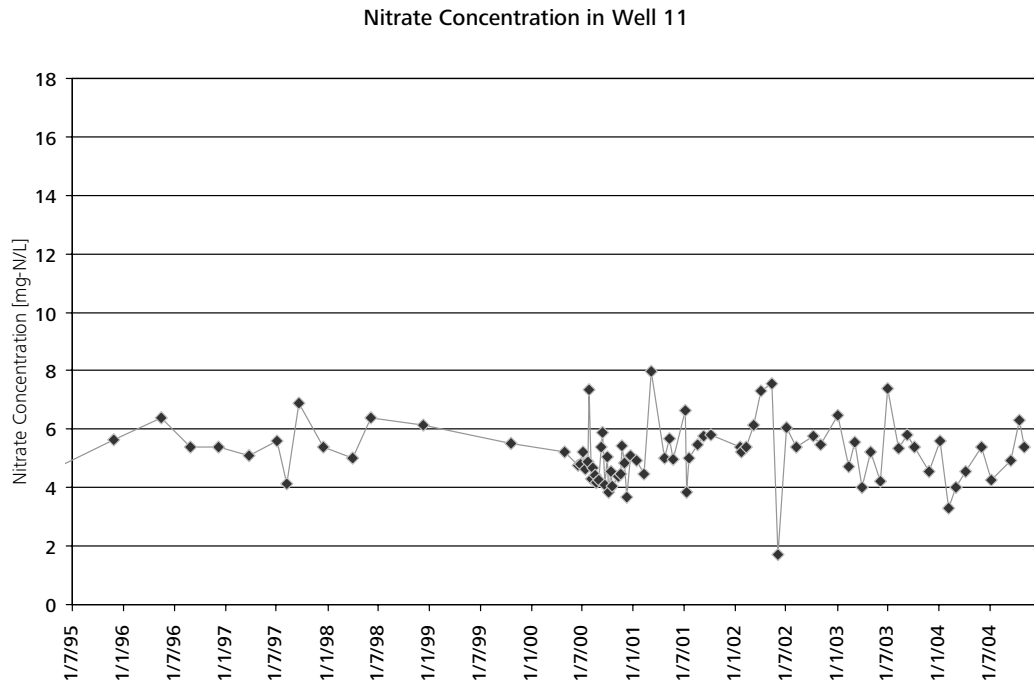
Figure A.19:
Trend of nitrate concentrations in Well 11

161
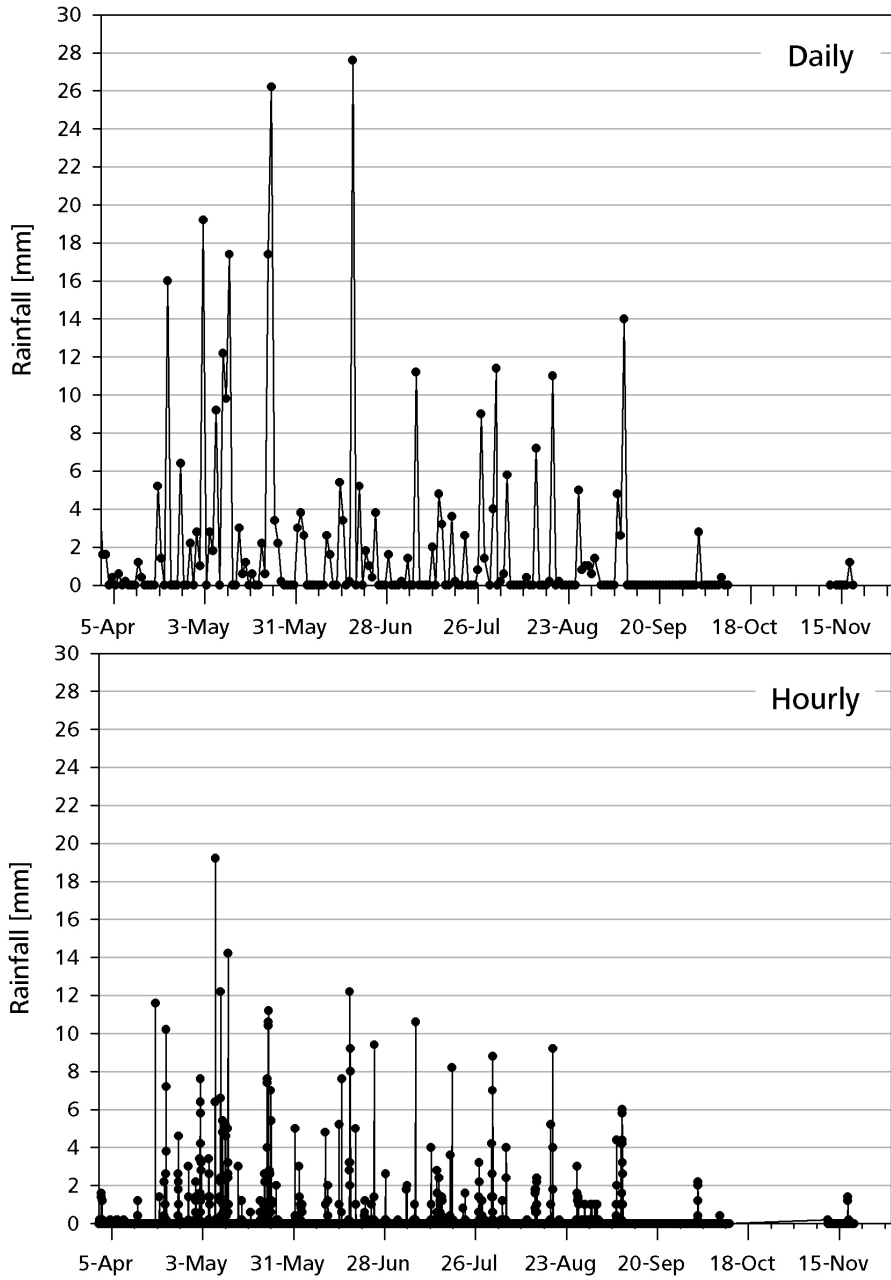
Figure A.20:
Precipitation over time at Well 01
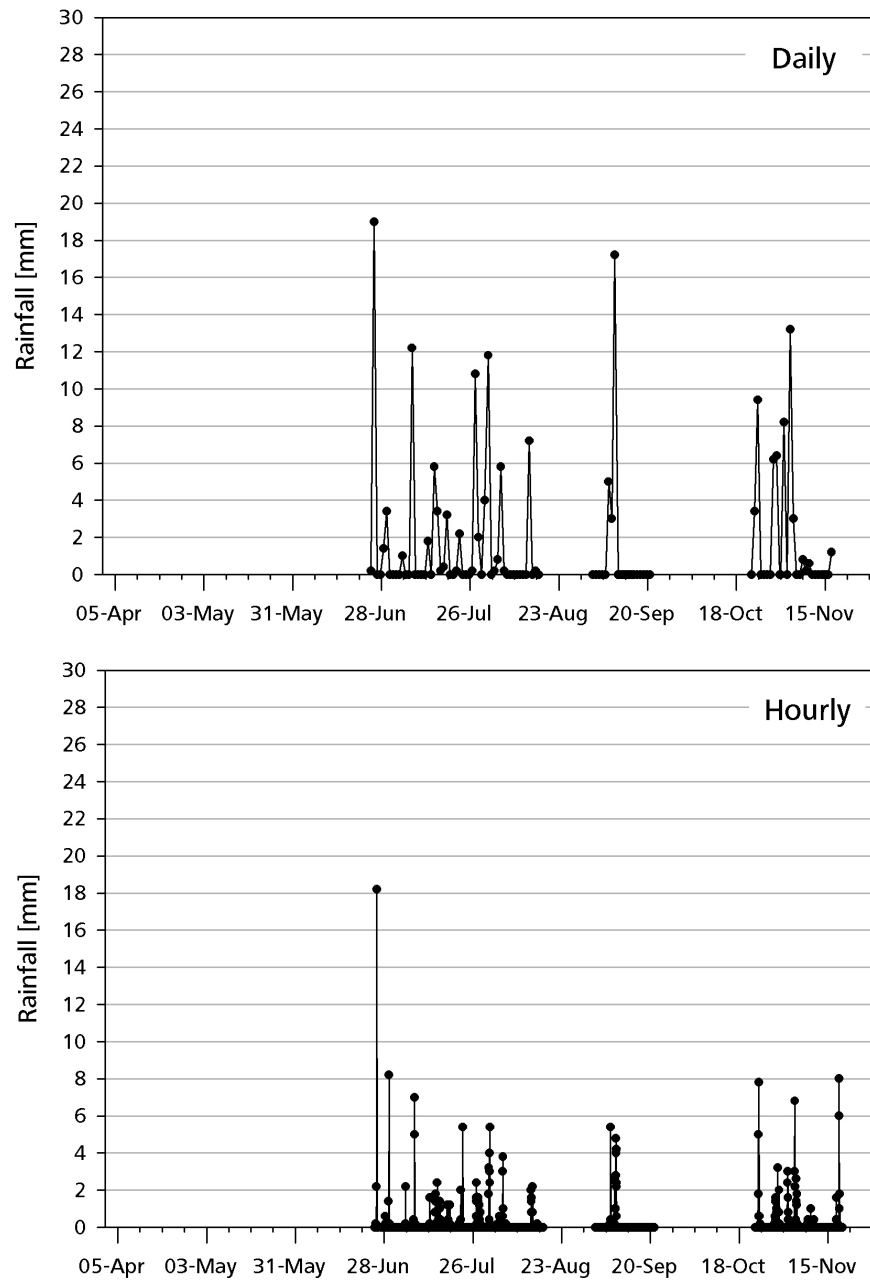
Figure A.21:
Precipitation over time at the Weir Box
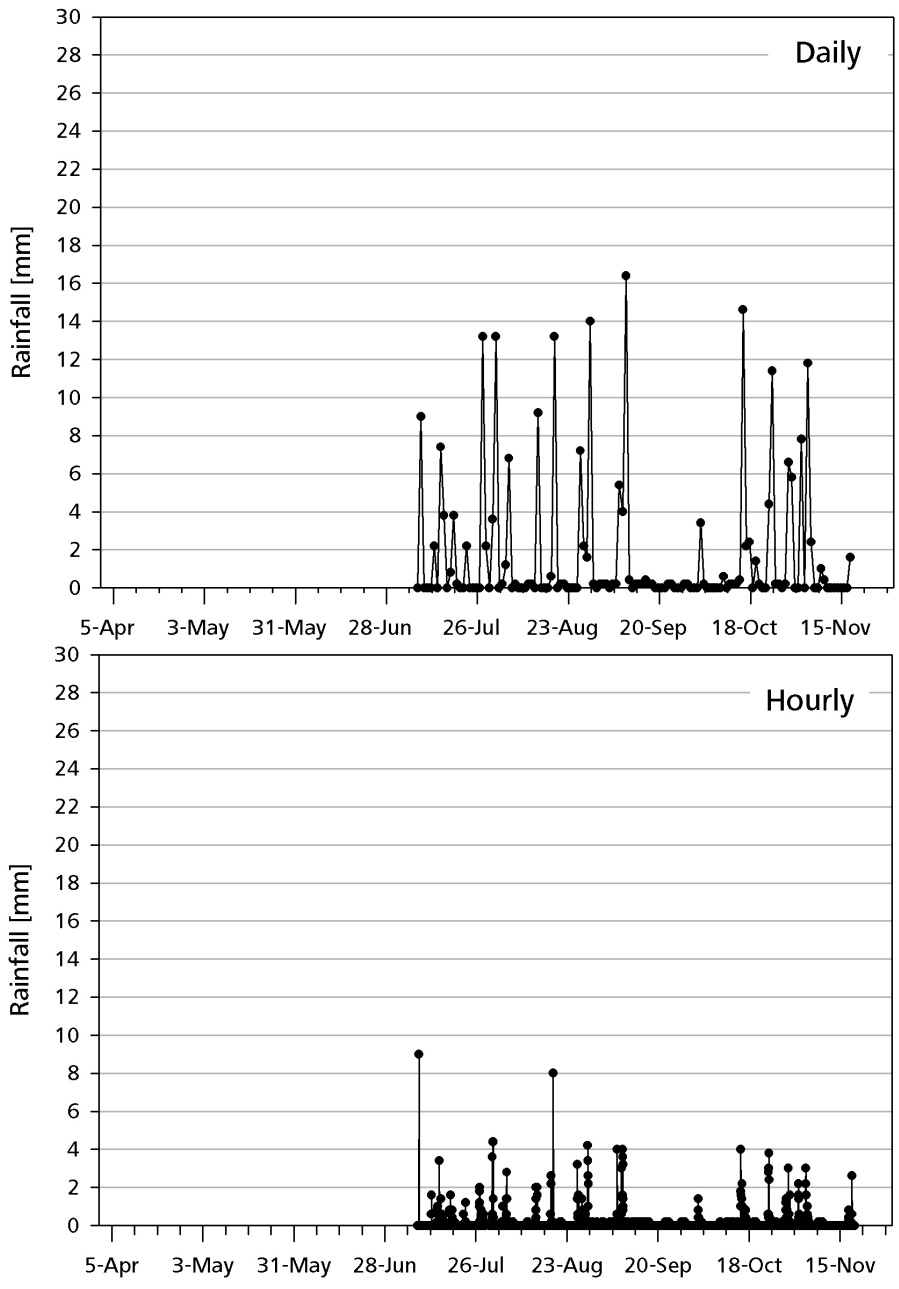
Figure A.22:
Precipitation over time at WO 28-D
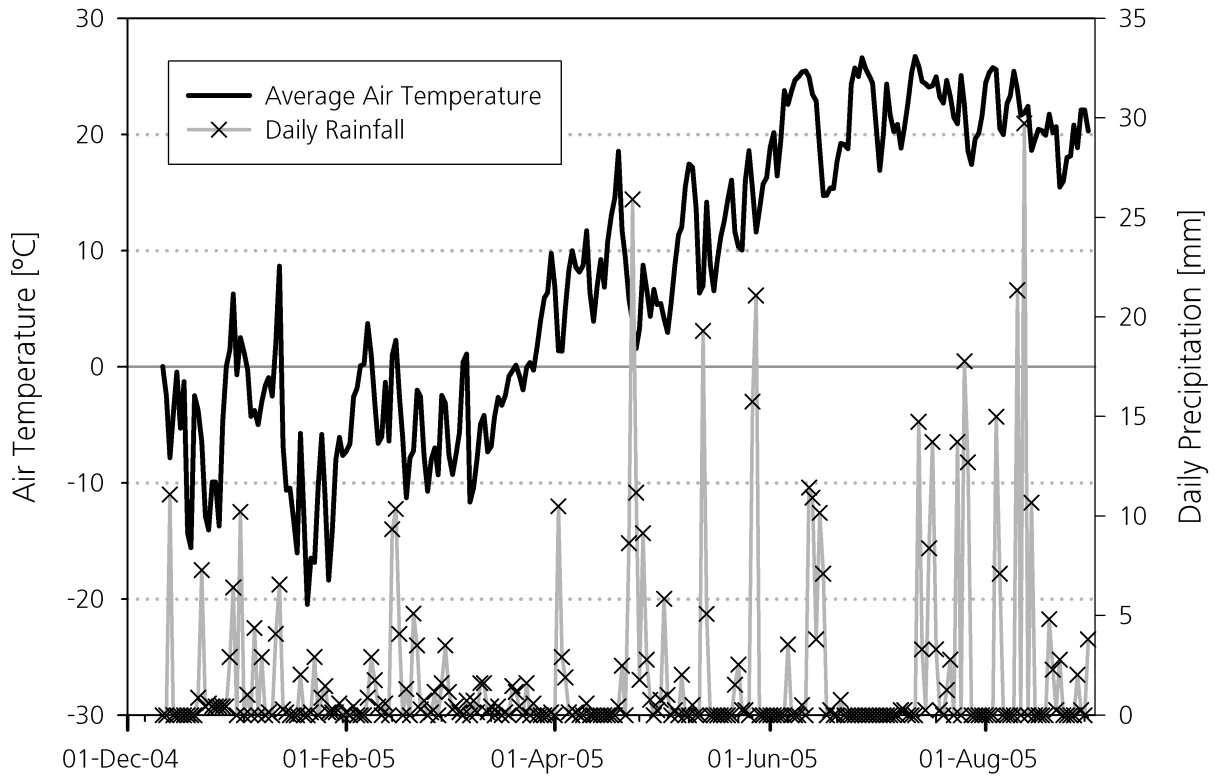
Figure A.23:
Precipitation over time at the meteorological station on site.

Core Logs and Profiles $\Big|$ A.13
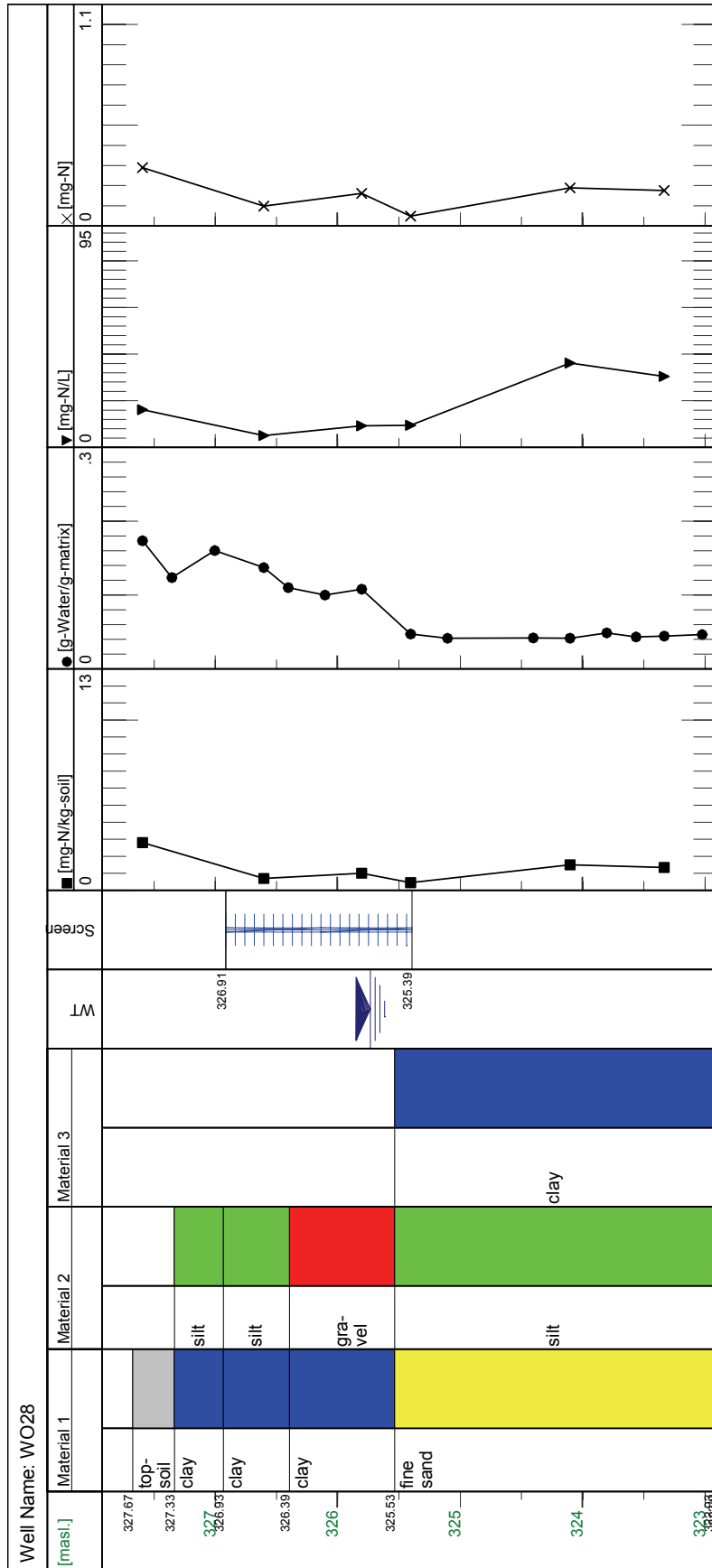
Figure A.24:
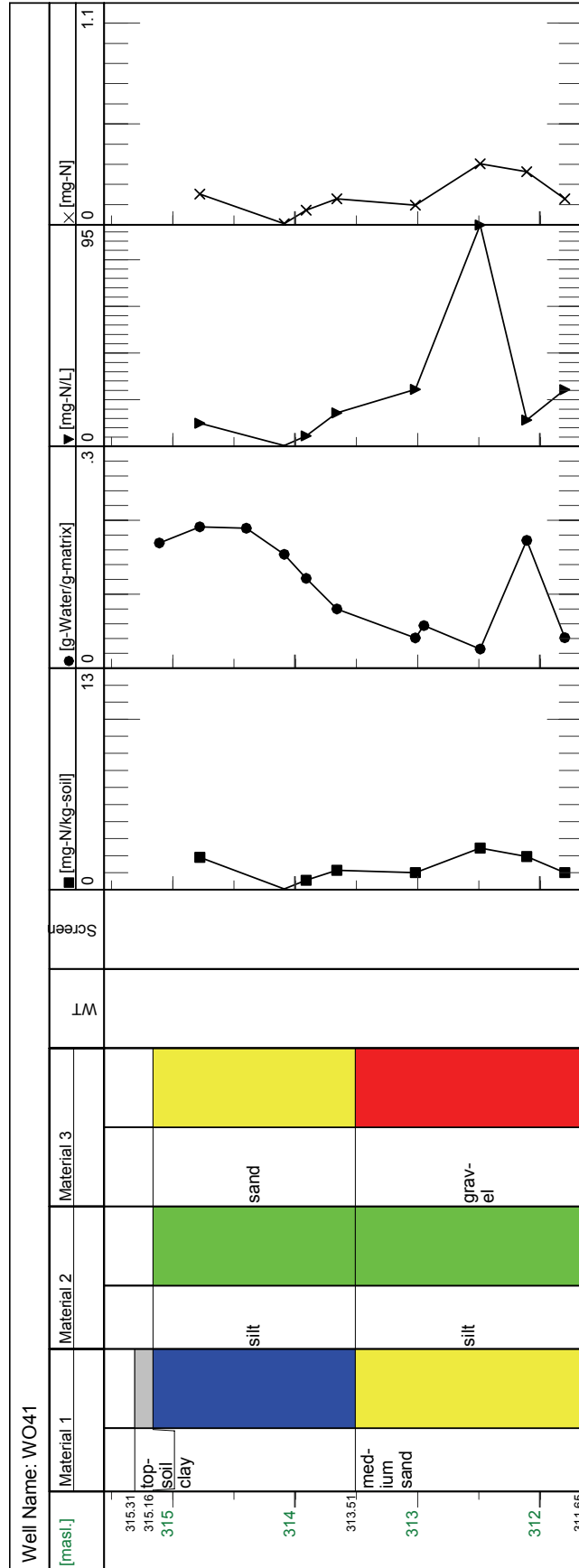Geologic log and nitrate profiles at location WO 28.

167
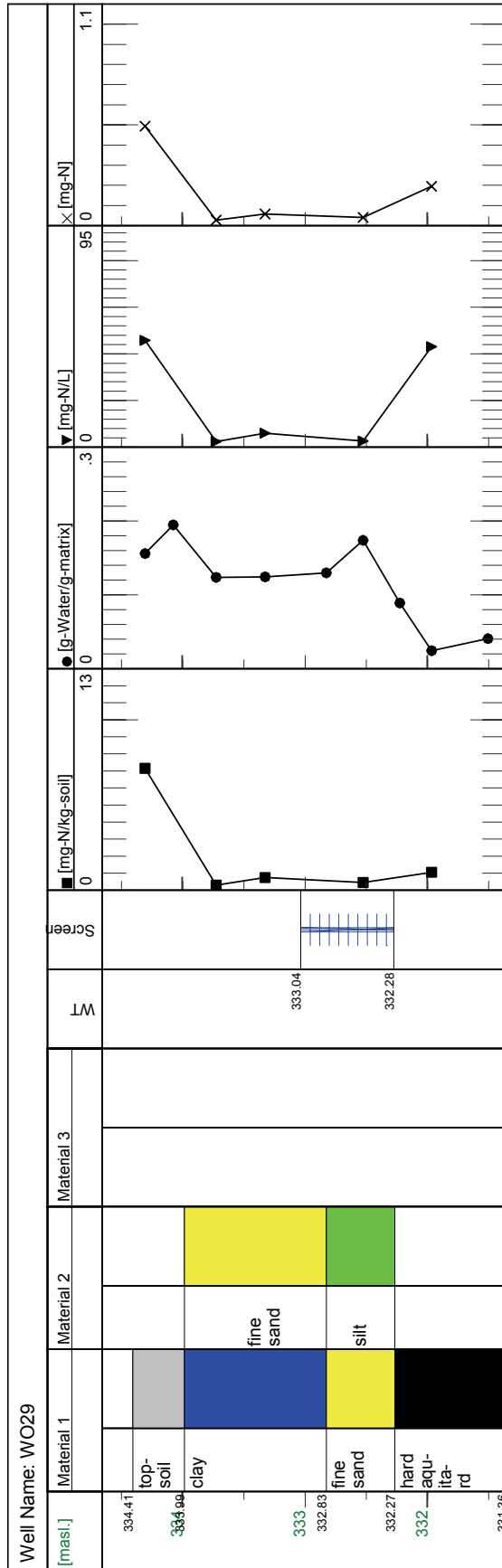
Figure A.25:
Geologic log and nitrate profiles at location WO 29.
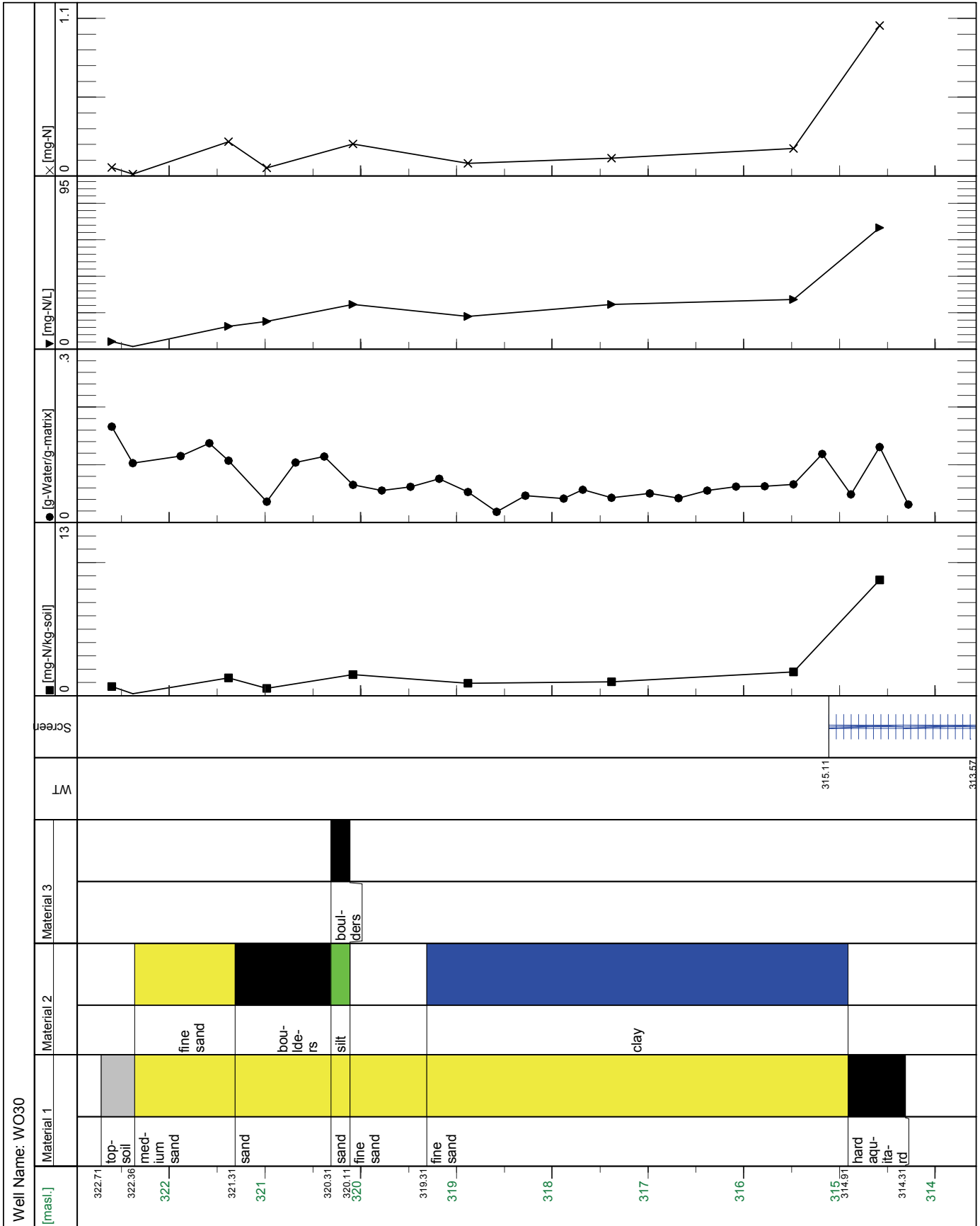
Figure A.26:
Geologic log and nitrate profiles at location *WO 30*.
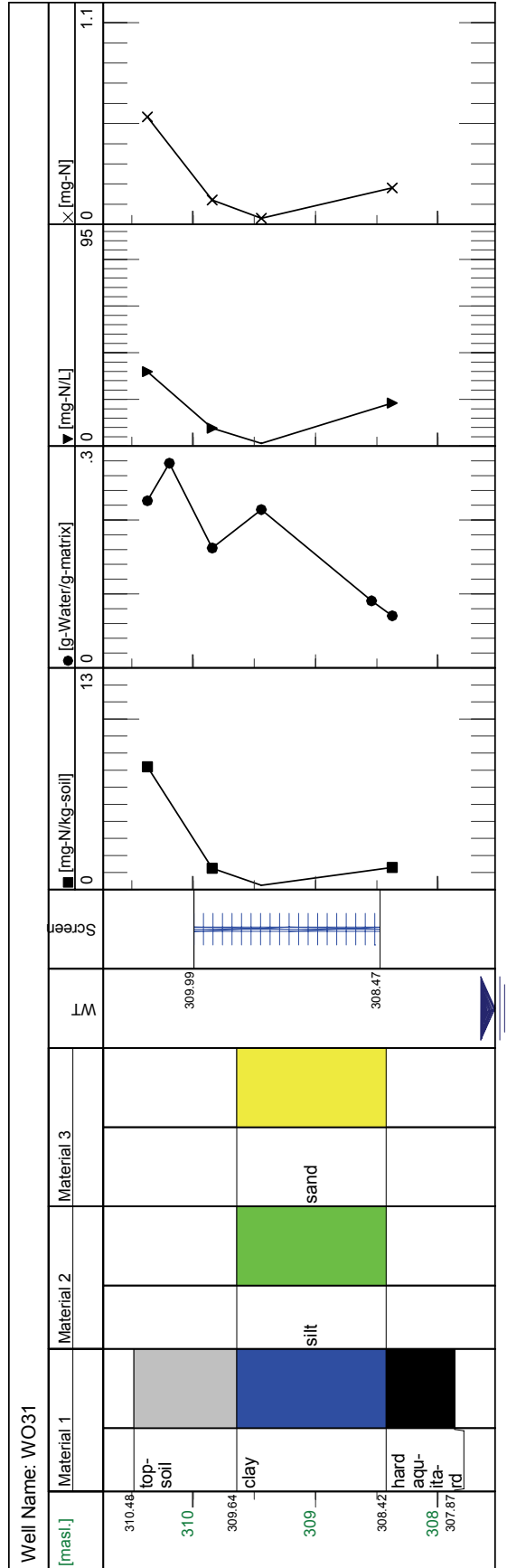
Figure A.27:
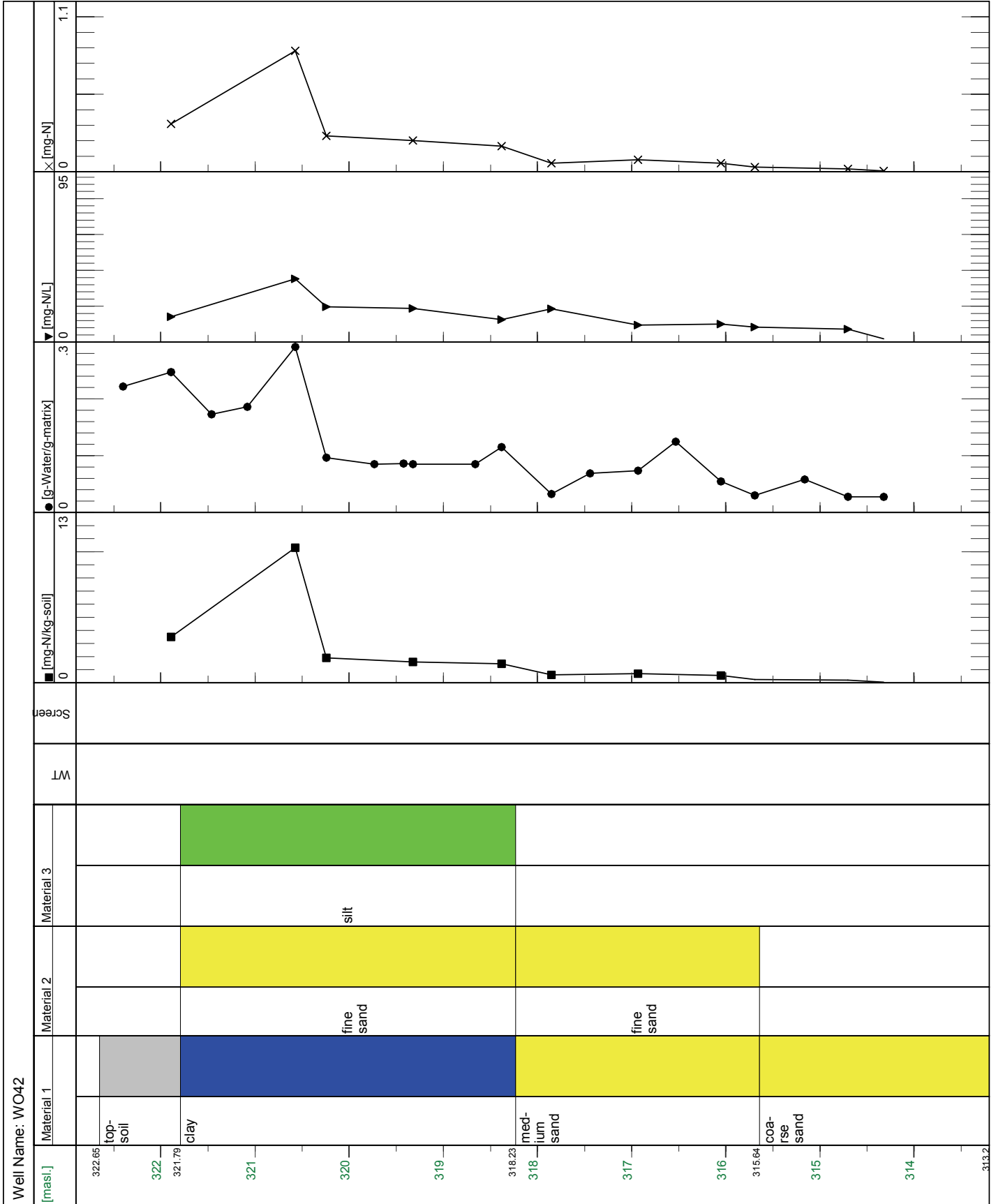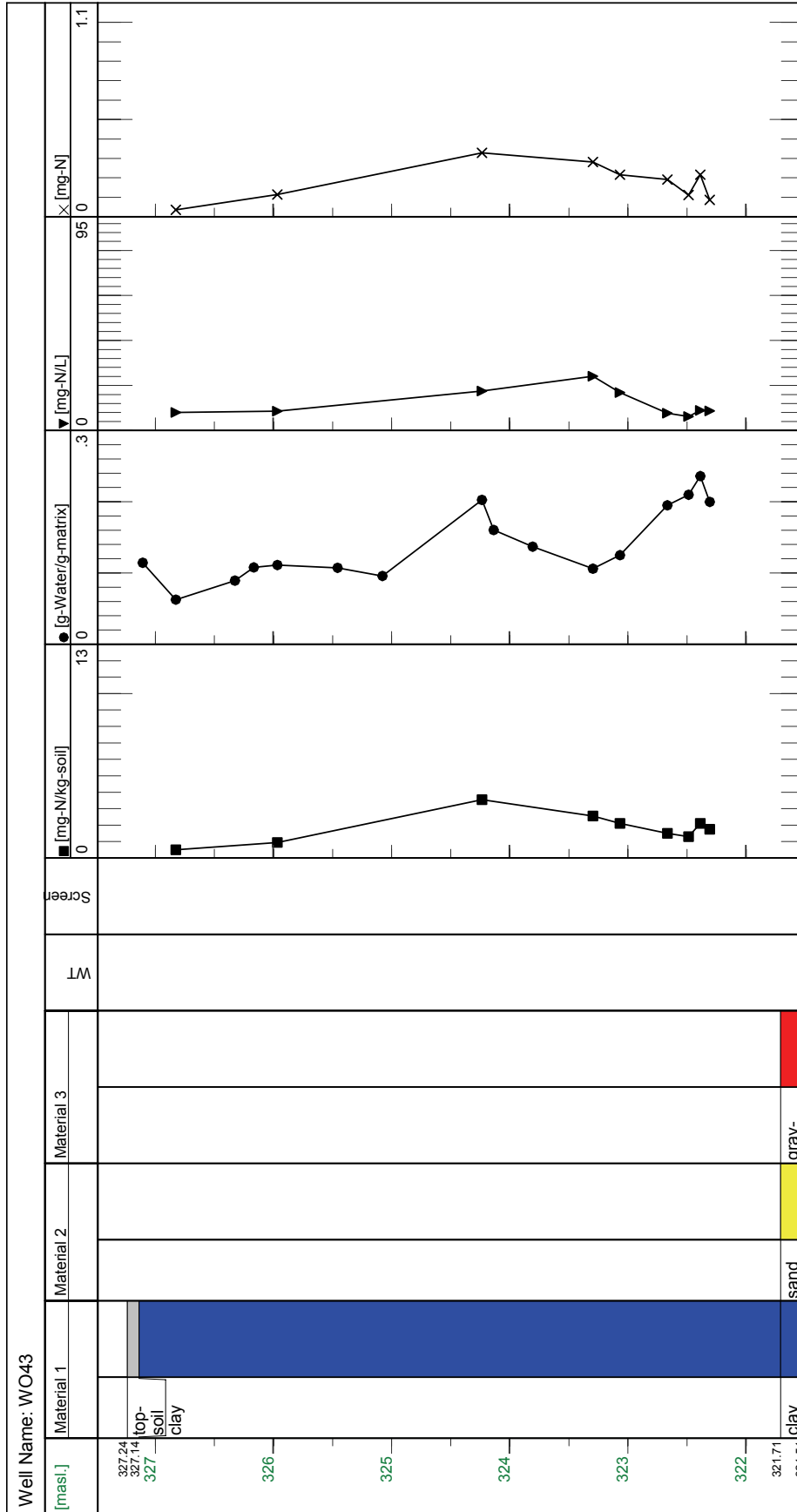Geologic log and nitrate profiles at location WO 31.
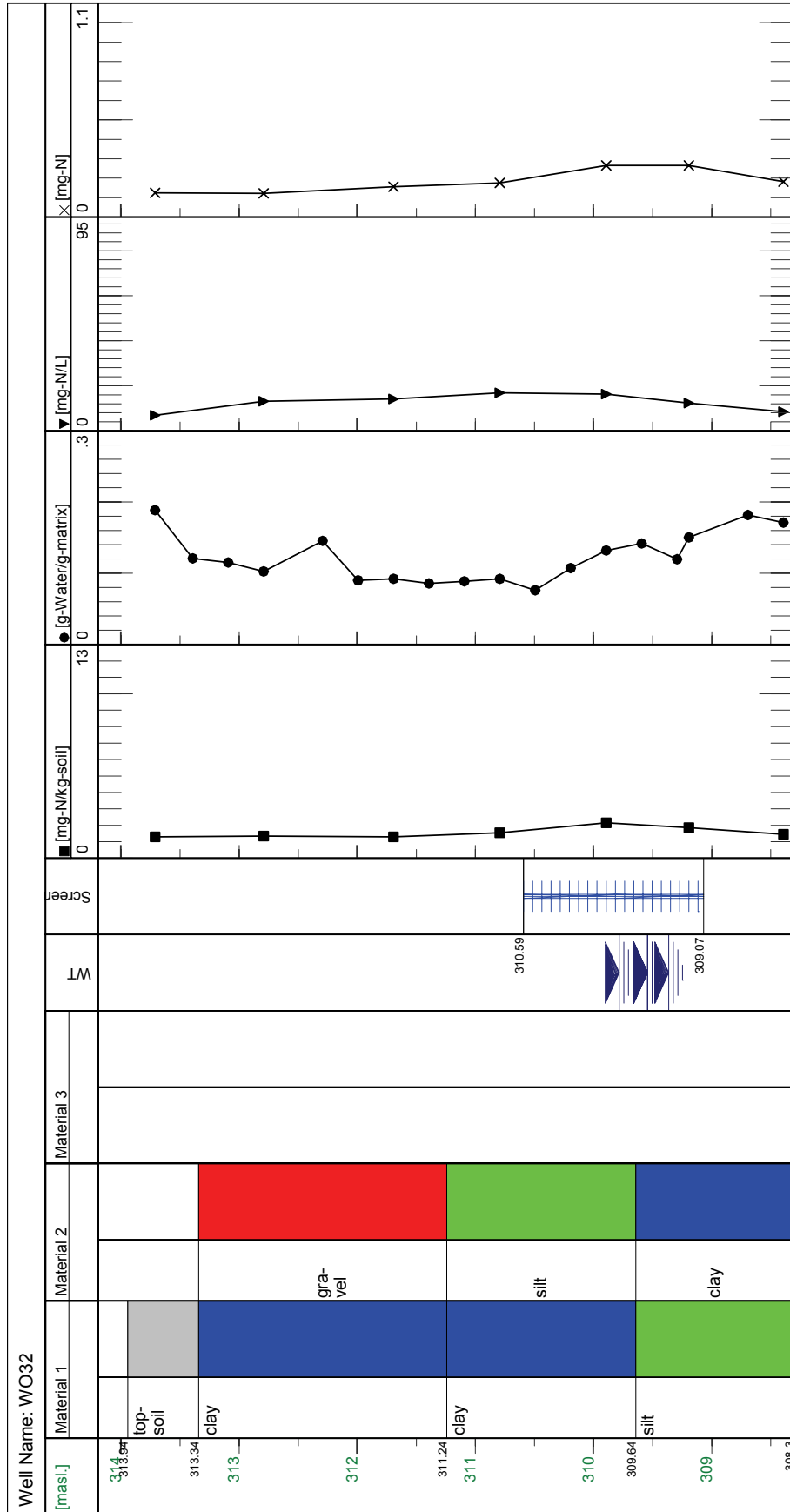
Figure A.28:
Geologic log and nitrate profiles at location WO 32.
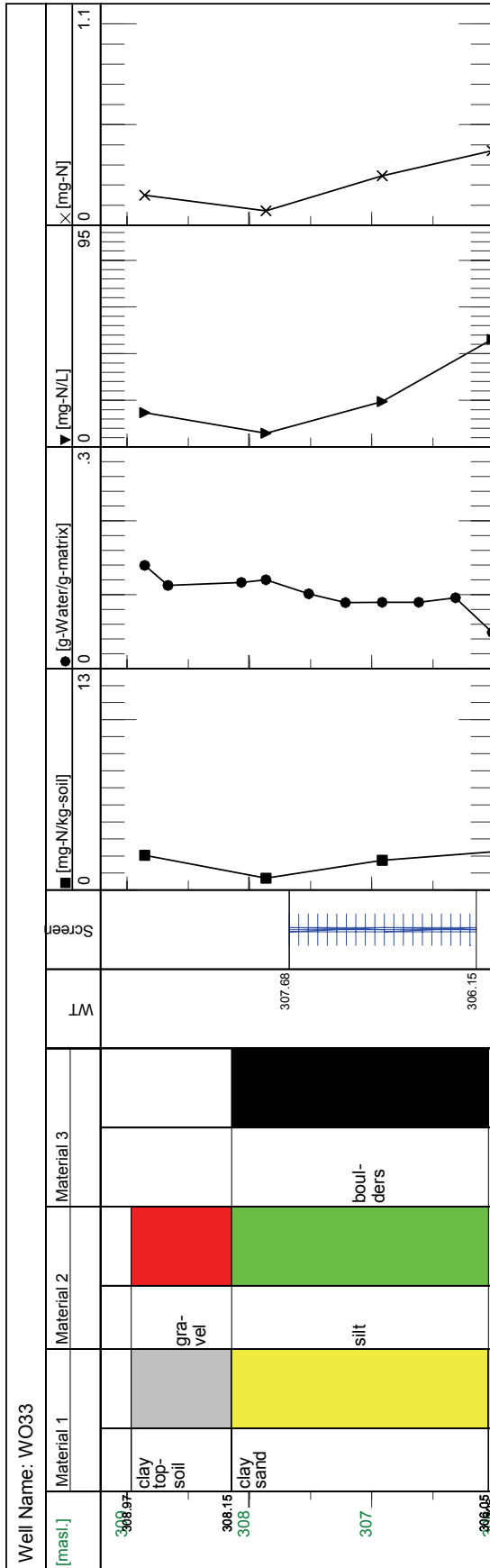
Figure A.29:
Geologic log and nitrate profiles at location WO 33.
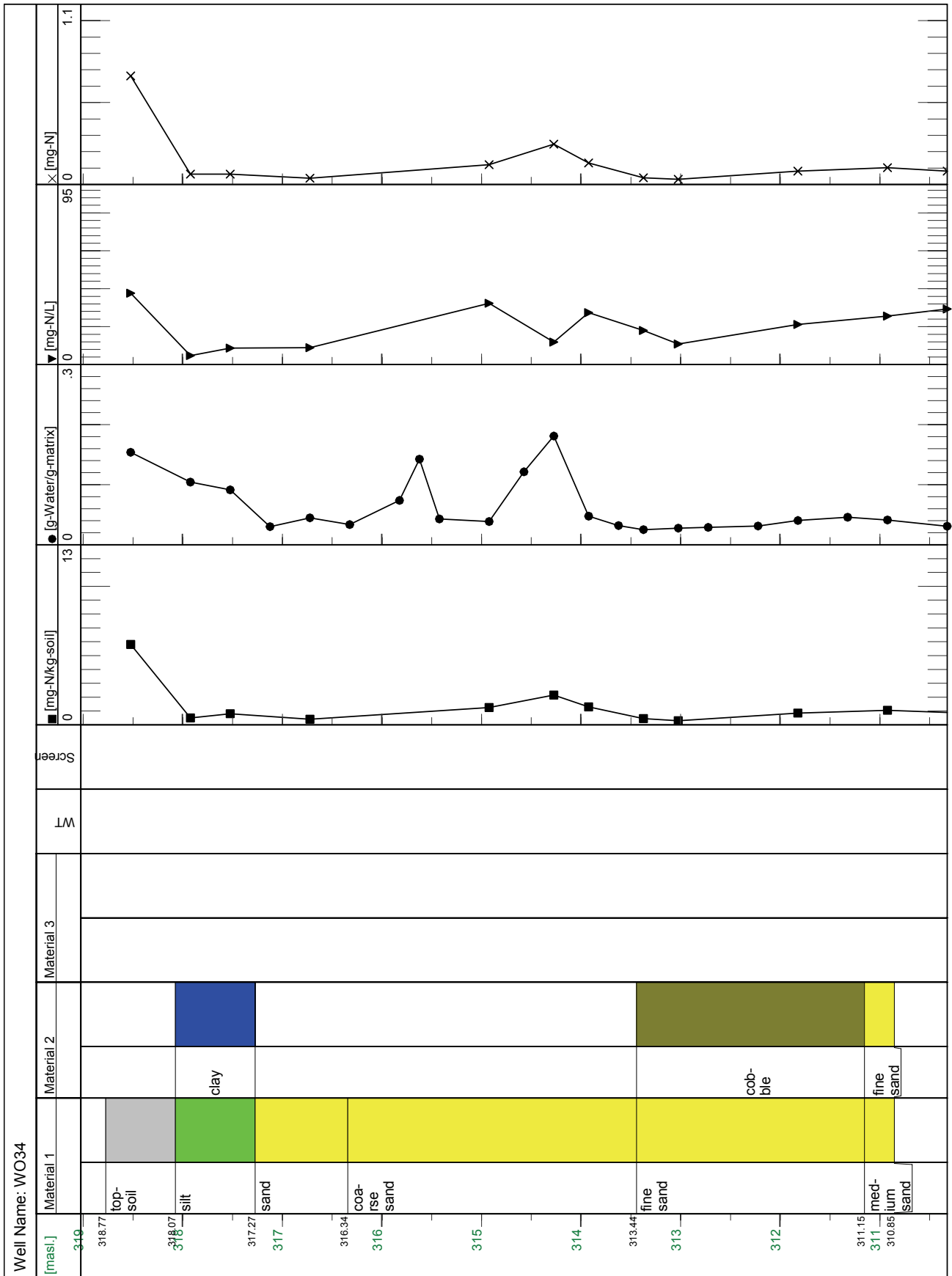
Figure A.30:
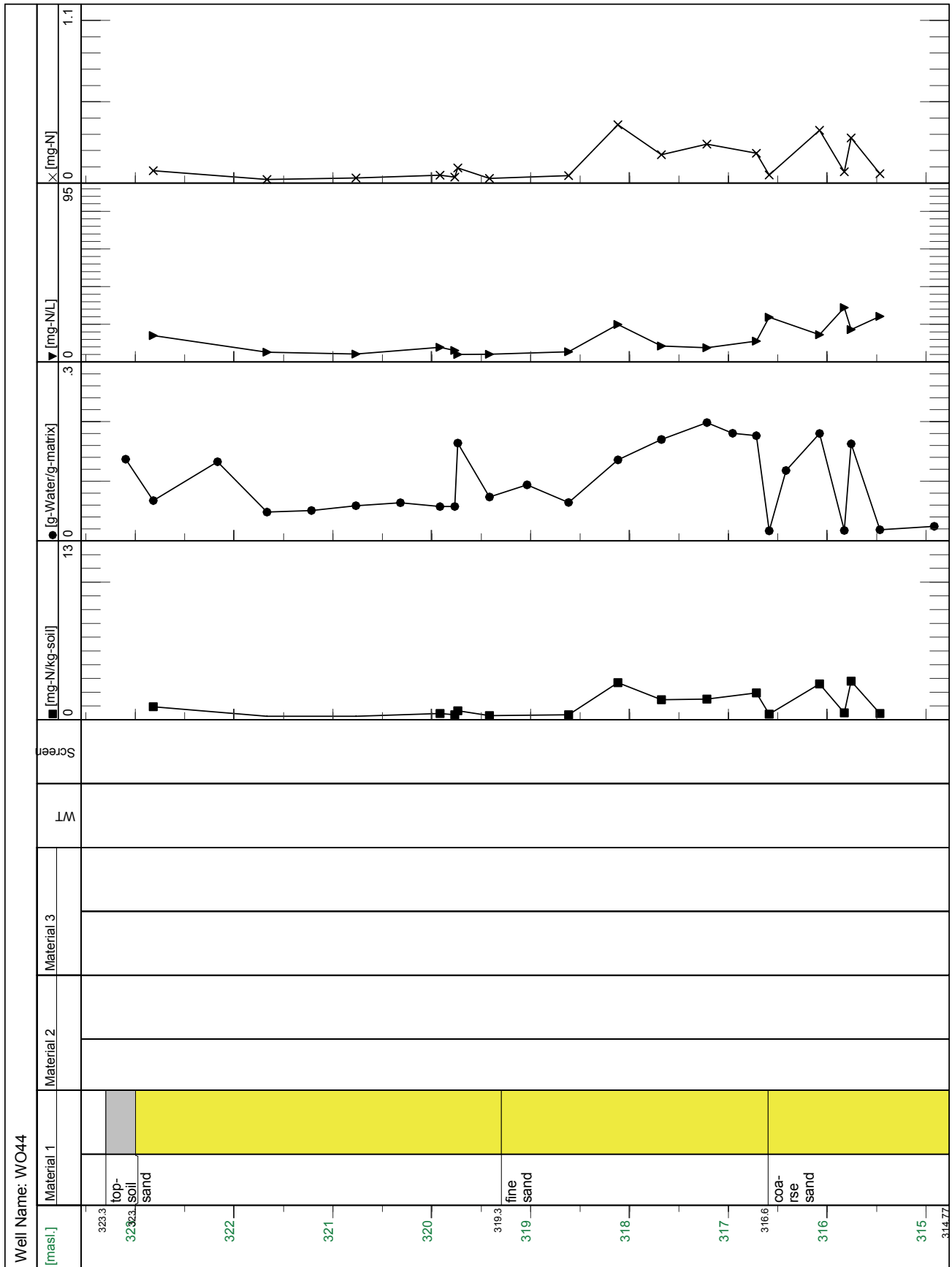Geologic log and nitrate profiles at location *WO 34*.
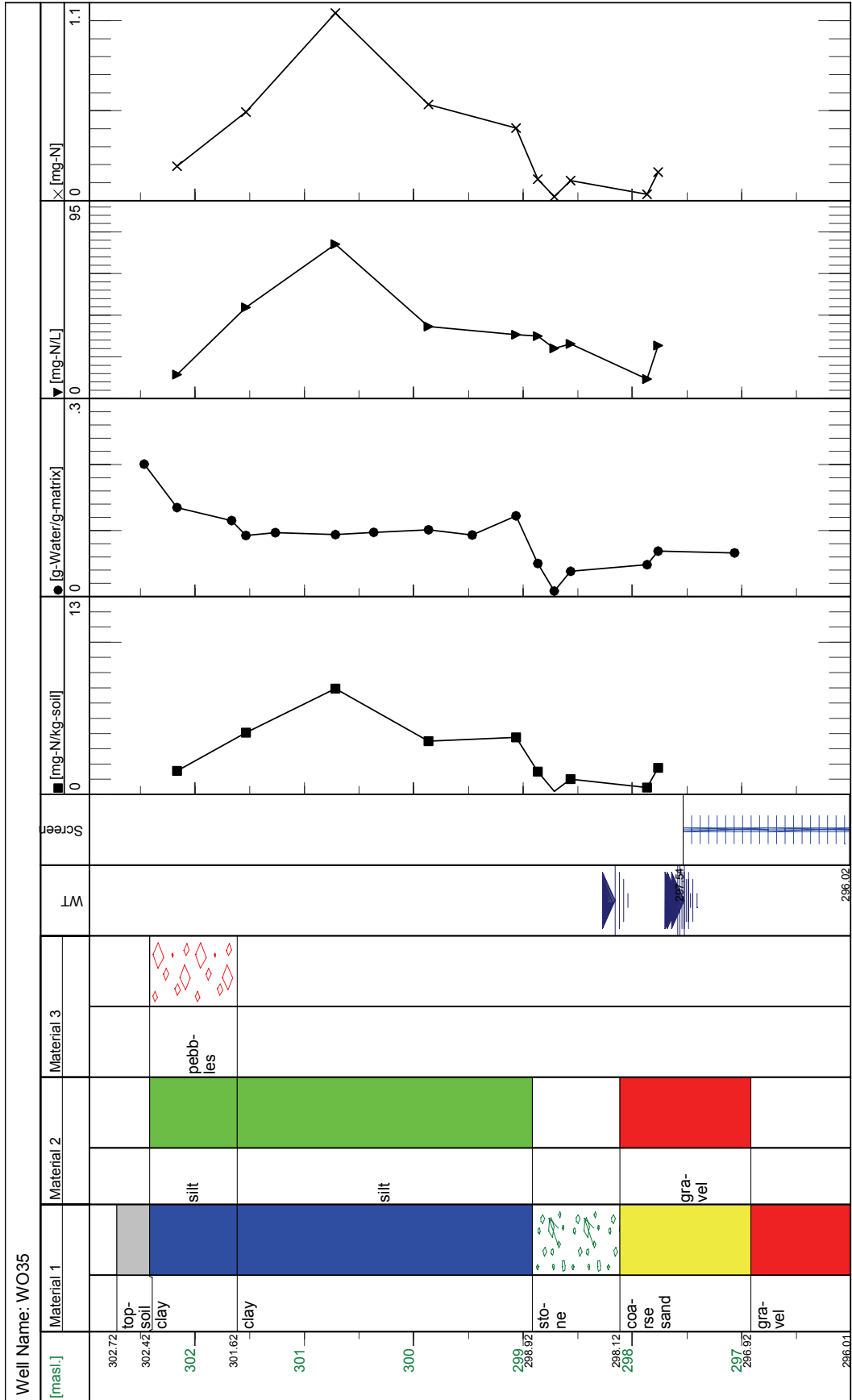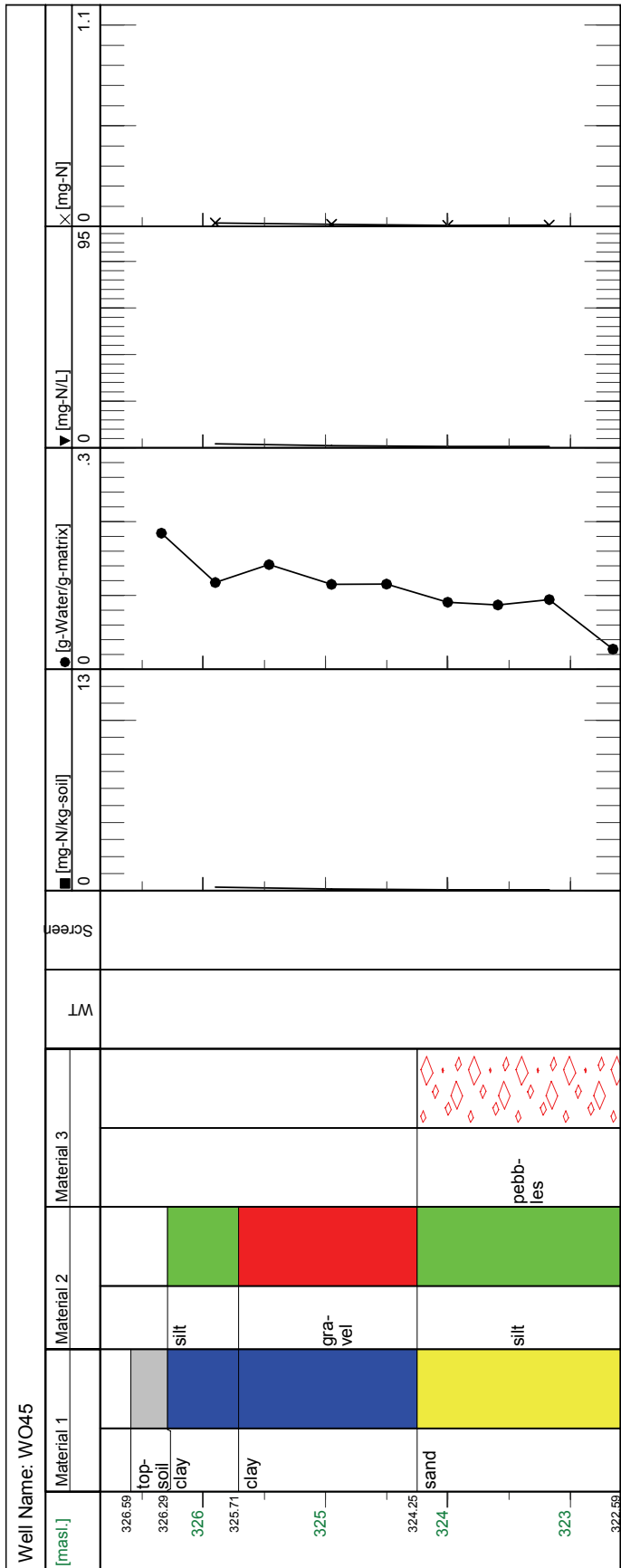
Figure A.31:
Geologic log and nitrate profiles at location WO 35.
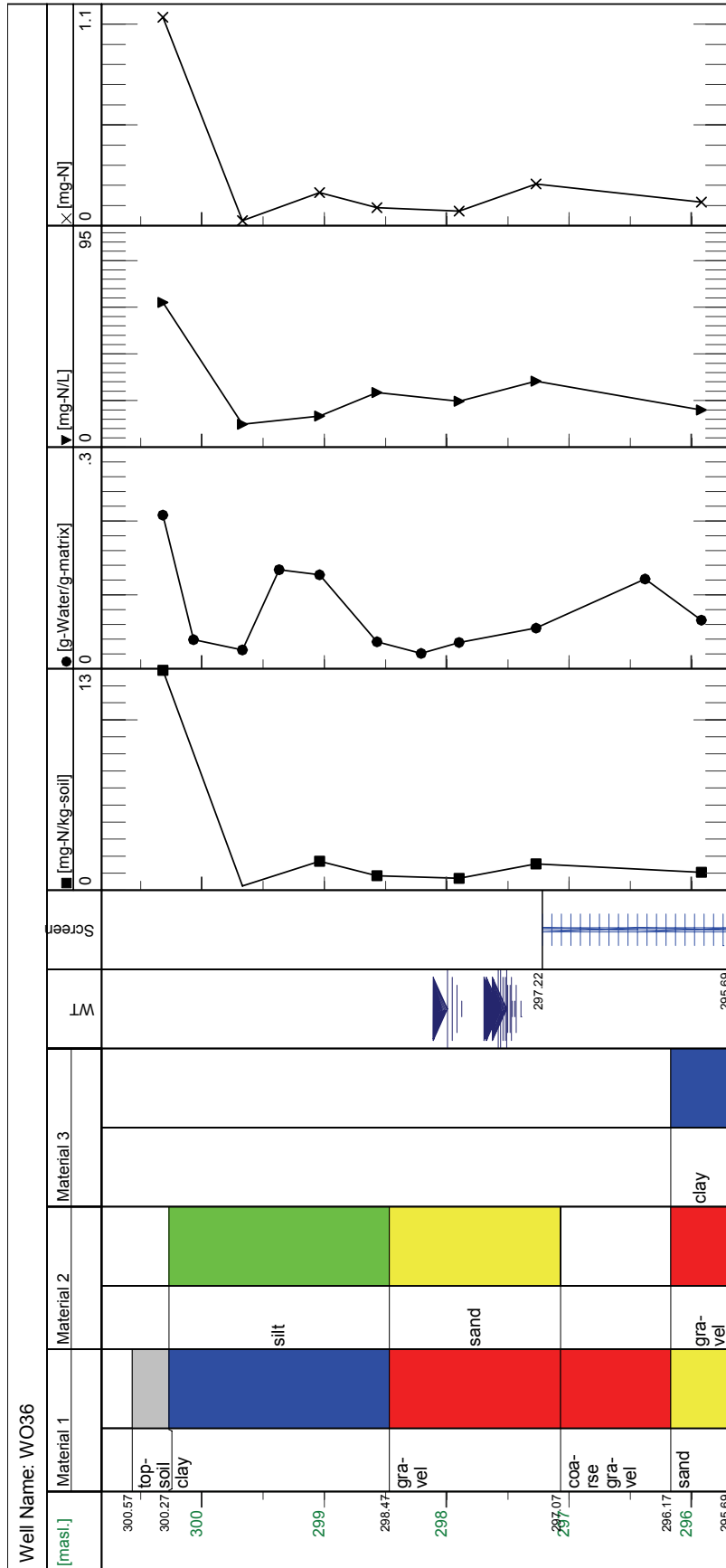
Figure A.32:
Geologic log and nitrate profiles at location *WO 36*.
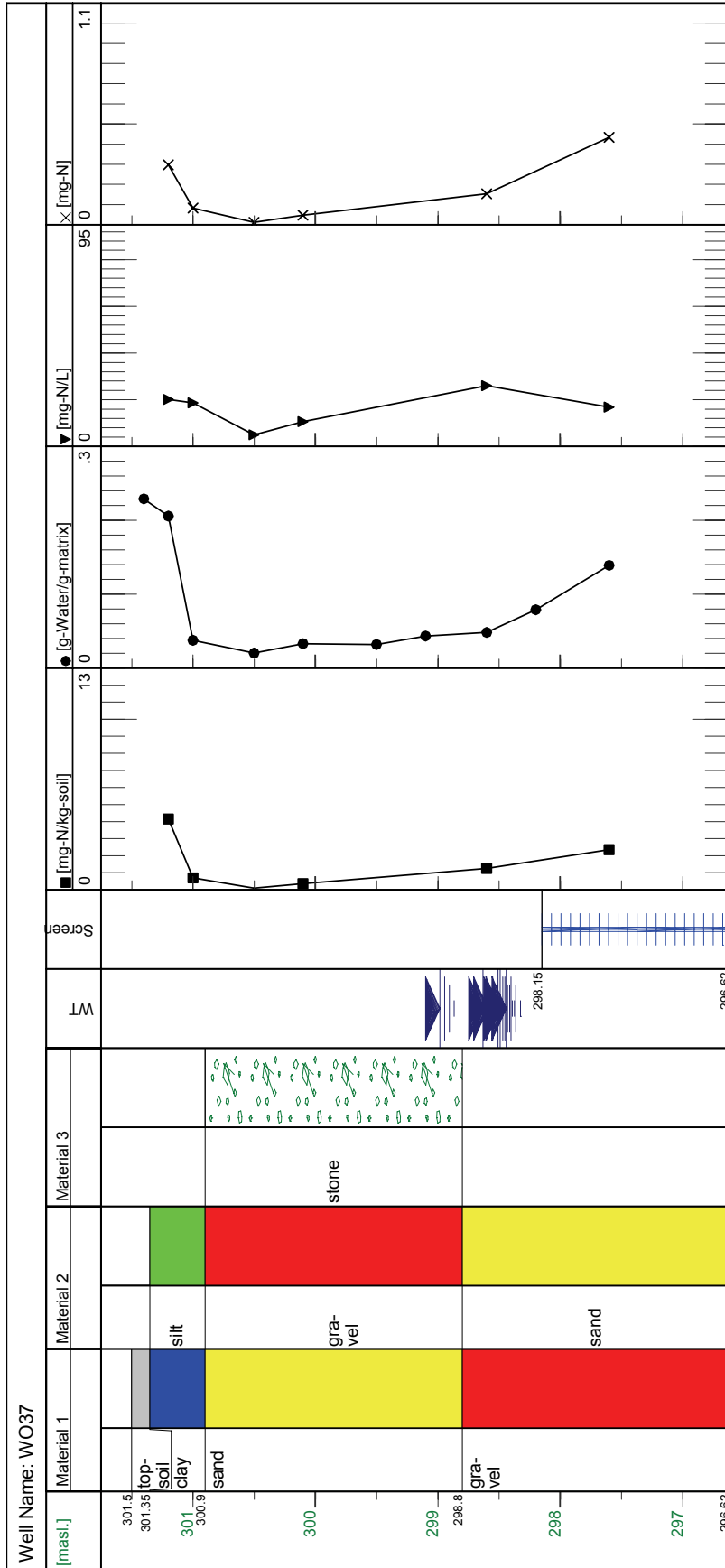
Figure A.33:
Geologic log and nitrate profiles at location WO 37.
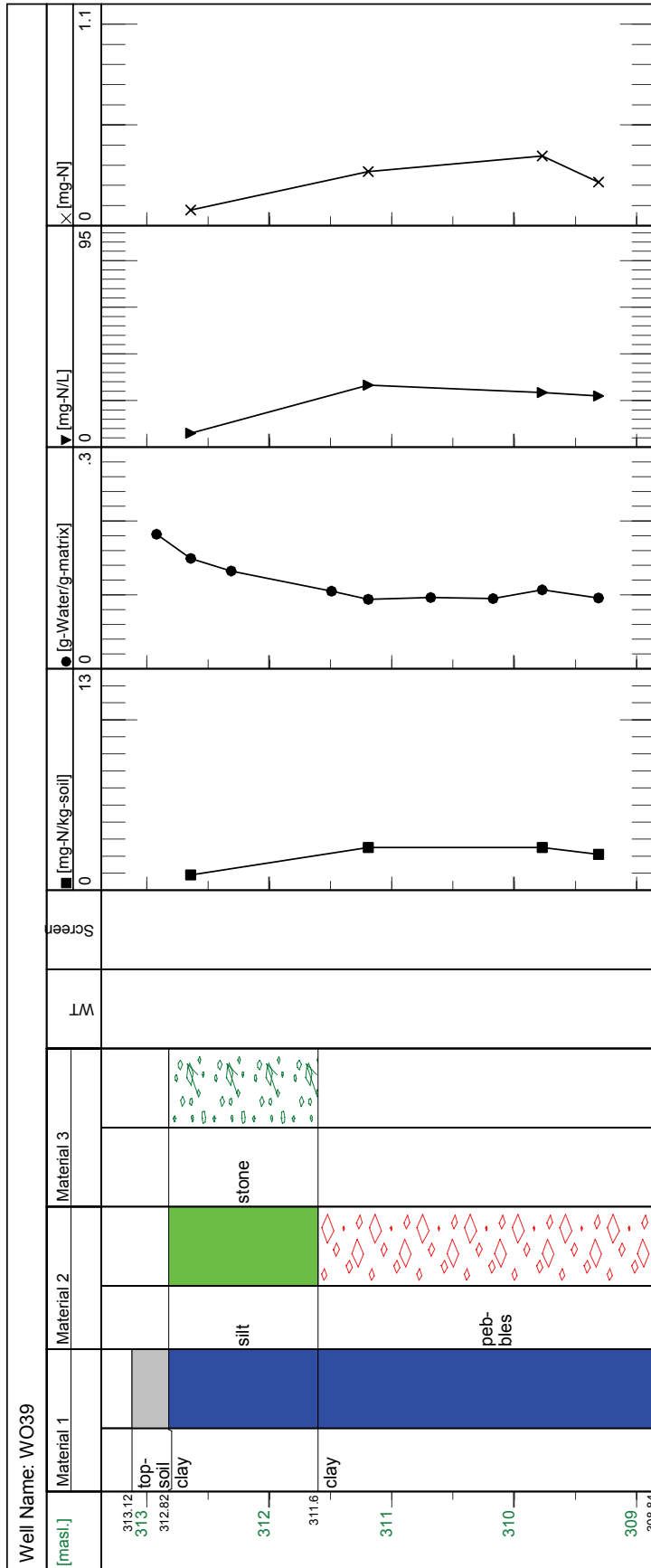
Figure A.34:
Geologic log and nitrate profiles at location *WO 39*.
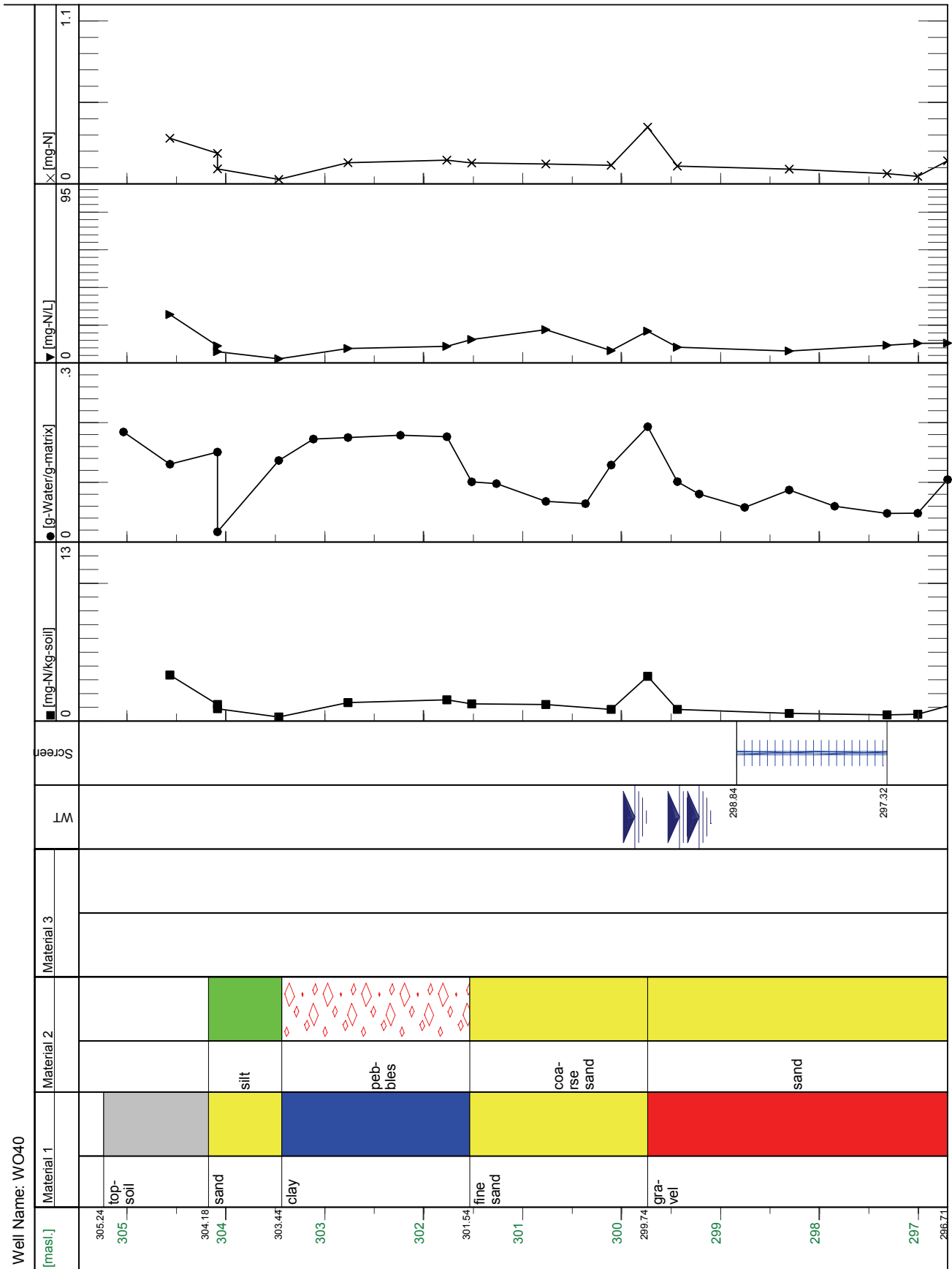
Figure A.35:
Geologic log and nitrate profiles at location WO 40.

Figure A.36:
Geologic log and nitrate profiles at location WO 41.

Figure A.37:
Geologic log and nitrate profiles at location WO 42.

Figure A.38:
Geologic log and nitrate profiles at location *WO 43*.

Figure A.39:
Geologic log and nitrate profiles at location WO 44.

Figure A.40:
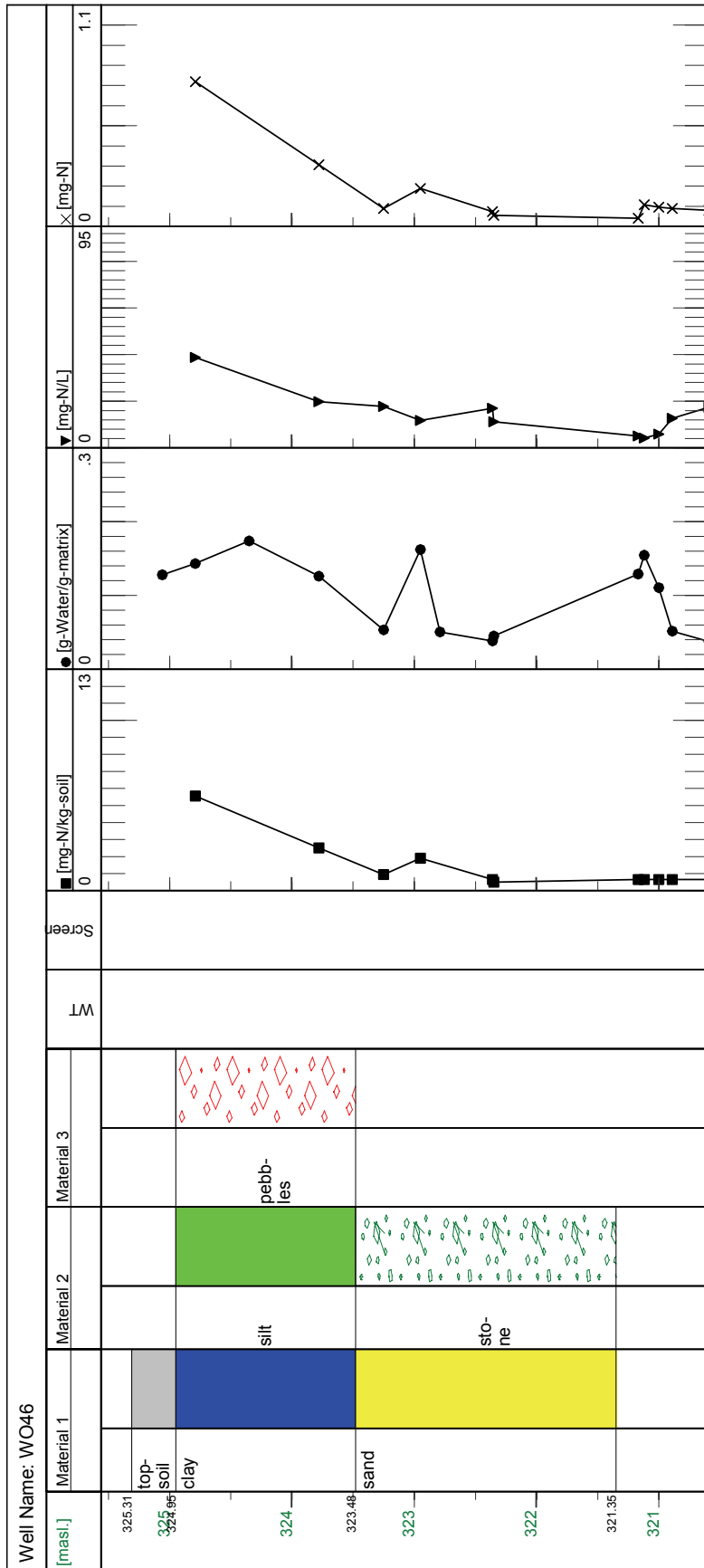Geologic log and nitrate profiles at location WO 45.

Figure A.41:
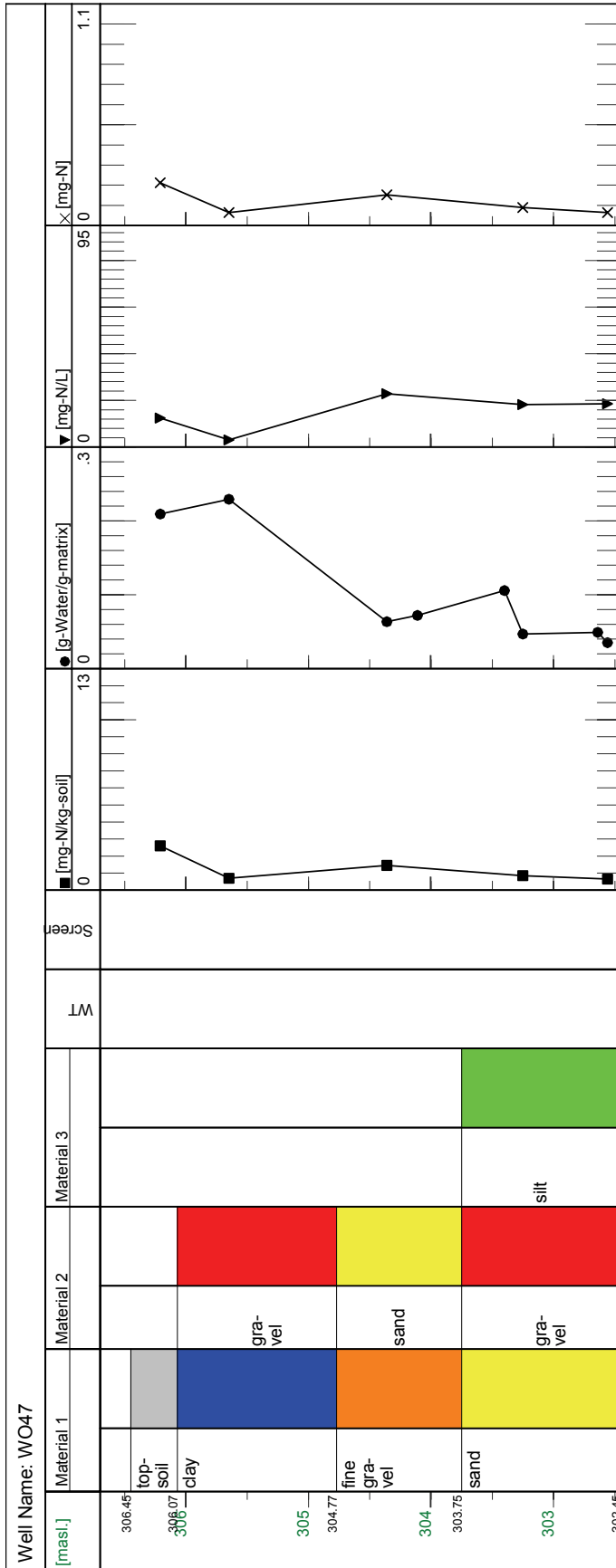Geologic log and nitrate profiles at location WO 46.

Figure A.42:
Geologic log and nitrate profiles at location *WO 47*.

185